The propagation of VHF and UHF radio waves over sea paths

Thesis submitted for the degree of

Doctor of Philosophy

at the University of Leicester

by

Chow Yen Desmond Sim

B.Eng.(Leicester)

Department of Engineering

University of Leicester

November 2002

The propagation of VHF and UHF radio waves over sea paths

by
Chow Yen Desmond Sim

Abstract

This thesis is concerned with the statistical studies of VHF/UHF radio wave propagation over the sea path at the limits of line-of-sight range. The objective is to provide a set of data that leads to the understanding of the characteristic of VHF/UHF radio wave over the sea path. A series of experiments were conducted using two paths of around 33 and 48 km across the English Channel. These two paths are between fixed land-based locations that provide an unobstructed condition. This allows a prolonged period of data collection under several sea states and atmospheric conditions without the heavy expenses of ship borne trial.

The statistic studies showed that the high signal strength variation observed at both receiving sites are the results due to ducting and super-refraction. It occurred around 43 to 76% and 31 to 48% of the total time (percentage of days) during summer 2001 and 2002 respectively. In comparison, the total time was below 10% during winter period. Across the Jersey-Alderney path (48 km), high fading phenomenon was observed which is a result due to interference fading between the diffracted and troposcattered signal. The statistics showed that it occurred at around 35 to 55% of the total times during summer with an average fading range of around 10 and 7 dB during autumn and summer respectively, with an average fading period of around 7 seconds.

The results from simulation showed that when the VHF/UHF signal reaches the radio horizon, the dominant propagating mechanism is smooth earth diffraction. Beyond the radio horizon, the attenuation rate increases dramatically and at a certain distance (depending on the frequency, antenna height and seasonal condition), the diffracted signals will be weaken and the troposcatter effect will become the dominant propagating mechanism.

Acknowledgements

I would like to express my gratitude to my internal supervisor Dr E.M.Warrington and co-supervisor Dr Alan Stocker of the University of Leicester, Engineering Department, for their help and guidance throughout my three years of research.

Many thanks go to Julian Thornhill from Radio and Space Plasma Physics for his advice and assistance with QNX in setting the system required for my experiment.

Finally, I am grateful to the technical staff from the Department of Engineering University of Leicester, for their help and assistance. I am also grateful to the Harbour Authority at St. Peter Port, Guernsey, the staff of Ronez Quarry, Jersey and Mr Jon Kay-Mouat, Alderney.

List of Contents

Glossary of symbols and abbreviation

A_0	Propagation attenuation
ADC	Analogue to Digital Converter
AGC	Automatic Gain Control
ψ	Incident angle
AGND	Analogue ground
A*r*	The receiving antenna captures area (or effective aperture)
β	Parameter that allows for type of ground and polarisation
BBC	British Broadcasting Corporation
c	Speed of light - 3×10^8 ms^{-1}
C	Ray path curvature
d	Distance (km)
d_{LOS}	Line-of-Sight distance
$d_{tx\text{-}rx}$	Distance between transmitter and receiver
D_n	Normalised path length
DAC	Digital Analogue Converter
ε	Relative permittivity
e	Water vapour pressure (mb)
e_a	Actual water vapour pressure (mb)
EHF	Extra High Frequency
ELF	Extra Low Frequency
ESS	Enhanced signal strength
f	Frequency
FIFO	First In First Out
GPS	Global Position System
G_r	Receive antenna gain (dBi)
G_t	Transmit antenna gain (dBi)
h	Height (km) or rms wave height deviation
h_{inc}	Height increment
h_{tx}	Height of transmitter antenna
h_{rx}	Height of receiver antenna
H	Applicable scale height
H_{RX}	Normalised Height for receiver
H_{TX}	Normalised Height for transmitter
Hz	Hertz
I/P	Input
k	Effective ray curvature (k factor)
k_{wave}	Wave number of the incidence wave
k_F	Fresnel zone layer
K_n	Normalised factor for surface admittance
λ	Wavelength (m)
γ	Rayleigh Roughness
LF	Low Frequency
LOS	Line-of-Sight

L_d	Diffraction path loss (dB)
L_{fs}	Free space loss between isotropic antennas (dBw)
L_p	Total path attenuation
L_r	Transmission line loss between receive antenna and received input (dB)
L_t	Transmission line loss between transmitter and transmit antenna (dB)
M	Modified Refractivity
MF	Medium Frequency
MO	Magnetic Optical
MUF	Maximum Usable Frequency
n	Reflective index
N	Refractivity
N_s	Refractivity at the height h
σ	Conductivity
O/P	Output
OCXO	Ovened Crystal Oscillator
θ	Grazing angle
PC	Personal Computer
Pd	Pressure of non polar air in mb (millibars)
ppm	Parts per million
P_r	Delivering power to the receiver antenna (watts)
P_t	Transmitter power output (dBW)
Q1PPS	Qualified 1 pulse per second
ρ	Radius of the ray path curvature
r	earth radius
r_0	$1/r_0$ is the corresponding earth curvature
$\rho_н$	Horizontal Polarization
$\rho_в$	Vertical Polarization
R_F	Fresnel zone radius (metre)
RX	Receiver
S	Power flux density
SHF	Super High Frequency
SSB	Single Side Band
T	Temperature (Kelvin)
T_{dew}	Dew point temperature in ºC
T_D	Tide differences ($T_D = T_H - T_L$) (metre)
T_H	Highest Tide (metre)
T_L	Lowest Tide (metre)
τ	Total wave bending
T_d	$T_{sea} - T_J$
T_J	Jersey airport temperature
TX	Transmitter
T_{sea}	Sea temperature
T_{LS}	Channel lightship air temperature

T_J	Jersey airport air temperature
U	Wind speed (m/s)
UHF	Ultra High Frequency
VHF	Very High Frequency
VLF	Very Low Frequency

Brief History of Early Radio Propagation

As early as 1820, Hans Christian Oersted from Copenhagan had found that when an electric current passed near a compass, the compass needle moved. These showed that there was some form of invisible energy that was coming from the electric current that passed near the compass.

In 1864, James Clerk Maxwell published a remarkable paper describing the means by which a wave consisting of electric and magnetic fields could propagate or travel from one point to another. This was known as Maxwell's Theory of Electromagnetic (EM) radiation.

In the late 1880's, German physicist Heinrich Hertz proved that this theory is correct during a series of careful laboratory experiments. These experiments included placing two small electrodes a short distance apart and generating high voltage sparks between them. When a large electric spark jumped across the gap, Hertz observed that a smaller spark appeared at a second instrument. Therefore, Maxwell's theory which post related that the electromagnetic energy did travel through the air and caused the second spark was proven. But Hertz saw no future in the devices and theory since the wave only travelled about a metre.

It was not until the last decade of the 19th century that an Italian scientist named Guglielmo Marconi (1874 - 1937) converted these theories into the first practical wireless telegraph system. Marconi well known as "the father of wireless" realised at the age of 19 that radio waves had a future in communication. He studied the works of Hertz and the mathematical conclusions of Maxwell. Soon, he built a transmitter based on the experiments of Hertz and together with Augusto Righi (his professor); he was sending signals across his father's vineyard in Northern Italy. Although Marconi succeeded in his first invention, the Italian authorities weren't interested in it. Hence, he travelled to Britain hoping that they would be interested in wireless communication. On December 12th 1896, he made his first public demonstration of his devices and it was a triumph.

In 1899, Marconi demonstrated his wireless communication technique across the English Channel and it was a success. In another landmark experiment on December 12, 1901, Marconi demonstrated transatlantic communication by receiving a signal in St.John's New Foundland that had been sent from Cornwall, England. Finally, in 1909, Marconi was awarded the Nobel Prize for Physics for his pioneering work in the use of wireless communication.

MARCONI

" I now knew that all my anticipations had been justified. I now felt for the first time absolutely certain that the day would come when mankind would be able to send messages around the world, not only across the Atlantic, but between the furthermost ends of the earth".

Chapter 1: Introduction

VHF/UHF and microwave signals can travel distances beyond the horizon under certain atmospheric conditions. Depending on the state of condition in the atmosphere, radio propagation between the transmitter and the receiver may occur by the mechanisms of scattering, reflection, refraction, diffraction and tropospheric ducting.

It is generally agreed that the radio-meteorological situation in the coastal areas can produce complicated structures due to the interaction between the sea and the land, Castel [1965]. Hence, it is useful to further investigate into this field since there is still insufficient information on meteorological effects and the various atmospheric mechanism that give rise to propagation over the sea using VHF/UHF. Although much work has been carried out (e.g. COST 210) throughout Europe to study the propagation mechanism over sea paths, land paths and mixed sea and land paths, the prediction of radio wave propagation is still not covered adequately. Moreover, there is relatively very little published on equivalent propagation over the sea for both VHF/UHF when the direct path is obstructed by the sea surface. The propagation path over sea is very different from over land, as the atmospheric conditions over the sea are the dominant influence of the propagation characteristics. In order to obtain the required additional information, non line-of-sight (LOS) paths were established by the University of Leicester Radio Systems Laboratory.

The main objectives of this research are to measure and model the propagation mechanisms appropriate to inter-ship communications at VHF/UHF. Of particular interest is where both ships are around the limits of propagation with each other. The aims of the work reported are:

(a) To test current understanding of over-sea VHF/UHF propagation for antenna heights commensurate with what might be found on ships.
(b) To identify any propagation effects that are not attributable to currently understood phenomena.
(c) Gather statistics of the various effects, in particular the occurrence of ducting and fading.
(d) Relate the above to prevailing weather conditions.

Chapter 2: Radio wave propagation at VHF/UHF

2.1 Introduction

This chapter introduces the concept of radio wave propagation and some of the terminology used in VHF/UHF communication such as refraction, reflection and line of sight propagation. Radio wave propagation includes everything that can happen to an energy radiated from a transmitting antenna to a receiving antenna. It includes the radiating properties of both antennas such as gain, power, directivity and polarisation. It also includes free space attenuation of radio wave with distance in addition of factors such as refraction, reflection, noise interference, diffraction, atmospheric absorption and scatter. Propagation is therefore dependent upon the properties of all transmission and boundary media.

The troposphere is the most important region of the atmosphere as far as VHF and UHF radio waves are concerned. It is the lower layer of the atmosphere surrounding the earth that extends to a height of approximately 10 km above the sea level. All weather on earth occurs in the troposphere during normal conditions. The temperature decreases as height increases, and generally drops with increased altitude at about 10°C per km until the tropopause is reached, the point at which the atmospheric temperature begins to rise with altitude (Hall [1979], Rishbeth and Garriott [1969], Picquenard [1974]). The basic theory of radio wave propagation within the troposphere is considered in this chapter.

2.2 Radio spectrum and free space propagation

2.2.1 The radio frequency spectrum

Radio wave communication can be extended from a few kilohertz to about 100 Giga-hertz as shown in Figure 2.1. The band that will be discussed is VHF/UHF band and the common applications for UHF are TV and cellular radio [Hall *et al*, 1996].

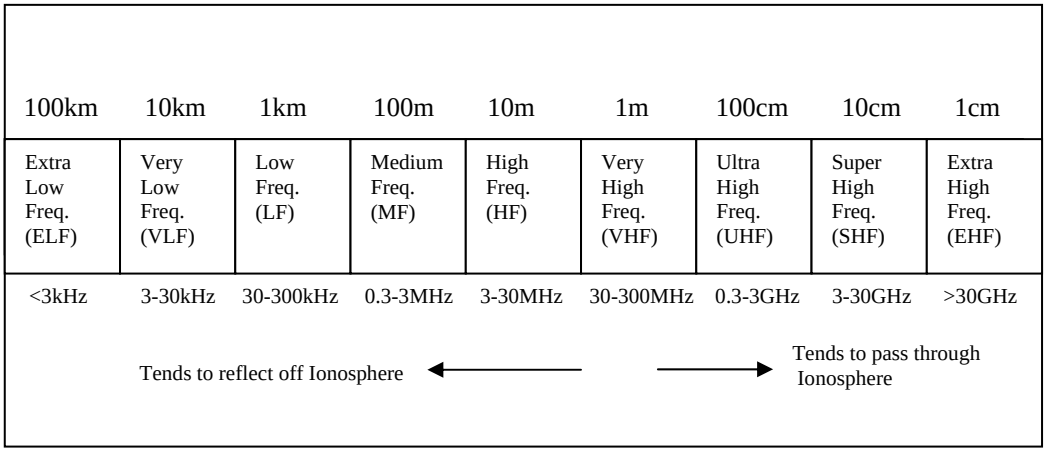

Figure 2.1: The radio frequency spectrum

2.2.2 Free space transmission loss

Before looking into various wave propagation related to VHF/UHF band, it is important to approach the free space transmission of radio wave. The calculation of free space transmission loss (Matthew [1965], Budden [1961], Castel [1966]) can be considered as below:

The power flux density, *S*, is given by:

$$S = \frac{P_t}{4\pi d^2} \qquad (2.01)$$

Where P_t is the transmitted power radiated equally in all directions. The radiated power is distributed uniformly over an area of $4\pi d^2$ where *d* is the radius of the surface area of a sphere.

The Transmission Loss for free space depends on how much is received by the receiving antenna. By considering A_r as the receiving antenna capture area (or effective aperture), the power delivered to the receiver antenna is:

$$P_r = SA_r \qquad (2.02)$$

For an isotropic receiving antenna ,

$$A_r = \frac{\lambda^2}{4\pi} \qquad (2.03)$$

Where λ is the wavelength.

By substituting equation (2.01) and (2.03) into (2.02), we will have

$$P_r = P_t\left(\frac{\lambda}{4\pi d}\right)^2 \qquad (2.04)$$

The propagation attenuation (A_0) is defined as the ratio of the power received to the power transmitted and is given by:

$$A_0 = \left(\frac{\lambda}{4\pi d}\right)^2 \qquad (2.05)$$

P_t / P_r is known as the free space loss (L_{fs}). By substituting $\lambda = c/f$ (where c is the speed of light - 3×10^8 ms^{-1}), we get

$$L_{fs} = \left(\frac{4\pi}{c}\right)^2 f^2 d^2 \qquad (2.06)$$

The free space loss can also be expressed in decibels as

$$L_{fs} = (32.4 + 20\log f + 20\log d)\text{dB} \qquad (2.07)$$

(*f* in MHz and *d* in km)

From equation (2.07), a further loss of 6 dB will occur when the distance *d* or frequency *f* doubles under free space conditions. The signal power P_r, which is at the receiver input, can be defined as below

$$P_r = P_t - L_{fs} + G_t + G_r \qquad (2.08)$$

As P_t = transmitter power output (dBW)

L_{fs} = free space loss between isotropic antennas (dB)

G_t = transmit antenna gain (dBi)

G_r = receive antenna gain (dBi)

Note that absorption effect and attenuation in the atmosphere is not a concern in this report as it is minor from 10 MHz to 3 GHz. Gough [1979] mentioned that the atmospheric absorption near to the earth's surface at a frequency of 774 MHz amounts to around 0.0047 dB/km mainly due to oxygen. Lavergnat and Sylvain [2000] provided more detail discussion on absorption or attenuation due to oxygen, water vapour, clouds, fog and rain.

2.3 VHF/UHF propagation mechanism

2.3.1 Types of radio wave propagation related to UHF band

There are many types of radio wave propagation as suggested by Reed & Russell [1966], e.g. ground wave, sky wave and tropospheric wave. At UHF, ground wave and sky wave (ionospheric wave) are considered as non-existant and only direct wave (line-of-sight), earth reflected and tropospheric wave remain to be considered [Reed & Russell, 1966].

2.3.2 Line of sight (LOS) and multipath propagation

For both VHF/UHF band, radio signals can travel in a direct path from the transmitter to receiver. This " line-of-sight" propagation requires a path where both antennas are visible to each other with no obstruction (e.g. buildings, mountains etc.) in between [Hall *et al*, 1996].

Having a LOS between two antennas does not mean that the path loss (L_p) will be equal to the free space condition as mentioned in equation (2.07). There are a few propagation mechanisms that may cause the path loss (L_p) to vary and they are sometimes perceived as multipath propagation. Multipath occurs when there is more than one path available for radio signal propagation. The phenomena of reflection, diffraction and scattering all give rise to additional radio propagation paths beyond the direct optical LOS path between the radio transmitter and the receiver. Multipath occurs when all the radio propagation effects combine in a real world environment. Hence, when multipath occurs, caused by whatever phenomenon, the actual received signal is a vector sum of all signals incident from any direction of arrival. These signals include those arising from reflection, refraction, scattering and diffraction etc. Some of these signals will add in

phase to the direct path signal, whereas other signals will add in anti-phase (e.g. tend to cancel) the direct signal path.

2.3.3 Reflection

LOS path may have adequate Fresnel zone (Section 6.2) and yet still have a path loss that differs significantly from free space loss under normal refraction conditions. If this is the case, the cause is probably due to multipath propagation as mentioned earlier (Reed & Russell [1966], Hall et al [1996]). In a radio path consisting of a direct path and a ground reflected path as shown in Figure.2.2, the path loss depends on the relative amplitude and phase relationship of the signals propagated by the two paths.

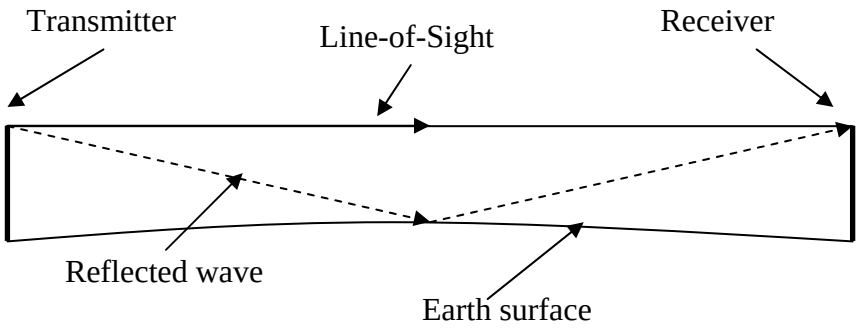

Figure. 2.2: LOS and reflected wave

2.3.4 Diffraction

Diffraction occurs when the radio path between the transmitter and receiver is obstructed by a surface that has sharp irregularities (edges) [Matthew, 1965]. This is sometimes known as “knife edge” diffraction. The secondary waves resulting from the obstructing surface such as sea waves are present throughout the space and even behind the obstacle, giving rise to a bending of waves around the obstacle, even when a line-of-sight path does not exist between the transmitter and the receiver. Similar to reflection, diffraction depends on the geometry of the object, as well as the amplitude, phase, and polarisation of the incident wave at the point of diffraction.

2.3.5 Refraction

Refraction occurs whenever there is a change in the refractive index. During unusual weather conditions, the refractive index in the atmosphere will change dramatically and this can lead to certain phenomenon such as “*super refraction*”. Super refraction occurs when the propagating wave is bending more than normal and the radio horizon are extended. In extreme cases, it leads to another phenomenon known as “*ducting*”, where

the signal can propagate over enormous distances beyond the normal horizon. A more serious phenomenon is “sub refraction”, in which the bending of radio wave is less than normal, thus shortening the radio horizon and reducing the clearance over obstacles along the path that might lead to an increase in path loss. Tropospheric refraction, scattering and ducting will be further discussed.

As discussed before, in the troposphere, both VHF and UHF radio waves propagate in a slightly deviated path instead of following a straight line as shown in Figure 2.3.

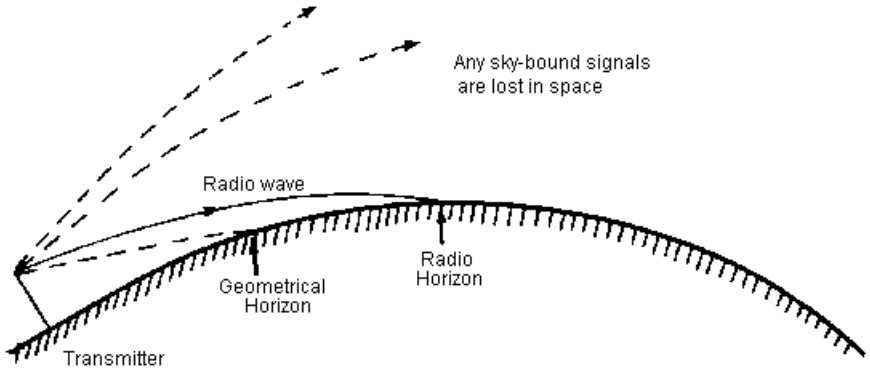

Figure 2.3: Normal Tropospheric propagation of a VHF or UHF radio wave

This is due to refraction and the extent and nature (the angle and distance) of the deviation depends on the refractive index profile of the troposphere. Under normal conditions, a radio wave is able to travel farther than the geometrical horizon to a point known as the radio horizon as illustrated in Figure 2.3 above.

Beyond the radio horizon, the signals will either attenuate rapidly or propagate away from the earth [Castel, 1966].

2.4 Refractive index in the troposphere

In free space, a ray will travel outward from its source along a radial line with a constant velocity equal to the speed of light. The refractive index of the troposphere is a function of pressure, temperature and water vapour content. Since the refractive index n is approximately =1 (typical value at 1.0003 at the Earth’s surface), the normal practice is to use N which is referred to as refractivity.

$$N = (n-1)\times 10^6 = \frac{77.6P_d}{T} + \frac{72e}{T} + \frac{3\times 10^5 e}{T^2} \qquad (2.09)$$

Where P_d is the pressure of non-polar air in mb (millibars), e is water vapour pressure in mb, and T is temperature in Kelvin's (Hall *et al* [1996], Biddulph [1993]). From equation (2.09), N varies inversely with temperature T and is strongly dependent on water vapour pressure e. The refractivity N may decrease exponentially in the troposphere as described by Hall *et al* [1996], whereby:

$$N = N_s\, e^{-h/H} \qquad (2.10)$$

Where N is the refractivity at the height h above the level where the refractivity is N_s while H is the applicable scale height. ITU-R Recommendation P.453-8 [2001] suggests that at average mid-latitude, N_s is 315 and H is 7.35 km. From Flock *et al* [1982], during average atmosphere, N_s has the value of 315 where

$$N = 315\, e^{-0.136\, h} \qquad (2.11)$$

with h in km. Values of N_s and ΔN have been compiled, with Ns sometimes reduced to sea level values. Bean and Dutton [1966] provided charts showing the distribution of N_s, at different height above the sea level.

Figure 2.4 shows different contours of refractivity (N) measured over the English Channel. Bean and Dutton [1966] provided a further study on surface variation of the radio refraction index in terms of reduced to sea level form of index. This yielded a more precise description of refractive index variation than the non-reduced form.

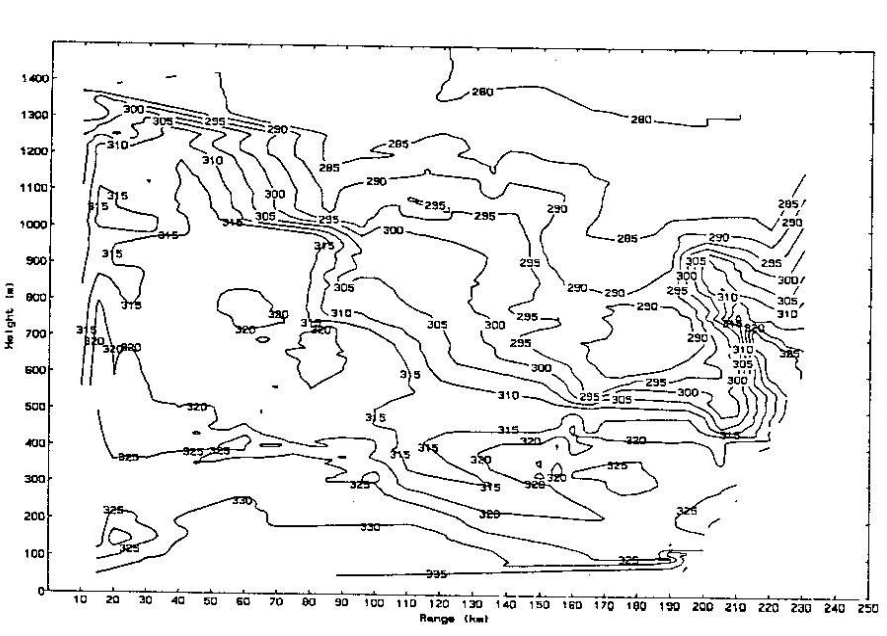

Figure 2.4: Contours of potential refractivity measured over the English Channel [after Hall *et at*, 1966]

2.4.1 *Refraction characteristic and effective Earth radius*

As mentioned earlier, radio wave does not travel in a straight line but experiences refraction. An important characteristic of this refracted ray path is its curvature C; defined as 1/ρ, where ρ is the radius of the curvature. Bean and Dutton [1966] and Hall [1996] showed that a ray path in a spherically stratified atmosphere has a curvature given by

$$C = -\frac{1}{n} \times \frac{dn}{dh} \cos\beta \quad \text{m}^{-1} \qquad (2.12)$$

Where β is the angle of the ray path measured from the horizontal and h is the height in km. Since the refractive index n is approximately unity, and if the angle β is close to zero, the expression of C can be simplified as

$$C = -\frac{dn}{dh} \qquad (2.13)$$

Equation 2.13 is normally used for terrestrial line-of-sight over a spherical earth. In this case, the difference in curvature between a ray path and the earth's surface is given by

$$\frac{1}{r_0} - C = \frac{1}{r_0} + \frac{dn}{dh} \qquad (2.14)$$

Where r is the Earth radius and $1/r_0$ is the corresponding curvature.

A geometric transformation may be applied such that the ray paths become linear and the Earth has an effective radius of k times the true radius $1/r_0$ thus

$$\frac{1}{r_0} + \frac{dn}{dh} = \frac{1}{kr_0} + 0 \qquad (2.15)$$

Which maintains the same relative curvature as in equation (2.14). The 0 has been included on the right-hand side of equation (2.15) to emphasize that it applies to the case that $dn/dh = 0$. In terms of N units, the relation is

$$\frac{1}{kr_0} = \left[157 + \frac{dN}{dh}\right] \times 10^{-6} \qquad (2.16)$$

Hall *et al* [1996] showed how the k factor, which is the effective ray curvature, associated with the Earth radius affects the rays propagating in a standard atmosphere with different k-factor representation. A typical value for *dN/dh* is –40 *N*/km and k is 4/3. Figure 2.5 shows an illustrative ray path, for several values of k for initially horizontal rays.

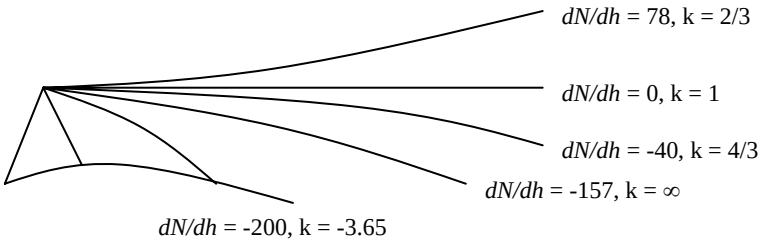

Figure 2.5: Illustrative ray paths for several values of k

If the lapse rate (*dN/dh*) is from positive lapse rate to –40 *N*/km (e.g 40 to –40 *N*/km), the ray path will curve downward, shortening the radio horizon and it is known as *sub-refraction*. Inversely, if the lapse rate is between –40 to –156 *N*/km, the ray path will increase hence extending the radio horizon. This is known as super refraction and Wait[1962] provided some very good discussion on super refraction in a stratified medium. If the lapse rate goes below –157 *N*/km (e.g. –175 to –200 *N*/km), the ray path

deviates in such a way that it is approaching towards the Earth surface, a phenomenon known as ducting will occur [Hitney *et al*, 1985]. Ducting is sometimes considered as beneficial if longer-range propagation is desirable. The downside is that the receiving antenna has to be within the height limits of the ducts, or else, if the receiving antenna is below or higher than the duct height, signal losses will increase dramatically [Hall, 1979]. Figure 2.6 below shows the illustrated classification of refractive condition,

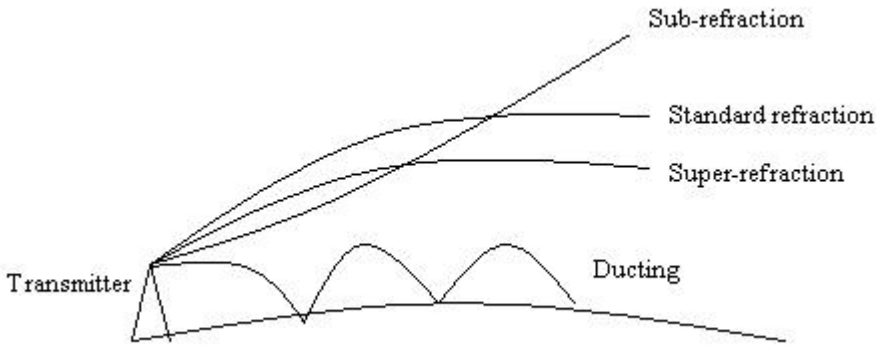

Figure 2.6: Refractive condition illustrations

Matthew [1965] provided a very detailed discussion on effective earth's radius for tropospheric propagation. The effective radius calculation was made by assuming under normal meteorological conditions (e.g. refractive index falls uniformly with height).

Various equations for calculating the refraction of the ray path and simple procedures for calculating refraction and elevation angle errors were revised by Weisbrod and Anderson [1959]. Crane [1976] further evaluated the refraction of angles at different elevation angles and showed that the exact values of bending angles vary depending on atmospheric conditions.

2.5 Tropospheric Ducting

Tropospheric ducting is the condition when communication of greater than a few hundred kilometres occurs. It is perceived as a severe refractive effect involving trapping of a wave in a duct between two boundaries, commonly a surface duct and hence the possible of propagating for an abnormally long distance. Ducting occurs frequently in some locations, but it is not a reliable means of communication [Dougherty and Hart, 1979].

As mentioned earlier, a necessary condition for ducting to occur is that the refractivity *N* decrease with height at a lapse rate of -157 *N* units per km or greater, (Hall *et al* [1996], Picquenard [1974], Hitney *et al* [1985]). Figure 2.5 shows that if the lapse rate is less than -157*N*/km, the ray path will deviate downward to the surface of the Earth when k factor is -3.65. In such a case, no signal will reach the receiving location and the use of space or frequency diversity may not improve the situation. The rays that bend downward to the Earth's surface may be reflected upwards, however, and then refracted down back to the Earth again, etc., giving rise to ducting as illustrated in Figure 2.7.

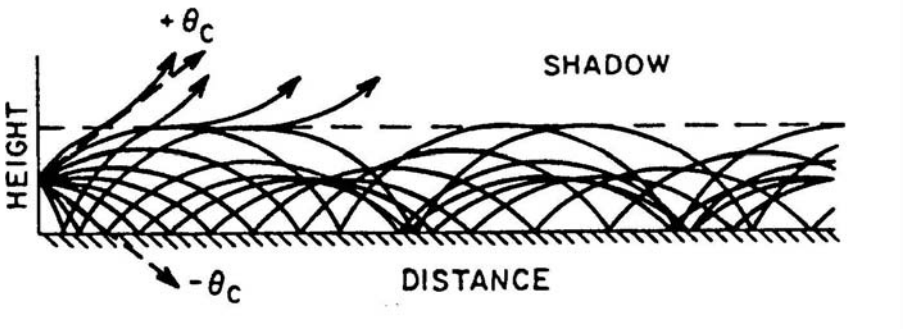

Figure 2.7: Example of ducting

From Reed and Russell [1966], White [1992], Hall *et al* [1996] and Hitney *et al* [1985], three types of ducting effects were described in the troposphere over the sea, surface-based ducts, elevated ducts and evaporation ducts.

The modified refractive index *M* is often employed to represent the variation of refractive index with height. Instead of using *n* (refractive index) over the earth radius (k), the modified refractive index can be considered as below:

$$M = N + 0.157h \qquad (2.17)$$

where *h* is the height in metre. From equation (2.17), *M* increases with *h* and hence the radio wave is deviated away from the ground. When *M* decreases with *h*, ducting occurs when the radio wave is deviated towards the earth. Duct height (h_d) is measured when *M* is at its zero gradient, Paulus [1985], Rotheram [1974].

Figures 2.8 shows the *N* (refractivity) and *M* (modified refractivity) profiles for all the three types of ducting.

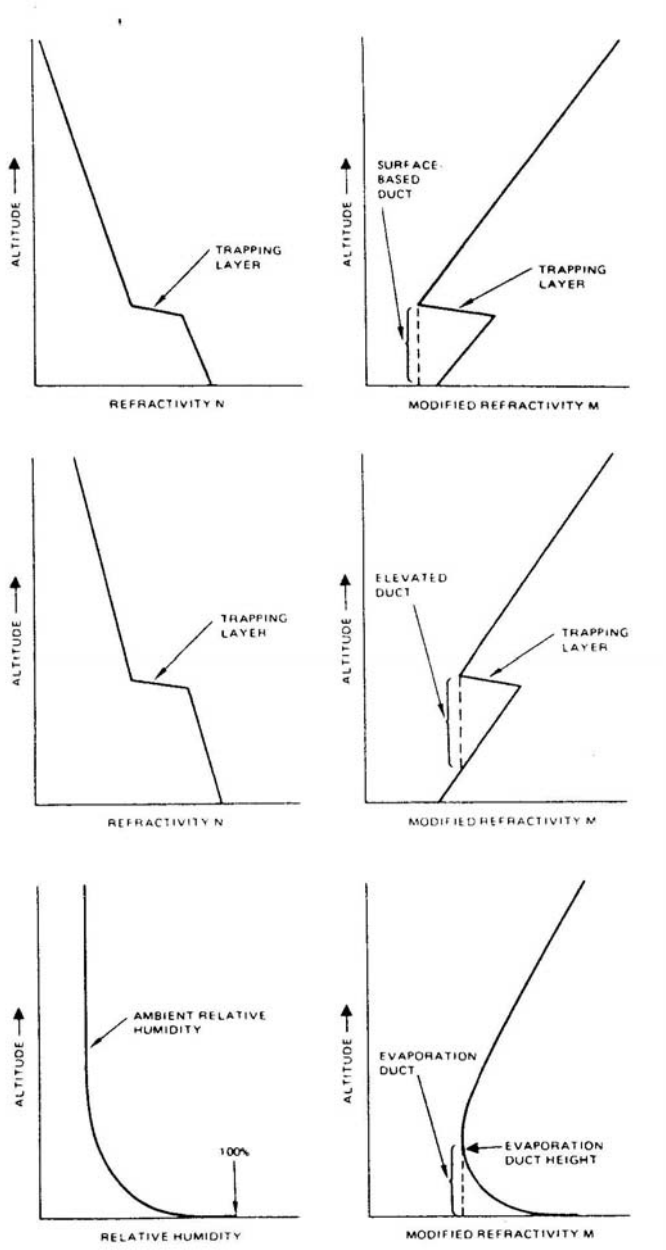

Figure 2.8: *N* and *M* profiles for 3 types of ducting over the sea [after Hitney *et al*, 1985]

A surface duct occurs when the upper boundary of the duct refracted the ray and the lower boundary is the earth surface that reflected the ray back into the atmosphere as shown in Figure 2.8. It is caused by temperature inversion, when warm air from the land moves over the cold water. In this case, the lapse rate increases and hence produces a much stronger surface duct. Surface duct can be easily identified when the top-trapping layer *M* value is less than the bottom-trapping layer and it is responsible for most of the trans-horizon propagation for frequencies over 100 MHz [Hitney *et al*, 1985]. The

effects on both VHF and UHF transmission depend mainly on the location of the receiving antenna. If the receiving antenna is within the duct, stronger signal will be received and transmission beyond the horizon is made possible.

Elevated ducting effects occur when the ray path is trapped between two boundaries in the troposphere caused by a double discontinuity in the refractive index. The upper boundary will deviate the ray path back towards earth and the lower boundary will deviate it back upwards. In this condition as shown in Figure 2.8, the duct height is the vertical extent from the top-trapping layer to the bottom-trapping layer with the same *M* value [Hitney, 1985]. Subsidence temperature inversion is sometimes considered as the main cause of this effect. In this case, tropospheric opening was developed due to the sharp contrast of temperature and humidity between the two layers of air boundary that produces substantial refraction for UHF signals. As for the effects on both VHF and UHF signals, it depends on the location of both receiving and transmitting antenna, whether if both are within, above or below the elevated ducting layer. Stronger signal strength is achieved if both the receiving and the transmitting antennas are in the same zone, especially within the ducts [Hall, 1979]. Elevated ducting can affect the propagation at frequencies higher than 100 MHz and is very common at a height of 3km although it might occur at a height up to 6 km. It plays an important role in producing high signal strength well beyond the horizon especially over the sea.

Evaporation duct is a phenomenon very common over sea and is due to rapid changes in humidity just above the sea surface. The duct height is measured at a minimum value of *M* and the rapid decrease in humidity results in a trapping layer adjacent to the surface as shown in Figure 2.8. Studies from Hitney and Vieth (1990) show that evaporation ducting can affect propagating frequencies that are above 2 GHz and its duct height normally varies from 0-40 metres. Such ducting is likely to occur in the afternoon due to prolonged solar heating and average duct thickness is 15 metres [Hall, 1979].

Ducting occurs more frequently over the sea than land since the land always tends to absorb or scatter radio waves [Matthew, 1965]. Although atmospheric absorption and rough sea surface increases the attenuation of signal, ducting effect over the sea is still able to provide longer radio wave propagation and lower loss than is essential for transhorizon propagation [White, 1992].

Hall [1979] and Hall *et al* [1996] provided a very good discussion on all types of ducting effects and how it is associated with temperature inversion will be discussed later.

2.6 Temperature Inversion and its effect on VHF/UHF propagation

As mentioned before, the occurrence of tropospheric ducting provided an opportunity for both VHF/UHF radio waves to propagate beyond the horizon. For a duct to occur, temperature inversion plays an important role.

Temperature inversion occurs when the air temperature increases with altitude instead of the usual temperature decrease with altitude. Inversion plays an important role in determining cloud forms, precipitation, and visibility. An inversion also acts as a lid on the vertical movement of air in the layers below. As a consequence, convection produced by heating the air from below is limited to levels beneath the inversion. Because the air near the base of the inversion is cool, fog is frequently present there. Bean and Dutton [1966] provide a very good background reading on the meteorological phenomena associated with radio refractive conditions caused by temperature inversion.

When temperature inversion occurs, the refractive index will increase dramatically to produce a longer-range reception as shown in Figure 2.9 for both VHF and UHF radio wave.

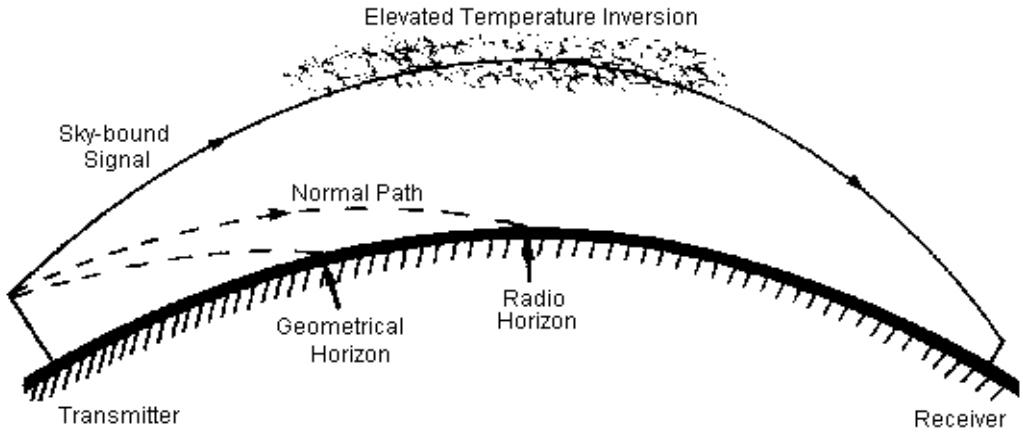

Figure 2.9: VHF/UHF radio wave propagation by refraction from an elevated temperature inversion

There are commonly three types of temperature inversion as described by Bean and Button [1966], Reed and Russell [1966] and Hall *et al* [1996].

Subsidence inversion develops when a layer of air is sinking and is compressed by the resulting increase in atmospheric pressure. The upper layer descending farther than the lower layers and hence resulting in reduction of temperature lapse rate. When these air masses descend low enough, its upper layer temperature will be higher than its lower layer and temperature inversion occurs. These temperature and humidity changes may result in an increase in refractive index within a few tens of meters height intervals, which extend horizontally over tens or hundreds of kilometres [Hall, 1979]. Subsiding air almost never continues descending towards the earth's surface. Hence this phenomenon is responsible for the occurrences of elevated ducts [Reed and Russell, 1966]. The layer of air beneath the base of the inversion layer and the layer of air above the top of the inversion layer are usually unstable, while the layer of air within the inversion layer is very stable. Subsidence tends to reduce sub-refraction layer while increasing chances of super-refraction to occur. Subsidence inversion can happen at any time of the year but more commonly during spring and autumn. It has been observed to occur frequently across the English Channel during the summer when several days of good weather occur [Bean and Dutton, 1966].

Advection inversion develops when an air mass advecting (e.g. shifting) across a surface of differing temperature. An example is the hot air from land blowing towards the sea to produce foggy air above the sea. Inversely, it can also occur over land during winter if warm, moist air from the sea is blown over cold ground to produce a layer of fog or moist [Picquenard, 1974]. Advection temperature inversion is responsible for ground base duct and super-refraction over the sea to occur [Al'pert, 1963].

The rapid cooling of the earth's surface especially after darkness fall causes Radiation/Nocturnal inversions. This type of inversion occurs particularly over the land as the ground can cool much faster than the sea after sunset.

Another type of inversion is called frontal inversion. It occurs when two air masses of different temperatures comes together and do not mix freely. Hence a transition zone called a "front" forms between these two air masses of different temperature. Fronts are commonly zones of steep horizontal temperature gradients and therefore are associated

with strong winds and causes complex inversion. These conditions are generally developed only for a short period of time, along a limited path, that is fairly significant.

2.7 Tropospheric Scattering

Tropospheric scattering (troposcatter) occurs due to the variations in refractive index dependent on meteorological irregularities such as humidity, temperature and pressure. Electromagnetic radio waves are scattered by these changes in irregularities and the usable frequency range is between 100 MHz to 10 GHz.

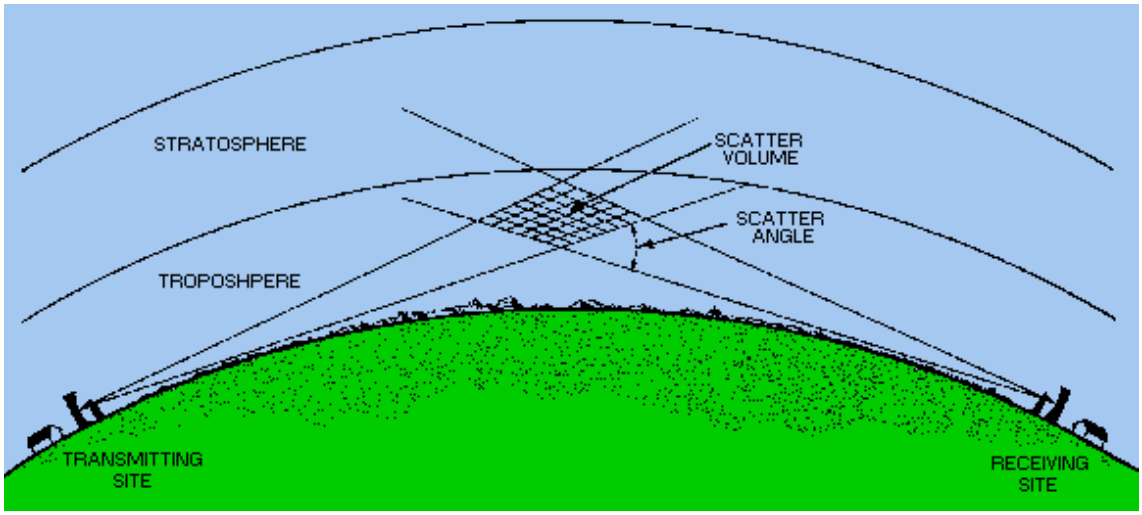

Figure 2.10: Tropospheric scattering propagation

The magnitude of the received signal caused by troposcatter depends on both the scatter volume and scatter angle as shown in Figure 2.10. The scattering volume, typically a few km above the ground level is able to provide a tropospheric scatter link of 70 to 700km. Low scattering angle will aid in preventing more radio signal losses and troposcatter mechanism is quite reliable especially on short distance and during summer or high pressure [Griffiths, 1987].

White [1992] and Picquenard [1974] mention two types of troposcatter mechanisms: Forward scatter is inherently multi-path and subject to fading as atmospheric irregularity and other tropospheric structure form, change and disperse. The fading characteristic is dependent on both tropospheric activities and the size of the scatter volume relative to the wavelength. Different band of wavelength (e.g. VHF and UHF band) will have its own distinct working range, depth and time scale of fading. Back

scatter on the other hand is a less useful mode of propagation but is desirable when the direct path is obstructed by large objects.

Hall *et al* [1996] provided a very good discussion on hydrometeor effects that included the scattering theory and attenuation effect from rain, cloud, ice and hail. These authors showed that the effects of rain, cloud etc. are only significant when the frequency is above 10GHz. Al'pert [1963] and Hall [1979] provided very detailed tables, graphs and experimental calculation to support this theory.

2.8 Concluding remarks

Propagation beyond the horizon (sometimes known as Trans-horizon propagation) is commonly caused by three kinds of mechanism at frequencies of more than 30 MHz; diffraction by the earth surfaces (e.g. sea), scattering due to atmospheric irregularities and ducting [Hall *et al*, 1996].

Beyond the horizon, diffraction can be used to establish communication at short distances. But as the propagating distance increases, the path loss increases rapidly and beyond a certain distance, scattering due to tropospheric irregularities (e.g. temperature inversion) are much more important than diffraction. This is due to the signal fading of scattering being relatively slow as the distance increases compared to high signal fading due to diffraction.

When the propagating signal strength is measured at some point beyond the horizon, the received signal is a combination of several signals of different amplitude and phases. At times, a signal level close to LOS can be achieved but more frequently, a slower, deep fading signal is achieved due to a combination of a few strong signals caused by multipath propagation. When multipath propagation exists, caused by whatever phenomenon, the actual received signal level is a vector sum of the signals incident from any direction or angle of arrival. Some signals will add to the direct path, while other signals will subtract (or tend to vector cancellation) from the direct signal path.

The curvature or deviation of a ray path depends on two conditions. The angle of incidence and the rate of change of refractive index N with height denoted as lapse rate

or *dN/dh*, where the refractivity *N* depends on the atmospheric condition such as temperature, pressure and moisture content [Reed and Russell, 1966]. Bean and Dutton [1966] give a very good discussion on equation (2.12) and the radio meteorology of refractive index.

In the troposphere, during normal conditions, pressure, temperature and water vapour content all decrease with height above the Earth's surface. In contrast, during temperature inversion, the temperature increases with height. Four types of inversion were mentioned and the inversions that of interest are subsidence and advection. In general, the refractive index does not vary linearly with height. In certain conditions as specified above, an inversion layer is formed within which, the refractive index increases rather than decreases with height. These phenomena occur frequently over the sea and due to the rapid decrease of humidity with height, an inversion layer is generally formed at the surface of the sea.

Ducting effect was first recorded during World War II in Egypt [Picquenard, 1974]. Instead of the wave propagating between the temperature inversion and the ground, the radio wave is trapped between two atmospheric layers thus creating a duct. Ducting constitutes a mechanism for interference between Earth stations and terrestrial line-of-sight systems. The surface duct ground base is the earth surface while a ground base of elevated duct is above the earth surface. The evaporation duct is a very common phenomenon over the sea affecting propagation frequencies above 2 GHz at a maximum height of 40 metres. Propagation along a duct leads to a very much smaller decrease in the field strength beyond the horizon. Ducting is more likely to occur with smaller wavelength (VHF/UHF) rather than longer wavelengths. This is because for layers of great thickness to behave as a duct, the gradient of the inversion needs to be very steep.

Chapter 3: Bibliographical survey on over sea VHF/UHF propagation

3.1 Probability of fading and path losses over sea and land

Castel [1965] (see Figure 3.1) showed that at microwave frequencies, the probability of fading increases dramatically over the sea/coast than over land as the propagation path length increases. The results from Figure 3.1 show that fading within the line-of-sight range occurs more in coastal and over the sea than over the land. In this case, the frequency used was 400 MHz and the antenna height for both transmitter and receiver was fixed at 10 metres.

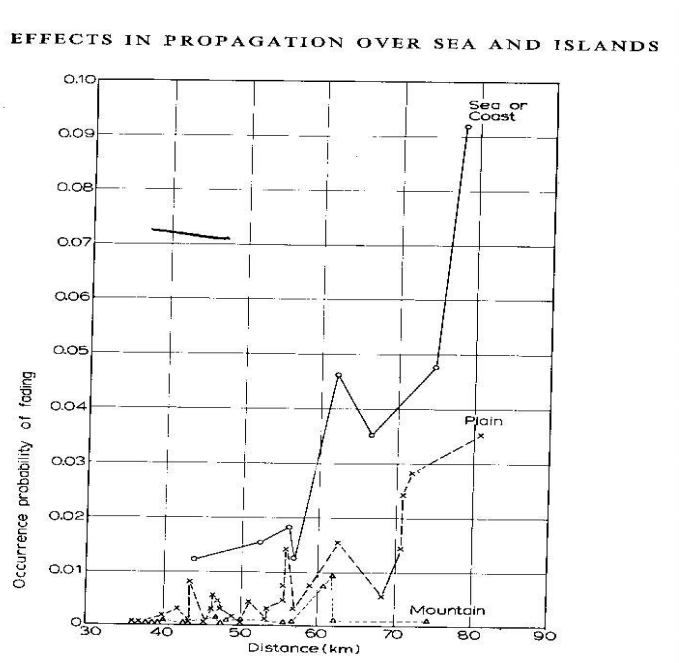

Figure 3.1: Occurrence probability of fading versus distance for various path conditions [after Castel , 1965]

Figure 2.4 shows that the surface refractivity values across the English Channel were higher over the sea than over the land [Hall *et al*, 1996]. Although the refractive index gradient (ΔN) is higher over the ocean, it is dependent on the distances from the coastline in the area where the sea and the land interact with each other, Castel [1965].

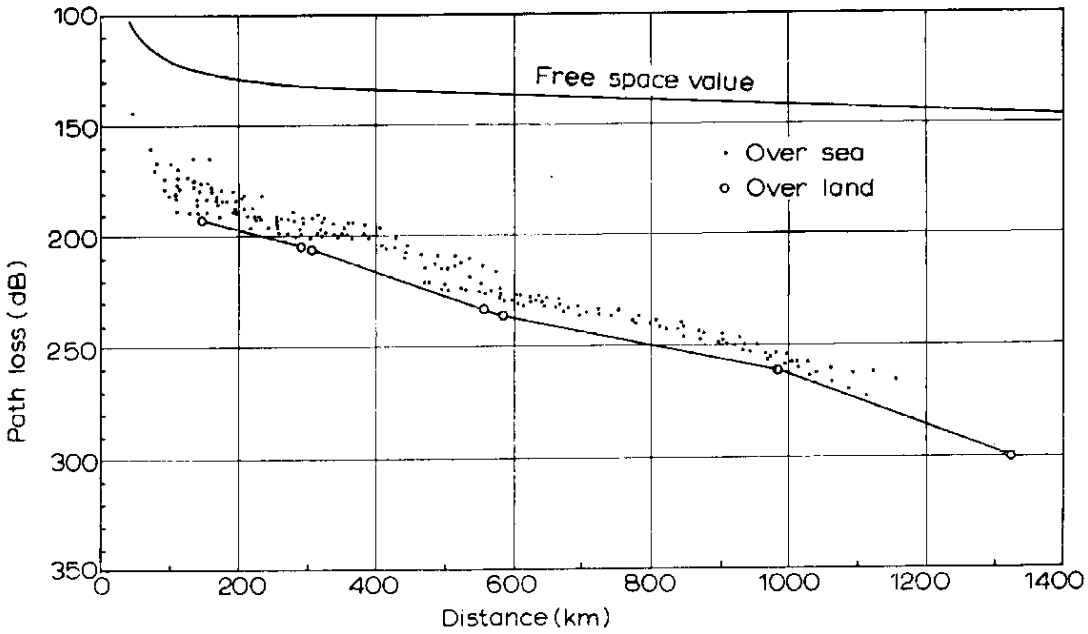

Figure 3.2: Comparison of over-water and over-land path losses versus distance (f = 400 MHz) [after Castel, 1965]

Figure 3.2 shows the differences in path loss between propagation path over the sea and over land. The results show that the path loss over the sea is around 10 dB less than over the land when transmitting at 400 MHz. Higher refractive index over the sea than land is also understood to be contributing to these results. Lower transmission losses could also be due to temperature inversion that occurs over the ocean.

3.2 VHF/UHF tropospheric propagation beyond the radio horizon over the sea

Since the amount of quantitative information available concerning tropospheric propagation over seawater is small, more research is needed to establish especially propagation beyond the horizon at VHF/UHF under different diurnal, seasonal, weather and sea states condition (Griffiths *et al* [1997], Castel [1965]). Ames *et al* [1955] established a 220MHz, point to point over the sea propagation at a distance of 200 miles (322 km) experiment. Results were obtained during winter and summer and it is as shown in Figure 3.3.

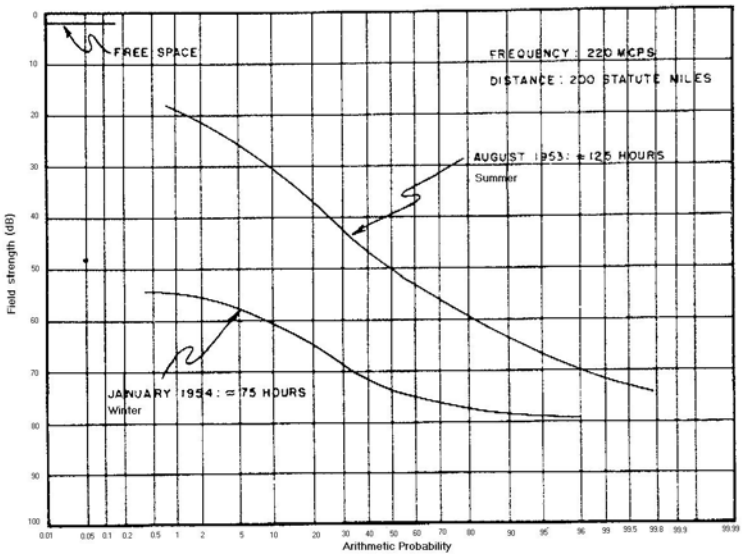

Figure 3.3: Field strength distributions for 200 miles (322 km) over water path during winter and summer at 220 MHz frequency [after Ames *et al*,1955]

Figure 3.3 shows that the path loss during the summer is less than during the winter. Further experiment had shown that the median loss over the water is still lower than over the land values. Higher signal levels were also observed during the summer whereby they approach close to free space value at certain short percentage of time.

For VHF/UHF at a distance beyond the horizon, enhanced signal levels might be received over a small percentage of time due to certain anomalous tropospheric mechanisms such as ducting. A simultaneous prolonged measurement that was done over the North Sea at 5 different receiving sites at 560 MHz and 774 MHz showed that the ratio of field strength exceeded for a specified time percentage is slightly higher at higher frequency (Bell [1968], Stark [1965]). Assumptions are made that the 50% field strengths are predominantly due to scattering in turbulent conditions whereas the propagation mechanism for small time percentages is refraction or specular reflection. It was also observed that seasonal variations are more pronounced over sea paths especially during the summer when the probability of occurrence of anomalous propagation reaches its maximum.

Table 3.1 shows the range of various of fading between various percentage times for two frequencies at each of the receiving sites. This table reveals that the range of fading between various time percentages increases with distance. It also confirms that the

transition to anomalous propagation for UHF signals occurs for the field strength values between 1% and 10% of the total time [Stark, 1965].

Table 3.1: Range of fading between various time-percentage [after Stark, 1965]

Receiving Site	Distance	Range of fading (dB) between various time-percentages					
		0.1 – 1.0%		1.0 – 10%		10 – 50%	
	km	560Mc/s	774Mc/s	560Mc/s	774Mc/s	560Mc/s	774Mc/s
Happisburgh	198	14.0	12.5	37.5	41.5	21.0	19.0
Flamborough Head	365	20.0	16.0	38.0	43.0	17.5	21.0
Newton-by-the-sea	543	20.5	28.5	42.5	40.0	-	-
Bridge of Don	690	26.5	23.0	-	-	-	-
Lerwick	950	26.5	26.5	-	-	-	-

Gough [1979] concluded that at average atmospheric conditions, if the diffracted signal is 50 dB below the free space level, tropospheric scattering becomes dominant as the distance increases. For refractivity lapse rate between -40 to -100 *N*/km, tropospheric scattering dominates diffraction at all ranges. Lapse rate that is less than -150 *N*/km will experience higher diffraction signals (such as ducting) that always dominates scatter at short to medium ranges. This can be seen from Figure 3.4 whereby both -40 and -100 *N*/km percentage incidents were left unchanged for a range up to 1500 km over the North Sea. Further results show that the standard lapse rate of -40 *N*/km remains at around 50% of the total percentage of time [Gough, 1979].

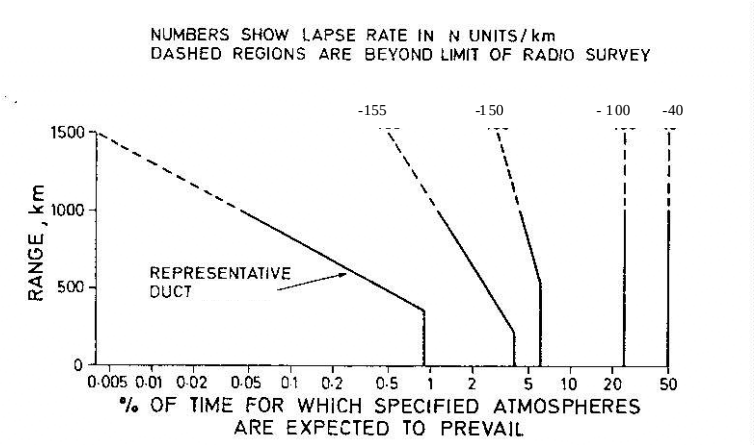

Figure 3.4: Model for incidence of North Sea atmospheric structures [after Gough, 1979]

Wickers and Nilsson [1973] characterised the signal into three different types:

Type A: Low mean signal level with rapid superimposed fading.

Type B: Higher mean level than type A. Signal fading is less rapid than type A mainly caused by reflection

Type C: Stable and high signal level which sometimes has deep fading minima of short duration.

Long term over the sea statistics (160 km path): Wickers and Nilsson [1973] concluded that during winter, scattering is more dominant than other propagation mechanisms (e.g. diffraction) at the higher frequencies (5 GHz) than the lower frequency (170 MHz) as shown in Figure 3.5 and Figure 3.6. In contrast, reflection is more dominant at lower frequency than higher frequency. Further prolonged over the sea propagation experimental results at 170 MHz shown in Figure 3.5 revealed that high signal levels occur more than 90% of the total time in summer and more than 50% in winter. This is mainly due to low level ducts that occur more frequently during the summer (70%) in comparison with the winter period (10%). It was also revealed that the total time that high signal level caused by either ducting or reflection during the summer decreases as the frequency increases.

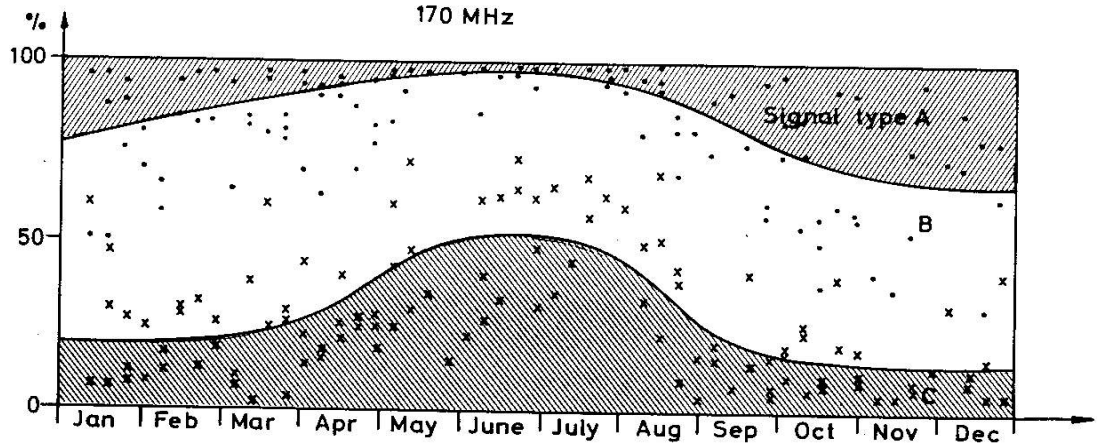

Figure 3.5: Annual occurrence of over the sea propagation signal type at 170MHz [after Wickers and Nilsson, 1973]

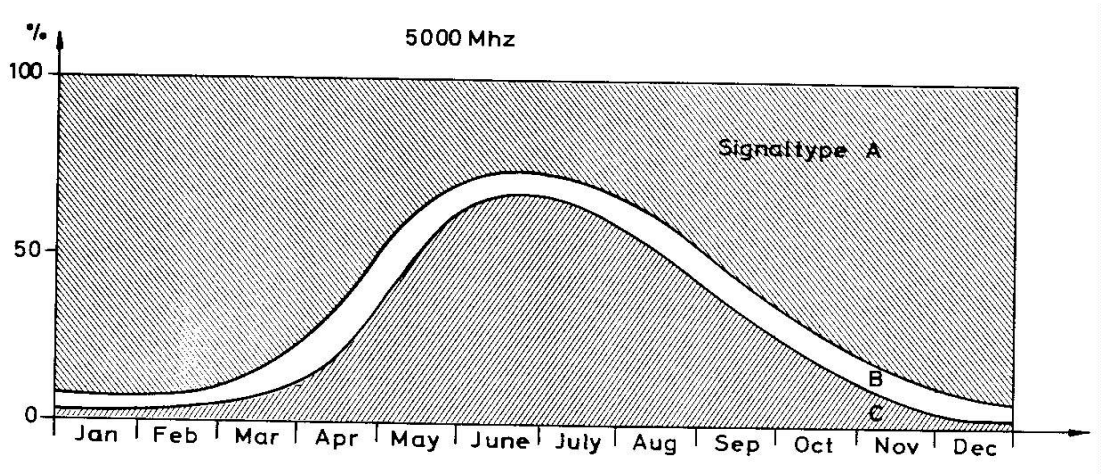

Figure 3.6: Annual occurrence of over the sea propagation signal type at 5GHz [after Wickers and Nilsson, 1973]

3.3 VHF/UHF radio wave propagation measurement over sea surface at different paths and sea states

Algor [1972] investigated propagation losses over sea paths up to 40 nautical miles (74km) during one-month period in September 1970. Three frequencies were used: 30, 140 and 412 MHz. The receiving site was an existing shore based radar station and the transmitter was a “mobile” 9-ft surfboard subjected to sea wave motion and variation. The antennas were vertically polarised and of particular interest is the 140 MHz receiving antenna as it is a log periodic type and similar to the cases employed in this thesis. The receiver elevation ranges from 50 to 100 ft.

Part of the objectives for this experiment is to determine the system parameter and analyse the signal levels and fading characteristic at various distances or frequencies. The effects from any other meteorological conditions are taken into consideration.

Figure 3.7 shows the normalised propagation signal strength against the various distances for all the three frequencies. It shows the usual decrease in signal strength as the distance increases.

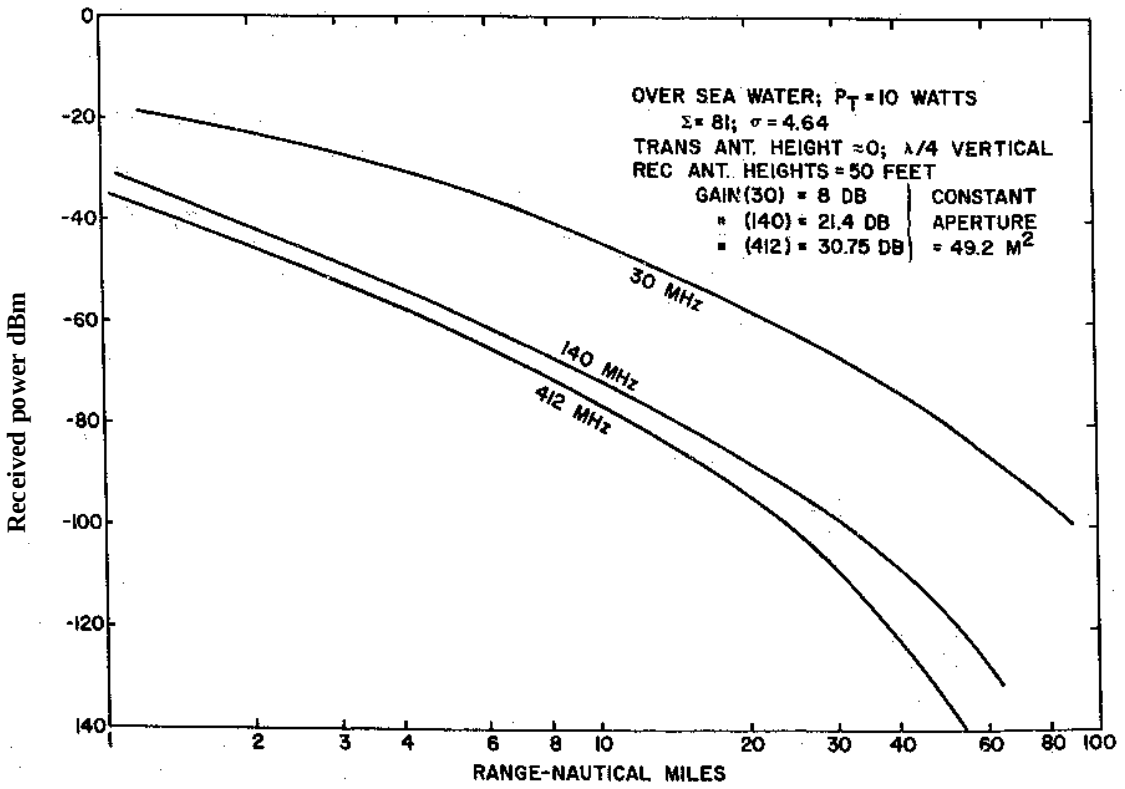

Figure 3.7: Normalised propagation signal strength against various distances [after Algor, 1972]

The following comments for signal fading characteristics were also suggested:

- Higher frequencies have greater fading range and faster fluctuation in level.
- Fading range is not a function of distance. The data obtained in this experiment show that signal level varies more at higher frequencies but for a fixed frequency, the variation of fading does not change accordingly with increase in distance.
- Fading range may increase with increased sea and wind states.
- Fading at one frequency is essentially uncorrelated with fading at other frequencies, with certain uncommon exceptions.
- Fading can be divided into two components, fast and slow which both may have different causes.

Algor [1972] observed a few results or phenomena during the experiment:
Dependence of much faster fading component at higher frequencies on wave action was less obvious as it might be due to the more random nature of the smaller waves. Only

occasional correlation of high fading components observed at all three frequencies at periods of 2 to 4 seconds corresponding to the large ocean waves.

Two sea conditions (calm and swell) were mentioned in this experiment. Figure 3.8 shows a calm sea state on 25 Nm (46.3 km) for both 140 and 30 MHz. Anomalous propagation was observed during this period for the 140 MHz as a “beat-frequency-like” appeared over several seconds. A possible cause was identified as interference by an aircraft flying across the propagation path. The same kind of signal fading was also observed at other times at 412 MHz.

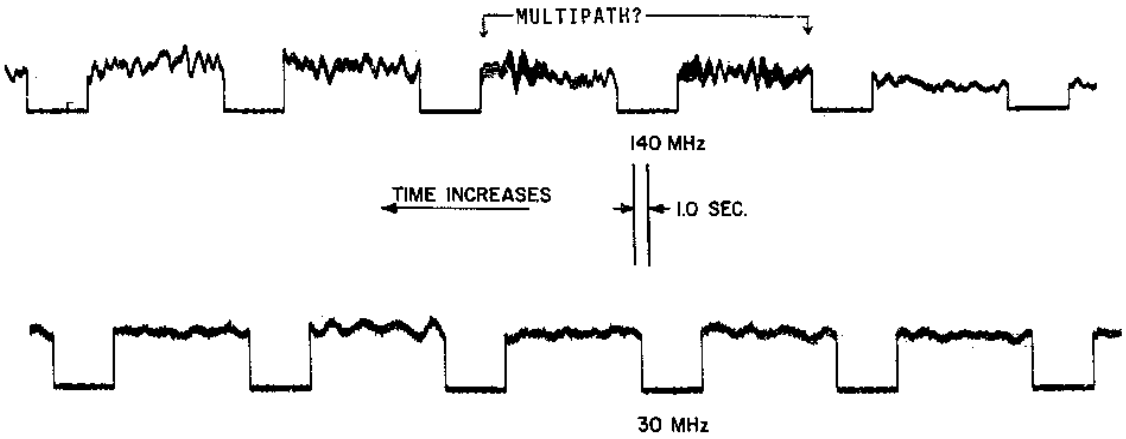

Figure 3.8: Calm sea states with anomalous propagation [after Algor, 1972]

Figure 3.9 demonstrated a condition when repetitive swelling about 2 feet in height was observed. Fast fading was observed at 140 MHz and became strongly periodic and this could be due to a well-defined, low amplitude chop of the sea wave.

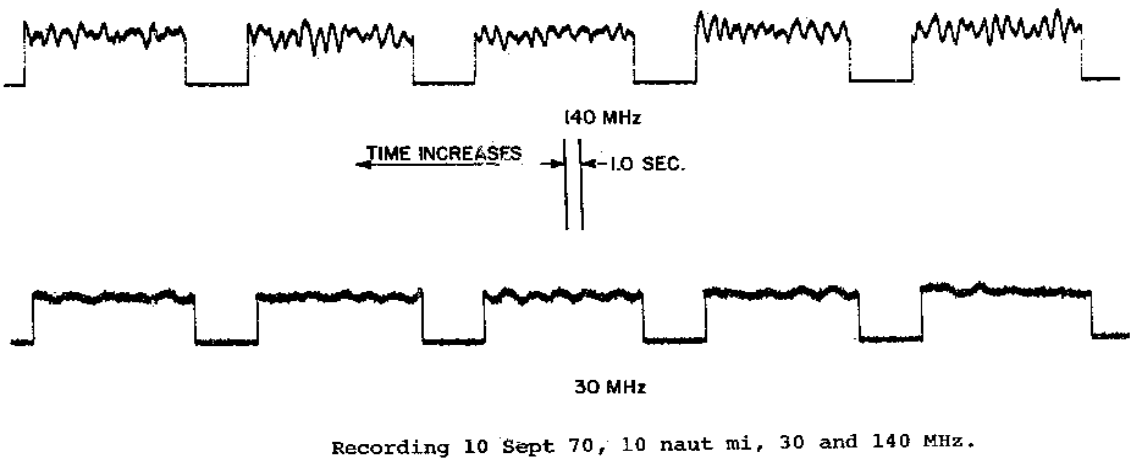

Figure 3.9: Rough sea states with swelling (2 feet in height) [after Algor, 1972]

An another observed phenomenon is shown in Figure 3.10 when signal drop out was due to washing over of the 412 MHz antenna by sea wave.

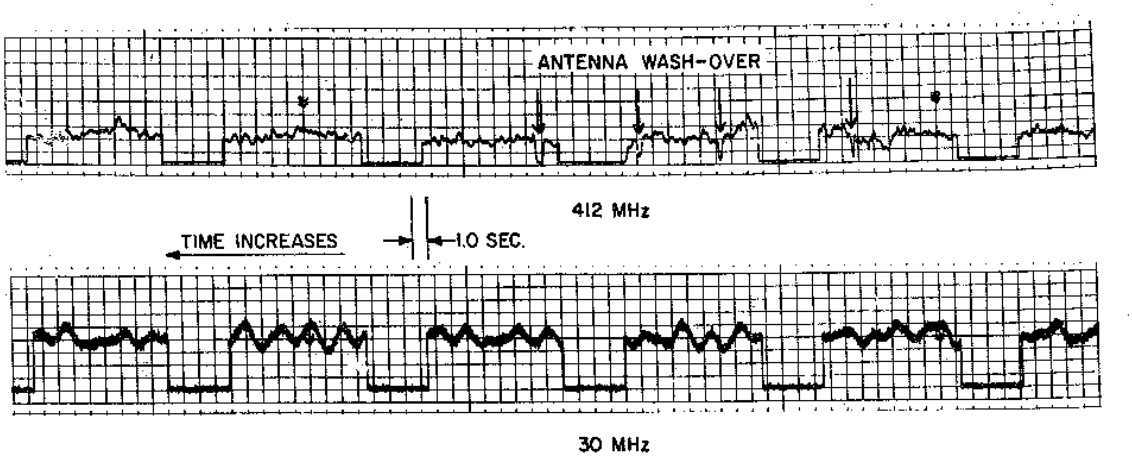

Figure 3.10: Signal “drop out” due to antenna over wash by sea wave [after Algor, 1972]

Griffiths et al [1997] conducted a similar experiment on two occasions in 1994, with the exception of investigating the signal variation as a function of different sea states from 2 to 5 and ranges up to 30 Nm (55.56 km). The main objective of this experiment was to derive a realistic model for the radio link over the sea surface and to determine the required transmitted power to guarantee a 20 dB of signal to noise ratio at a range of 20 Nm (37 km). The frequency band in this experiment ranges from 136 to 173.5 MHz with two bandwidths of 180 and 300 kHz.

Cumulative results from sampled signal strength showed a variability not exceeding 4.5dB for 90% of the time. Equation 3.01 was applied to the signal strength received during the experiment.

$$P_r(dBm) = 10\log_{10} C - \text{n}.\log_{10} r + 30 \qquad (3.01)$$

where C is the propagation constant and r the range of the floating transmitter.

The above equation goes well with the data showing a strong relationship between the different sea states and signal spectrum width as shown in Table 3.2 provided by Griffiths *et al* [1997]. The results concluded that the signal strength for non line-of-sight

VHF propagation over the sea surface varies with range approximately $1/r^4$, independently of sea states. Griffiths *et al* [1997] further suggested a 3W transmitting power would ensure a reliable detection at a maximum range of 20 Nm (37 km).

Table 3.2: Non line-of-sight over the sea propagation parameters for different sea states [after Griffiths *et al*, 1997]

	Frequency	C/r^n	Constant (signal strength)	Correlation fix	Max. Range
Sea States 3					
Receiver 1	167.500 MHz	n = 4.12	-38.4 dBm	0.9920	41.30 km
Receiver 2	165.625 MHz	n = 4.28	-38.4 dBm	0.9977	26.69 km
Receiver 3	158.500 MHz	n = 4.09	-38.4 dBm	0.9983	37.43 km
Sea States 3/4					
Receiver 1	167.500 MHz	n = 4.32	-39.6 dBm	0.9990	31.50 km
Receiver 2	165.625 MHz	n = 4.35	-44.6 dBm	0.9990	24.83 km
Receiver 3	160.375 MHz	n = 4.22	-39.1 dBm	0.9982	34.47 km
Sea States 4/5					
Receiver 1	162.625 MHz	n = 4.07	-43.9 dBm	0.9834	31.13 km
Receiver 2	162.625 MHz	n = 4.11	-45.9 dBm	0.9813	27.24 km
Receiver 3	162.625 MHz	n = 4.08	-43.8 dBm	0.9827	31.32 km

3.4 The effect of sea state on propagation loss above the ocean

Barrick [1971] derived a method of analysing radiation and signal propagation above a sea surface by employing an effective surface impedance method to describe the effect caused by different sea states. The main area of concern in the experiment was the estimated effect on both HF and VHF ground wave propagation on perfectly smooth and rough sea surface.

Figure 3.11 shows the basic transmission loss across the ocean with increasing frequency and range. Figure 3.12 shows the added transmission losses due to various sea states and range at 50 MHz. From both figures, Barrick [1971] concluded that the transmission loss is higher during rougher sea states, higher frequencies and longer ranges.

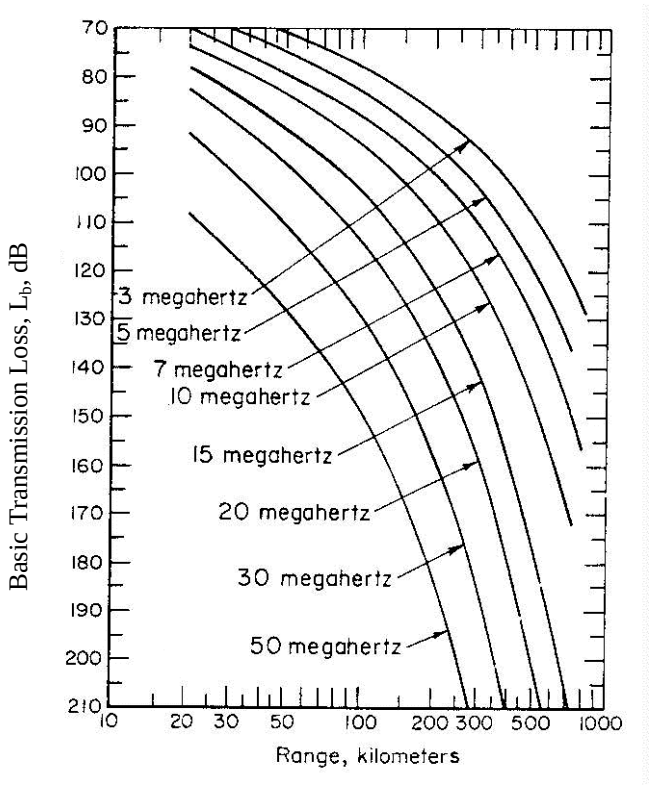

Figure 3.11:Basic transmission loss across the ocean between points at the surface of smooth spherical earth. Conductivity is 4mhos/m and an effective earth radius factor of 4/3 is assumed [after Barrick, 1971]

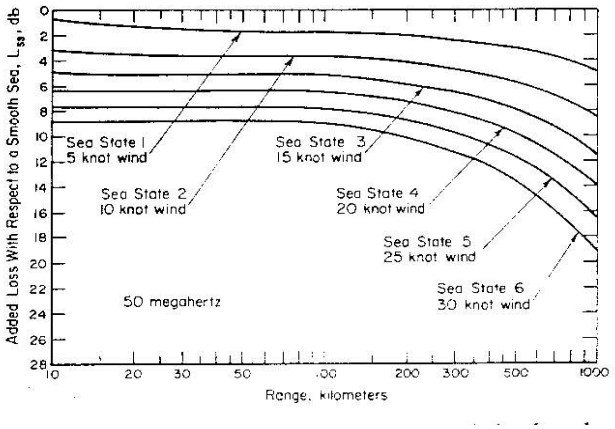

Figure 3.12: Added transmission losses due to sea state at 50 MHz [after Barrick, 1971]

3.5 Reflection from a sea surface

If the reflected surface is not smooth, scattering of the wave will occur at the surface and power is retransmitted in all directions. For a surface with random roughness (e.g. seawater), the maximum in power reflection will be in the direction of specular reflection**.** A surface may be regarded, as rough if the variations of the surface are such

as to cause variations in the path length of more than an eighth of a wavelength [Matthew, 1965]

For oblique incidence over seawater as shown in Figure 3.13, at angle ψ above the surface of the sea level, $2H \sin \psi < \lambda/8$ can be expressed in degrees as

$$H\,\psi < 3.6\lambda \qquad (3.02)$$

where,

ψ – angle of incidence

H – height of the sea wave (m)

λ – frequency wavelength (m)

The surface of the sea will be considered smooth if it satisfies equation 3.02.

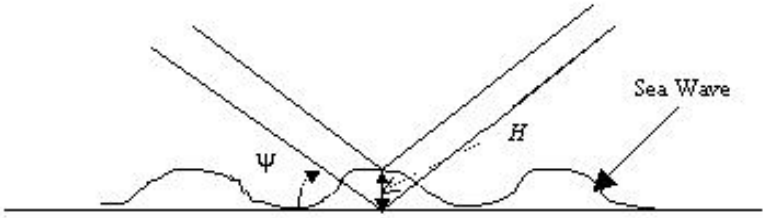

Figure 3.13: Reflection from a rough sea surface [after Matthew, 1965]

For the example shown in Figure.3.14, the transmitter above the ship is 20 metres in height, and at a distance of 20 km, the angle of incidence ψ is $\tan^{-1}$ (20/20000)= 0.0573°. If the transmitting frequency is 3 GHz, λ is 0.1metre. Assuming the wave height H across the English Channel is at an average of 2 metres, then:

$H\psi = 2 \times 0.0573 = 0.1146$

$3.6\,\lambda = 3.6 \times 0.1 = 0.36$

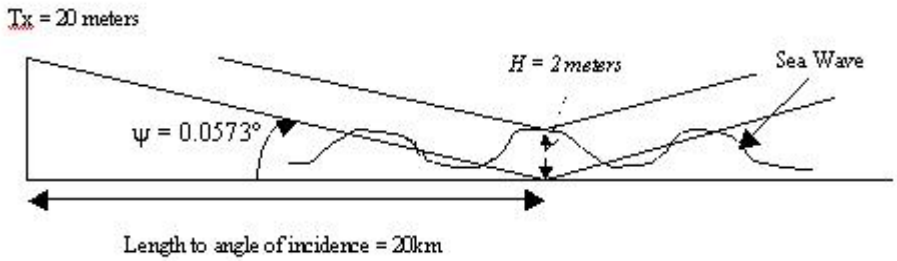

Figure 3.14: Example of a rough sea surface with angle of incidence

Hence, equation 3.02 was satisfied and the above sea condition can be considered as smooth. If ψ is more than 0.18°, the sea condition will then be considered as rough.

3.6 Sea surface roughness and spectrum

The Rayleigh roughness parameter γ expresses the difference in phase between two rays with grazing angle θ reflecting from parts of the surface each separated by the wave rms height deviation *h* and is given by:

$$\gamma = 2k_{wave}H\sin\Psi \qquad (3.03)$$

where,

k_{wave} - wave number of incidence wave

Ψ- *angle of incidence (or* grazing angle)

H = height of sea wave (rms height deviation in metre)

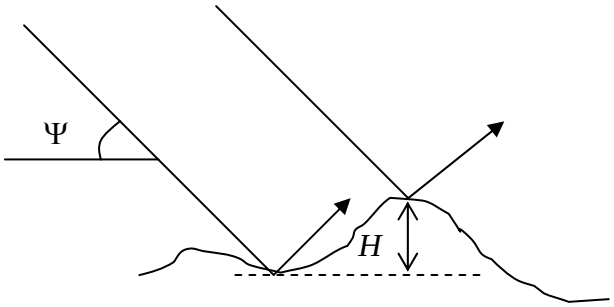

Figure 3.15: Rayleigh roughness parameter [after Levy, 2000]

From Figure 3.15, even if γ is small, the surface can be considered as smooth since the reflected ray is approximately in phase. If γ increase, the surface is considered as rough and due to the decrease in intensity of the specular reflection, the propagating ray is scattered in various directions.

Table 3.3 gives the semi-isotropic Phillips spectrum that was proposed to fully developed sea for a given sea state and wind speed and is given by:

$$h = 0.0051U^2 \qquad (3.04)$$

where h is the rms wave height in metre and U is the wind speed.

Table 3.3: Sea states, wind speed and rms wave height [after Levy, 2000]

Sea States	Wind Speed (U)	rms wave height (h)
2	10 knots (5.14 m/s)	0.135 m
3	15 knots (7.72 m/s)	0.304 m
4	20 knots (10.29 m/s)	0.540 m
5	25 knots (12.86 m/s)	0.843 m

Tables 3.3 above provided an ideal basis on how various sea states affect the wave height that might be applicable to this experiment.

3.7 Evaporation duct propagation

An evaporation duct is perceived as a shallow simple surface duct, which occurs over the sea almost all of the time. It occurs when the moisture above the sea decreases rapidly at levels several metres above the sea level. The decrease in vapour pressure above the sea results in a decrease of M (modified refractivity) and hence a trapping layer is formed adjacent to the sea level, Paulus [1985], Hitney *et al* [1985].

The evaporation duct height can be calculated by obtaining measurement of wind speed, air/sea temperature and relative humidity. These formulae can be found in Rotheram [1974]. Paulus [1985] also observed that the air-sea temperature differences play an important role in calculating the unrealistically high evaporation duct height, and the relative humidity above the sea is the most important factor that the duct height is dependent on. Typical calculated evaporation duct heights vary from 10 to 40 metres (maximum).

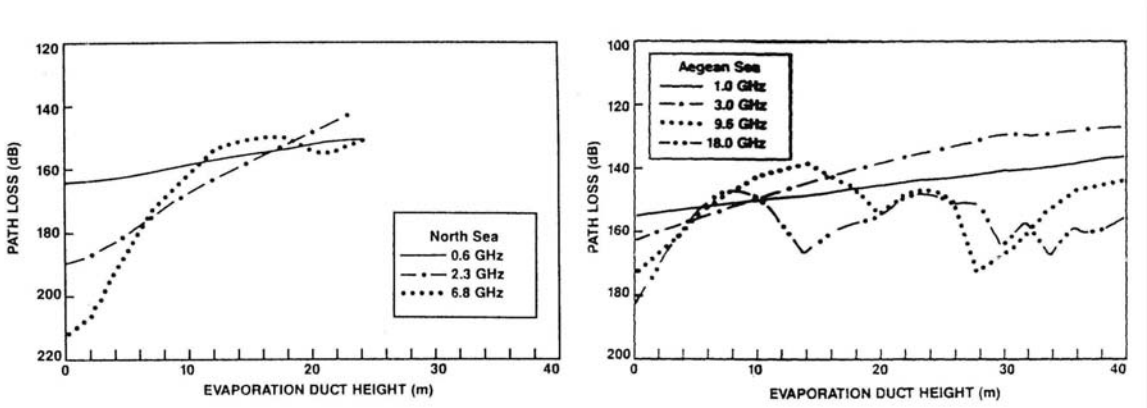

Figure 3.16: Path loss vs evaporation duct height across the North and Aegean Sea [after Hitney and Vieth, 1990]

A series of path loss versus duct height measurement were conducted in both the North Sea and Aegean Sea by Hitney and Vieth [1990]. Both the transmitter and receiver antenna heights were located at 4.5 and 19.2 metres above the mean sea level respectively and the path was 35.2-km entirely over sea water. The experimental results from 0.6 to 18 GHz are shown in Figure 3.16. From the figure, the path loss is monotonically decreasing over the entire duct height at lower frequency. At much higher frequency (9.6 and 18 GHz), the path loss increases and decreases alternatively with duct height. This behaviour is due to multiple waveguide mode interference, which is absent at lower frequencies due to the duct supporting only one waveguide mode.

The above-mentioned experiment concluded that the evaporation duct is the dominant one in over-the-horizon propagation mechanism at frequencies above 2 GHz. Lower frequencies (below 500 MHz) are less sensitive to evaporation duct since such ducting becomes progressively invisible. But other propagation mechanisms such as surface duct, super-refractive effects and scattering are the dominant effects.

By using theoretical methods, Rotheram [1974] gives a very detailed description of radiowave propagation and beyond the horizon propagation in the evaporation duct. Effects of the rough sea are taken into consideration so as to minimise the discrepancies between the theoretical and experimental results.

3.8 Summary

During abnormal conditions over the sea, VHF/UHF signals are able to travel at a distance much further than the normal distance. This anomalous propagation occurs more on over sea paths than on overland paths due to phenomena such as temperature inversion.

Ames et al [1955] concluded that the path loss over the water is still lower than over the land and the same happens during summer and winter periods. These results were further confirmed by Castel [1965] who showed that the probability of severe fading across the sea is much higher than across the land. On the other hand, statistical results provided by Barrick [1973] and similar sets of experiments conducted by both Algor [1972] and Griffiths [1997], showed that higher frequency, sea roughness, sea states and longer transmitting range will contribute to more transmission loss along the sea path. Anomalous propagation observed by Algor [1972] also showed how a plane flying across the propagating path, and antenna over washed by sea waves affects the propagating signal. A realistic equation modelled by Graffiths *et al* [1997] showed corresponding results with the experimental data and suggested that a 3 watts transmitter power would certainly provide a good reception at 20 nautical miles maximum (37 km).

Prolonged over the sea propagation experimental results by Wickers and Nilsson [1973] showed that at 170 MHz, high signal level occurred more than 90% of the total time in summer and more than 50% in winter. These high signal levels are mainly contributed by ducting that occurs more frequently during the summer (70% of total time) in comparison with less than 10% in total time during winter periods. Besides seasonal variation, Stark [1965] concluded that there was a tendency for higher signal levels to occur in the late afternoon and early evening for over the sea paths due to temperature inversion. Further investigation in the North Sea with different sites showed that, the range of fading between time-percentage increases with distance. The results also show that the range of fading between 1% to 10% is very much greater than other time percentages such as 0.1% to 1% and 10% to 50%. Further results concluded that the transition to the abnormal type of propagation at UHF occurred between 1% and 10% of the total time.

For propagation mechanism such as troposcatter, it is the controlling factor at lower lapse rate (e.g. -40 *N*/km). But for lapse rate that is lower than -157 *N*/km, troposcatter propagation can be ignored. This is due to the dominant diffraction mode at higher lapse rates that extend the radio horizon by super-refraction or tropospheric ducting as discussed in Chapter 2. Radio measurement results obtained from Gough [1979] concluded that at a range much shorter than 200 km over the sea, the lapse rate of real atmospheres have unchanging percentage incidence at all shorter ranges.

As for ducting effects, over-the-horizon propagation measurement from 0.6 to 18 GHz was done by Hitney and Vieth [1990]. The experiment concluded that the evaporation duct could substantially increase beyond-the-horizon radio signal above diffraction level for frequencies that are above 2 GHz. The result show that evaporation duct is dominant at 2 GHz and above while surface duct and super-refractive effects are the more important propagation mechanism at lower frequencies.

With respect to sea surface effects on propagation, Matthew [1965] suggested that a smooth surface would only be considered if the variations of the surface are such as to cause variations in the path length of less than an eighth of a wavelength. On the other hand, Rayleigh roughness parameter discussed by Levy [2000] suggested that even if γ is small, the surface can be considered as smooth if the reflected ray is approximately in phase. In addition, the Phillip spectrum equation provided a basic insight on how various sea states affect the wave height.

Chapter 4: Design of the experiment

The initial aim of this experiment is to investigate VHF/UHF propagation characteristic between two ships. Due to a lack of available ships and the prohibitive expense, the experiment was undertaken between three of the Channel Islands as shown in Figure 4.1. Propagation characteristic such as the effect of signal level and fading characteristics, seasonal and diurnal effects such as temperature inversion, and capability of the propagation are the main concern in this experiment. Propagation mechanisms such as line-of-sight, reflection, diffraction, surface wave, ducting and tropospheric scattering while propagating over the sea surface are to be analysed and simulated if possible.

The map in Figure 4.1 shows the location of the transmitter in Jersey and both receivers at Guernsey and Alderney. Both paths (Jersey-Guernsey) and (Jersey-Alderney) are unobstructed. This enables the signal to be measured without the heavy expenses of prolonged ship-borne trials. Figure 4.2 shows the location of the transmitting site in Ronez quarry on the north coast of Jersey. Figure 4.3 and 4.4 shown the location of both receiving site at St. Peter Port Light House (Guernsey) and Isl de Raz (Alderney).

Since the experiment is simulating ship communication, the assumption is made that the ship height is around 15 metres above mean sea level. Figure 4.5 shows the basic design of antenna height for the transmitting site at Jersey that is 15 metres above mean sea level (around 10 or 20 metres during high and low tide respectively). This corresponds to the lowest, average and highest tide in Sark (0.5m, 5m and 10m respectively). The antenna height for both receivers at Guernsey and Alderney are also around 15 metres above the mean sea level.

From Figure 4.5, two poles of 6 metres height are required to support two antennas (either horizontal or vertical). These poles are mounted next to the transmitting system and the GPS antenna is mounted on top of one of the poles. The antenna position for both receivers are much simples with only two antennas (both vertical and horizontal) pointing at the transmitter site.

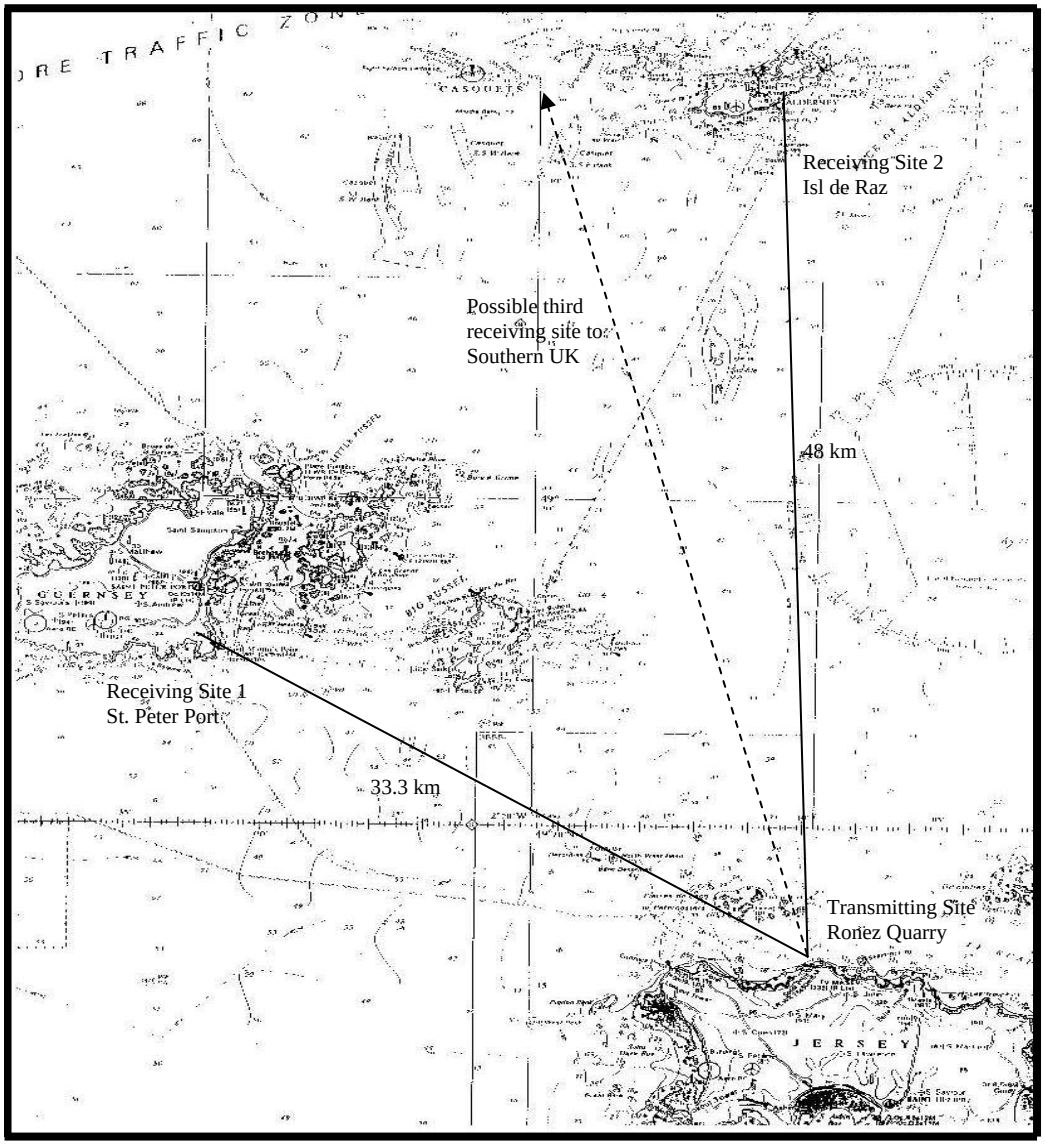

Figure 4.1: Transmitter and receiver sites in the Channel Island

Figure 4.2: Transmitting Site- Ronez Quarry (Jersey)

Figure 4.3: Receiving Site (1)- St. Peter Port Light House (Guernsey)

Figure 4.4: Receiving Site (2)- Isl de Raz (Alderney)

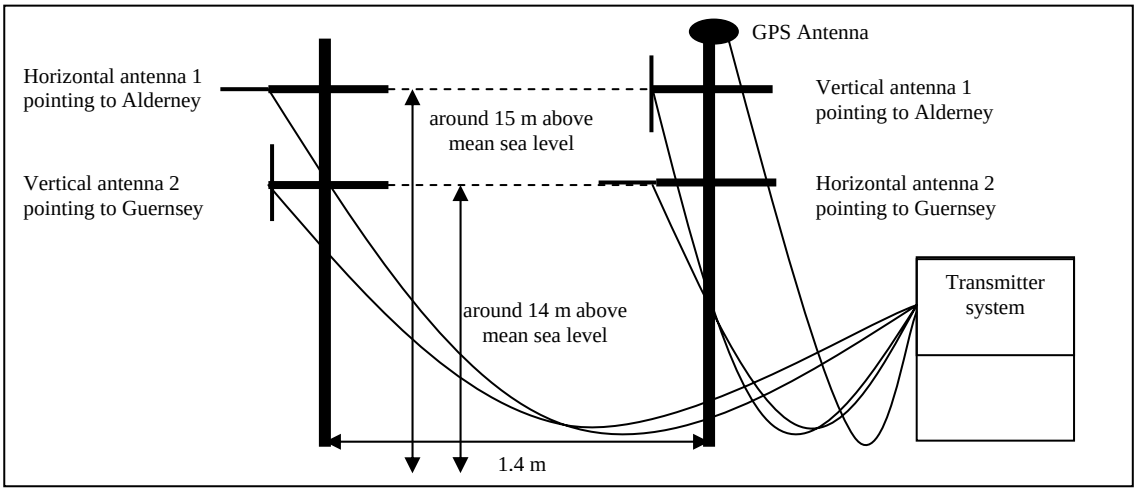

Figure 4.5: Antenna design for transmitter at Ronez Quarry (Jersey) pointing at both receiving sites

4.1 Design of the transmitter and the receiver system

4.1.1 Design of the transmission system

The basic design of the transmission system is as shown in Figure 4.6. From Figure 4.6, the transmission system is a combination of several vital circuits / equipment. The signal from the signal generator (IFR 2023B) is output into the transmission amplifier

set as shown in Figure 4.7. The amplifier (720FL) is able to provide a maximum of 25watts of power to the antenna for transmission but can only support up to 1 GHz frequency. The transmitting signal from the amplifier set is sent to the log periodic antenna via the RF relay. These relays are controlled by the parallel port i/o converter (PPIO) that decides which antenna to transmit.

The PC running under QNX OS controls the whole transmission system including the signal format to be sent to the signal generator. From Figure 4.8, two analog signals are produced by each of the DAC channels from the DAC (PCI 234). One is the amplitude modulated signal and the latter is a phase frequency producing either 0° or 180° signal. These two signals are input into the signal generator that allows pulse modulation to generate the amplitude modulated. The aim of using a GPS card is to achieve an accurate time base for both transmission and reception. To achieve this synchronisation between the receiver and the transmitter, the qualified 1 pulse per second (Q1PPS) from the GPS card is fed into the GPS synchronisation card. The GPS synchronisation card will in turn send a trigger signal to the external clock of the DAC card at the next pulse from the GPS card.

The combination of both carrier on (amplitude modulation) and phase shift frequency (0°/180°) (phase modulation), and the desired output from the signal generator is as shown in Figure 4.9. Note that PSK barker sequence was not used in this experiment.

The completed transmission set is connected up in 2 wall sheds as shown in Figure 4.10. The use of wall shed is to protect the transmission equipment from the weather. Figure4.11 shows the completed transmission system in Ronez quarry (Jersey), with both sets of antennas (horizontal / vertical) pointing at St. Peter Port Light House (Guernsey) during the period from April 2001 until November 2001.

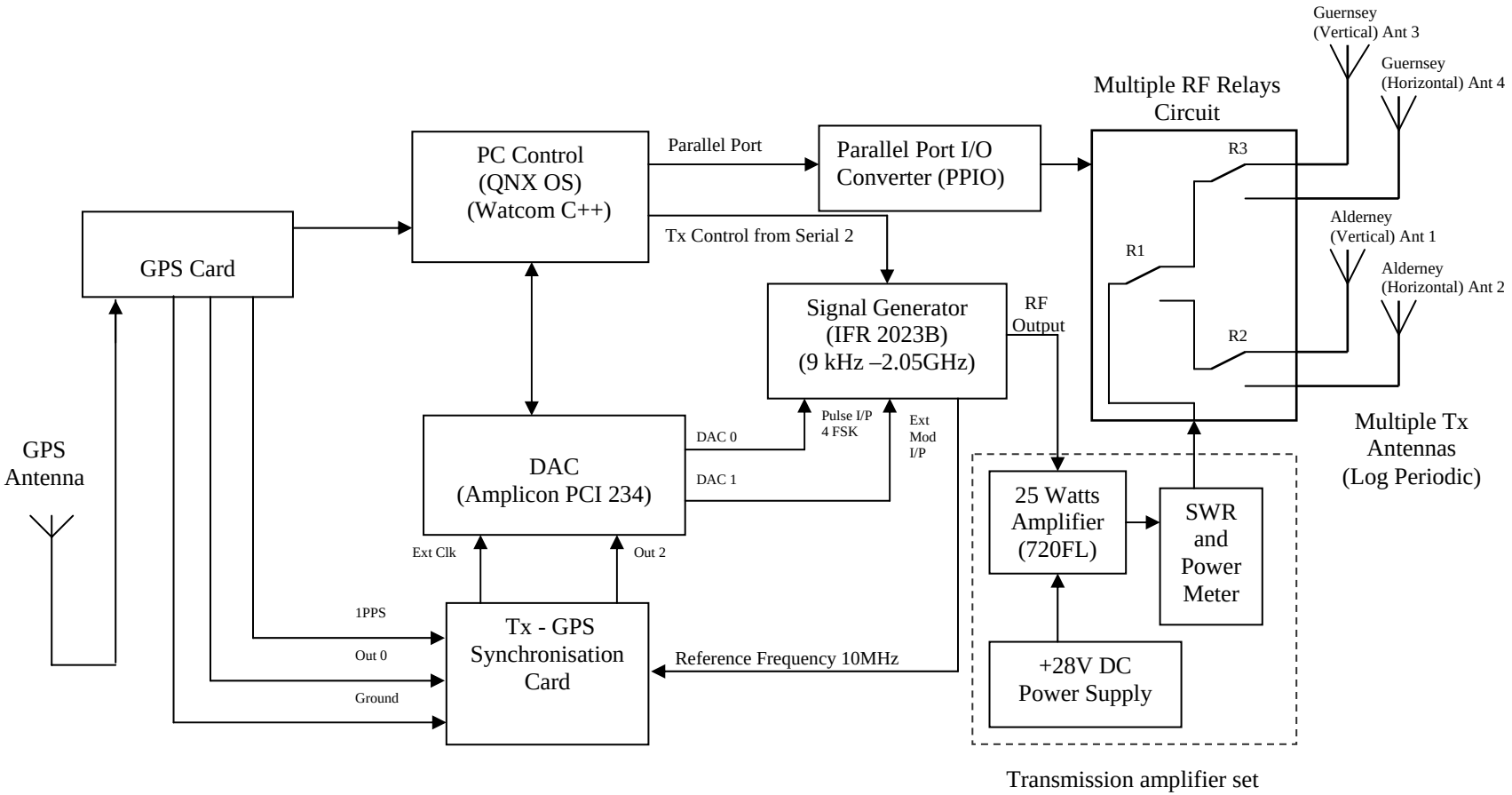

Figure 4.6: Over the sea propagation transmission system

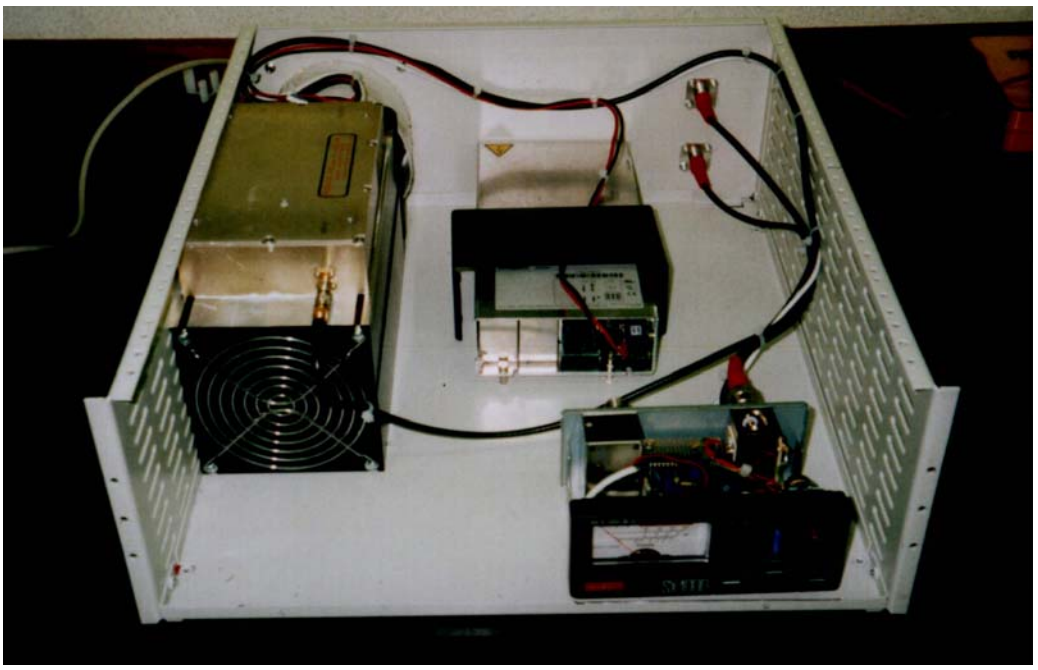

Figure 4.7: Transmission amplifier set

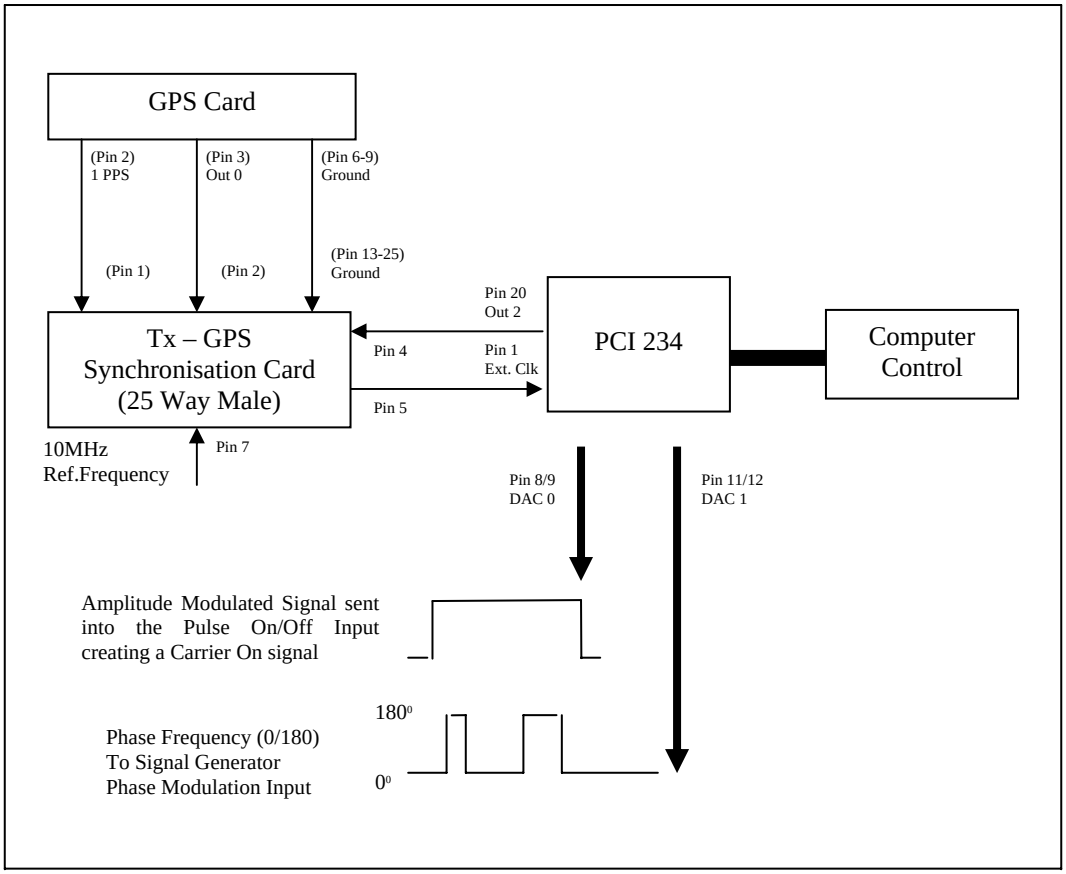

Figure 4.8: Block diagram of PCI 234 connection

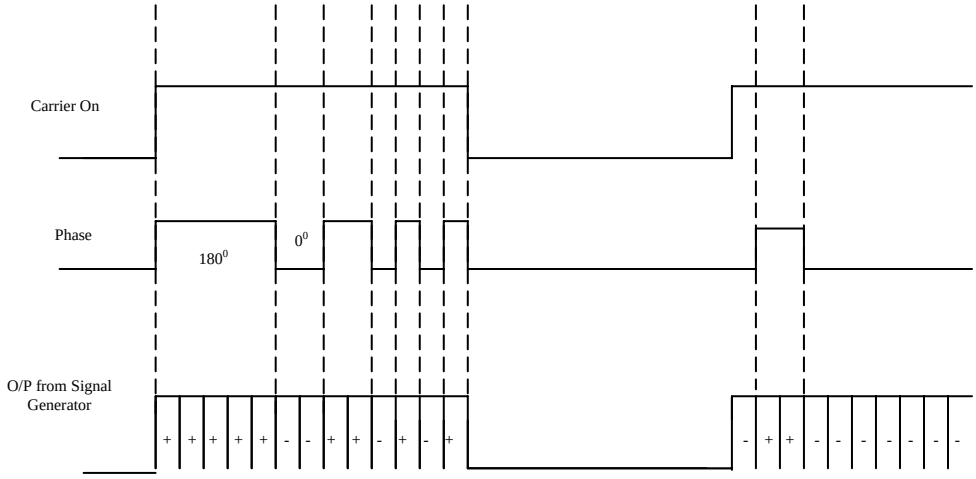

Figure 4.9: Graph of carrier on, phase and output of signal generator

Figure 4.10: Completed transmission set

Figure 4.11: Completed transmission system in Ronez Quarry (Jersey) pointing at Guernsey only

4.1.2 Design of the receiving system

The basic design of the receiving system is as shown in Figure 4.12. From Figure 4.12, the receiver employed in this experiment is AOR5000 with a frequency range of 10 kHz to 2600 MHz. Its extensive RS232 command list allows the user to issue various commands via the serial port from the PC control. In order to increase the frequency stability of the receiver, a 10MHz precision OCXO source is connected externally and at the same time clocking the ADC (PCI 260) via the external clock input.

From Figure 4.13, the received signal goes through a low pass filter (LPF) before being sampled by the ADC. This is due to the fact that the AOR5000 inherits a noise of around 50 kHz, which will integrate into the received signal. Since the bandwidth of the received signal is set at 25 kHz, the cut-off frequency of this LPF is set to 30 kHz. The design of the receiver GPS synchronisation card is similar to the transmitter type except that it provides its own 10 MHz references from an ultra precision ovened oscillator with a frequency tolerance of 0.005ppm.

Since the transmitting signal is at 25 kHz SSB, in order to avoid aliasing, the basic requirement for the ADC is to provide at least a conversion rate of 50 kHz. PCI 260 in this case provided a 300 kHz per channel conversion rate that satisfies the requirement

perfectly, whereby the analogue signal received is being sampled and stored into the Magnetic Optical disk. These data will then be used for further analysis.

In order to communicate with the main control, an external modem and card phone are used in both receiving sites (1) and (2) respectively. In addition for receiving site (1) in St. Peter Port Light House (Guernsey), a wireless radio modem (Air Link-RT) is connected to the receiver system at the lighthouse so as to connect to the telephone line at the port. As for receiving site (2) in Isl de Raz (Alderney), it runs under solar power that provides 48V DC to the whole receiving system.

The completed receiving system (1) is in St. Peter Port Light House (Guernsey) and the antenna set-up are shown in both Figure 4.14 and Figure 4.15 respectively. The completed receiving system (2) is in Isl de Raz (Alderney) and the set up for the antenna, solar power and equipment are shown in Figure 4.16, Figure 4.17 and Figure 4.18 respectively.

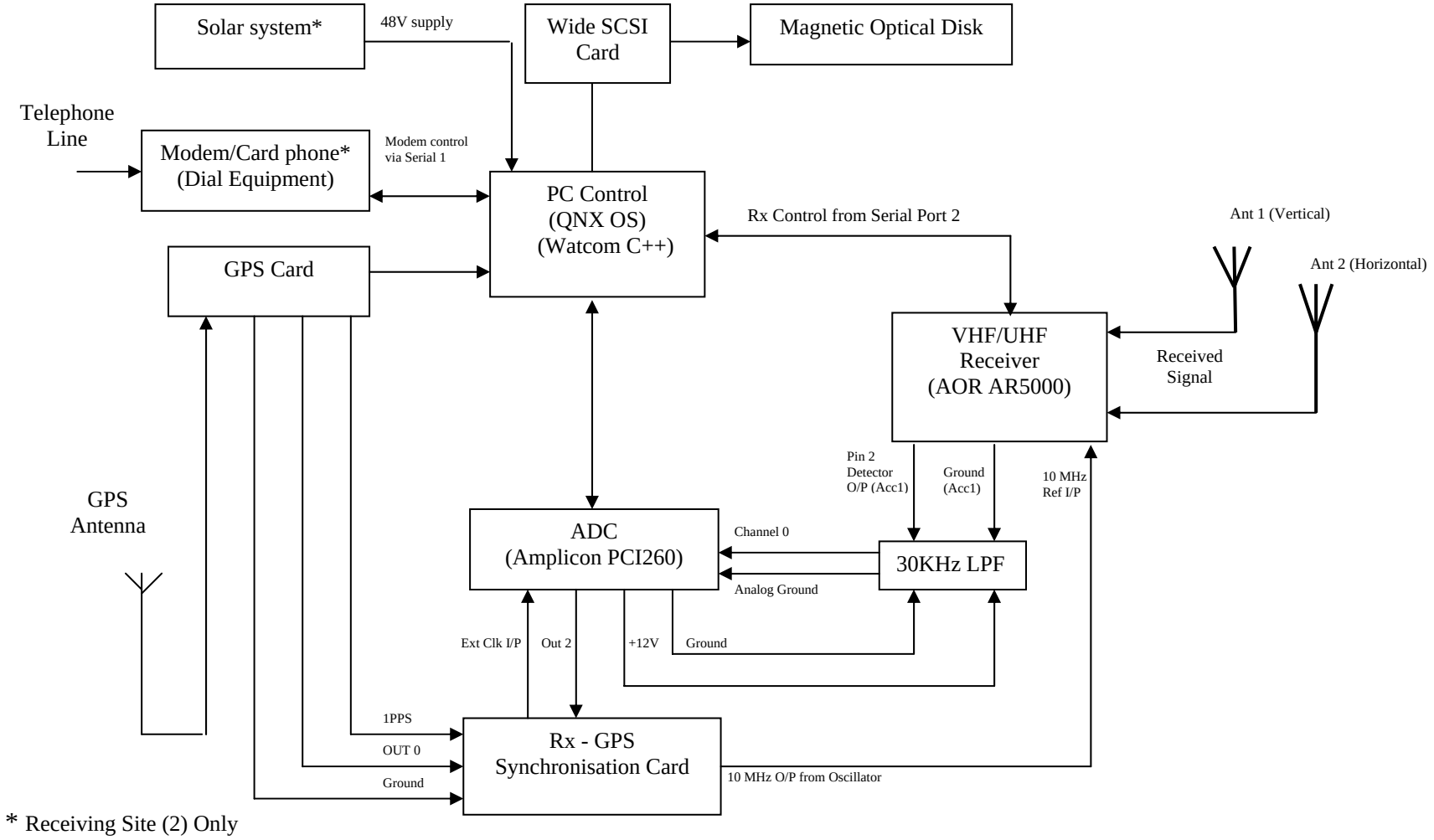

Figure 4.12: Over the sea propagation receiving system

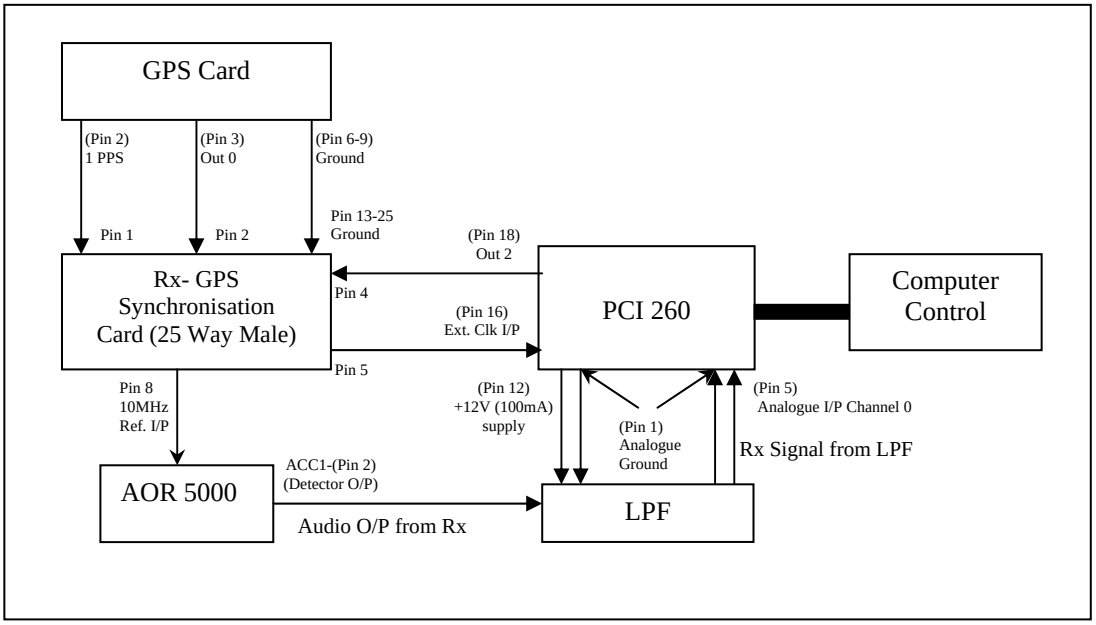

Figure 4.13: Block diagram of PCI 260 (ADC) connections

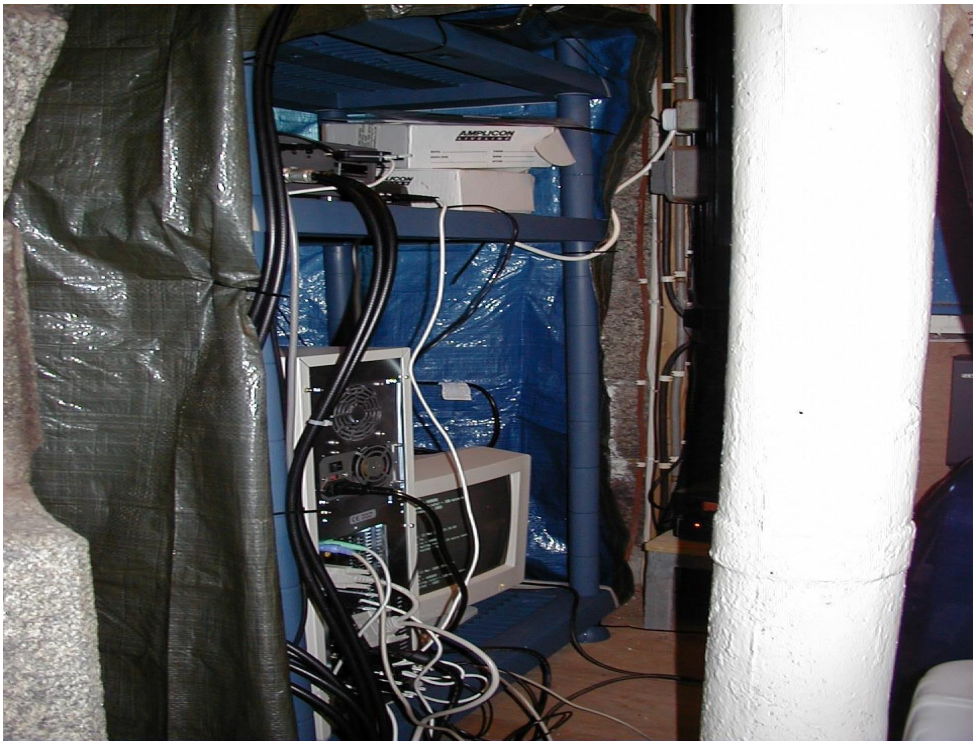

Figure 4.14: The completed receiver system (1) in St. Peter Port Light House

Figure 4.15: Antenna setup in St. Peter Port Light House

Figure 4.16: Antenna set up in Isl de Raz (Alderney)

Figure 4.17: Solar panel set up

Figure 4.18: Equipment set up in the bunker of Isl de Raz (Alderney)

4.2 Narrow pulse sounder

Since the propagation characteristics are dependent upon the modal structure of the received signal, it requires a transmission of continuous carrier frequency modulated with a regular interval pulse transmission.

The structure of this pulse signal is as shown in Figure 4.19. The whole pulse signal is repeated every 0.1 second with an interval break of 2.1ms. The interval pulse is 100 μs. An example is shown in Figure 4.20. It is obtained by transmitting the signal across the laboratory with 10 metres apart from both transmitter and receiver system. By setting the sampling duration to 25 μs and receiving duration set to 0.1 second, 4000 samples were collected which will in turn produce a total of 10 pulse signals.

The objective of this pulse signal is used to identify periods with anomalous or long time delay (e.g. multipath propagation) particularly over longer paths. Due to the short distances available for both receiving paths, for a pulse of 100 μs, the travel distance is around 30 km. Hence, there is a probability that nothing will be observed from this particular signal at both Jersey-Guernsey (33 km) and Jersey-Alderney (48 km) paths. However, it provides the possibility to operate over significantly longer paths (e.g. Jersey-Weymouth) in addition to the two paths already mentioned.

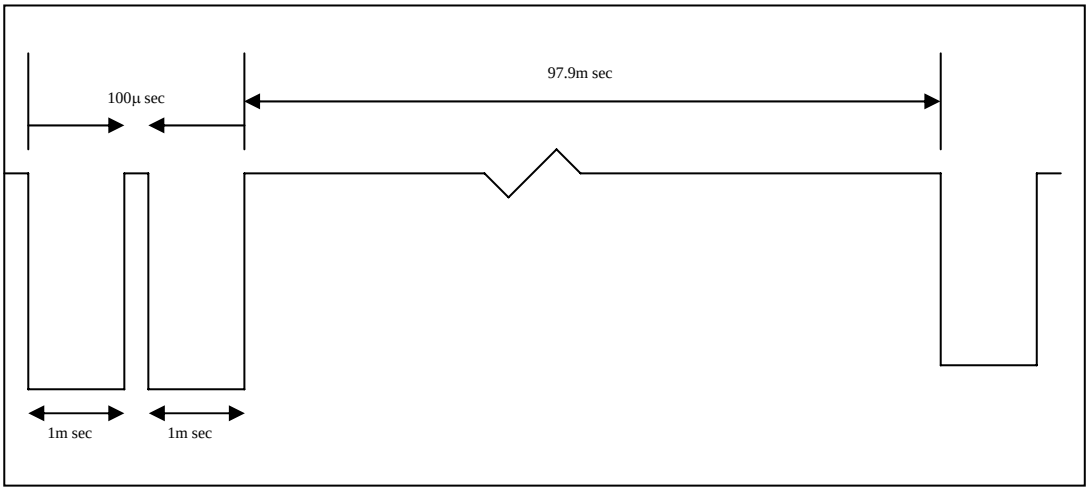

Figure 4.19: Pulse signal structure

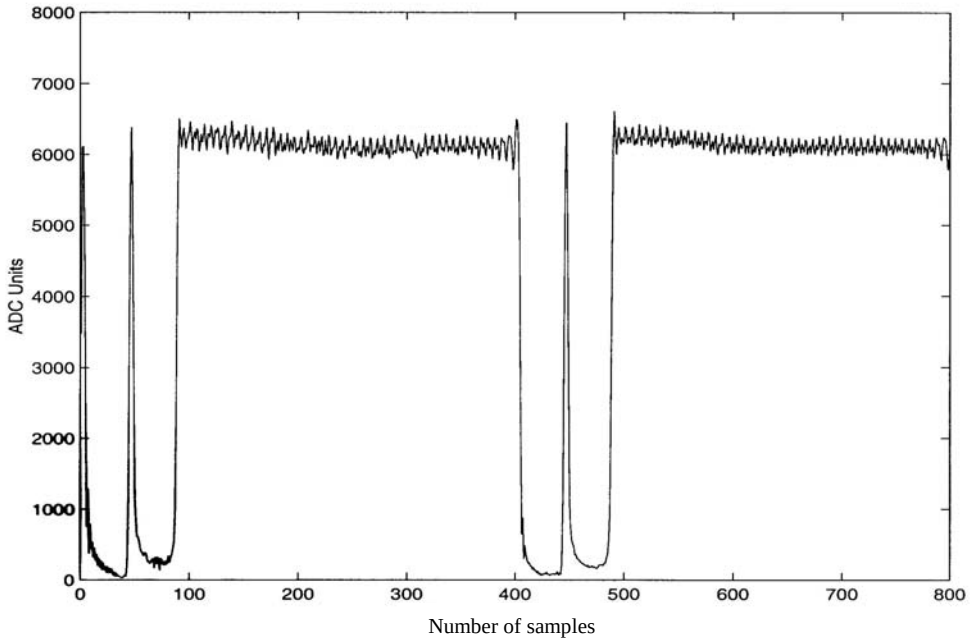

Figure 4.20: Propagated pulse signal across laboratory

4.3 Operating system and data acquisition

4.3.1 Operating system

The operating system used in this experiment is QNX as it is a real time, multitasking OS. The multitasking capability of QNX allows a modular approach to enable testing and modification of required software. The real time capability enables the data to flow at a rate close to real time. The message passing and data flow through a radio are much faster due to the synchronisation mechanism of QNX (send, receive and reply). Its robustness and real time performance was required for the experiment.

QNX OS also enable the computers, of both transmitting and receiving systems to share data and files via the telephone network from the main control station as shown in Figure 4.21. This includes data issue (e.g. transmitter/receiver sequence file), data collection (e.g. downloading received digital signal) and controlling program needed for the experiment.

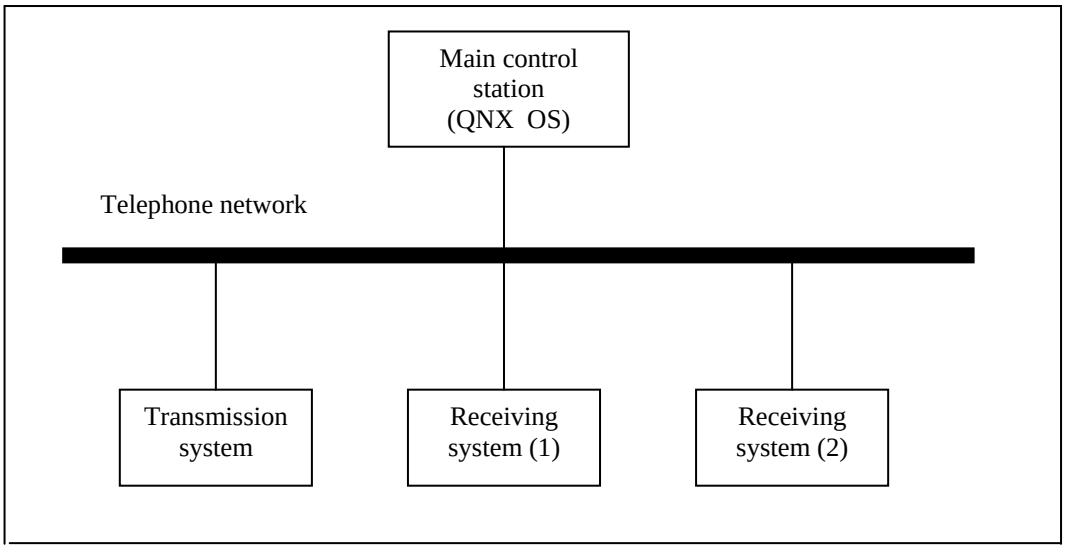

Figure 4.21: Diagram showing network connection

4.3.2 Transmitter/Receiver control program

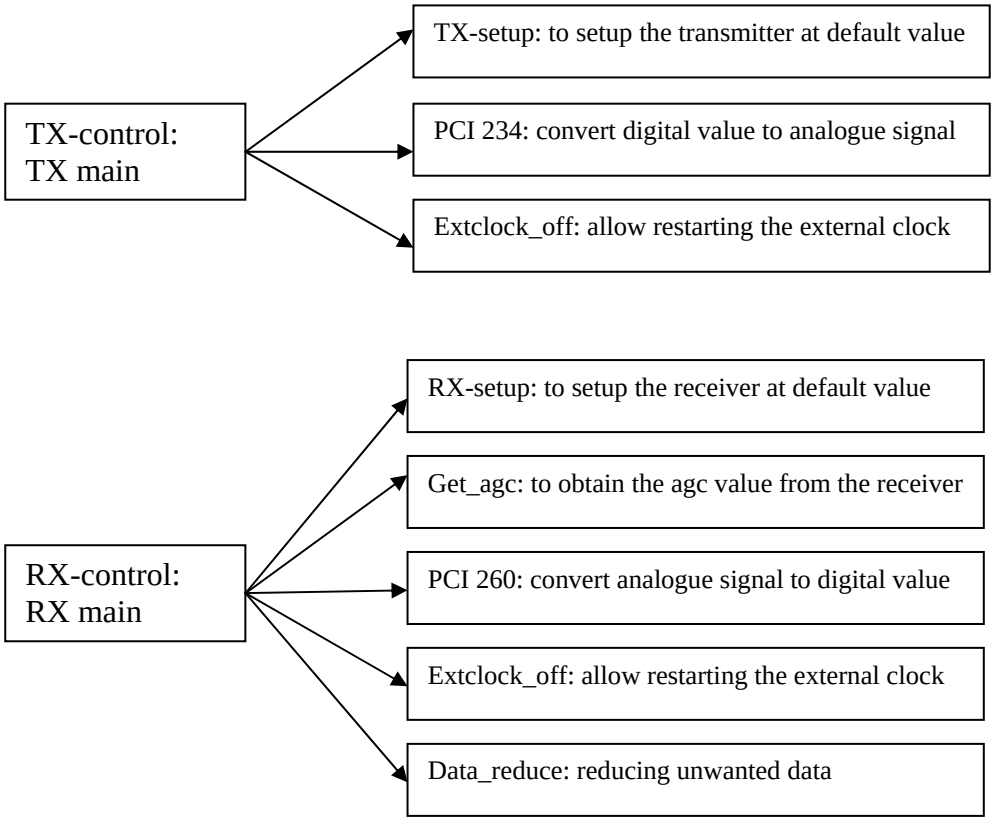

Figure 4.22: Transmitter/Receiver program chart

There are three major programs required in this experiment, transmitting/receiving control and GPS. Both transmitting and receiving control programs are similar except that one samples the data and output it while the latter receives the data and samples it.

Therefore, the structure for both transmitting and receiving control programs is the same except that the receiver had more request command. Both Transmitter and Receiver program charts are as shown in Figure 4.22. The flexibility of the receiver program is that it enables the collection of both the pulse sounder data and the AGC value in one single file.

4.3.3 Tide/Weather data collection

In this experiment, weather conditions such as wind speed, tide height, wave height, pressure and temperature across the Channel Islands are particularly important as it adds to the findings of propagation characteristic due to different weather conditions.

The following weather parameters are collected:

- Daily tide height (metre) variation at Sark [1].
- Air/sea temperature (°C), wave height (metre) and wind speed (knots) across the channel lightship [2].
- Jersey (airport) air temperature (°C) above the sea, air pressure (hPa), wind speed (knots) and direction of the wind [3].
- Guernsey wind speed (knots) and direction [4].

These data are collected by automatically collecting information from different web-site with online data at a fixed timestamp.

4.4 Conclusion

The design of both the transmitting and receiving systems were briefly described in this chapter. Both the transmitter system at Ronez Quarry (Jersey) and receiver system at St.Peter port lighthouse have been successfully installed during the period of March-April 2001. Minimum changes were done on the transmitting site when receiving system (2) at Isl de Raz (Alderney) was set up during the period October-November 2001. The only significant different is that the receiving system at Alderney is powered up by the solar power system.

Due to its small data size, the AGC measurements were routinely transferred over the telephone link to Leicester. Other types of files (e.g. pulse signal) were included to help identify any anomalous propagation mechanisms which might have been observed, particularly over the longer paths. These types of files are normally too long and costly to allow transfer by telephone link and hence required a visit to both the receiving sites to copy the data and transfer back to Leicester. As for the collection of weather data from the web site, it is done on a fixed timestamp and these data provide further information of the effect from different weather conditions.

Both the transmitting and receiving hardware/software design were subjected to changes as the development of the experiment progressed.

Chapter 5: Measurements

5.1 Frequencies and signal format

Two frequencies (VHF/UHF) were used in this experiment, 248.375 and 341.375MHz with both horizontal and vertical polarisation. In addition to co-polar measurements, cross-polar reception was also undertaken. During the entire experiment, there were three major changes in the transmission and reception schedule especially when Alderney receiving site was set up during Oct/Nov 2001. The three periods of change were as follows:

(a) *Apr 2001 until Oct/Nov 2001:*

Only 2 transmitting antennas (horizontal and vertical) were employed pointing at the Guernsey receiving site.

(b) *Nov 2001 until May2002*:

Four transmitting antennas were employed at the transmitting site, with 2 antennas (horizontal and vertical) pointing at each receiving site. The transmitter alternates between these two receiving sites on a 6 minute cycle.

(c) *Jun2002 until Sep2002:*

Employed the same schedule as of (b) above but with only 2 transmitting antennas (horizontal and vertical) pointing at Alderney receiving sites.

During these 3 periods, the transmission and reception schedule employed were as follows:

- Frequency: The transmitter alternates between the two mentioned frequencies on a 3 minute cycle
- Polarisation: Within each 3 minute period, 1 minute on each of vertical, horizontal and cross polar (horizontal transmit, vertical receive).
- Calibration: once per hour on each frequency. The transmitted power is reduced in 1dB steps and the receiver AGC value recorded.
- Receiver AGC values: Recorded for 30 seconds within each minute period.

- Receiver AF output: Recorded for 10 seconds within each minute during alternate 6 minute periods.
- Narrow pulse signal: recorded for 0.1 seconds during the same minute that the receiver audio output is recorded.

5.2 Signal behaviour from receiving site (1)- St. Peter Port Lighthouse (Guernsey)

The receiving system in St. Peter Port Lighthouse (Guernsey) was set up during the period of March /April 2001 and the observation of signal behaviour during the one-year period can be segregated into a few different categories e.g. calm sea / rough sea / cool summer day / hot summer day. The receiver AGC level in Guernsey was collected while the transmitter was transmitting to both Guernsey [Jersey-Guernsey (1)] and Alderney [Jersey-Guernsey (2)] receiving sites. The AGC level [Jersey-Guernsey (1)] was the direct transmission (transmitting antenna pointing directly to Guernsey) from Jersey to Guernsey. AGC level [Jersey-Guersney (2)] was the indirect transmission (transmitting antenna pointing to Alderney) and is used for comparison with the AGC level in Alderney at the same time [Jersey-Alderney (1)].

5.2.1 Data plotting

Before analysing all the effects observed from the data that have been collected from both receiving sites, it is best to describe the plotting of these data that has been mentioned in the previous section. Note that the calibration of the radio receiver (dBm to AGC value) is dependent on the initial conversion table (see Appendix A – Script 1) obtained from a direct signal input (via a cable) from the transmitter that ranges from –107 to 8dBm into the receiver.

In this section, 4 major matlab scripts will be shown:

Script 1 (see Appendix A and refer to Figure 5.1), displays all the various weather parameter measured as a function of time in comparison with the signal amplitude measured in dBr (no references at the receiving sites). The AGC values (converted from binaries into numbers) were used to compare with the signal amplitude table (see Appendix 1: Script 1). This AGC signal amplitude (in dBr) was eventually added with another 107 dBr that results in Figure 5.1 (d).

Script 2 (see Appendix A) displays the median, mean and fading range of the signal amplitude (in dBr) against the changing tide height for both polarisation and frequencies (refer to Figure 5.2).

Script 3 (see Appendix A) displays the AGC level (in dBr) within a 30 seconds period for either Guernsey or Aldeney data (with selection of either F1 or F2, horizontal or vertical polarisation).

Script 4 (see Appendix A) makes use of the files containing the AF output from the receiver within a 10 seconds period. The AGC level (dBr) obtained from the AF [see Figure 5.9(a)] was used to multiply with the AGC linear voltage gain that results in Figure 5.9 (b) showing the actual fading range (in dB). An FFT operation was then used to perform on this data [see Figure 5.9 (c)], so as to observe if there are any anomalous signals in the AF. The rest of the minor scripts will also be mentioned in this chapter.

5.2.2 Calm sea (Jersey to Guernsey)

The first major effect observed from the sea parameter during the period that maybe categorised as calm day in spring, autumn or winter, the measurements are shown in Figures 5.1 and 5.2. From these figures, the signal amplitude (in dBr) displays approximately linear relationship with the tide height (in metres) obtained from Sark since it is located approximately between Jersey and Guernsey. Lower signal amplitude was observed at high tide with a reduction of approximately 1.1 dB per metre increase in tide height. For this day, the tidal range was around 9 metres with wave heights of between 1.2 and 2 metres measured at the Channel Light Vessel.

The changes in signal amplitude within 30 seconds period for both F1 and F2, with both horizontal and vertical polarisation respectively are shown in Figures 5.3 and 5.4. From these figures, a fading range of around 2 dB is apparent in the data. During these “calm sea” periods with low signal amplitude fading, the sea temperature (T_{sea}), the Channel Light Vessel air temperature (T_{LS}) and the temperature at Jersey Airport (T_J) are either similar or T_J is lower than T_{sea} and T_{LS} during the winter period.

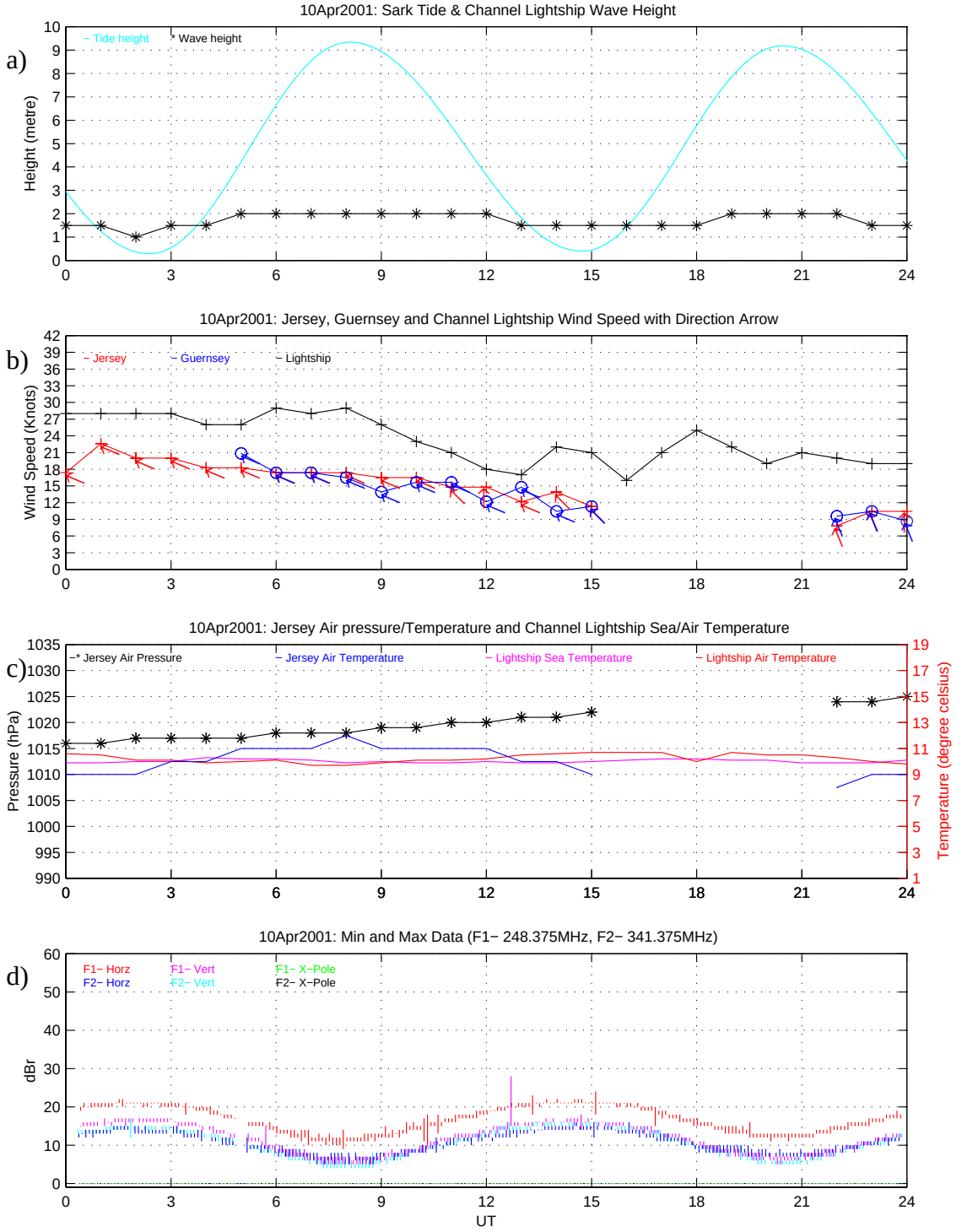

Figure 5.1: Various parameters measured as a function of time on a calm spring day (10th April 2001): (a) Tide height and wave height, (b) Jersey, Guernsey and Channel Lightship wind speed with direction arrows, (c) Jersey air pressure, Jersey/Channel Lightship air temperature and Channel Lightship sea temperature, (d) Signal strength (minimum and maximum value plotted) for both F1 and F2 (horizontal, vertical and cross polar).

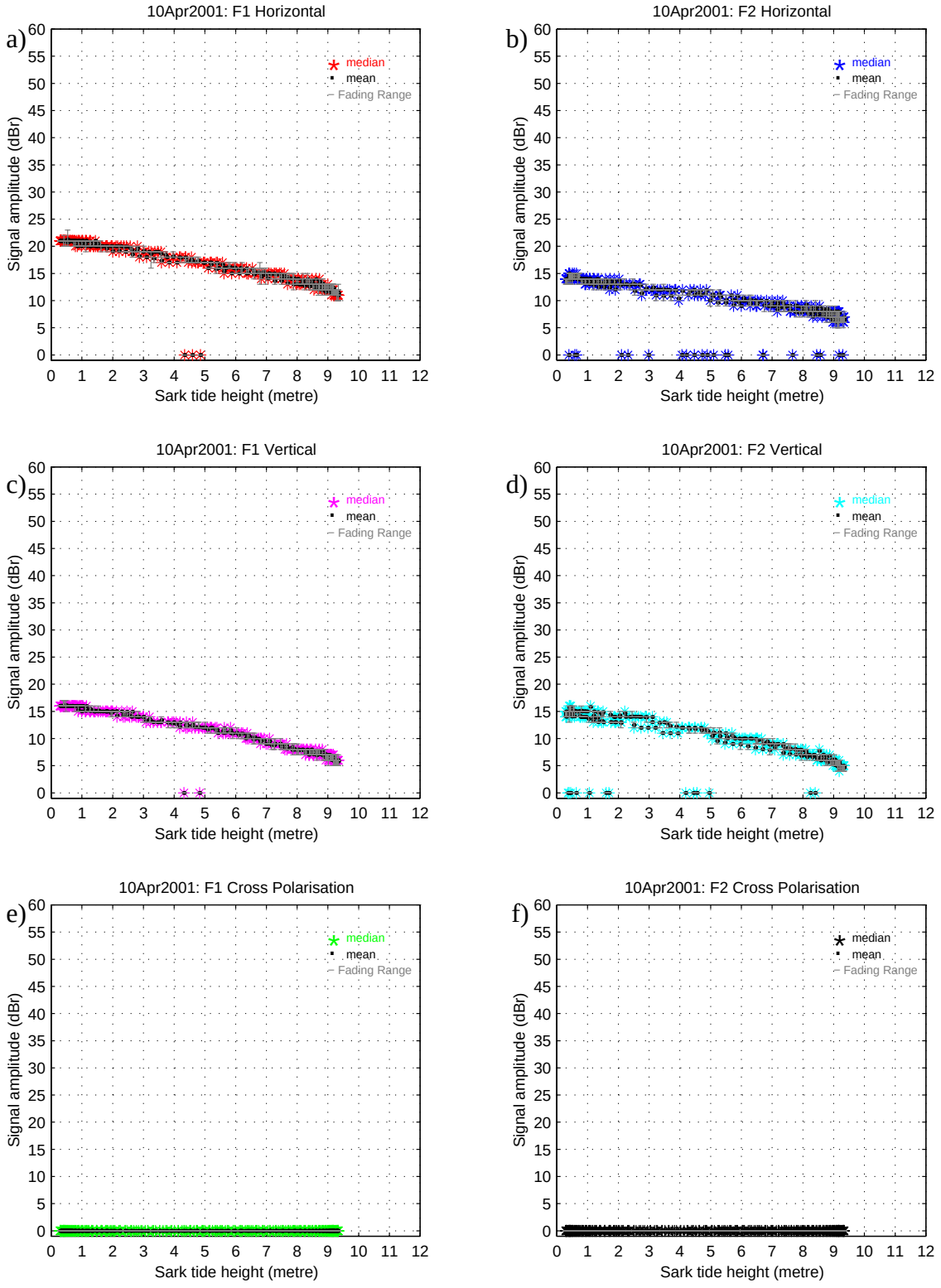

Figure 5.2: Signal amplitude (dBr) vs tide height (metre) on a calm spring day (10th April 2001) for frequencies of F1- 248.375 MHz and F2- 341.375 MHz:
(a) F1- Horizontal polarisation, (b) F2- Horizontal polarisation, (c) F1- Vertical polarisation, (d) F2- Vertical polarisation, (e) F1- Cross polarisation (transmit horizontally and received vertically), (f) F2- Cross polarisation (transmit horizontally and receive vertically).

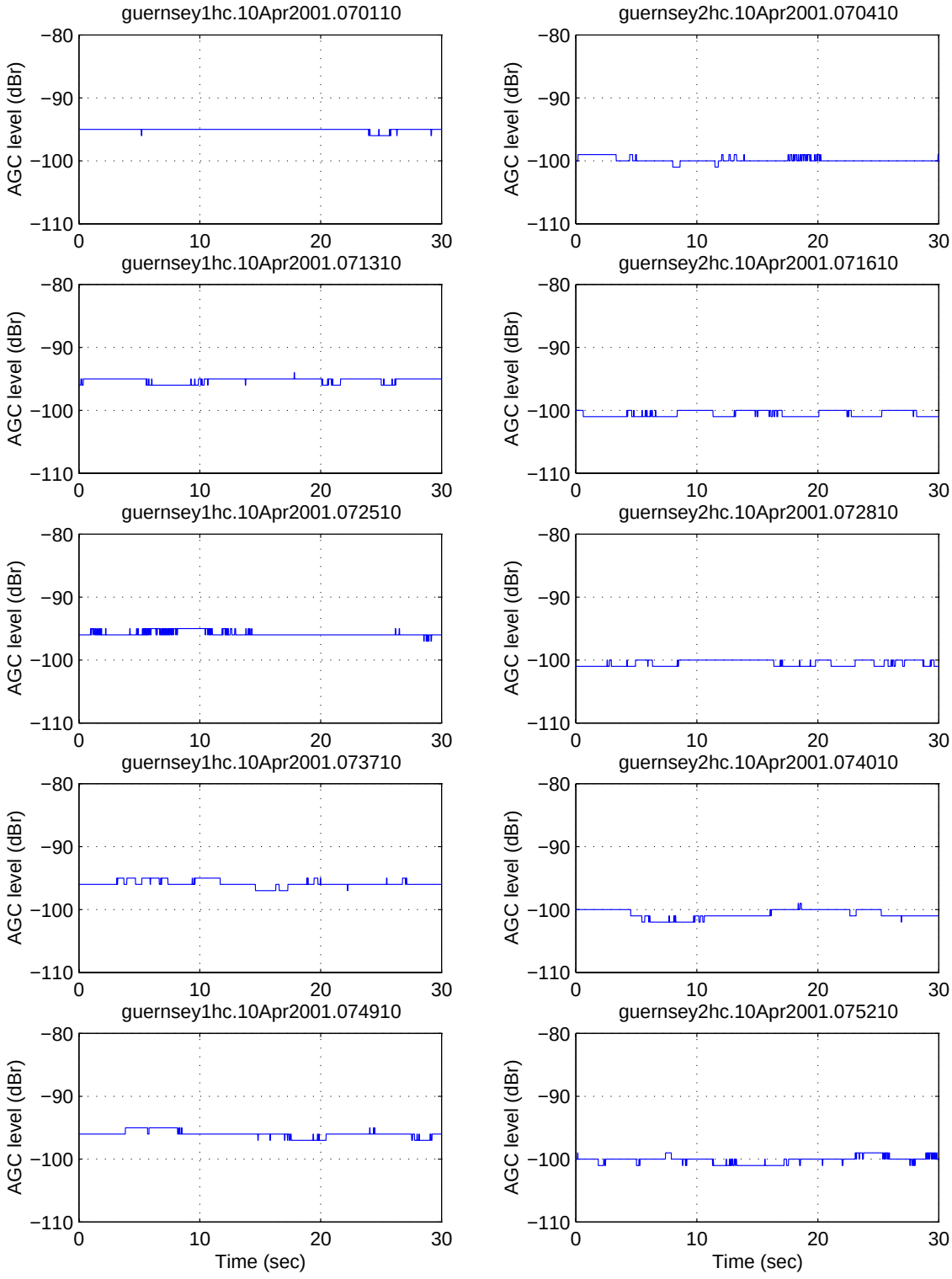

Figure 5.3: Signal strength vs time for (Jersey-Guernsey) F1 (left panel) and F2 (right panel) horizontal signal during a calm spring day (10^{th} April 2001)

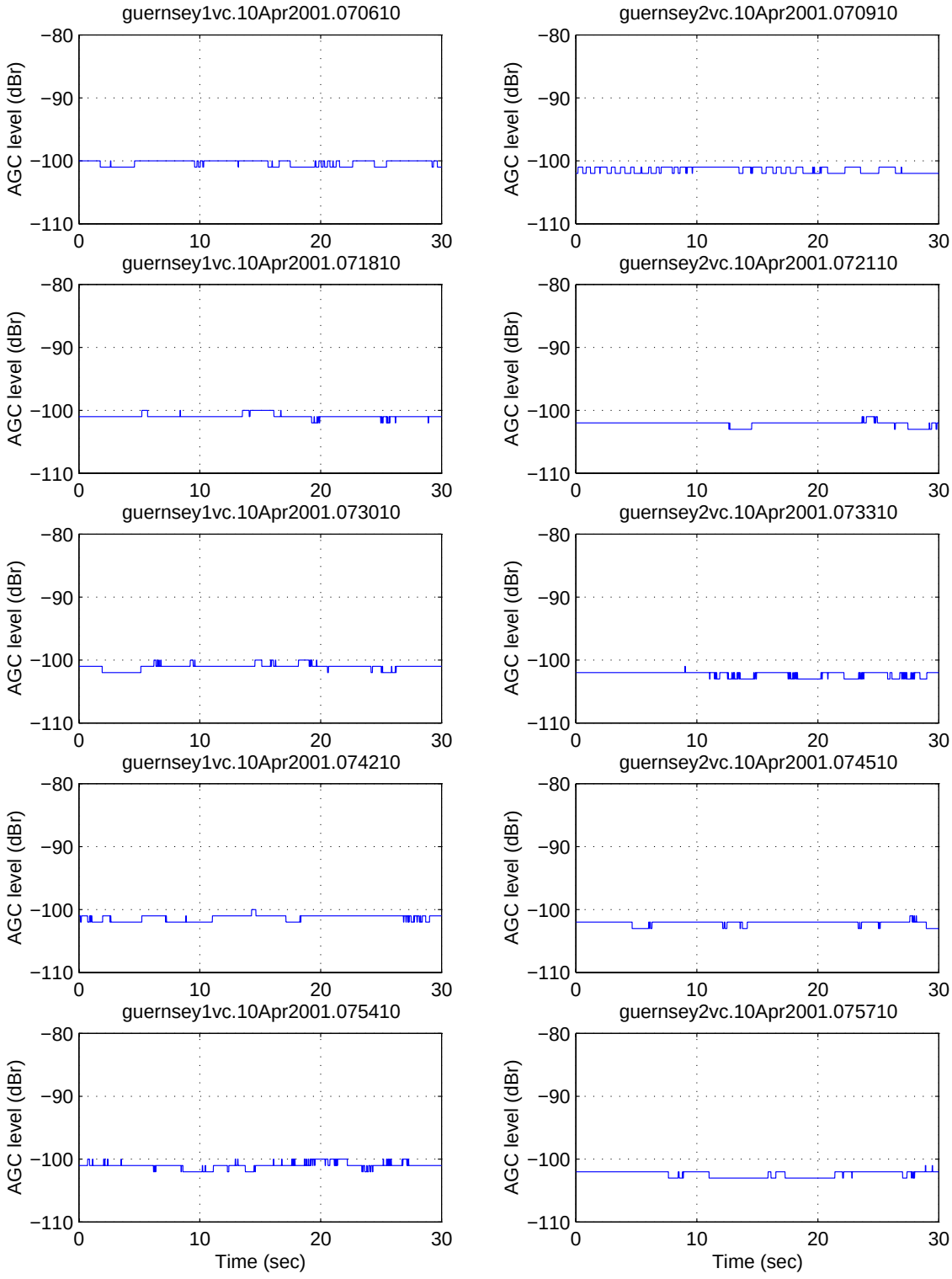

Figure 5.4: Signal strength vs time for (Jersey-Guernsey) F1 and F2 vertical signal during a calm spring day (10th April 2001)

5.2.3 Rough sea (Jersey to Guernsey)

Theoretically, the wave height, wind speed and the direction of the wind affect the propagation of signals. Barrick [1971] explains that rougher sea state (e.g. high wind speed) will add to the basic transmission loss when either the frequency or the distance increases (see Section 3.4). Although rough sea states or high wind speeds were observed from the weather data on some occasions, there were only three occasions on different days where anomalous propagation was observed during spring 2001 (Jersey-Guernsey) on a rough sea state day. These amount to less than 0.1 percent of the total time.

Figure 5.5 is illustrative of measurements obtained during a rough-sea day when this type of anomalous propagation occurred in the spring. For this day, the wave height varies between 2 to 4 metres while the wind speed measured at the Channel Light Vessel varies between 12 to 35 knots (6 to 18 m/s). This corresponds to a sea state level between 2 to 7 as compared to Table 3.3 obtained from Levy [2000]. The weather parameter on this day showed that both the wave height and wind speed were correlated especially during high wind period (rougher sea state). This was also mentioned by Levy [2000] as the increase in wind speed will contribute to higher wave height and sea state.

Both Figures 5.5 and 5.6 show that the horizontally polarised signal was not much affected whereas the amplitude of the vertically polarised signal was reduced by between 3 and 6 dB. In addition, fast fading of up to 15 dB within a 30 seconds period was observed from horizontally polarised signal only (see Figure 5.7 and Figure 5.8) during high tide and rough sea states. In contrast, the vertical signal shows fast fading of around 3 dB only. The signal characteristic of both F1 and F2 horizontal/vertical signals are shown in Figure 5.9 and Figure 5.10. It provides further evidence that during rough/spring conditions at high tide, fast fading with periods of several seconds may occur, with reductions in amplitude in excess of 10 dB. In contrast, the vertical signal showed a fading of around 3 dB. No similar report has not been found in the literature.

Matthew [1965] explains that if equation 3.02 is not satisfied (see Section 3.5), a surface can be considered rough. By applying the parameters for Jersey-Guernsey during a rough sea day, the transmitter antenna was around 20 metres in height above the sea

level (at low tide) and at a distance of 16.65 km (half of Jersey-Guernsey distance), the angle of incidence ψ is:

$$\tan^{-1}(20/16650) = 0.0688°$$

By selecting F2, the wavelength (λ) is 0.861 metre and since the maximum wave height (H) during rough sea state was around 4 metres, then:

$$H\psi = 4 \times 0.0688 = 0.2753 \text{ metres}$$

and

$$3.6\,\lambda = 3.6 \times 0.861 = 3.1 \text{ metres}$$

The above calculation shows that equation 3.02 was satisfied and if it is applied to the rough sea day in spring as mentioned above, the surface of the sea will be considered smooth. Therefore, if equation 3.02 is applied to Jersey-Guernsey, or even Jersey-Alderney (48 km path), the sea surface will always remain smooth.

The data analysis for cross-polar signals showed that during calm sea conditions or cool summer time, the received cross-polar signal strength was normally around 20 dB less than the co-polar signal. The signal amplitude fading range for cross-polar signals (see Figure 5.11) was around 10 to 13 dB and suspected to be noise interference as the AGC level of the receiver has reached its minimum.

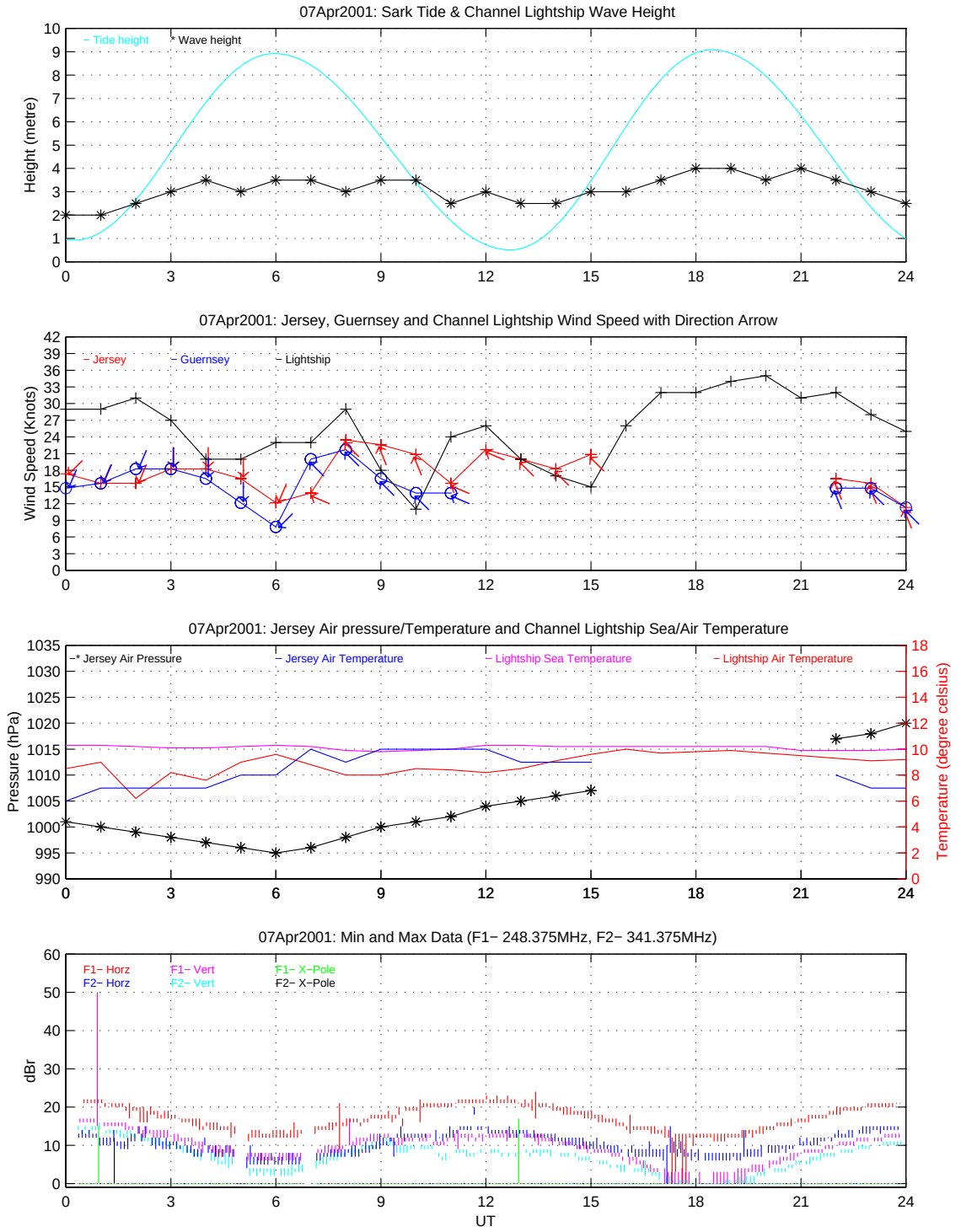

Figure 5.5: Signal amplitude plot on a calm day (07th April 2001) with respect to various weather parameters

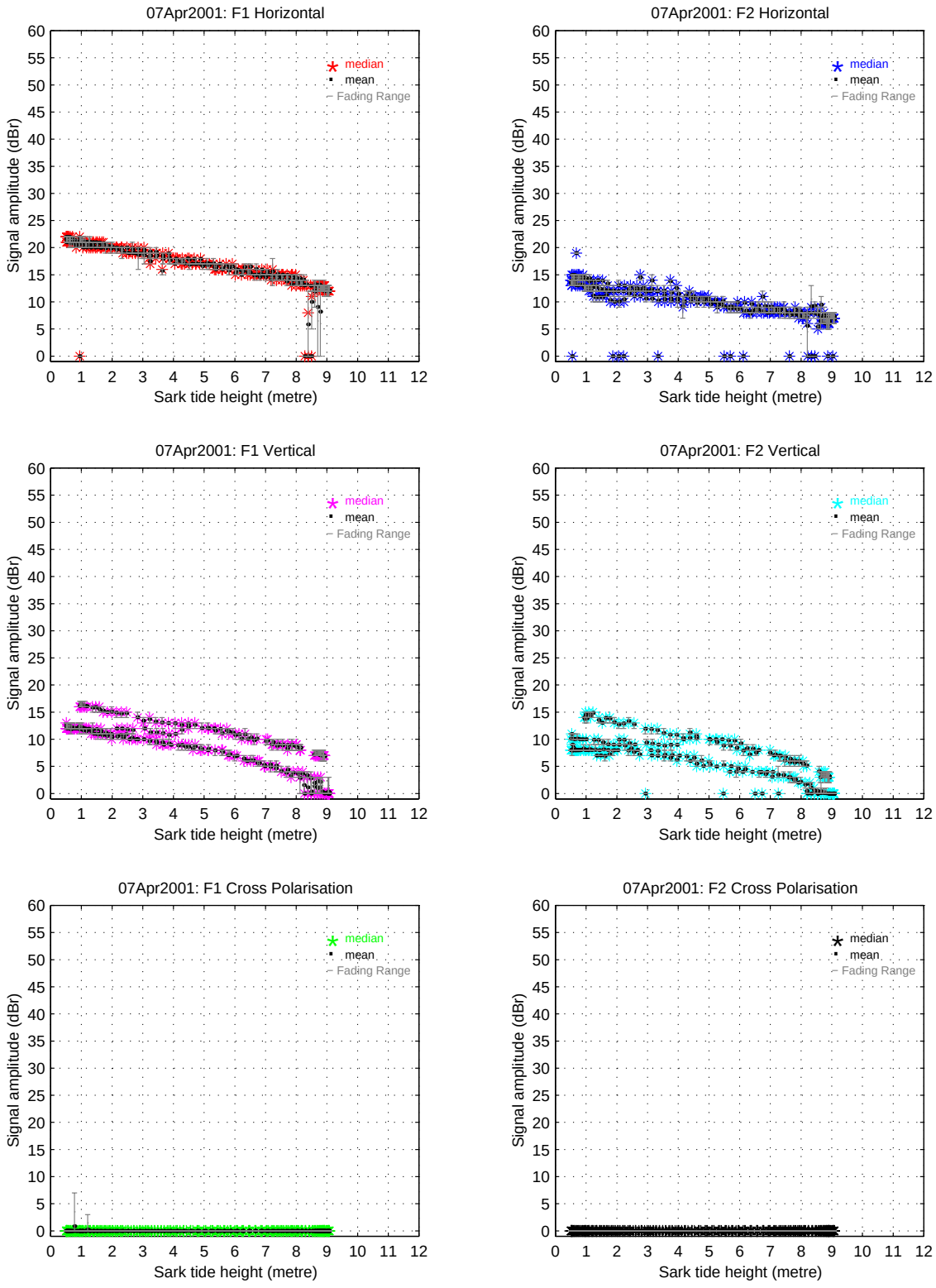

Figure 5.6: Signal amplitude vs tide height on a rough day (07th April 2001)

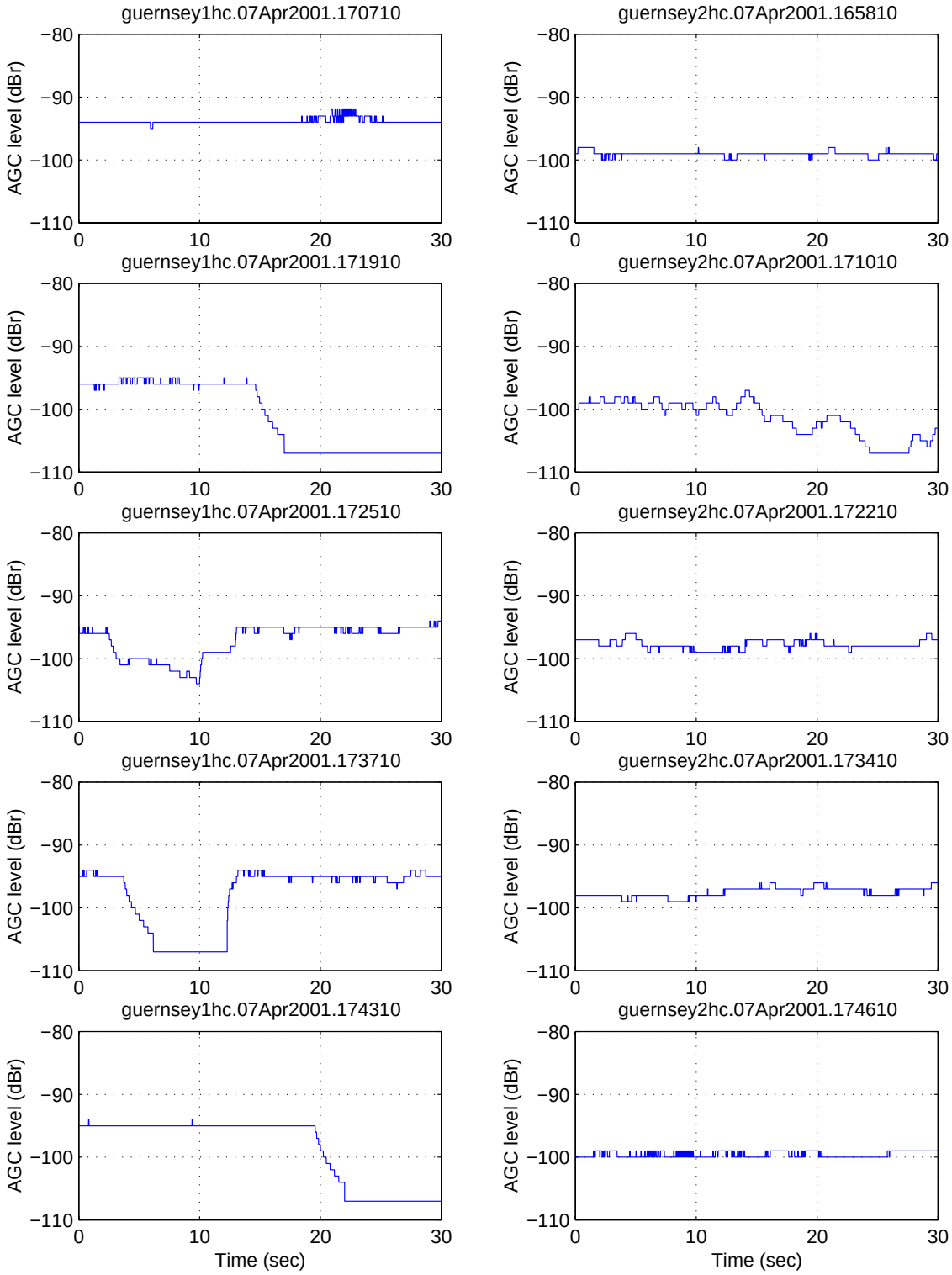

Figure 5.7: Signal amplitude vs time for Jersey-Guernsey F1 and F2 horizontal signal during a rough day on 07th April 2001

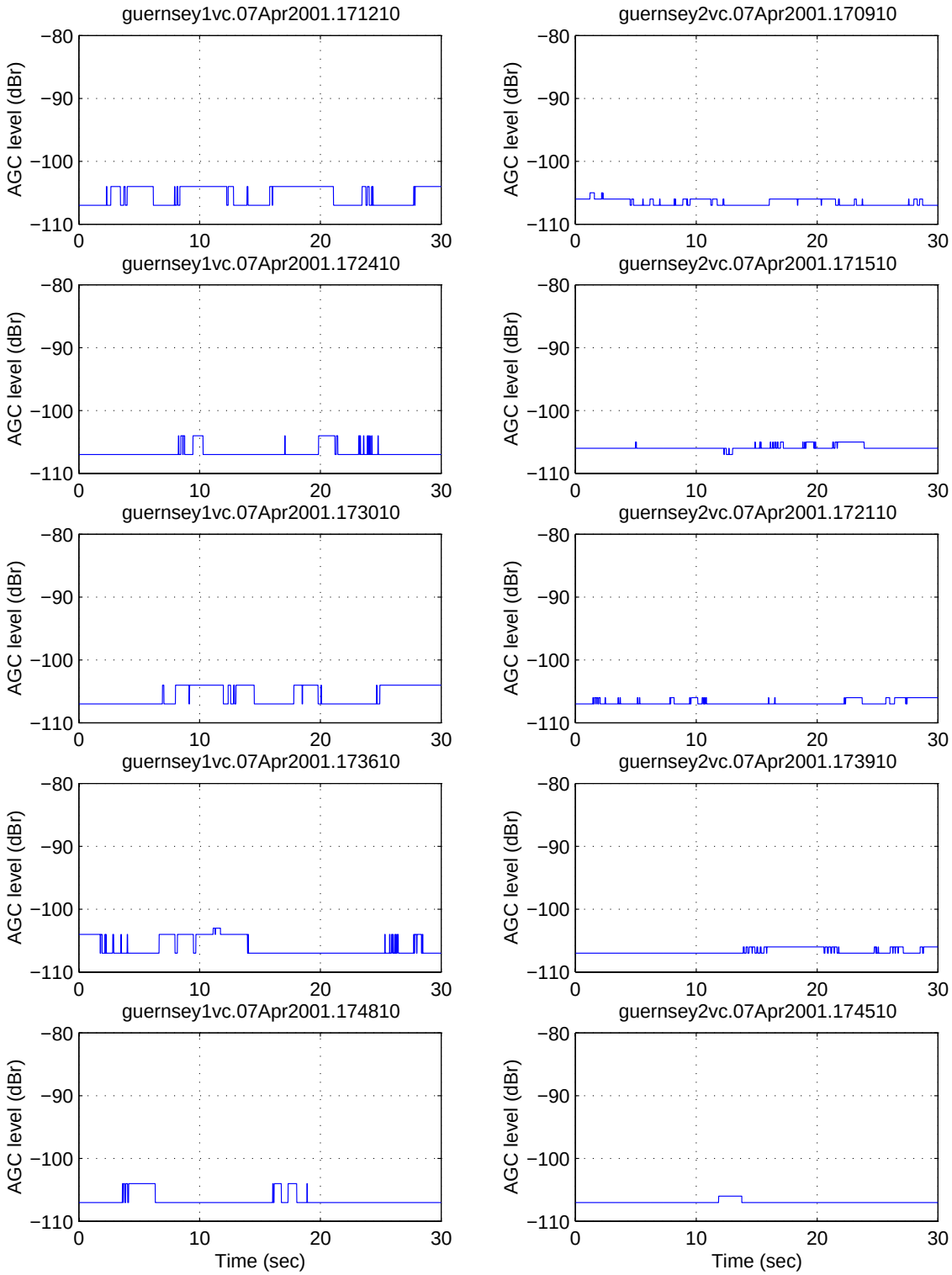

Figure 5.8: Signal strength vs time for Jersey-Guernsey F1 and F2 vertical signal during a rough day on 07th April 2001

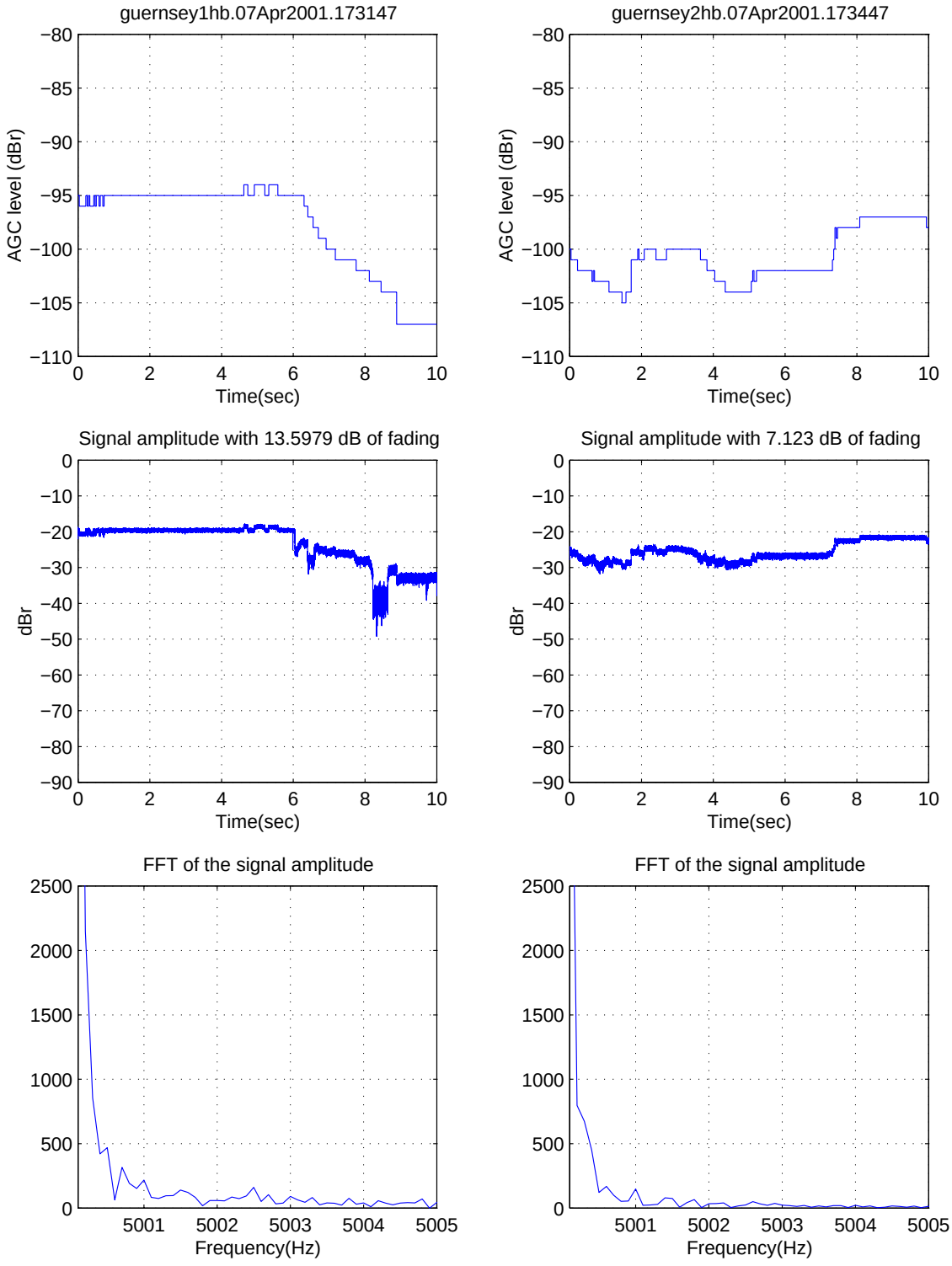

Figure 5.9: Rough spring signal characteristic for both F1 and F2 (Horizontal)

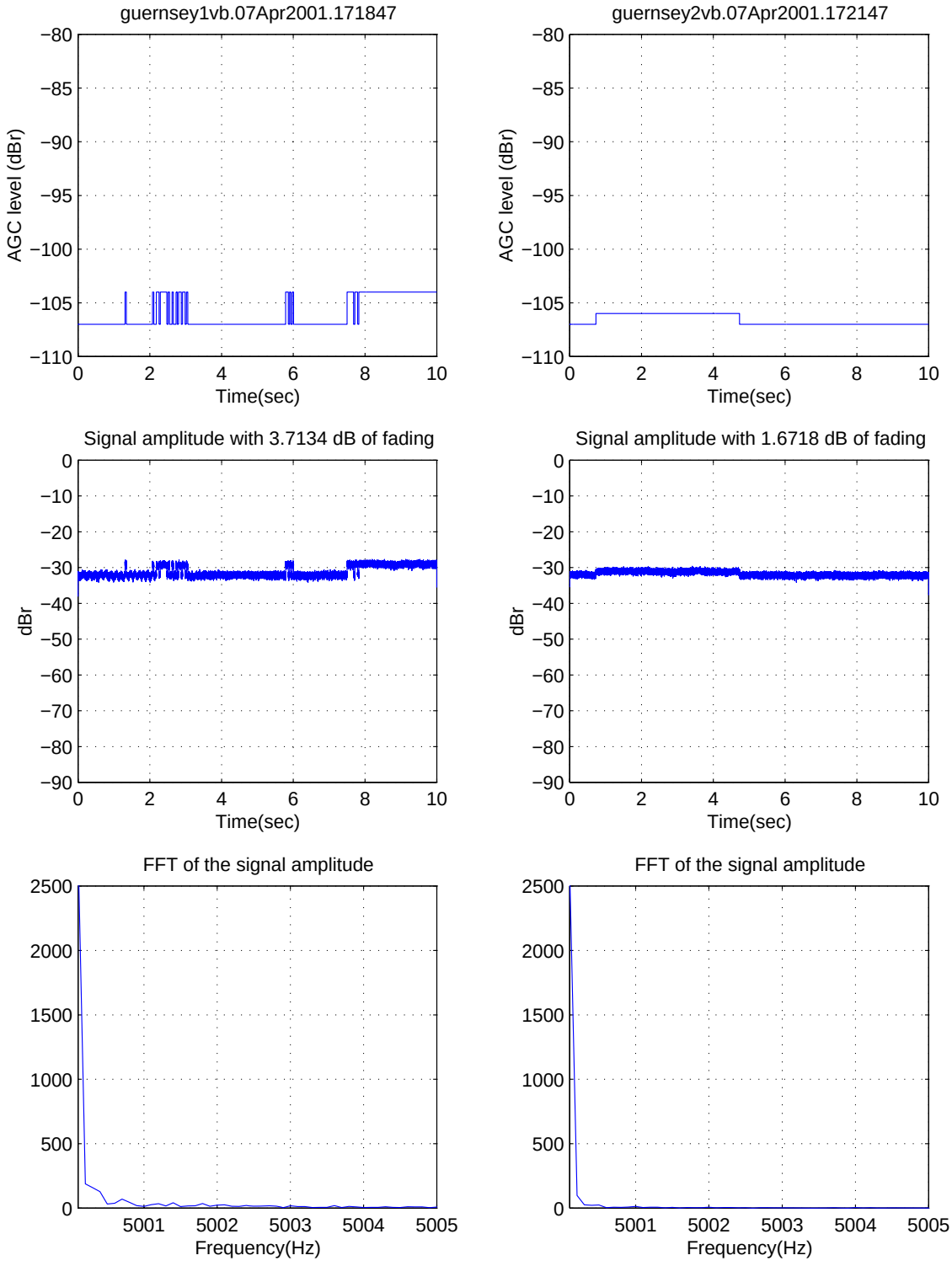

Figure5.10: Rough spring signal characteristic for both F1 and F2 (Vertical)

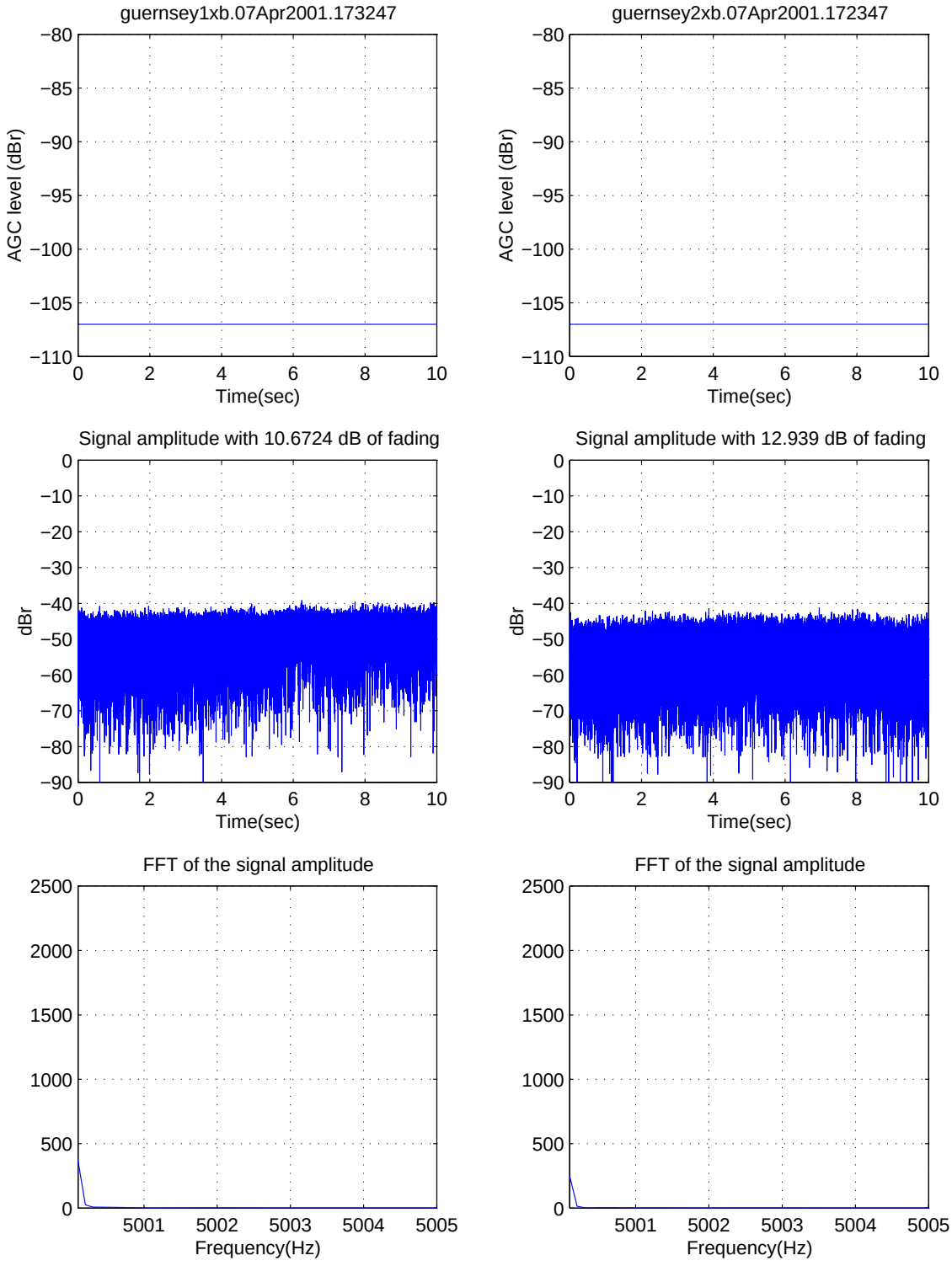

Figure 5.11: Cross-polar signal characteristic during spring

5.2.4 Summer (Jersey to Guernsey)

During "cool" summer days when the temperature at Jersey airport (T_J) is either similar or below sea temperature (T_{sea}) and the Channel Light Vessel air temperature (T_{LS}), the only fading is due to the tidal effects as mentioned in Section 5.2.1. In contrast, during hot summer days when T_J significantly exceeds T_{sea} and T_{LS}, the received signal strengths were observed to be often up to 20 dB (sometimes more) greater than those observed on a "cool" summer or other days such as spring. An example is shown in Figure 5.12 and Figure 5.13 on 26th July 2001, during which the Jersey air temperature (T_J) exceeded the sea temperature (T_{sea}) by up to 10°C.

Figure 5.14 and Figure 5.15 show the fading characteristic within a period of 30 seconds for both the Jersey-Guernsey horizontal and vertical signal with both F1 and F2 respectively on the same day. From these two figures, a fading range of around 1 dB occurred. Although the fading range is low within a 30 seconds period, fading up to 20 dB is evident with time-scales of tens of minutes as shown in Figure 5.16 display the enhanced signal strength (ESS) characteristics. Fading effects due to tidal variation and changes in the ESS propagation are also evident in this figure. As regard to signal fading for cross-polar signal during summer time when ESS occurs, the fading range was around 1 dB or so as shown in Figure 5.17.

The occurrence statistics for the period of April 2001 until September 2002 on a monthly basis for threshold temperature differentials of 3,4 and 5°C are given in Figures 5.18, 5.19 and 5.20. These suggest a threshold temperature differential of approximately 4°C. During these observations, periods of ESS lasting from a few hours to 9 days occurred. Therefore, the above measurement indicates that ESS occurs more frequently when T_d (the temperature difference between T_J and T_{sea}) is equal to or more than 4°C. Note that there are no data available during April 2002.

The total percentage of days with ESS and mean T_{dmax} [1] from April 2001 until September 2002 is shown in Figure 5.21, whereas the statistic occurrence of total percentage and number of hours of time during ESS are shown in Figure 5.21. From these figures, the ESS occurrence during both summers 2001 and 2002 respectively was observed to be different. For summer 2001, the total percentage of days with ESS has a

[1] Mean T_{dmax} is the monthly average value of (maximum air temperature at Jersey Airport subtracted by maximum sea temperature at Channel Light Vessel).

monthly distribution between 55 to 76% from May until August 2001. In comparison, the distribution for total percentage of time (in hours) during the same period was between 43 to 61%. The mean T_{dmax} in this case was around 4 to 5°C and the total number of ESS hours occurred monthly varied between 267 to 409 hours. In comparison, summer 2002 (May until August 2002) showed a gradually increasing ESS monthly occurrence (percentage of days) from 31 to 48% and the total percentage of time (in hours) from 19 to 37%. In this case, the mean T_{dmax} was around 4°C and the total ESS hours monthly increased gradually from 84 to 272 hours. This was evident as the number of days with high temperature and sunshine day during the year 2002 was less than the previous year (information provided by the Jersey Met office). Furthermore, the occurrence of ESS and mean T_{dmax} declined drastically during the period of autumn, winter and spring. These changes were more obvious especially during Nov/Dec 2001 as ESS reached zero level when T_{dmax} was less than -2°C. During this "low temperature period" from September 2001 until March 2002, the ESS monthly occurrence for both total percentage of days and time (in hours) were 0 to 20% and 0 to 13% respectively. Further observation also revealed that it was below 10% of the total time during winter.

Figure 5.23 shows the monthly distribution of ESS duration during a day (maximum 24 hours) for Jersey-Guernsey path from April 2001 until September 2002. From this figure, the total statistic showed that the upper/lower decile values were 24 and 7 hours respectively and the total median value was 18 hours. By considering both summer days, the ESS duration can be considered to vary between a median value of 17 to 22 hours during both summers 2001 and 2002.

In comparison with the monthly distribution of ESS duration, the signal strength increases during the same period is shown in Figure 5.24. From this figure, it shows that summer 2001 is higher than summer 2002 and by comparing June 2002 to June 2001, the latter median value was 6 dB higher with a maximum signal strength increase of 33 dB. In comparison with summer, the winter period showed signal strength improvement of up to 5 dB as shown in both Figures 5.24 and 5.25. The total statistic during winter period showed that the increase in signal strength upper/lower decile values were 5 and 1 dB respectively and the median value was 3 dB.

The overall statistics from the above agreed with the sea path experiment conducted by Wickers and Nilsson [1973] (160 km path with frequency between 60 to 5000 MHz) where low level ducting occurred around 70% during summer and less than 10% during winter period (see Section 3.3).

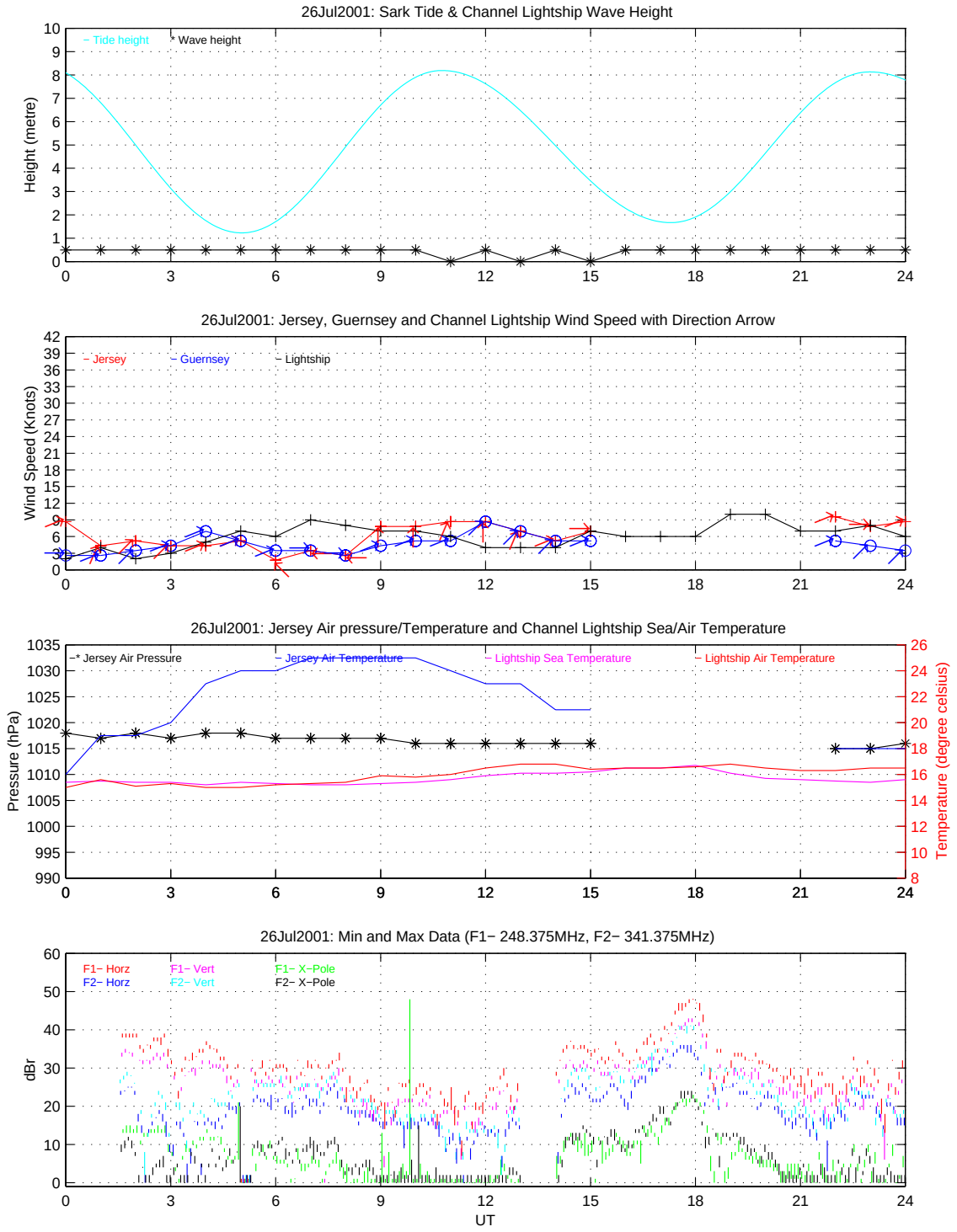

Figure 5.12: Signal strength variation on a hot day with respect to high Jersey airport temperature (26th July 2001)

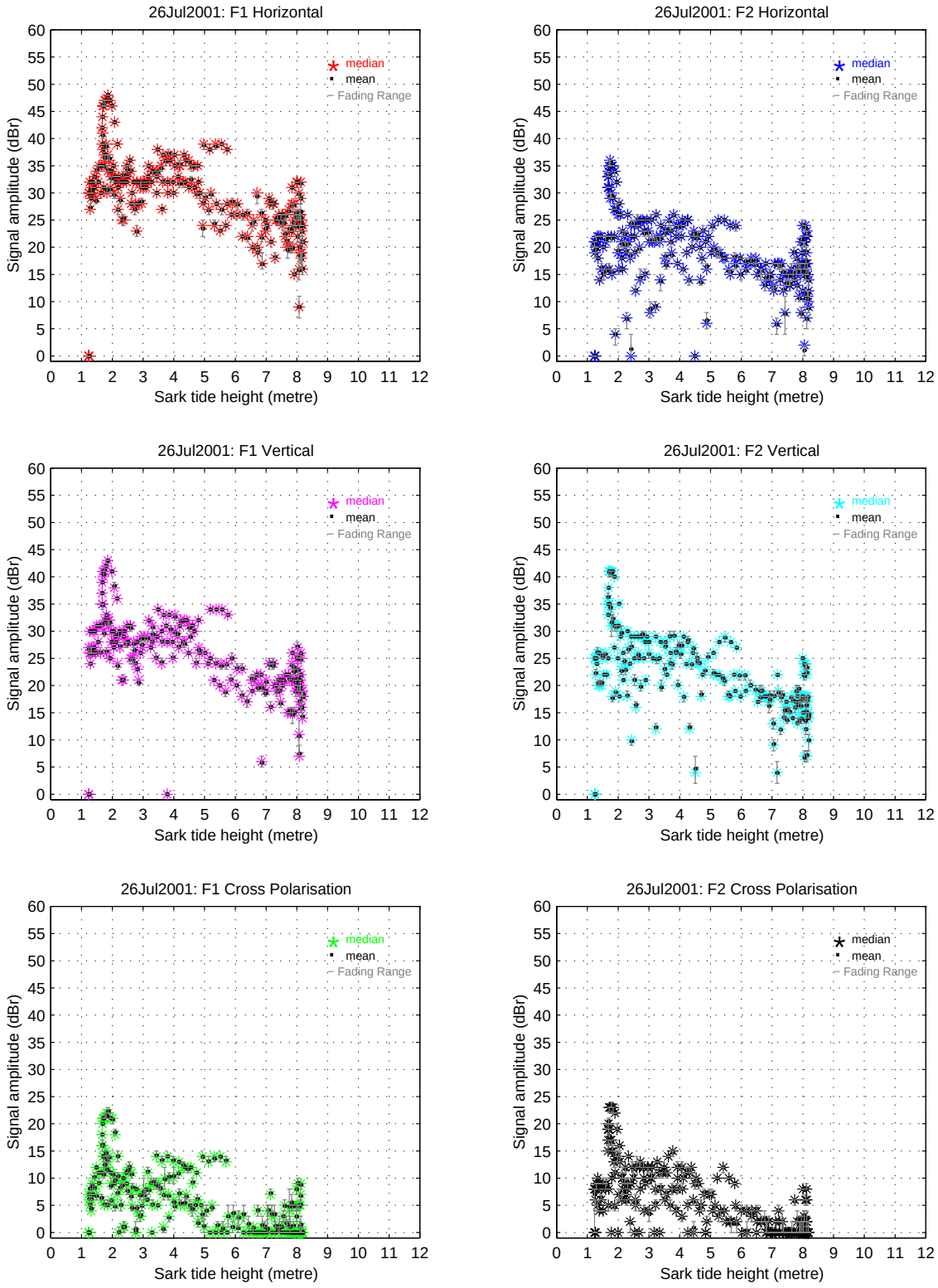

Figure 5.13: Enhanced signal strength (ESS) vs. tidal height on a hot day

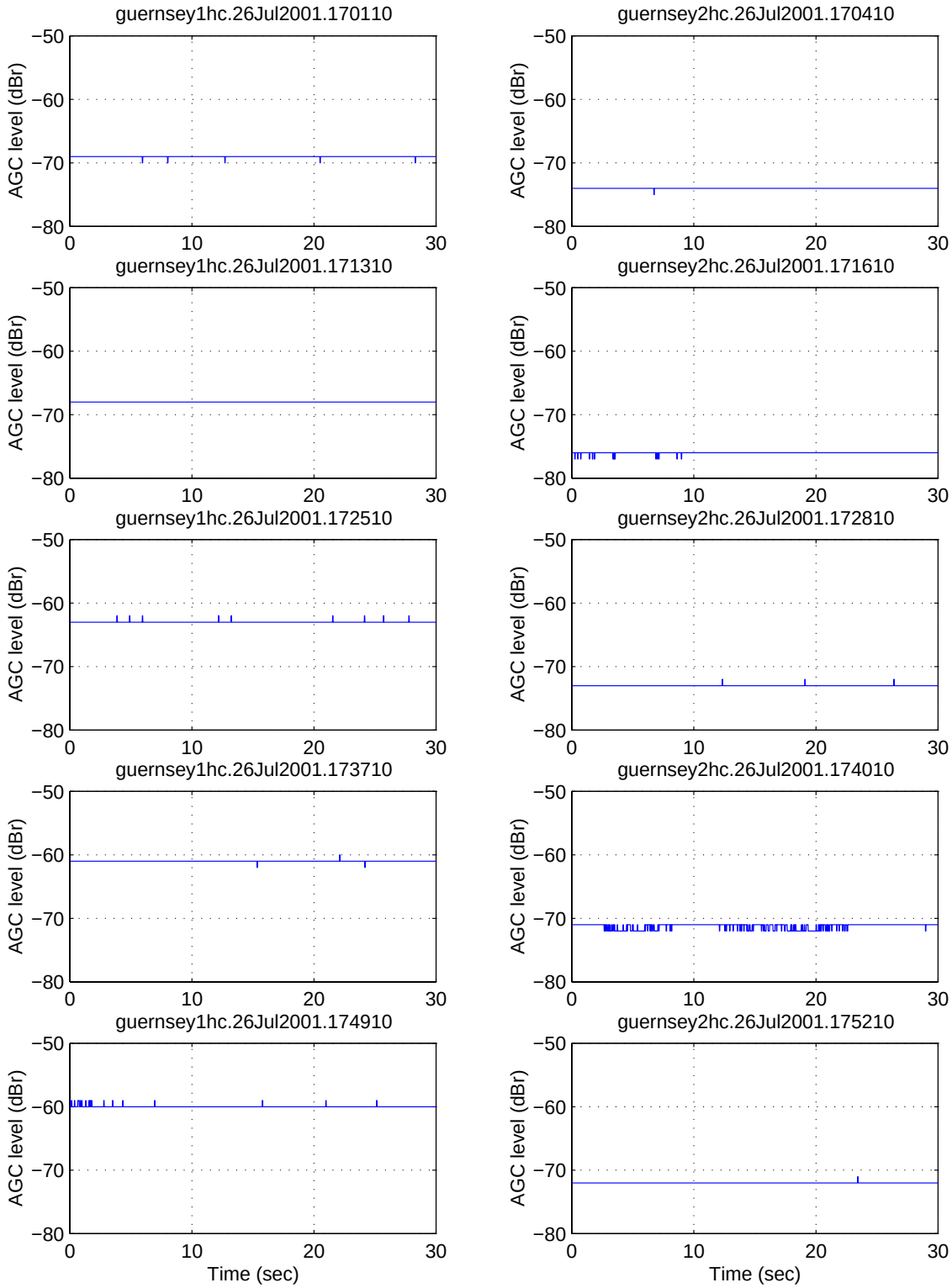

Figure 5.14: Signal amplitude vs time for Jersey-Guernsey F1 and F2 horizontal signal during ESS on a hot day

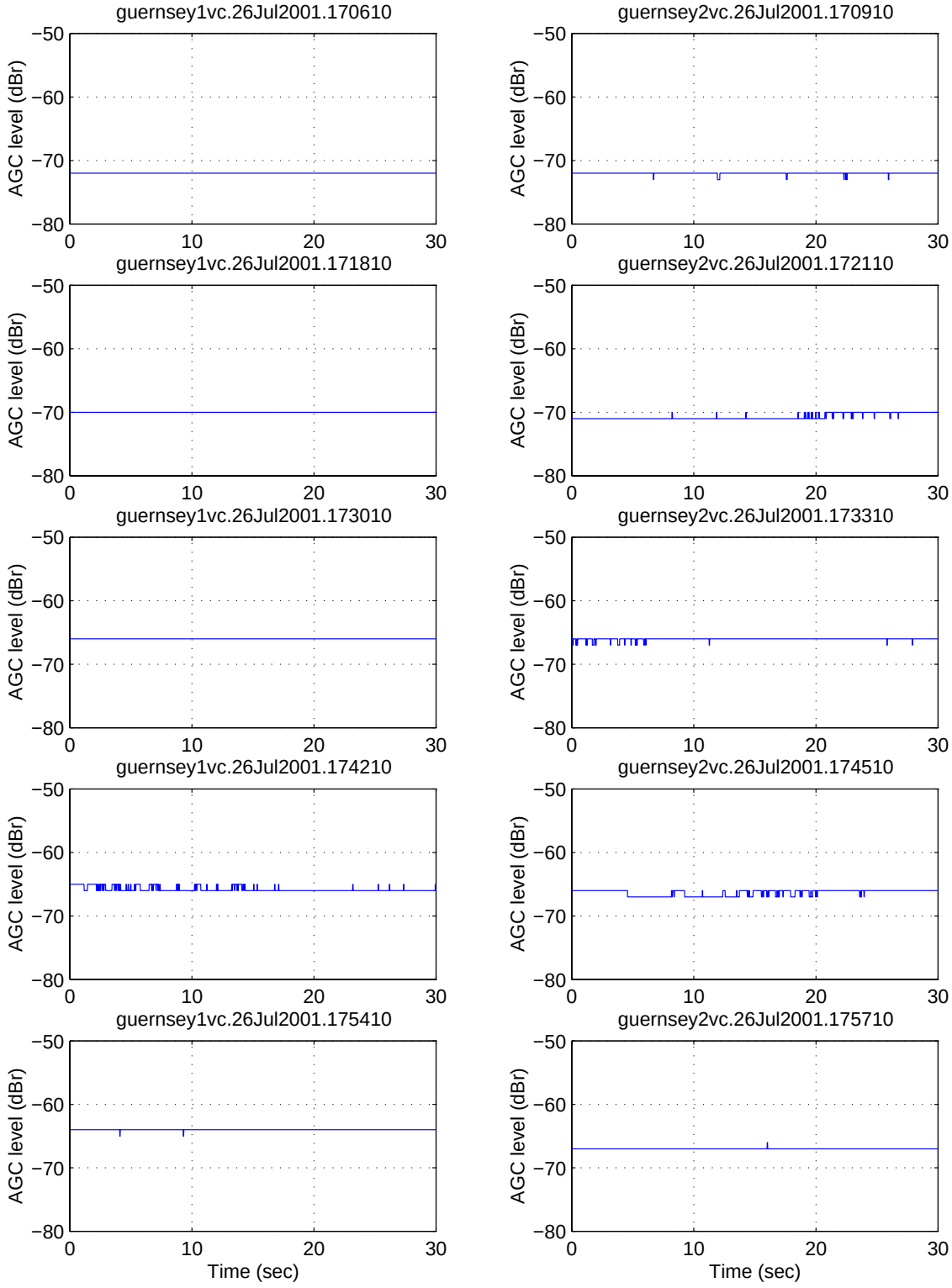

Figure 5.15: Signal amplitude vs time for Jersey-Guernsey F1 and F2 vertical signal during ESS on a hot day

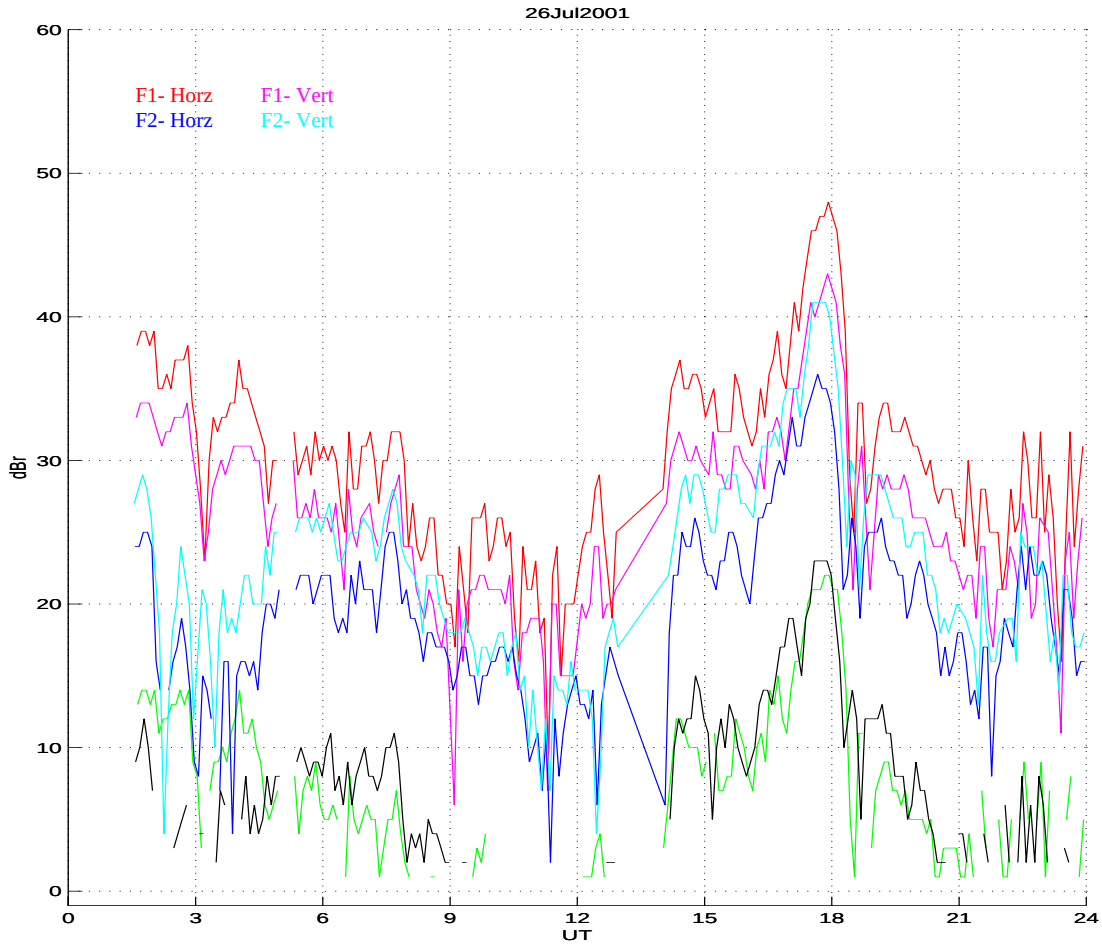

Figure 5.16: Signal strength variation on 26th July 2001 (mean value plotted)

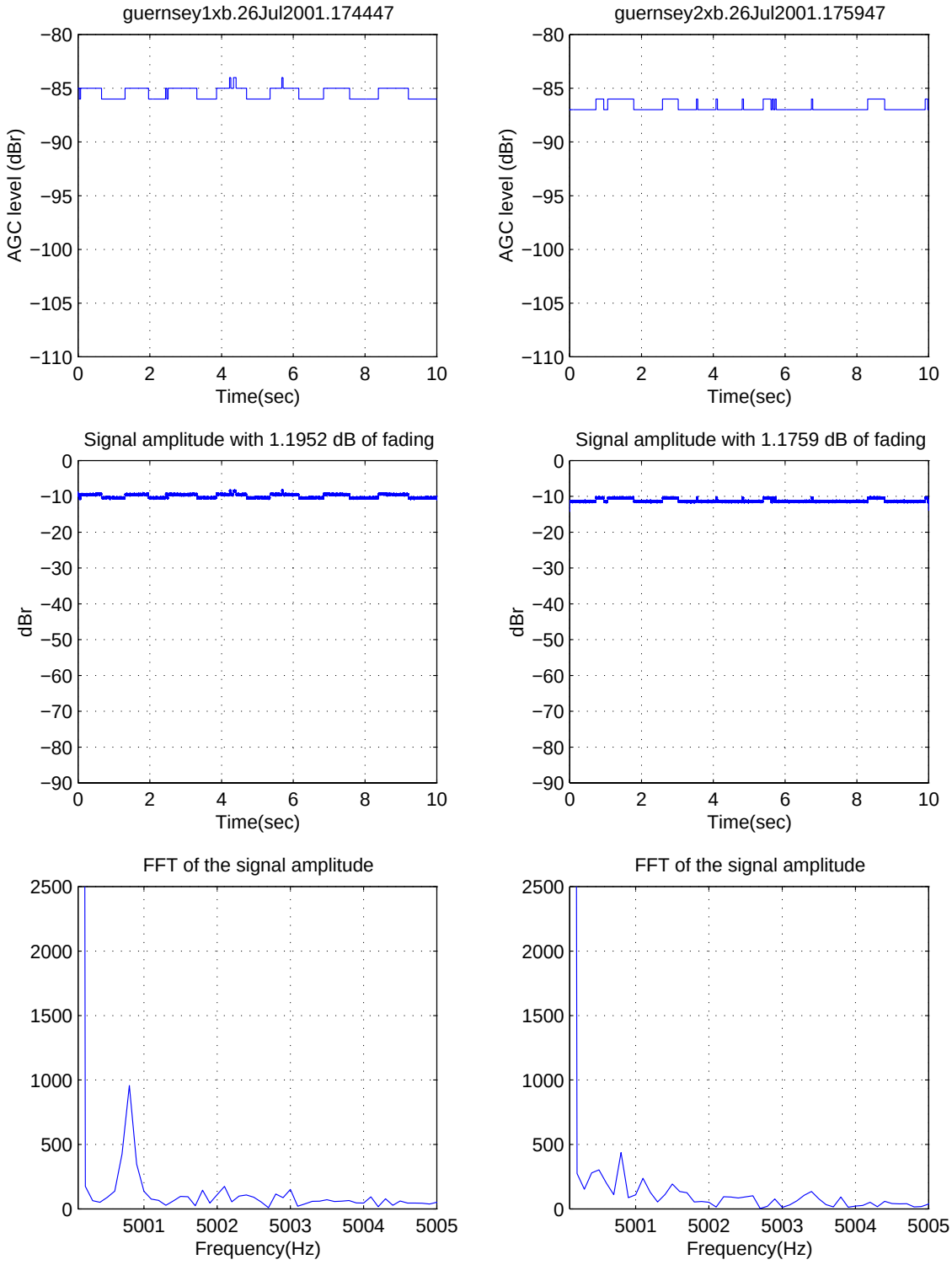

Figure 5.17: Cross polar signal characteristic during summer time when ESS occurred

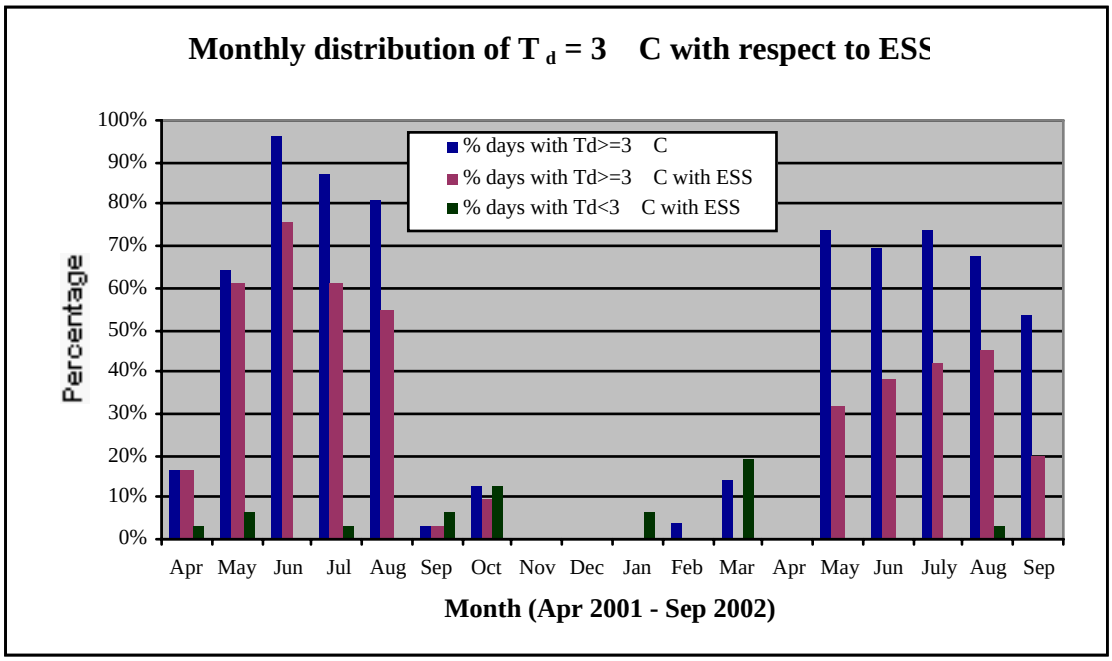

Figure 5.18: Monthly distribution with T_d threshold set at 3°C (Note* no data available for April 2002)

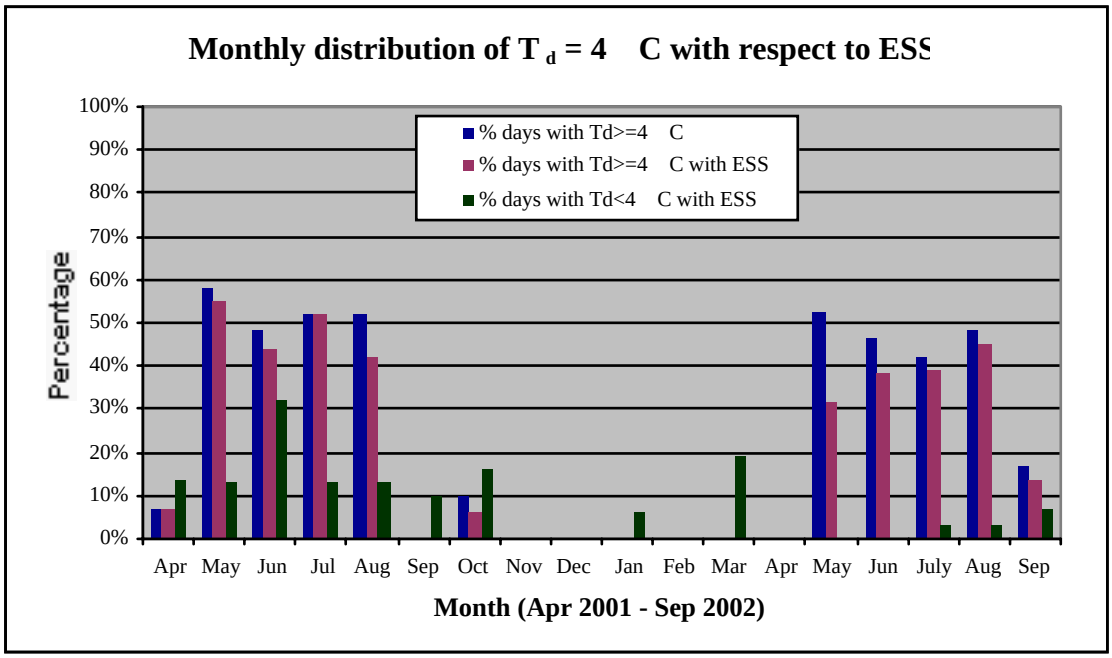

Figure 5.19: Monthly distribution with T_d threshold set at 4°C

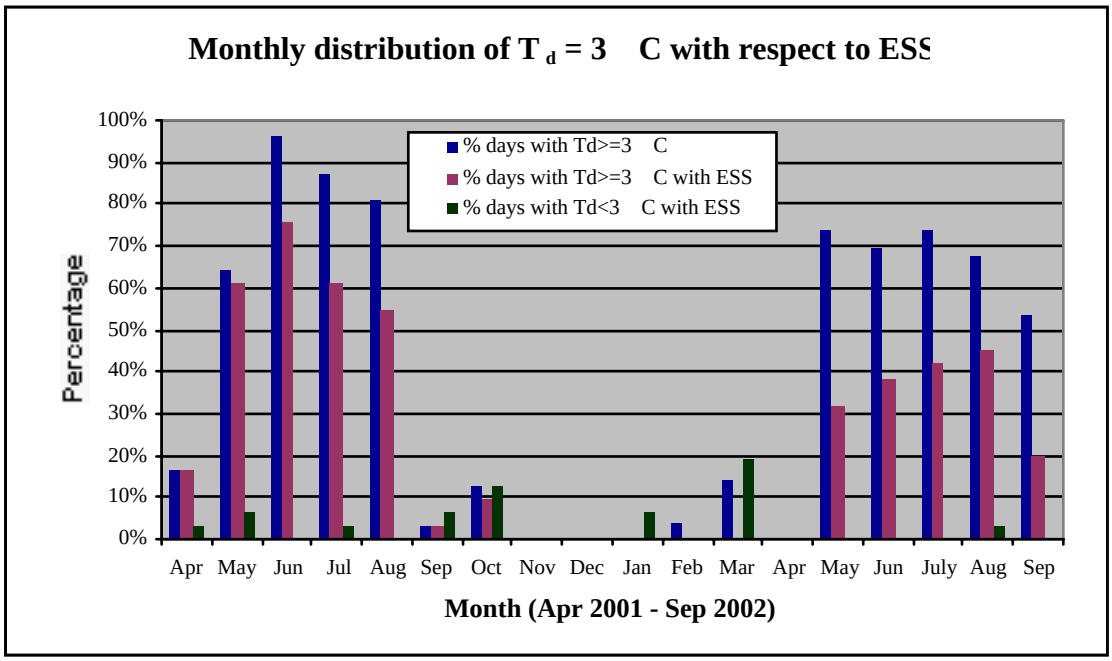

Figure 5.20: Monthly distribution with T_d threshold set at 5°C

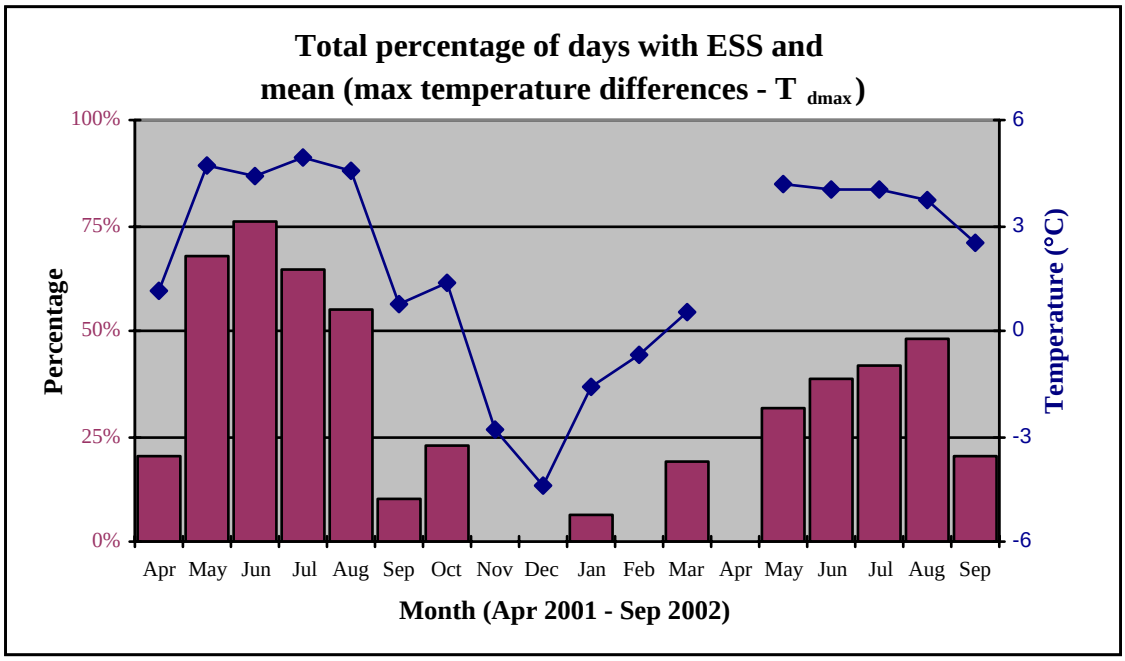

Figure 5.21: Monthly statistic displaying ESS from April 2001 until September 2002 with respect to mean T_{dmax}

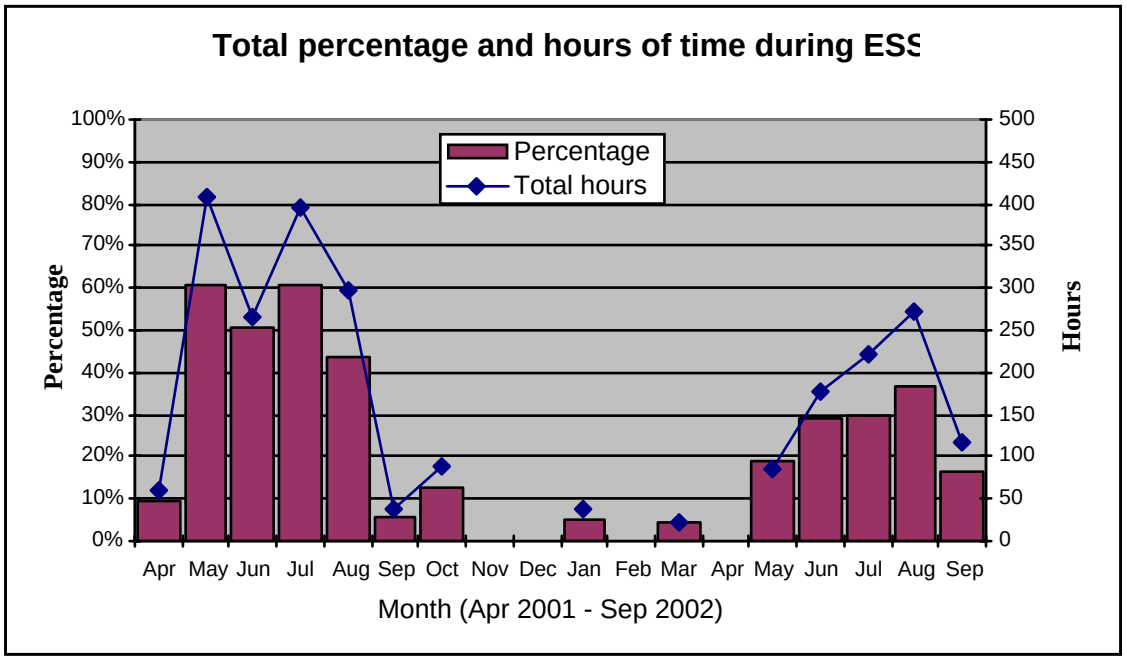

Figure 5.22: Monthly statistic displaying total percentage and number of hours of ESS occurred from April 2001 until September 2002 for Jersey-Guernsey

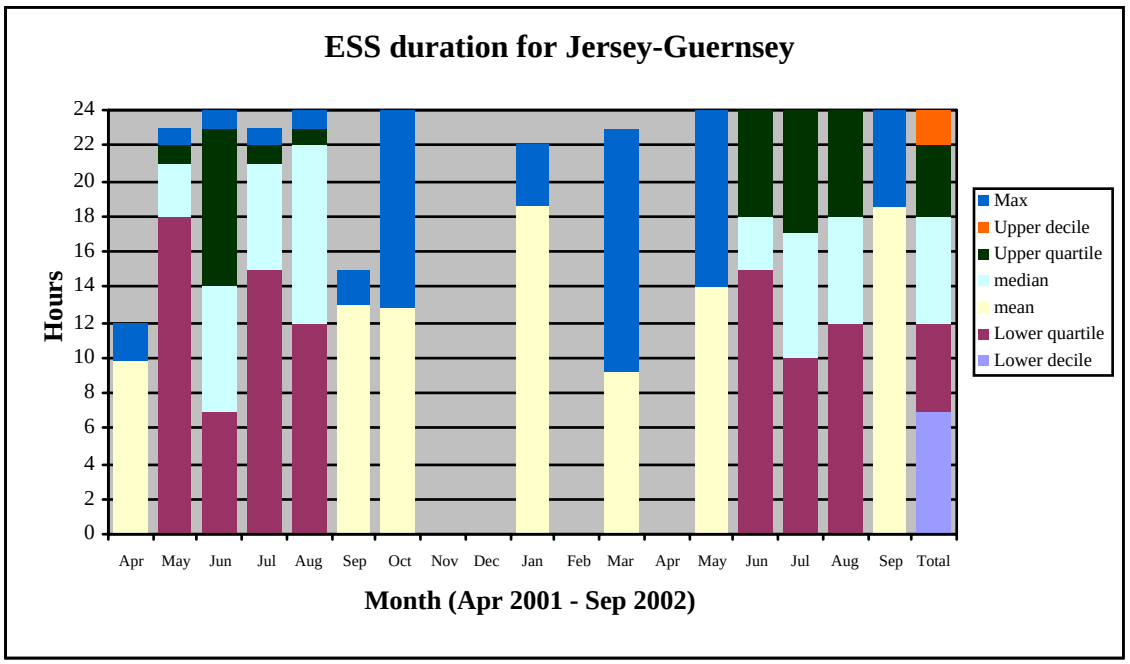

Figure 5.23: Monthly statistic displaying the duration (showed at the top of each colour code) of ESS occurrence for Jersey -Guernsey path. The total statistic between April2001 until September 2002 was showed at the far right of the chart (note that the upper decile value is the same as the maximum hours). Maximum and mean values were only used for Apr/Sep/Oct 2001 and Jan/Mar/May/Sep 2002 due to fewer number of ESS days occurred during these months. Note that the upper quartiles of Jun/Jul/Aug 2002 are the same as the maximum hours

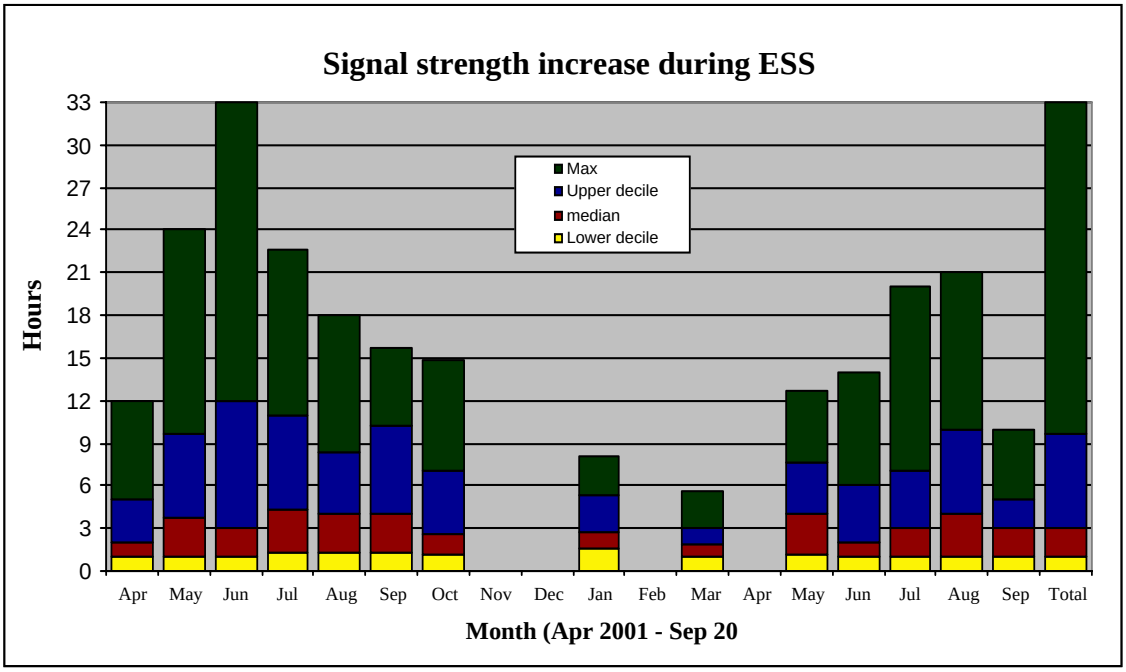

Figure 5.24: Monthly statistic displaying the maximum, median and upper/lower decile value of signal strength increase during ESS for Jersey-Guernsey (Note that the total statistic from April 2001 until September 2002 is shown on the right side of the chart)

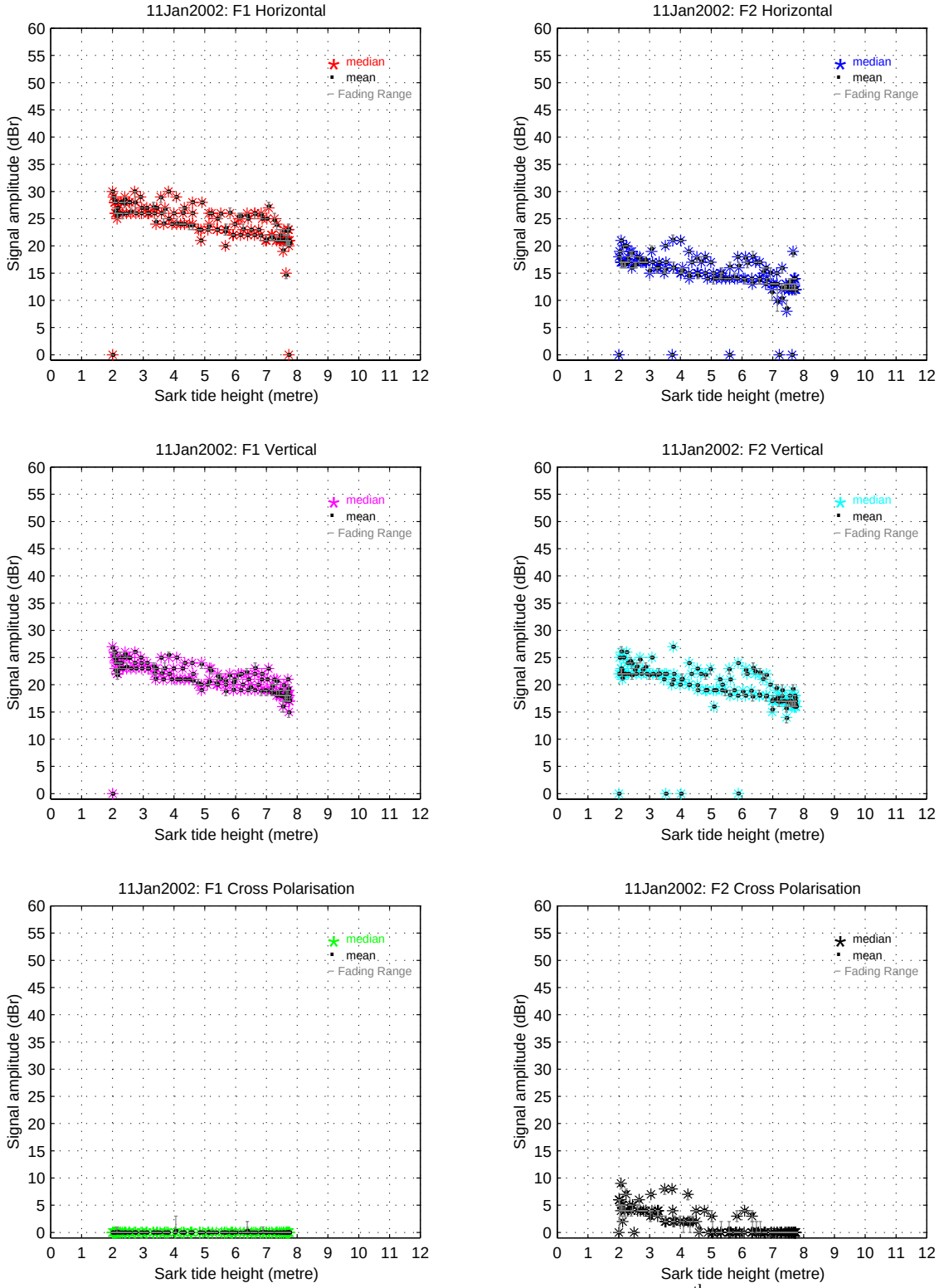

Figure 5.25: Signal strength vs. tide height on a winter day (11th Jan 2002) when ESS occurred

5.3 Signal behaviour from receiving site (2)- Isl de Raz (Alderney)

The receiving system in Isl de Raz (Alderney) was set up during the period of Oct/Nov 2001and since it is dependent on solar power, missing data within a day is expected especially during the spring, autumn and winter periods due to lesser daylight. Data from Alderney receiving site was disrupted a number of times due to failing transmitter system and wind damaged receiver antenna etc. As a result, data during the period of February until April 2002 was sparse and of low quantity. Nevertheless, data received for all seasons were analysed and from these data, the signal behaviour during the period of measurements in Alderney can be segregated into a few different categories such as calm sea, high fading and summer day.

5.3.1 Calm sea (Jersey to Alderney)

The weather and amplitude plot of a calm day in autumn (18th Nov 2001), which is similar to the observation for calm day (Jersey to Guernsey) is shown in Figure 5.26. The tide height versus amplitude plot with half a cycle of tide is shown in Figure5.27. From these figures, fading range of around 2 dB and slight irregular linear shape (signal fluctuation along the linear function) were observed as compared to Figure 5.2 (calm day for Jersey-Guernsey path).

5.3.2 High fading (Jersey to Alderney)

Three different days with high fading will be discussed in this section during autumn, winter and spring (approaching summer). Figure 5.28 shows the weather data with amplitude plot during a high fading autumn day (17th Nov 2001). Figure 5.29 shows both the Jersey-Alderney (1) and Jersey-Alderney (2) signal amplitude plot and Figure 5.30 shows the tide height vs. signal amplitude for half a tide height cycle for Jersey-Alderney (1). From these figures, high fading range of around 10 dB and the usual pattern which signal strength varies steadily with changing tide height (around 1.2 dB per metre) was observed. In addition, signal amplitude scattering around the linear region was also observed.

Figure 5.31 and Figure 5.32 showed the signal amplitude with weather parameter and against the tidal effect respectively during a high fading day in winter on 10thDec2001when only the vertically polarised signal was available (horizontal antenna broken). For this day, the high signal-fading characteristic within a short period of time

(30 seconds) is shown in Figure 5.33 and fading around 3 to 10 dB was observed. From these figures, it is evident that the winter period produces the same high signal-fading characteristic as in autumn. Further analysis was done on this high fading phenomenon by applying the FFT to the AF measurement. Both the FFT and sounder plot for both F1 and F2 (vertical polarisation) on the above mentioned winter day are shown in Figure 5.34. The matlab script can be found in Appendix A (script 5). From this figure, 2 and 3 different components in the received signal were observed for both F1 and F2 respectively. In addition, the signal characteristic plot in Figure 5.35 shows fading of up to 6 dB. These show that the received signal was a result of multipath propagation.

During a calm spring day in May 2002 when the temperature began to rise, the high fading phenomenon changes its usual pattern. Instead of it occurring over the whole period of the total time as shown in Figure 5.30 during autumn, the fast fading range increases substantially by a few dB only when the tide is approaching its peak. These are shown in Figure 5.36 and Figure 5.37 during half a tidal cycle. In addition, Figure 5.38 and Figure 5.39 show the signal amplitude versus time characteristic within an hour period at both low and high tide respectively.

The statistics for high fading days in comparison with low fading days for Jersey to Alderney path are shown in Figure 5.40. From this figure, the total percentage of time for high fading phenomenon decreased from around 80 to 30% during the autumn/winter period from November 2001 until January 2002. Note that during this period, the equipment in Alderney has just been set up and due to winter period, the total data hours collected within this period of time are much lower than during summer 2002. Therefore, it was observed that the total time (hours) for high fading occurrence ranges from 60 to 20 hours during the above-mentioned period. During the period from May 2002 until September 2002, the receiving system at Alderney was working much more properly and together with the approaching summer period, more data in a day were collected. From Figure 5.40, the high fading phenomenon occurrence ranges around 35 to 48% of the total time (in hours) during the summer period and increased to around 66% when it approached September 2002 when autumn began. The fading range/period statistics for both autumn (17^{th} Nov 2001) and "cool" summer day (12^{th} Jun 2002) respectively are shown in Table 5.1. From this table, the maximum fading ranges for both autumn and summer day were around 10 dB and 7 dB respectively and the average fading period for both days was around 7 seconds. Therefore, from the

above results in comparison with the data from Jersey-Guernsey, it is evident that high fading phenomenon only occurred across Jersey-Alderney path.

In regards to cross-polar signal in Jersey-Alderney (1) during a high fading day, the signal amplitude plot in Figure 5.41 shows a fading of around 10 dB. Since the receiver agc level has reached its minimum level, the signal obtained above could be noise interference.

5.3.3 Summer day (Jersey to Alderney)

Two types of summer or hot days are discussed in this section, the first is a relatively average T_d (temperature difference between T_J and T_{sea}) type on a warm day and the latter will be a high T_d type during a hot day. Figures 5.42 and 5.43 show the signal strength with weather plots and the signal amplitude comparison plot for both Jersey-Alderney (1) and Jersey-Guernsey (2) when T_d was around 4°C respectively on 12thMay2002. Figures 5.44 and 5.45 showed the signal amplitude versus tide height plot for both Jersey-Alderney (1) and Jersey-Guernsey (2) respectively on the same day. Note that for this day, the horizontal receiving antenna was not working properly, hence horizontal data for both F1 and F2 were not available. These figures show that the signal amplitude at Jersey-Alderney (1) could increase up to around 10 dB higher than its normal value when ESS occurred. In contrast, the signal amplitude increases at Jersey-Guernsey (2) was around 3 dB. Nevertheless, the fading range for both Jersey-Alderney (1) and Jersey-Guernsey (2) when ESS occurred was around 2 dB. By comparing the ESS occurrences for both receiving locations during August 2002 with respect to Alderney total data time (266 hours), Figure 5.46 showed that ESS occurred almost at the same period for both receiving locations.

Figures 5.47 and 5.48 show that during a hot day in the summer when T_d was above the threshold temperature of 4°C, ESS occurred with signal amplitude up to 35 dB. Although the fading range during ESS is very small, high fading phenomenon will resume itself when ESS is not present or only present for a couple of hours in a day as shown in Figure 5.49.

5.3.4 Jersey -Guernsey (1) and Jersey-Alderney (2) - signal analysis

During the period of Oct/Nov 2001, the 2nd receiving site at Isl de Raz (Alderney) was set up and AGC signals are collected at both receiving sites as the transmitter is

transmitting to either of the receiving station. This is to observe the difference in signal strength at both ends of the receiving sites at the same period of time scale though both receiving sites are approximately 60° apart from each other from the transmitter point of view (see Figure 4.1). Note that the receiving site at Alderney is around 15 km further than the receiving site in Guernsey. This section will discuss and compare the AGC signal [Jersey-Guernsey (1) to Jersey-Alderney (2)] and [Jersey-Guernsey (2) to Jersey-Alderney (1)] collected at both the Guernsey and Alderney receiving sites. The descriptions of these four types of AGC signals are as follows:

- Jersey-Guernsey (1): AGC signal obtained as a result of direct transmission from Jersey to Guernsey
- Jersey-Guernsey (2): AGC signal obtained as a result of indirect transmission from Jersey to Guernsey
- Jersey-Alderney (1): AGC signal obtained as a result of direct transmission from Jersey to Alderney
- Jersey-Alderney (2): AGC signal obtained as a result of indirect transmission from Jersey to Alderney

Figure 5.50 shows both sets of signal amplitude plots during autumn (17th Nov 2001). The top figure shows the Jersey-Guernsey (1) signal amplitude plot while the bottom figure shows the Jersey-Guernsey (2) signal amplitude plot. From this figure, the signal amplitude plot for Jersey-Guernsey (2) follows the usual steady variation with the tide height. Figure 5.51 shows both sets of amplitude plot of Jersey-Guernsey (1) and Jersey-Alderney (2) on the same day. From this figure, the Guernsey signal received at Alderney receiving site [Jersey-Alderney (2)] was experiencing more attenuation and fading. Figure 5.52, 5.53, 5.54 and 5.55 show the F1/F2 signal amplitude (dB) plot of both Jersey-Guernsey (1) and Jersey-Alderney (2) signal, within an hour of time period with respect to both horizontal and vertical signals. Both signals are compared and fading of around 7 dB within a 30 seconds period is shown in Jersey-Alderney (2) signal. In contrast, agc level across Jersey to Guernsey [Jersey-Guernsey (1)] provided no evidence of high fading due to whatever sea states effects.

Figures 5.56, 5.57, 5.58 and 5.59 compare the signal amplitude plot between Jersey-Alderney (1) and Jersey-Guernsey (2) within an hour period for both F1 and F2, with both horizontal and vertical polarisation respectively. From these figures, fading of 10dB within a 30 seconds period was observed at Alderney receiving site [Jersey-

Alderney (1)] while in contrast, the Guernsey receiving site [Jersey-Guernsey (2)] experienced fading of 2 dB. These provided further evidence that on the same day, high fading occurred in Jersey-Alderney path only.

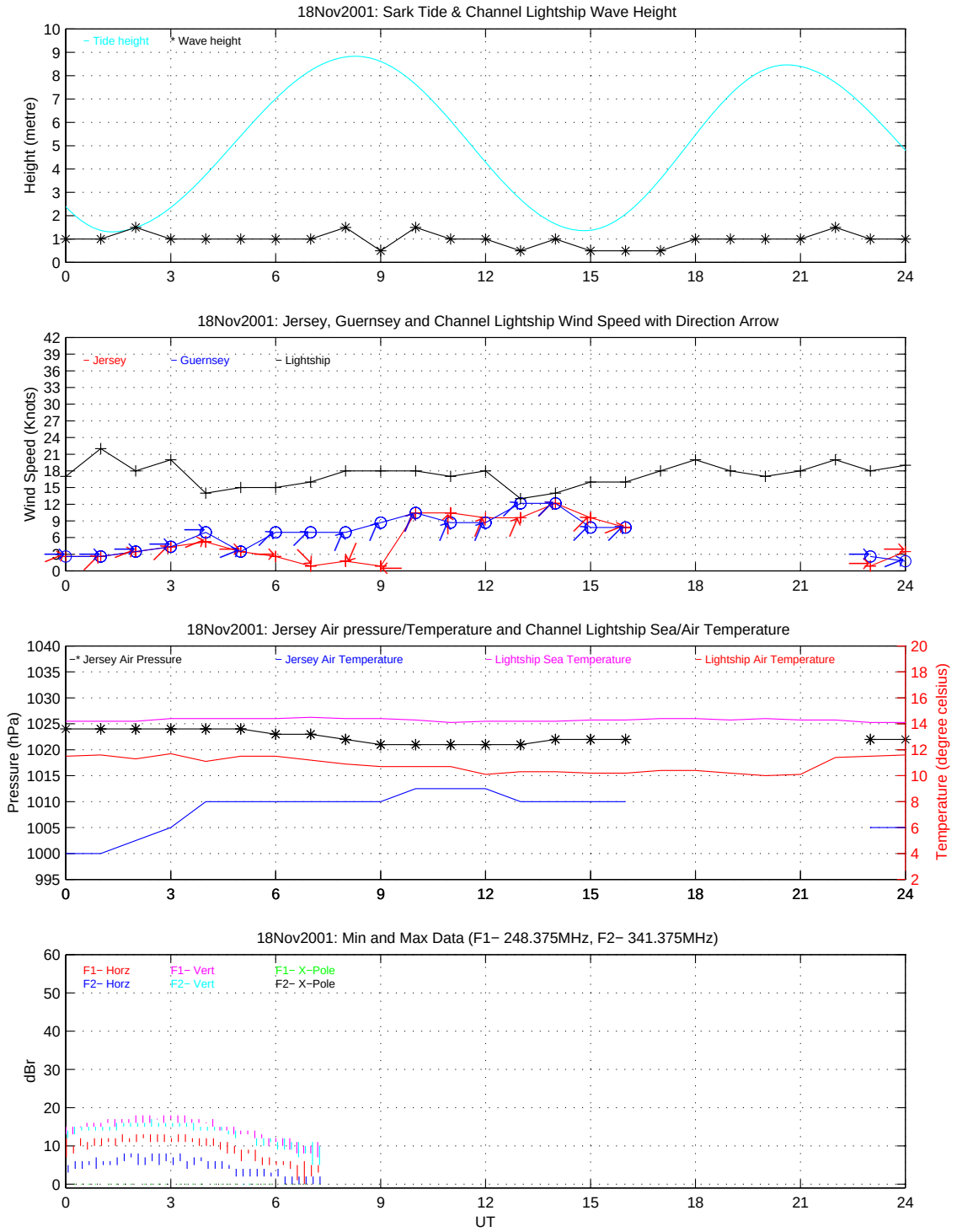

Figure 5.26: Signal strength plot on a calm autumn day (18th Nov 2001) with respect to various weather parameters

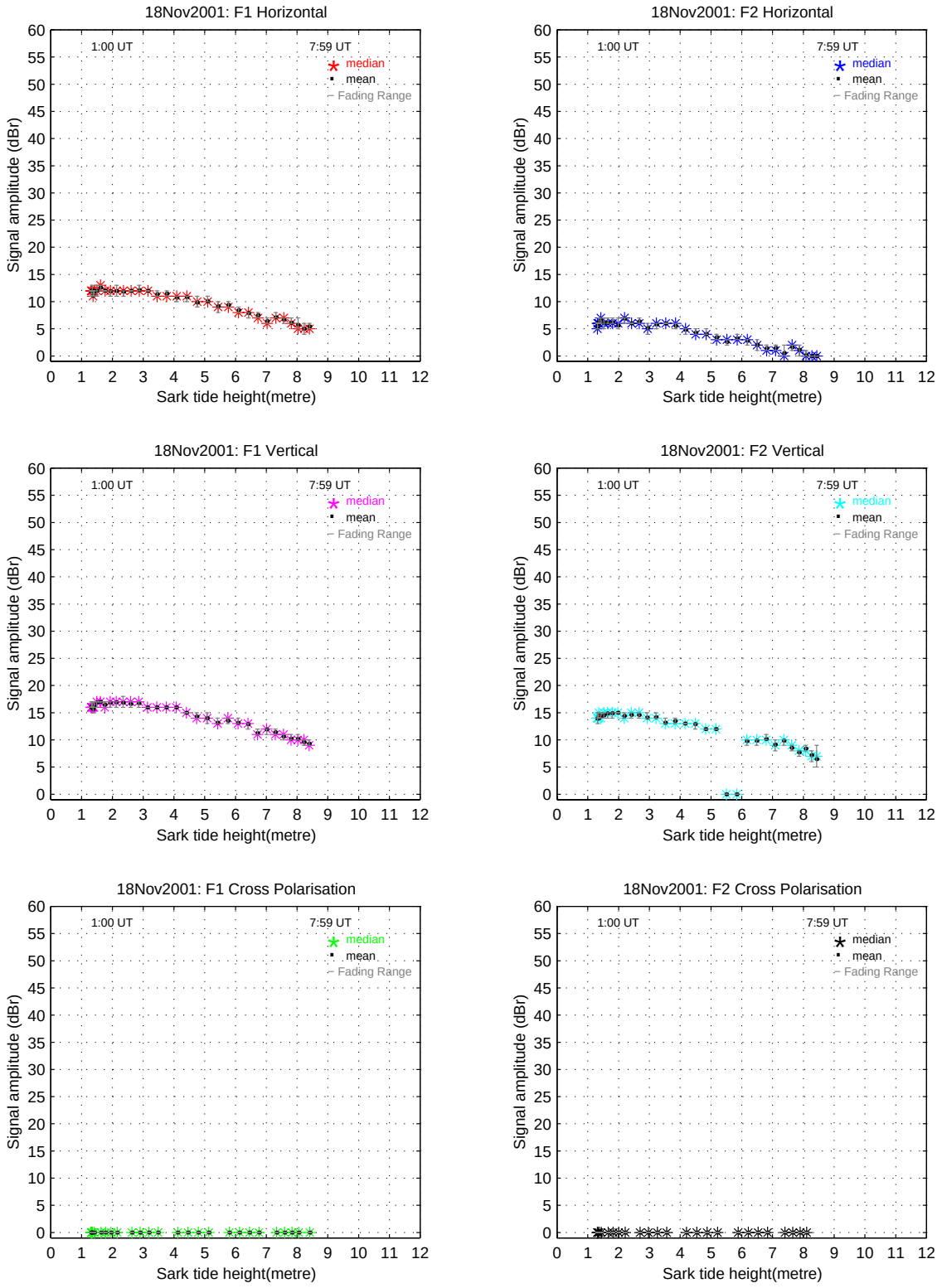

Figure 5.27: Signal strength vs tide height (half cycle from 01:00 until 07:59 UT) on a calm day in autumn (18th Nov 2001)

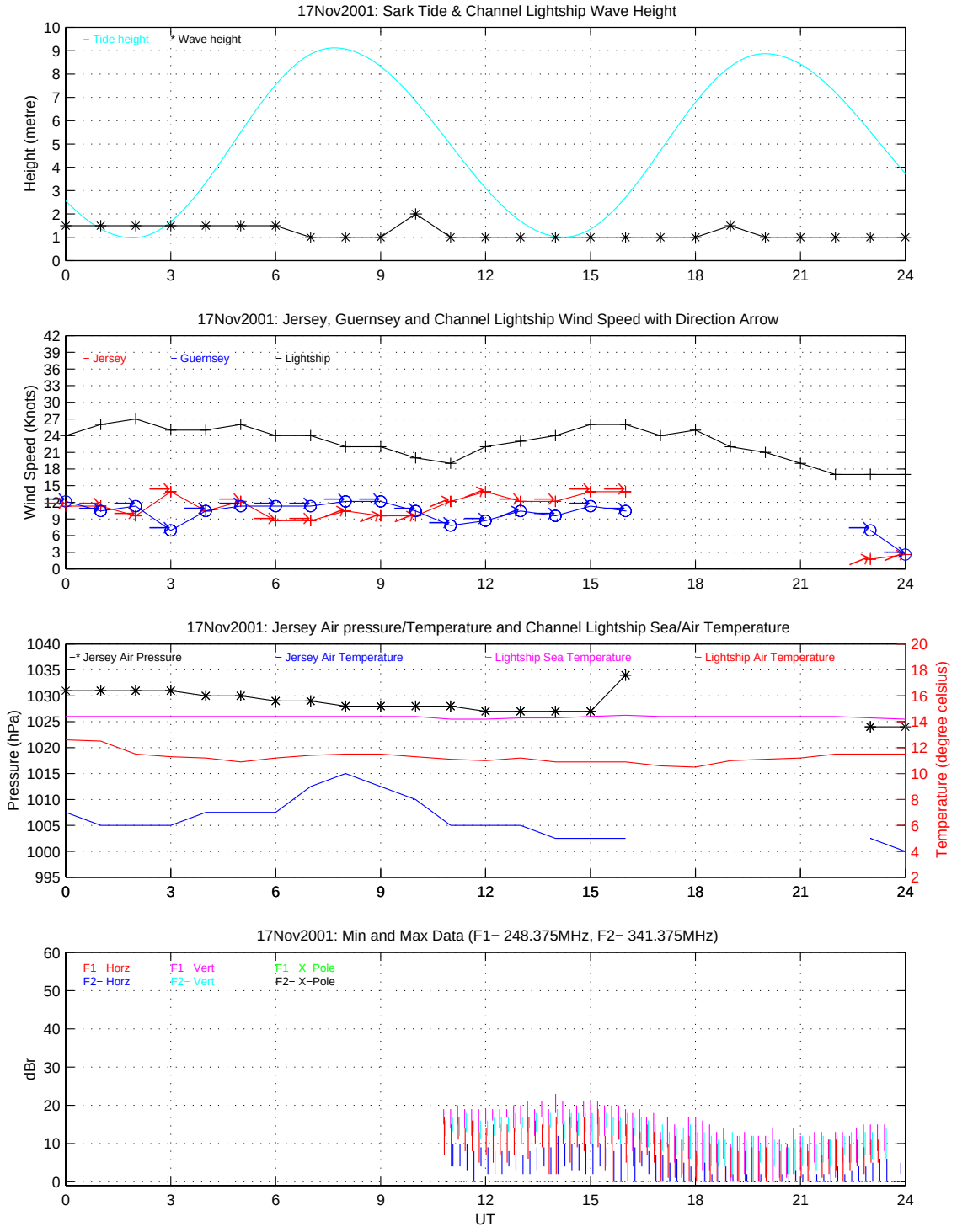

Figure 5.28: Signal strength plot on a high fading autumn day (17th Nov 2001) with respect to various weather parameters

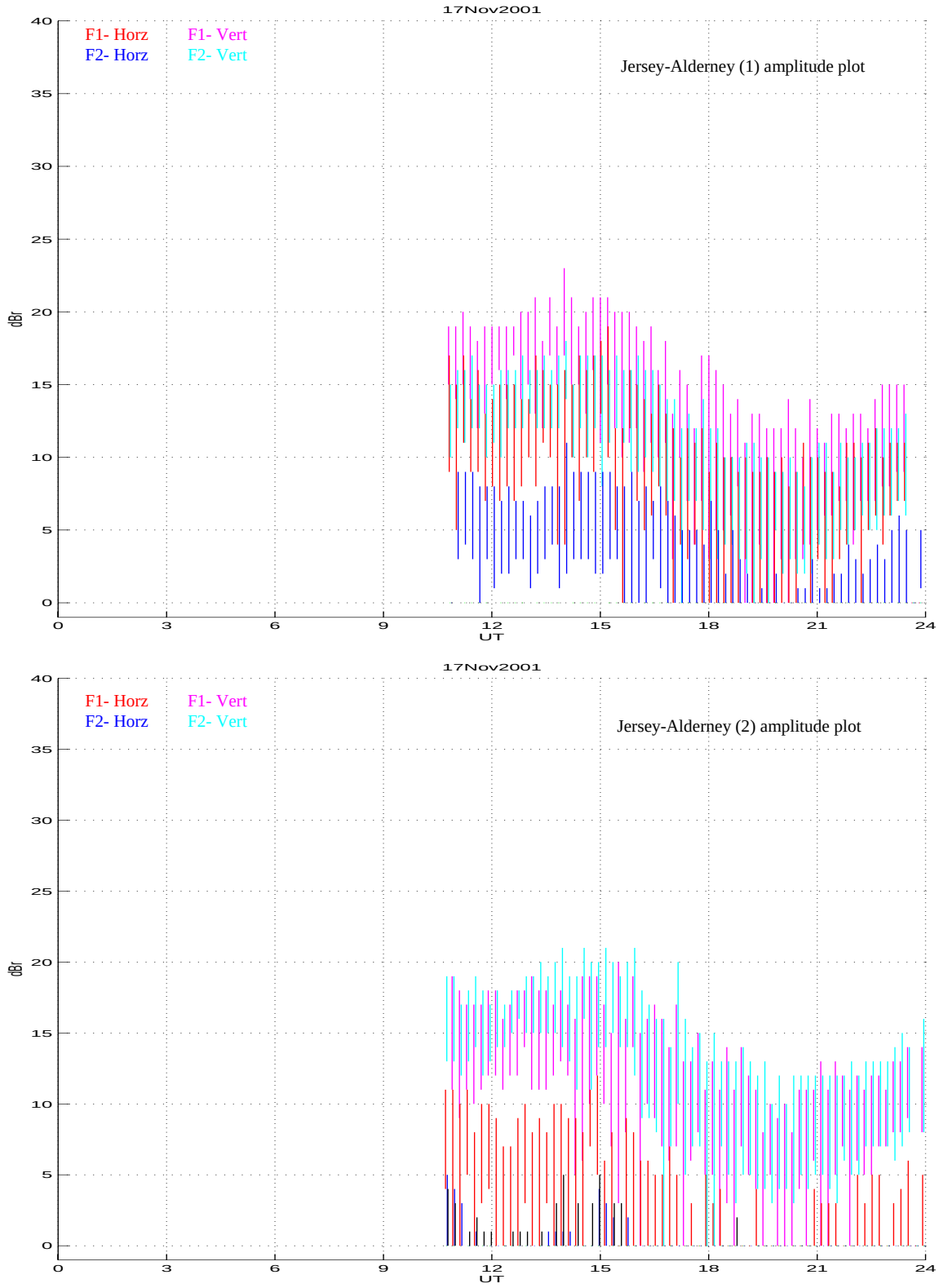

Figure 5.29: Jersey-Alderney (1) vs. Jersey-Alderney (2) amplitude plot

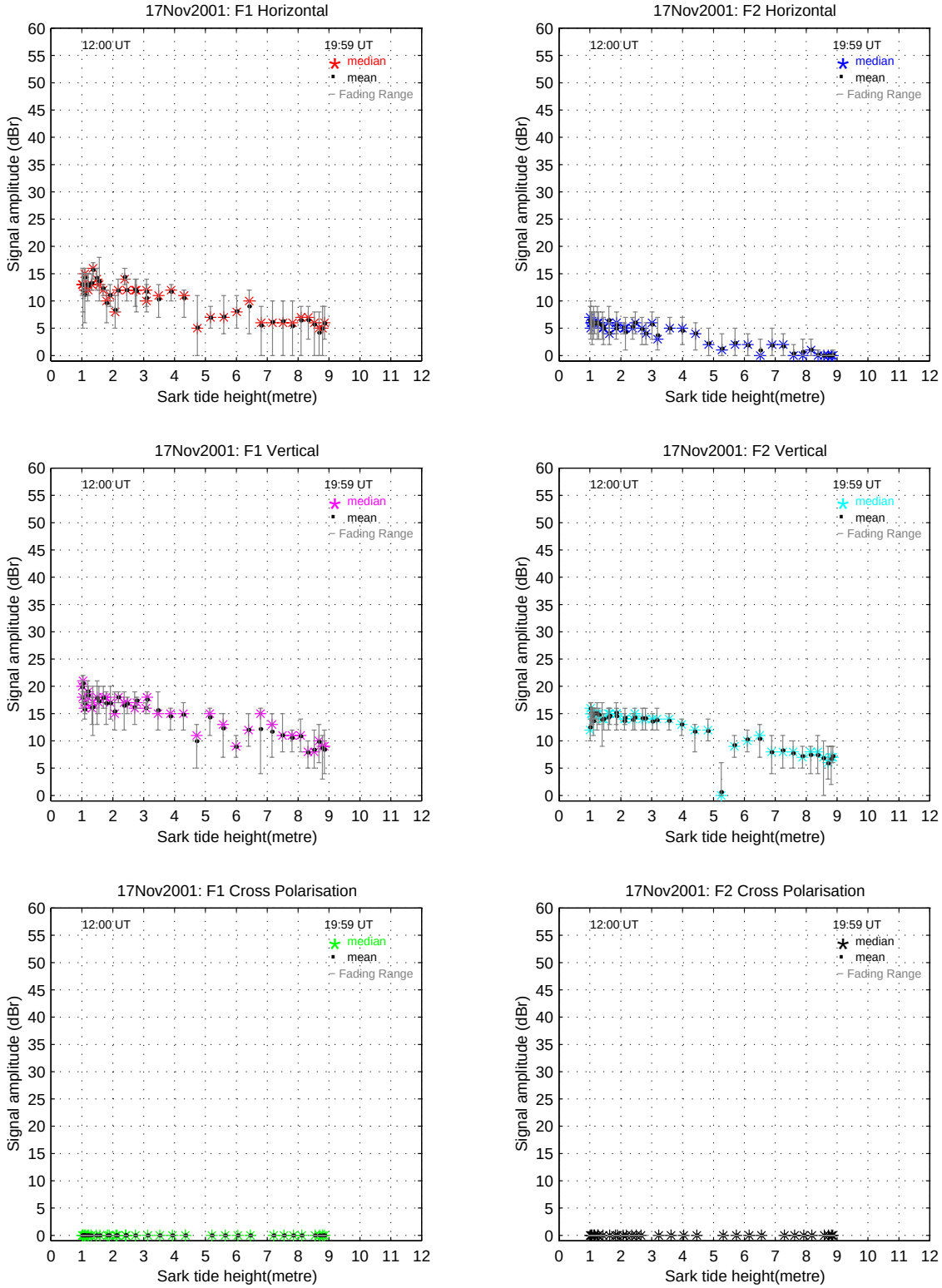

Figure 5.30: Jersey-Alderney (1) amplitude vs. tide height (half cycle from 12:00 until 19:59 UT) plot on a high fading day

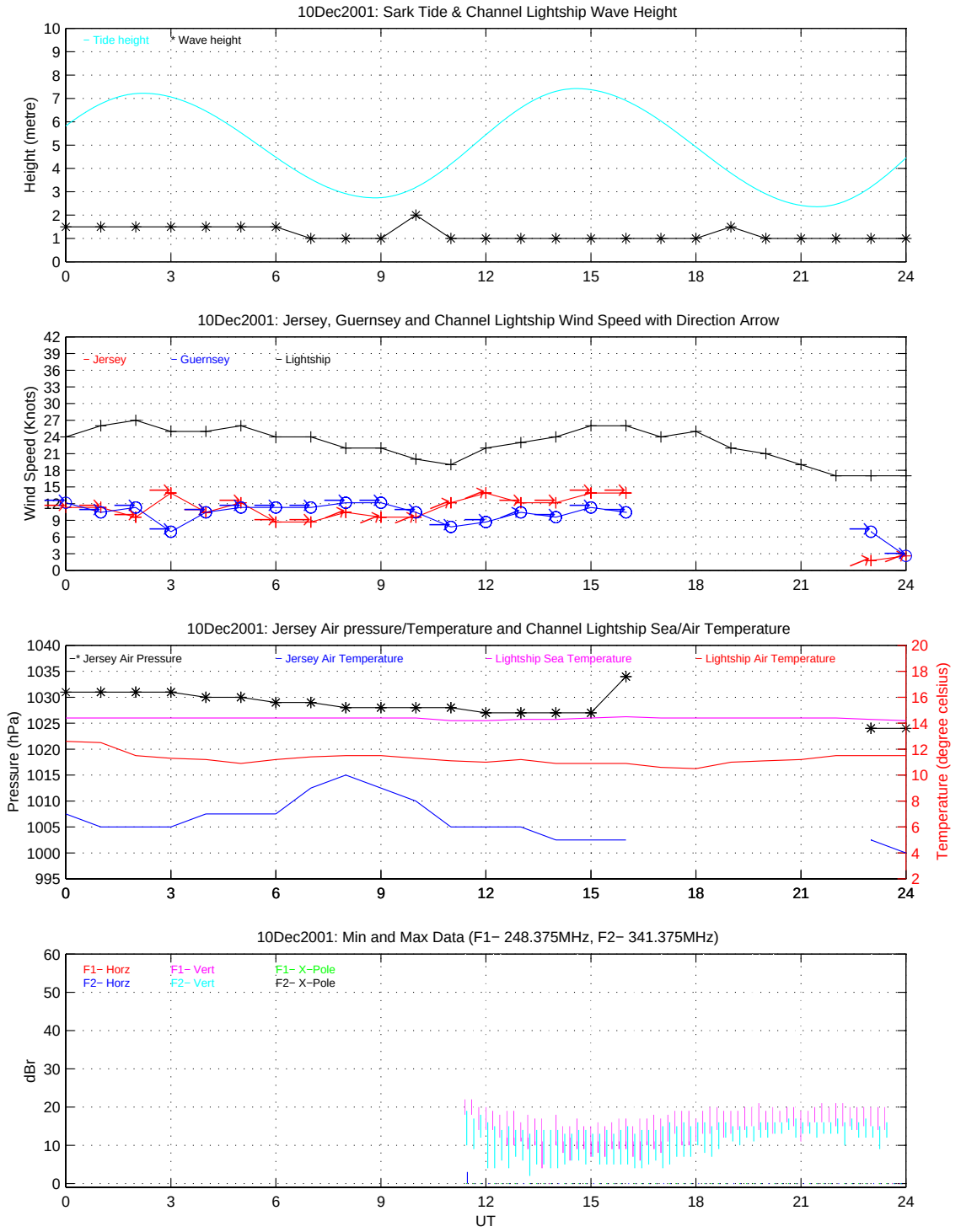

Figure 5.31: Signal strength plot on a high fading winter day (10^{th} Dec 2001) with respect to various weather parameters (horizontal signal not available due to broken antenna)

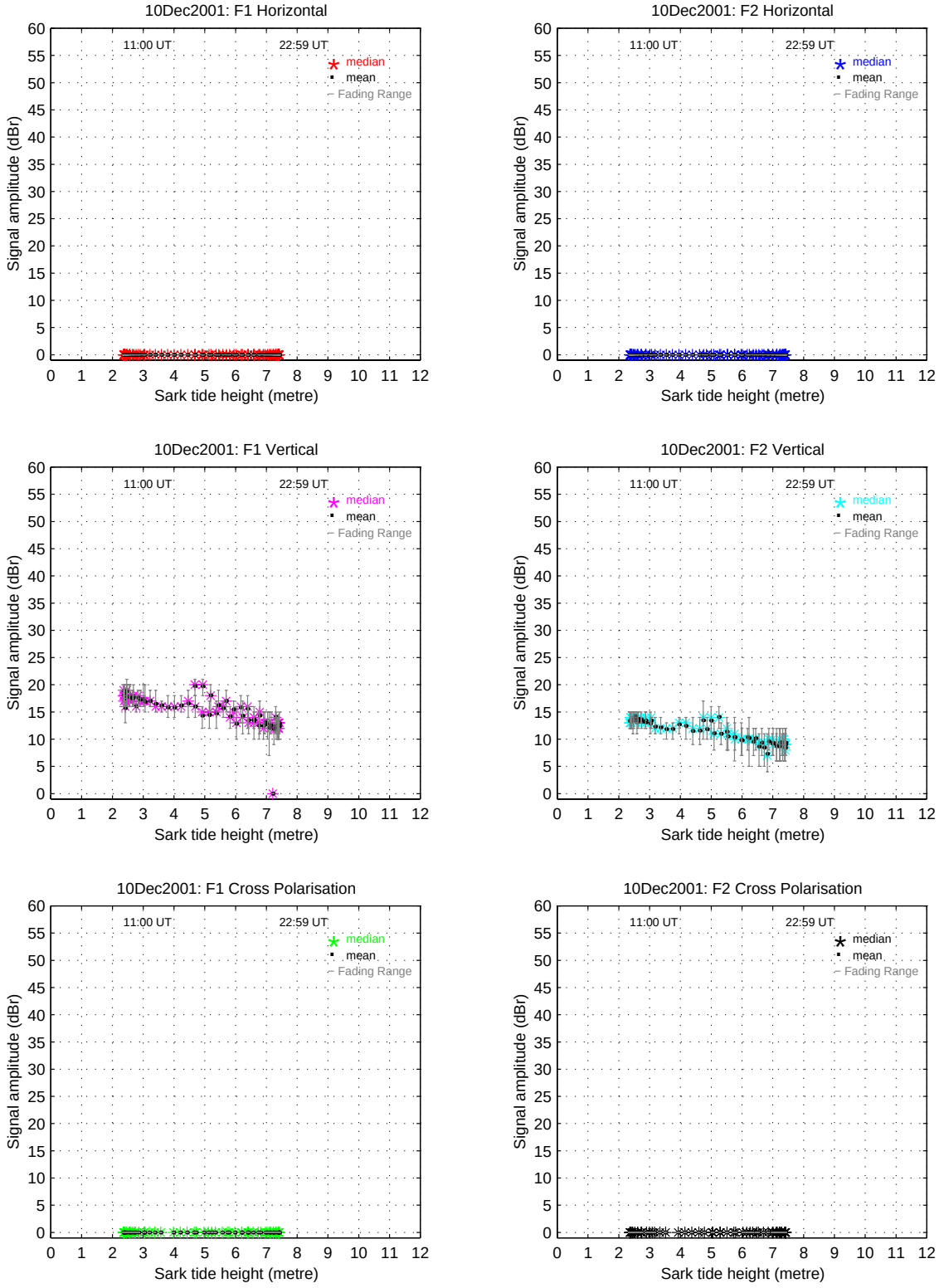

Figure 5.32: Signal strength vs tide height during a high fading day in winter (from 11:00 until 22:59 UT)

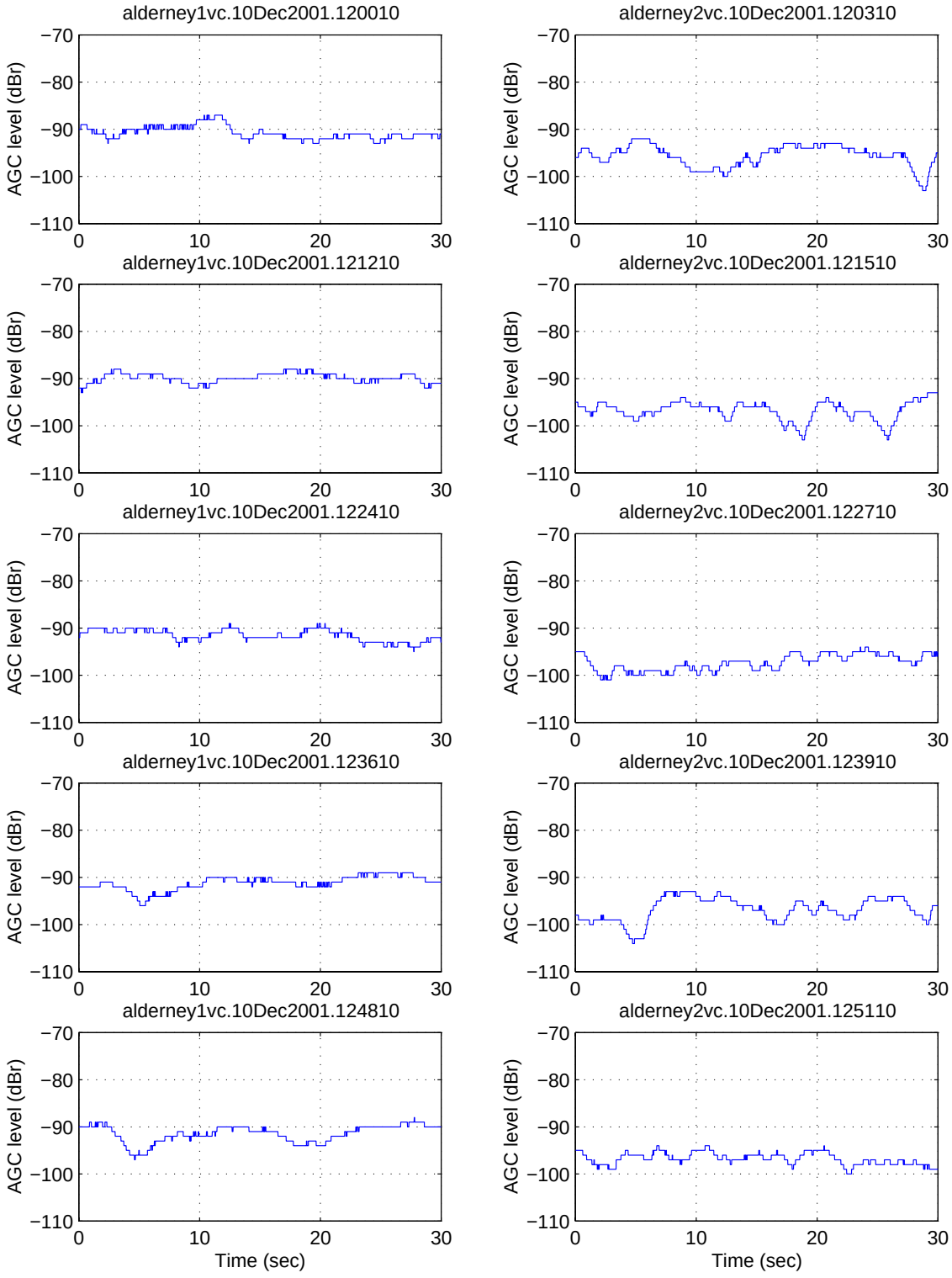

Figure 5.33: Signal amplitude vs time for Jersey-Alderney (1) F1 and F2 vertical signal on a high fading day during winter

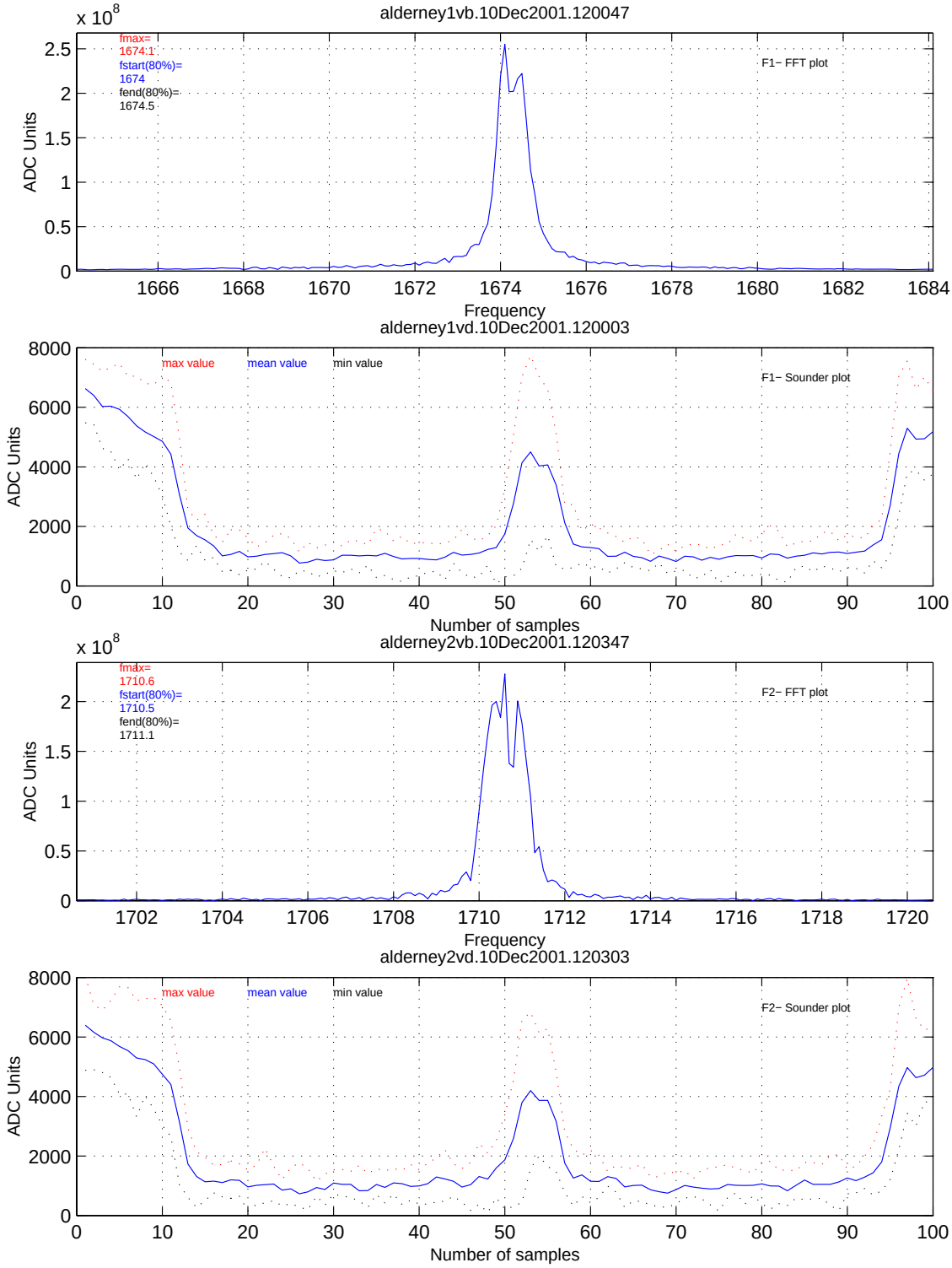

Figure 5.34: FFT and sounder plot during a high fading day in winter for both F1 and F2 (vertical)

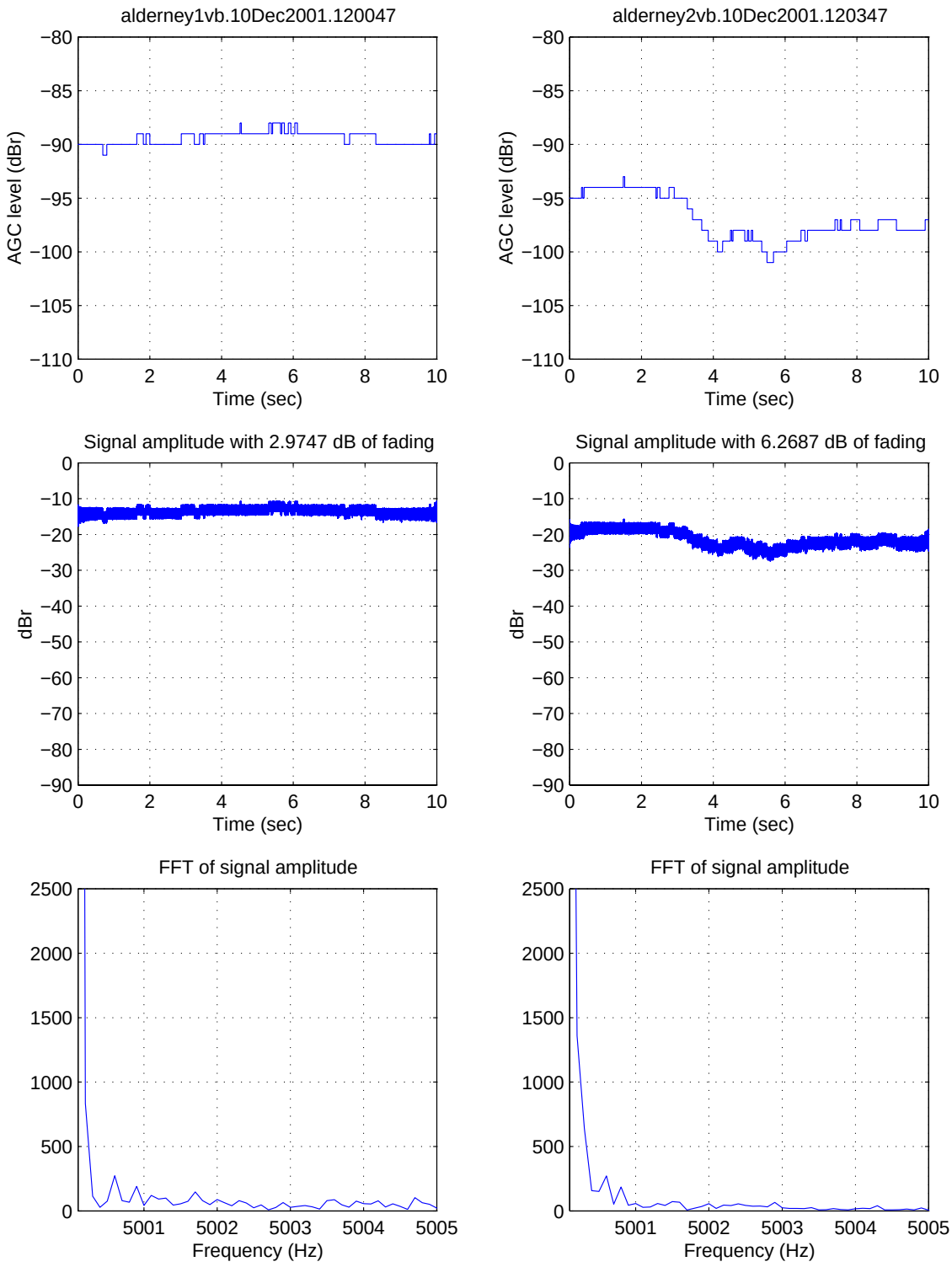

Figure 5.35: High fading signal characteristic for Jersey-Alderney (1): F1 and F2 (vertical)

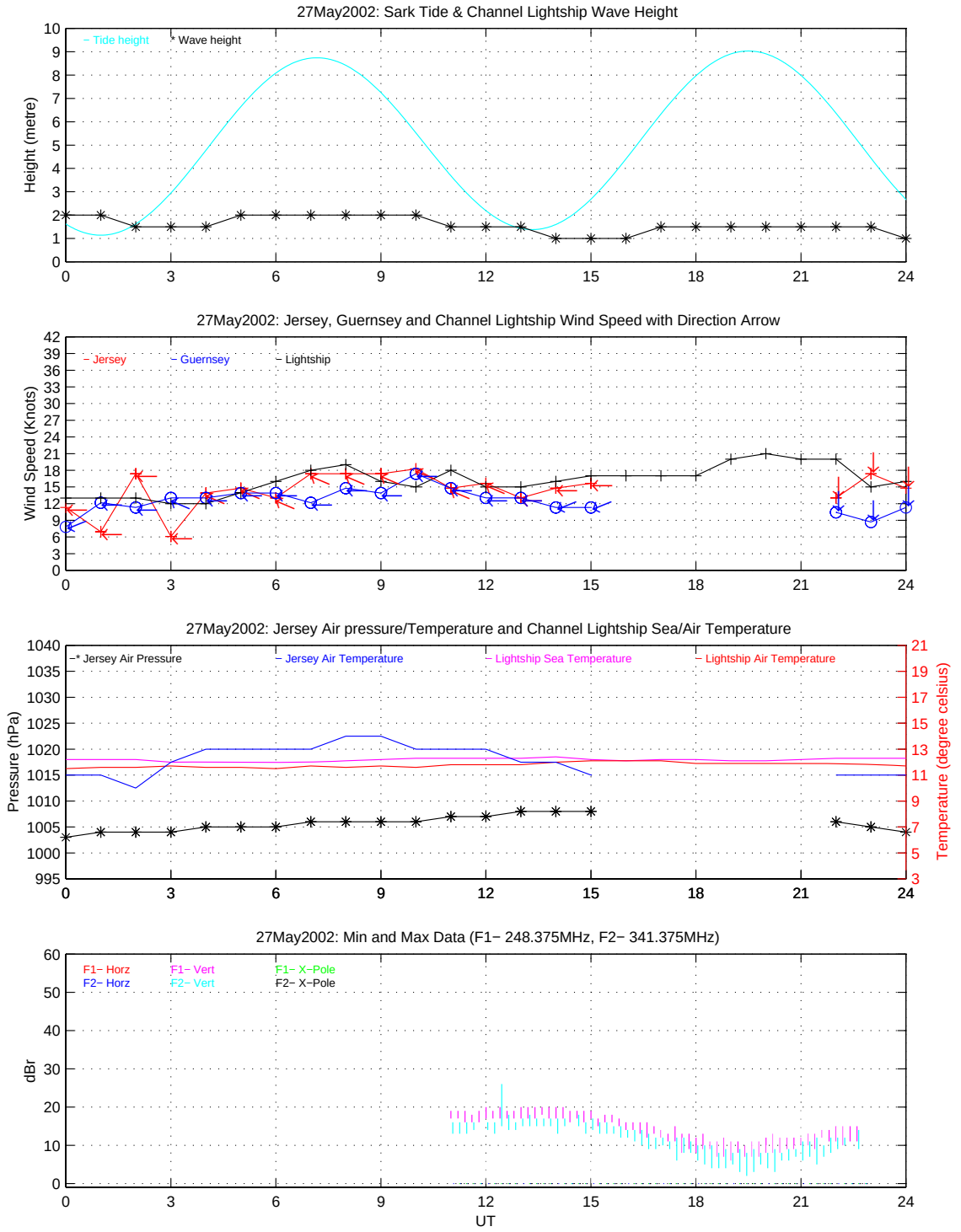

Figure 5.36: Signal strength plot on a calm spring day (27th May 2002) with respect to various weather parameters for Jersey-Alderney

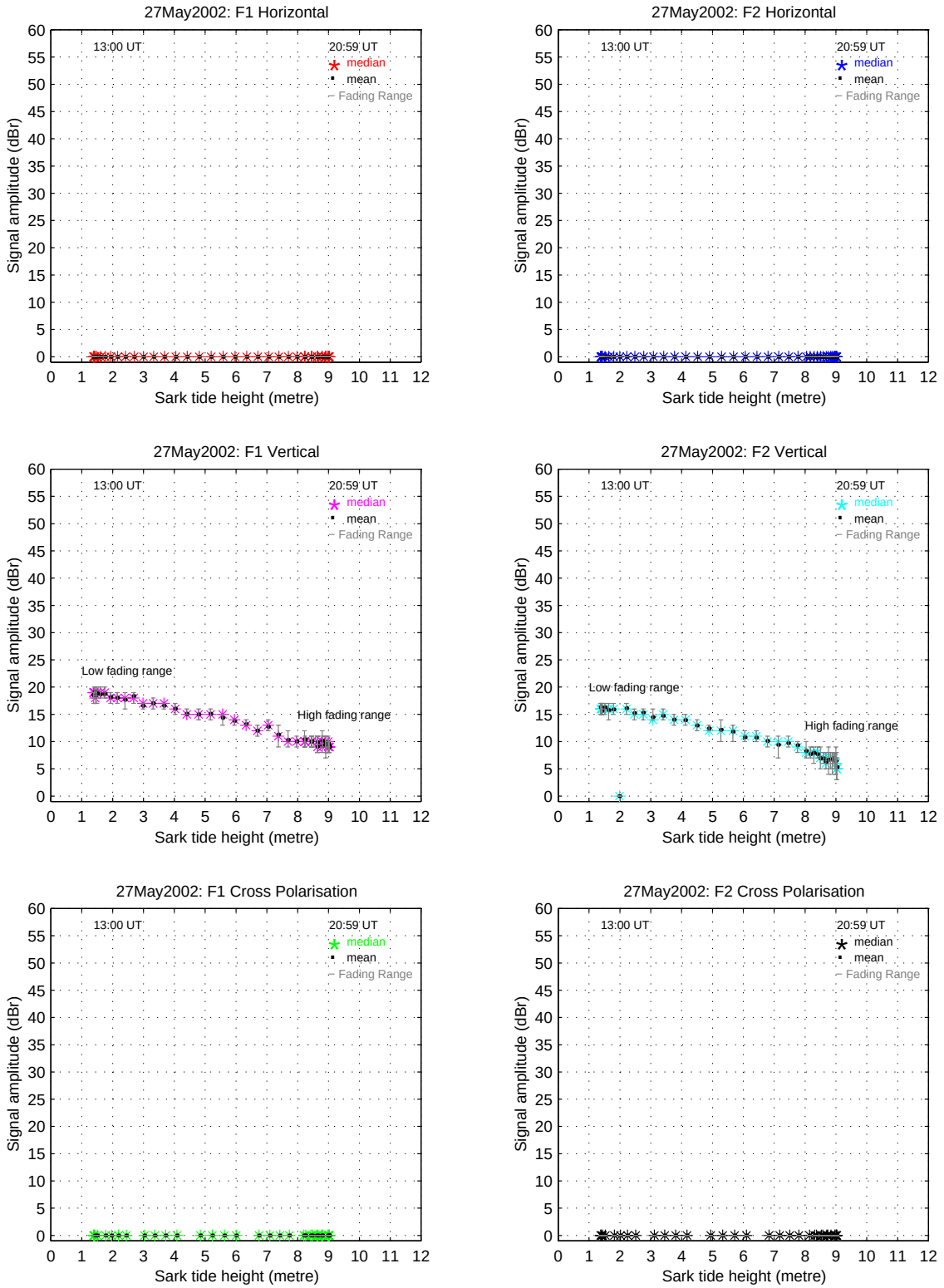

Figure 5.37: Signal strength vs tide height (half cycle from 13:00 until 20:59 UT) on a calm spring day (27th May 2002) with low and high fading range indication

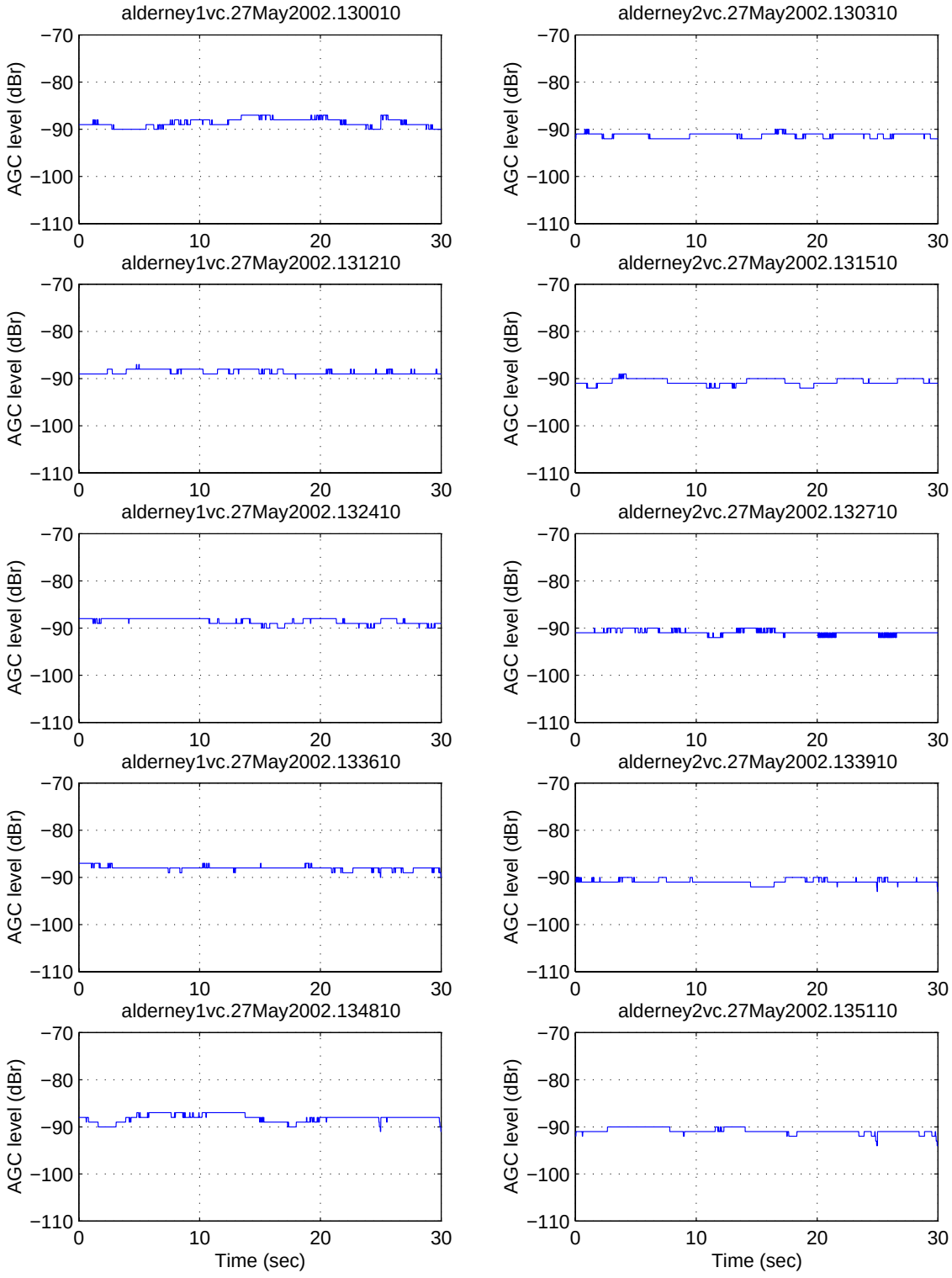

Figure 5.38: Signal amplitude vs time for Jersey-Alderney (1) F1 and F2 vertical signal on a calm day in spring during low tidal period (13:00 UT – 27th May 2002)

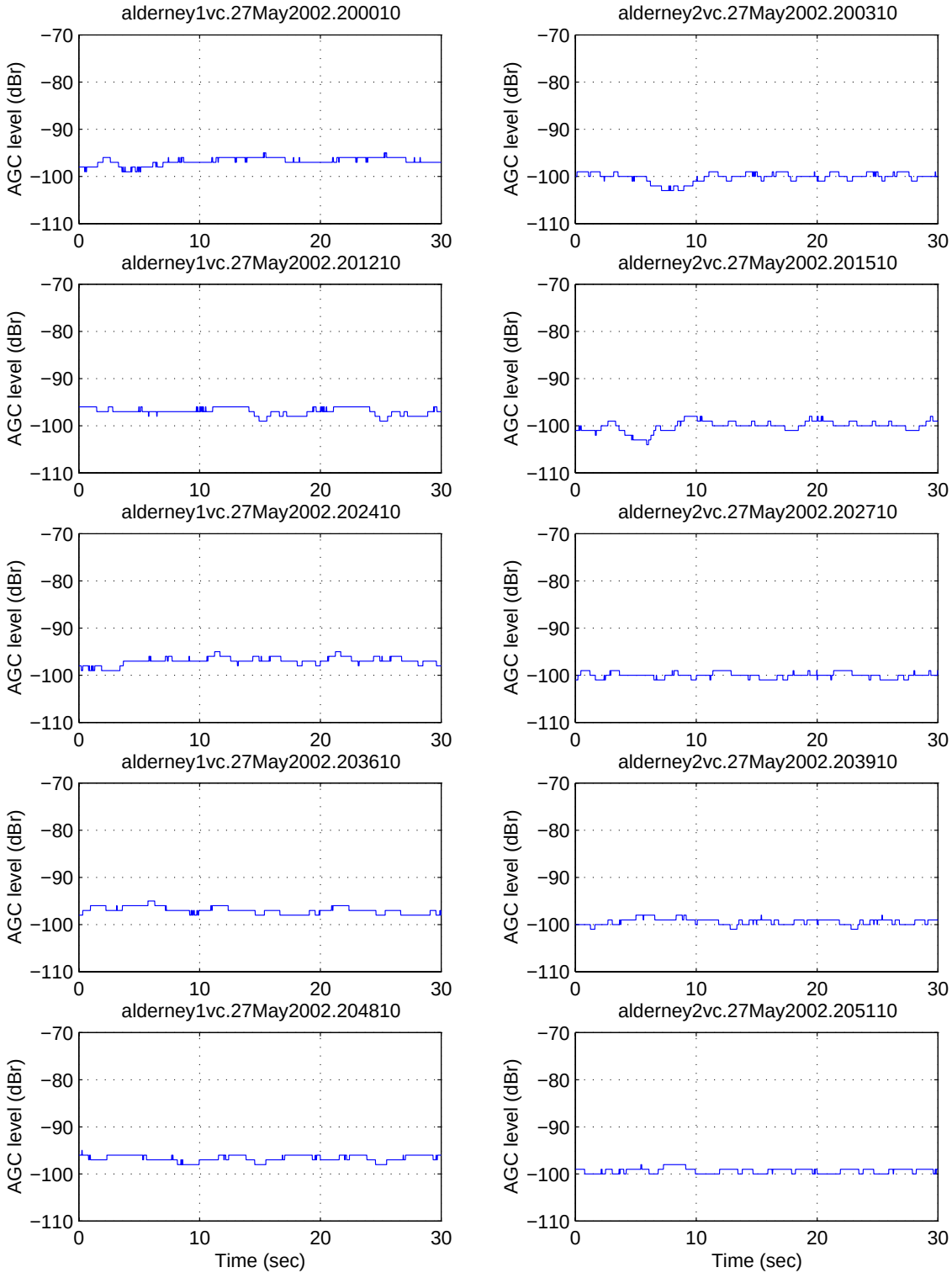

Figure 5.39: Signal amplitude vs time for Jersey-Alderney (1) F1 and F2 vertical signal on a calm day in spring during high tidal period (20:00 UT – 27th May 2002)

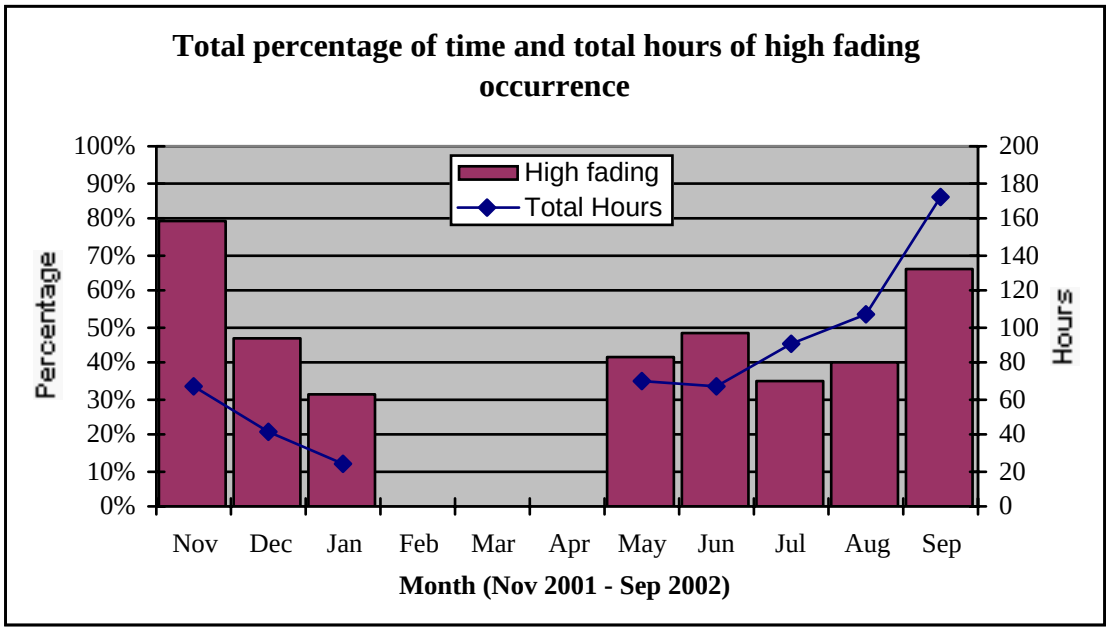

Figure 5.40: High fading statistic for Jersey-Alderney path from November 2001 until September 2002 (Note* data not available from Feb 2002 until Apr 2002)

Table 5.1: High fading statistics (fading period and range) on both autumn and "cool" summer day respectively

	17th Nov 2001 (autumn)				12th Jun 2002 (cool summer)			
	F1 Horz.	F1 Vert.	F2 Horz.	F2 Vert.	F1 Horz.	F1 Vert.	F2 Horz.	F2 Vert.
Max. fading range (dB)	11	12	8.5	10	6	7.5	7.5	7.5
Max. fading period (secs)	20	21.5	22	16	17	16.75	18	17.5
Avg. fading period (secs)	6.58	9.2	8.4	6.2	7.1	7.32	7.5	7.6

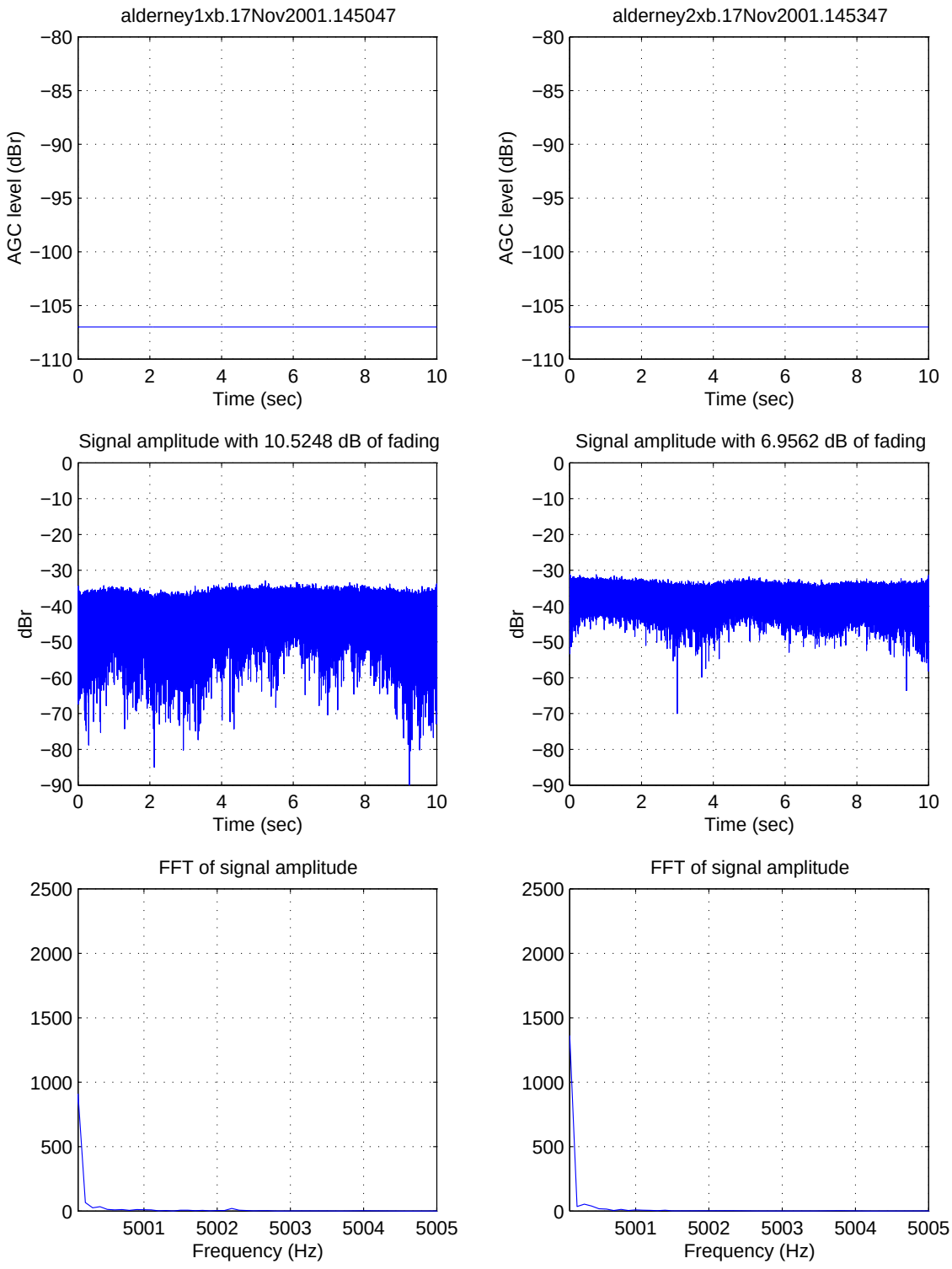

Figure 5.41: Cross-polar for Jersey-Alderney (1)

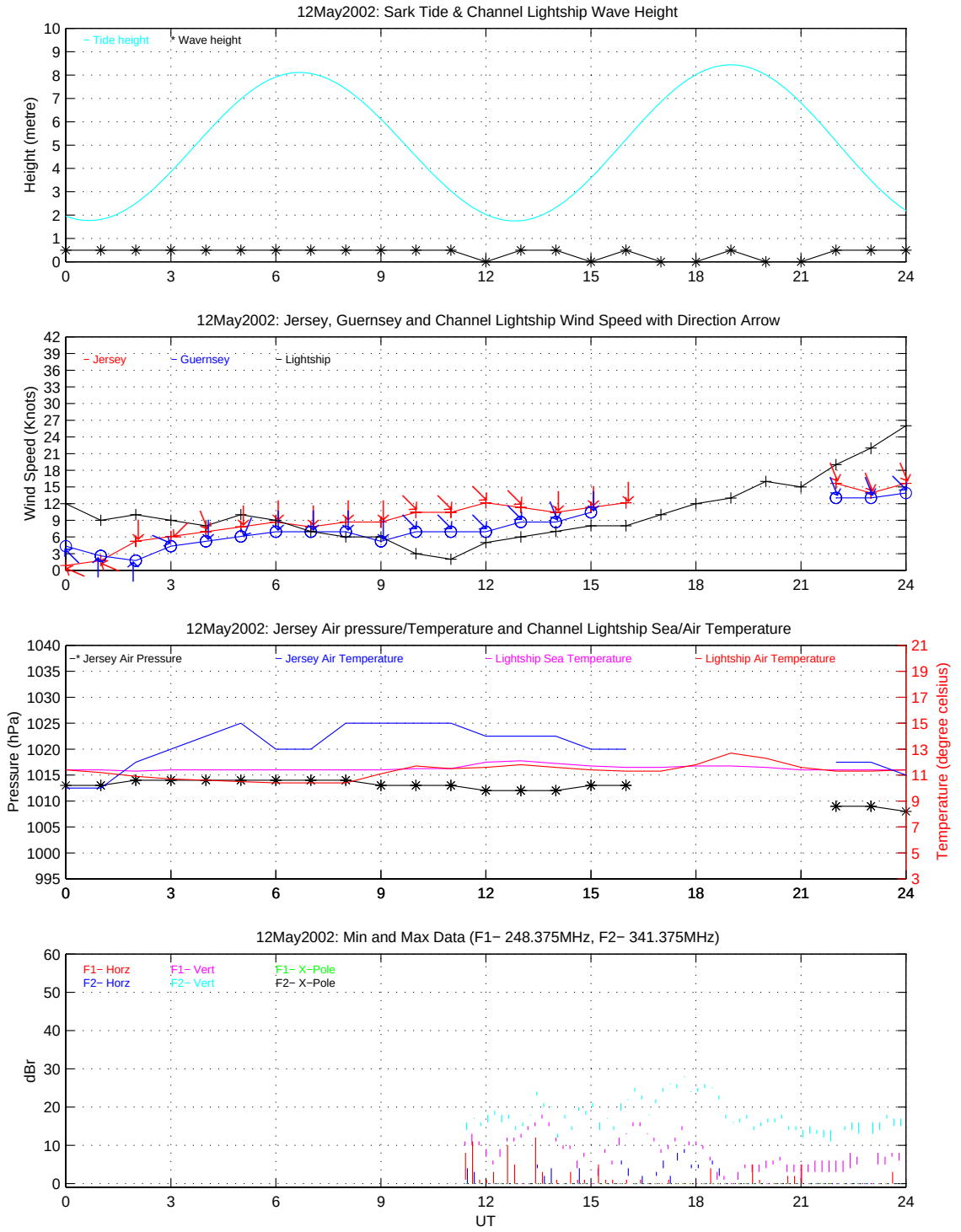

Figure 5.42: Signal strength plot with respect to various weather parameters on 12th May 2002 when T_d is around 4 degree celsius

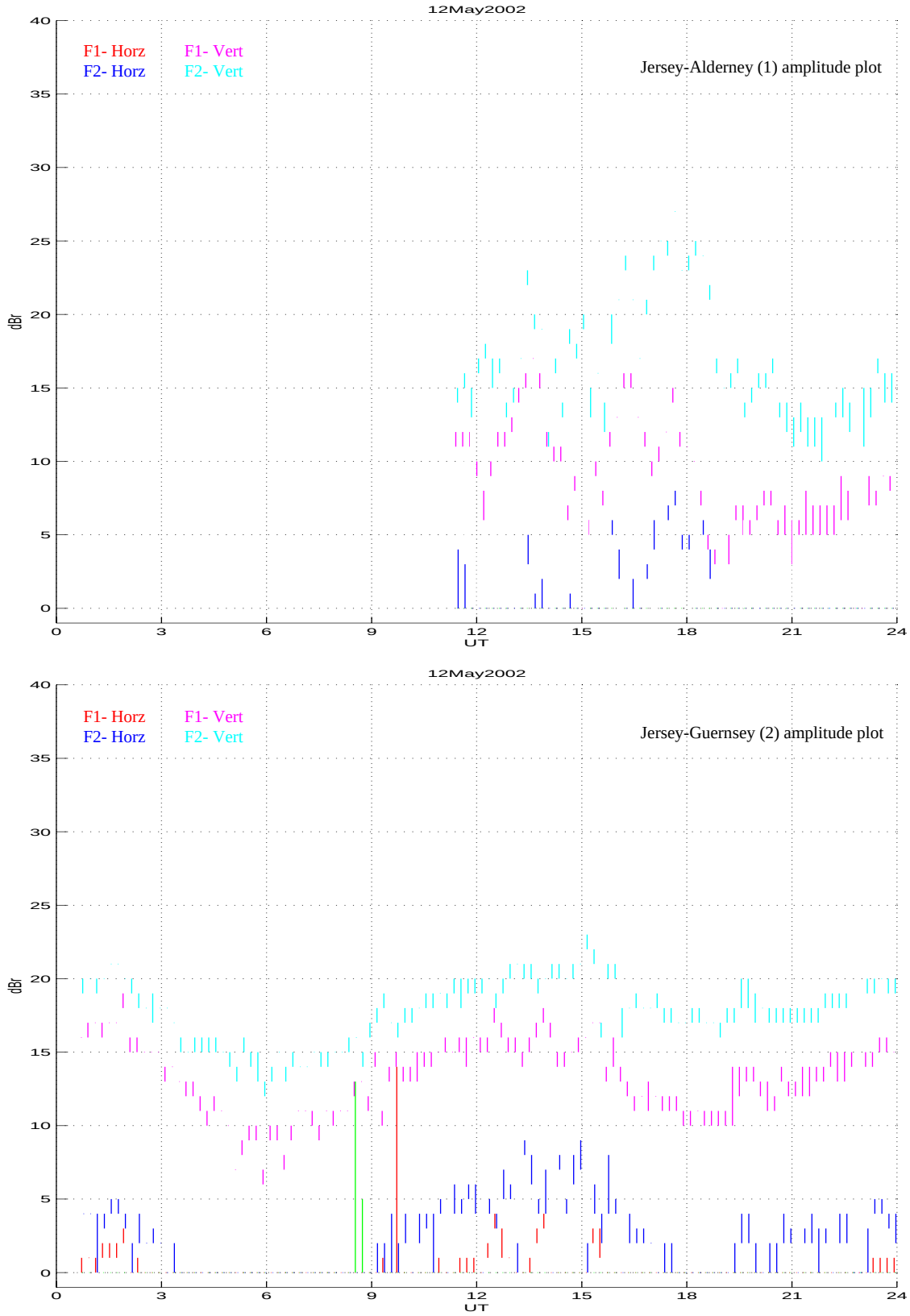

Figure 5.43: Signal amplitude comparison plot for both Jersey-Alderney (1) and Jersey-Guernsey (2) during an average warm day on 12th May 2002

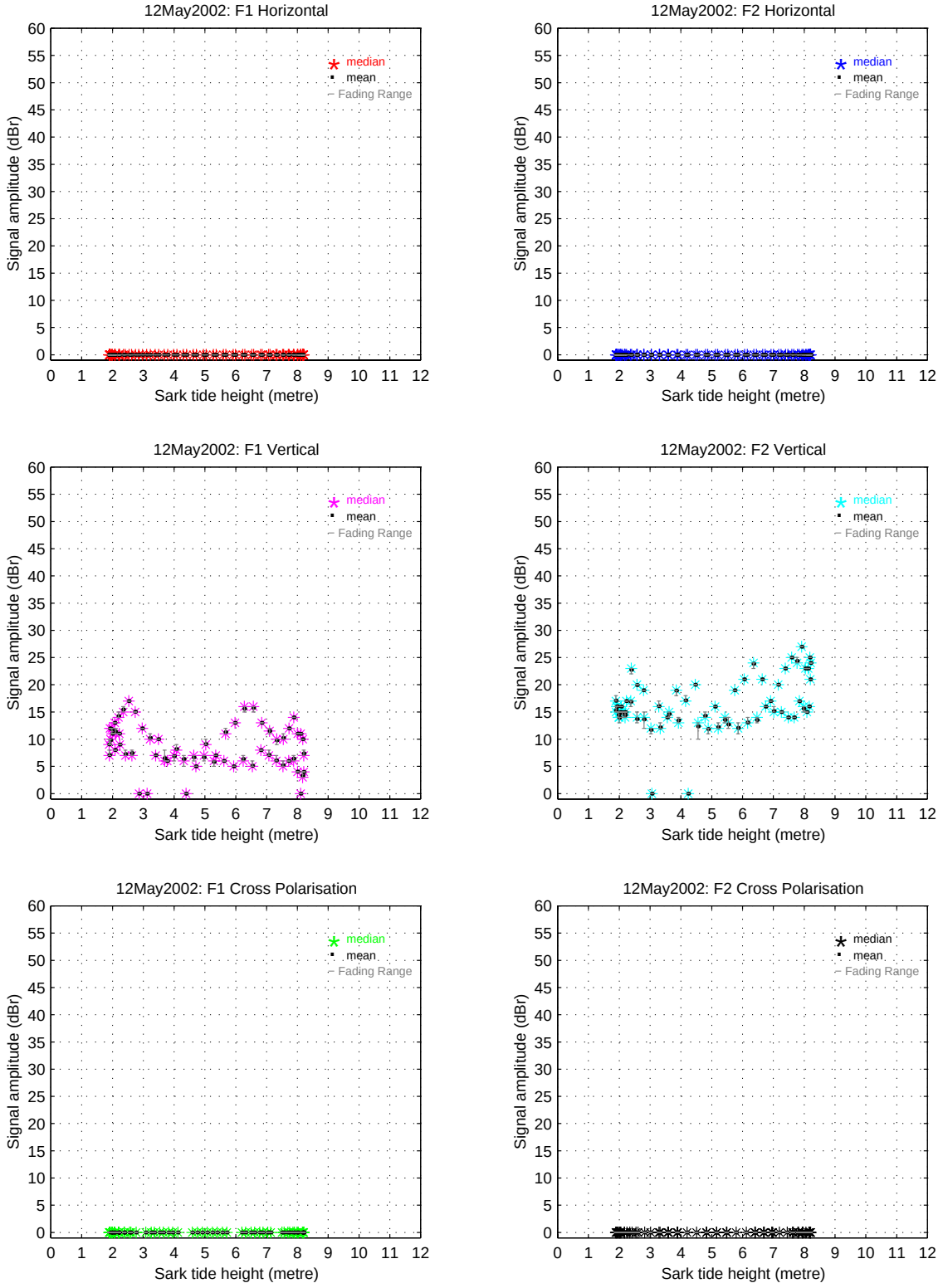

Figure 5.44: Signal amplitude vs tide height for Jersey-Alderney (1) during an average warm day on 12th May 2001 (Note* horizontal data not available)

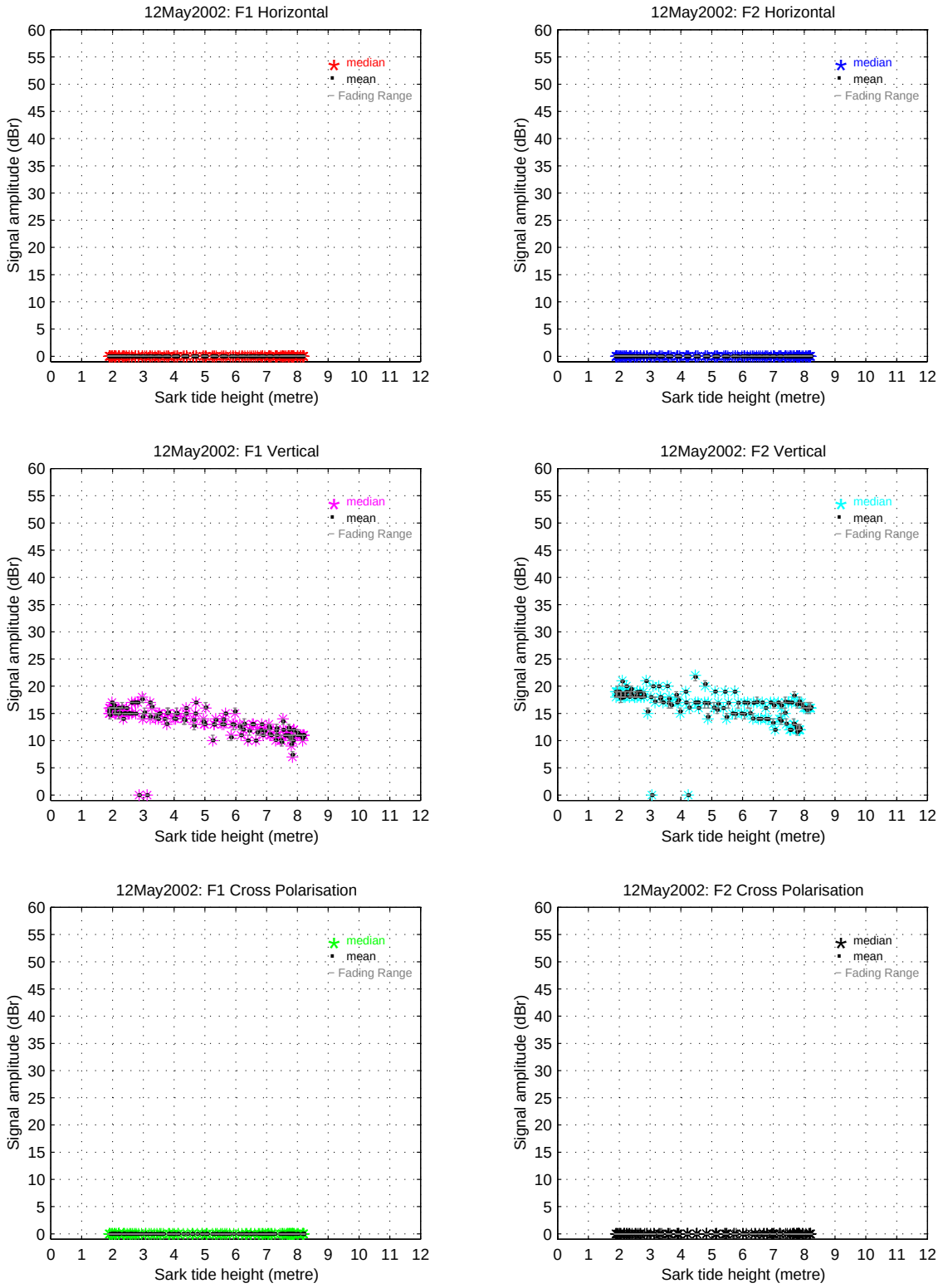

Figure 5.45: Signal amplitude vs tide height for Jersey-Guernsey (2) during an average warm day on 12th May 2001 (Note* horizontal data not available)

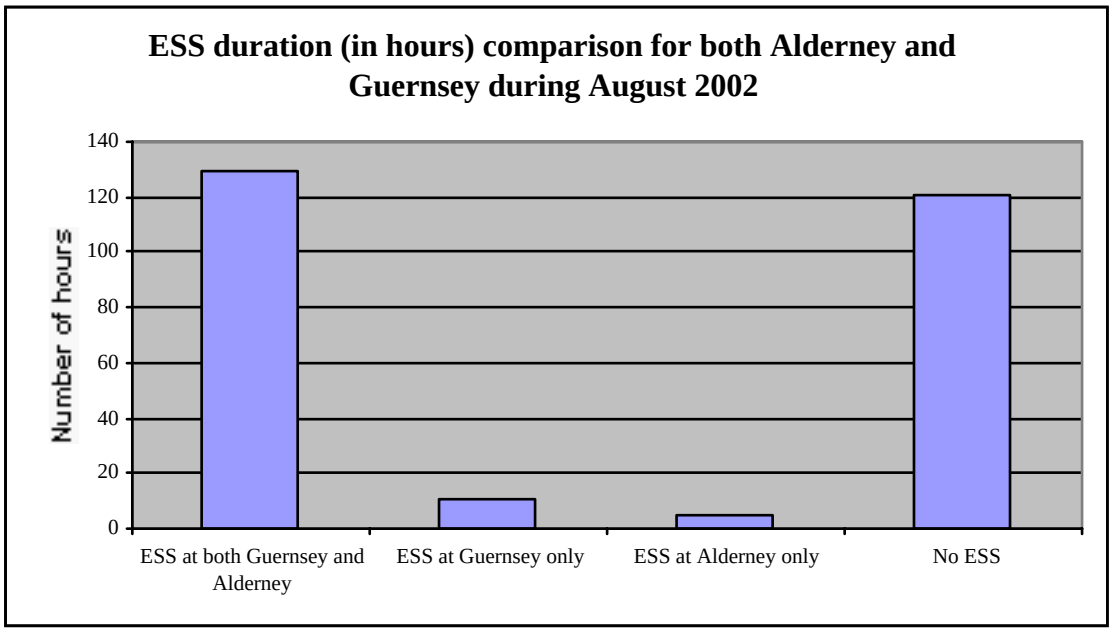

Figure 5.46: ESS duration comparison (August 2002) for both receiving locations with respect to Alderney total data time (266 hours)

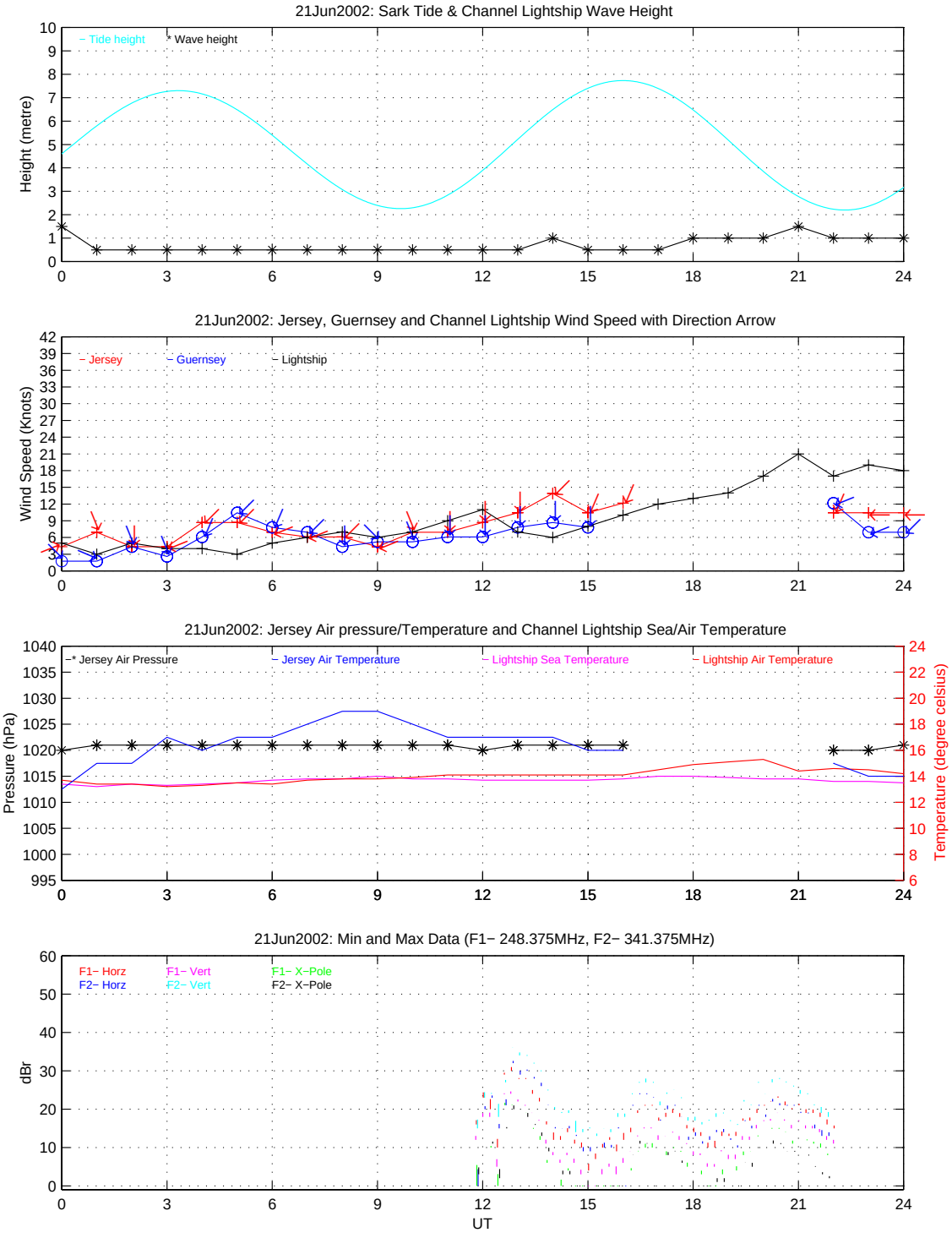

Figure 5.47: Signal strength plot during a hot summer day (21st Jun 2002) with respect to various weather parameters

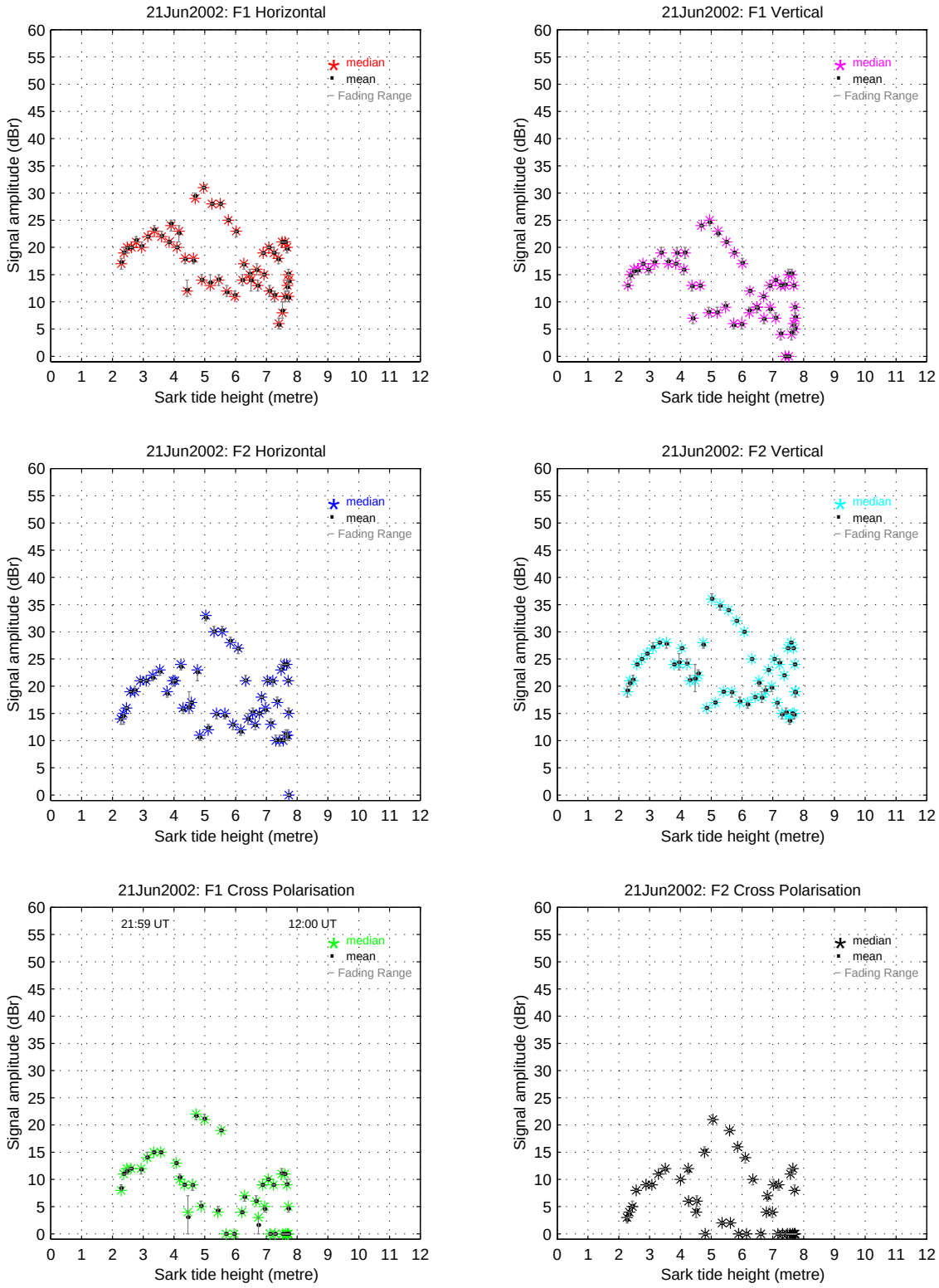

Figure 5.48: Signal strength vs tide height during a hot summer day for Jersey-Alderney (1) on 21st Jun 2002

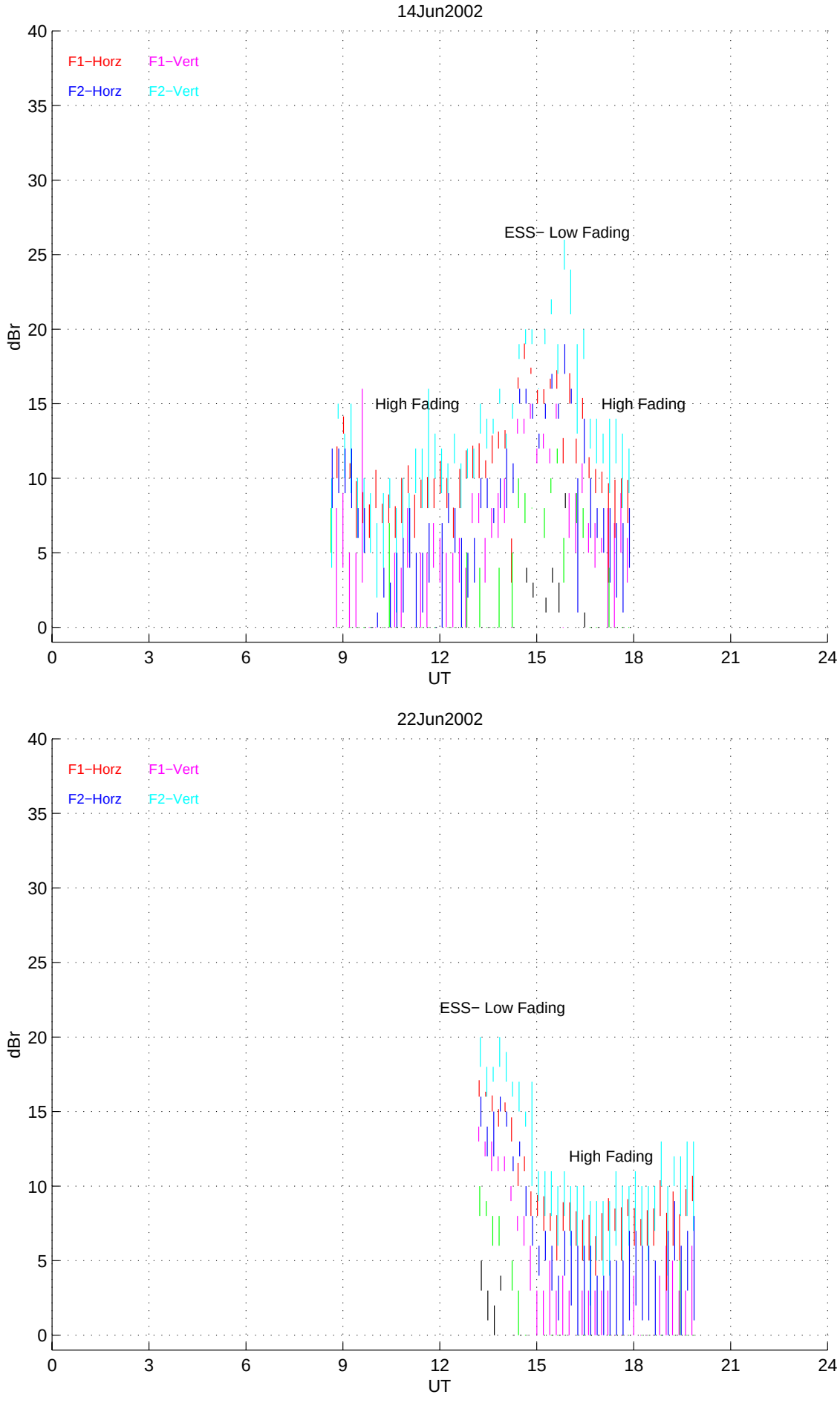

Figure 5.49: ESS with high fading phenomenon during summer time

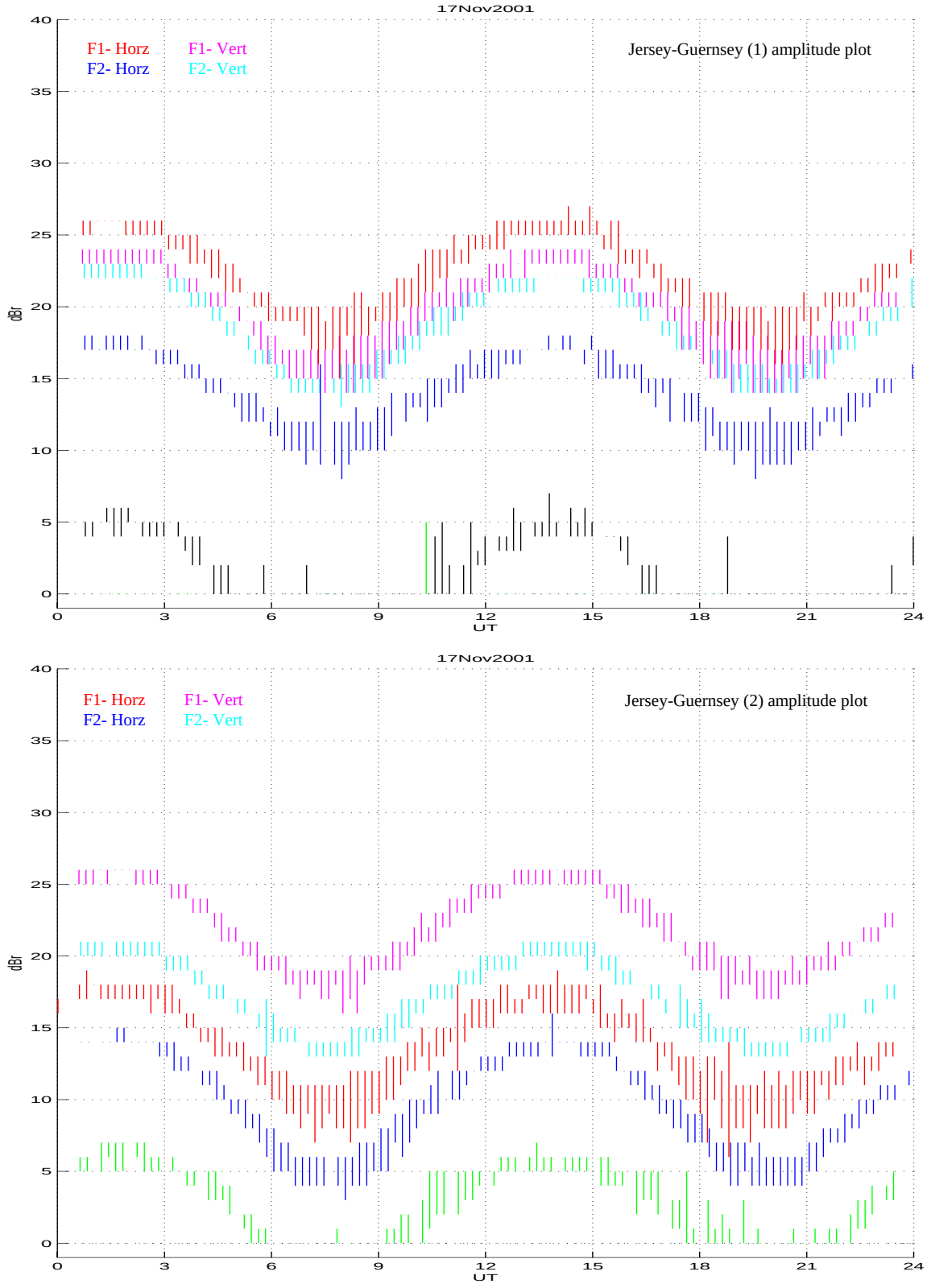

Figure 5.50: Jersey-Guernsey (1) vs. Jersey-Guernsey (2) amplitude plot

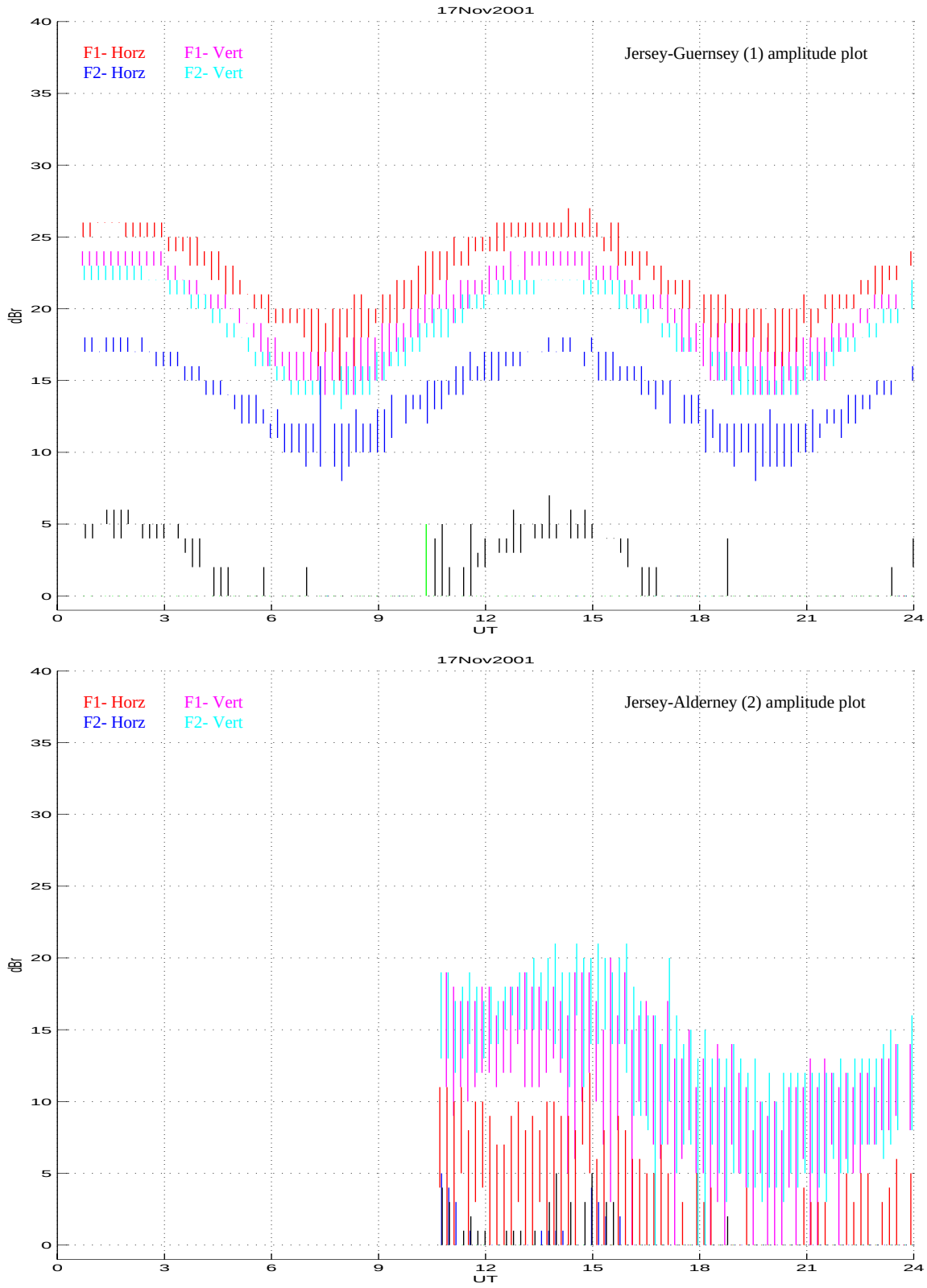

Figure 5.51: Jersey-Guernsey (1) vs. Jersey-Alderney (2) amplitude plot

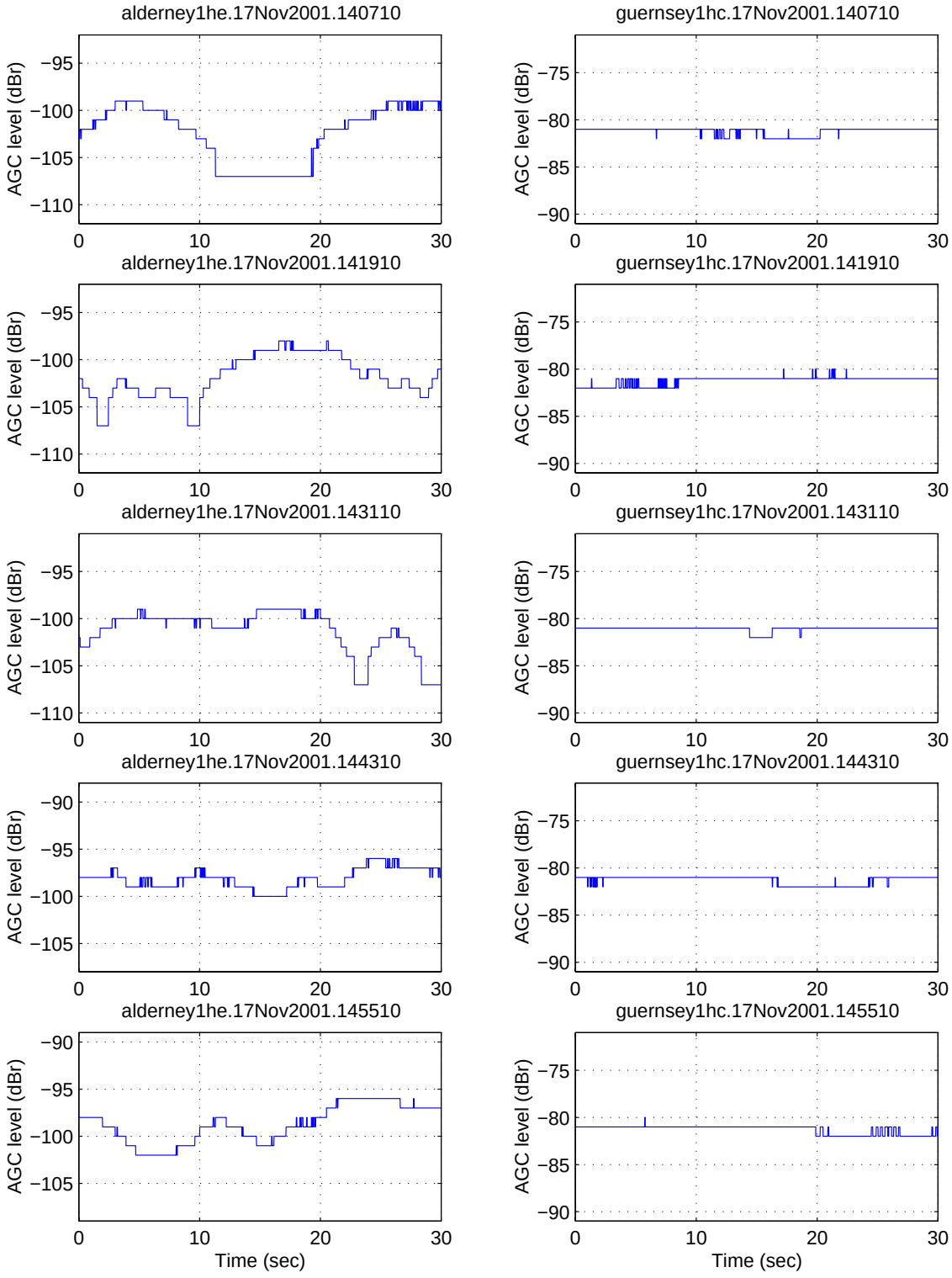

Figure 5.52: Jersey-Guernsey (1) (right panel) vs. Jersey-Alderney (2) (left panel) amplitude comparison plot for F1 (Horizontal) within an hour period

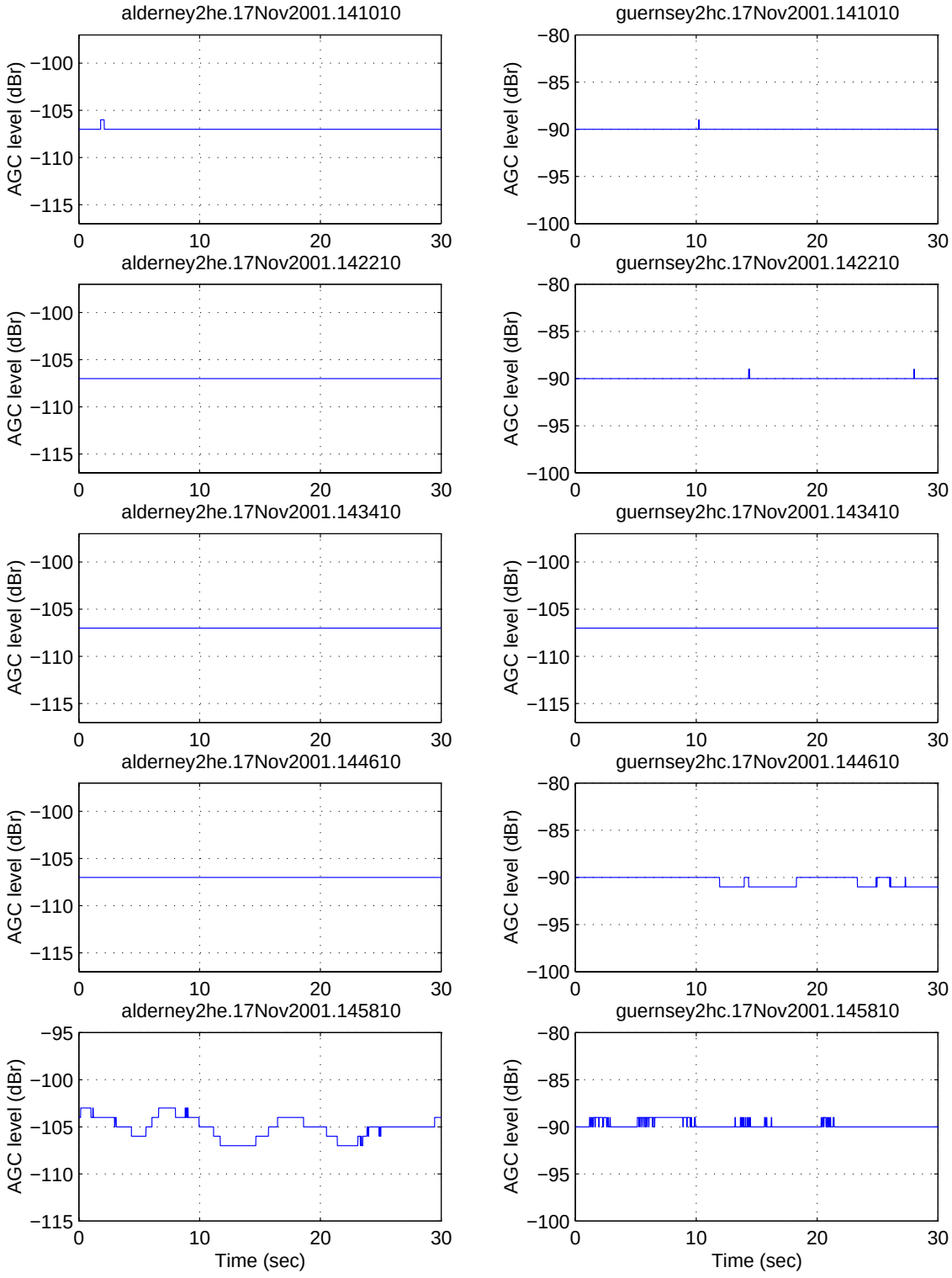

Figure 5.53: Jersey-Guernsey (1) vs. Jersey-Alderney (2) amplitude comparison plot for F2 (Horizontal) within an hour period

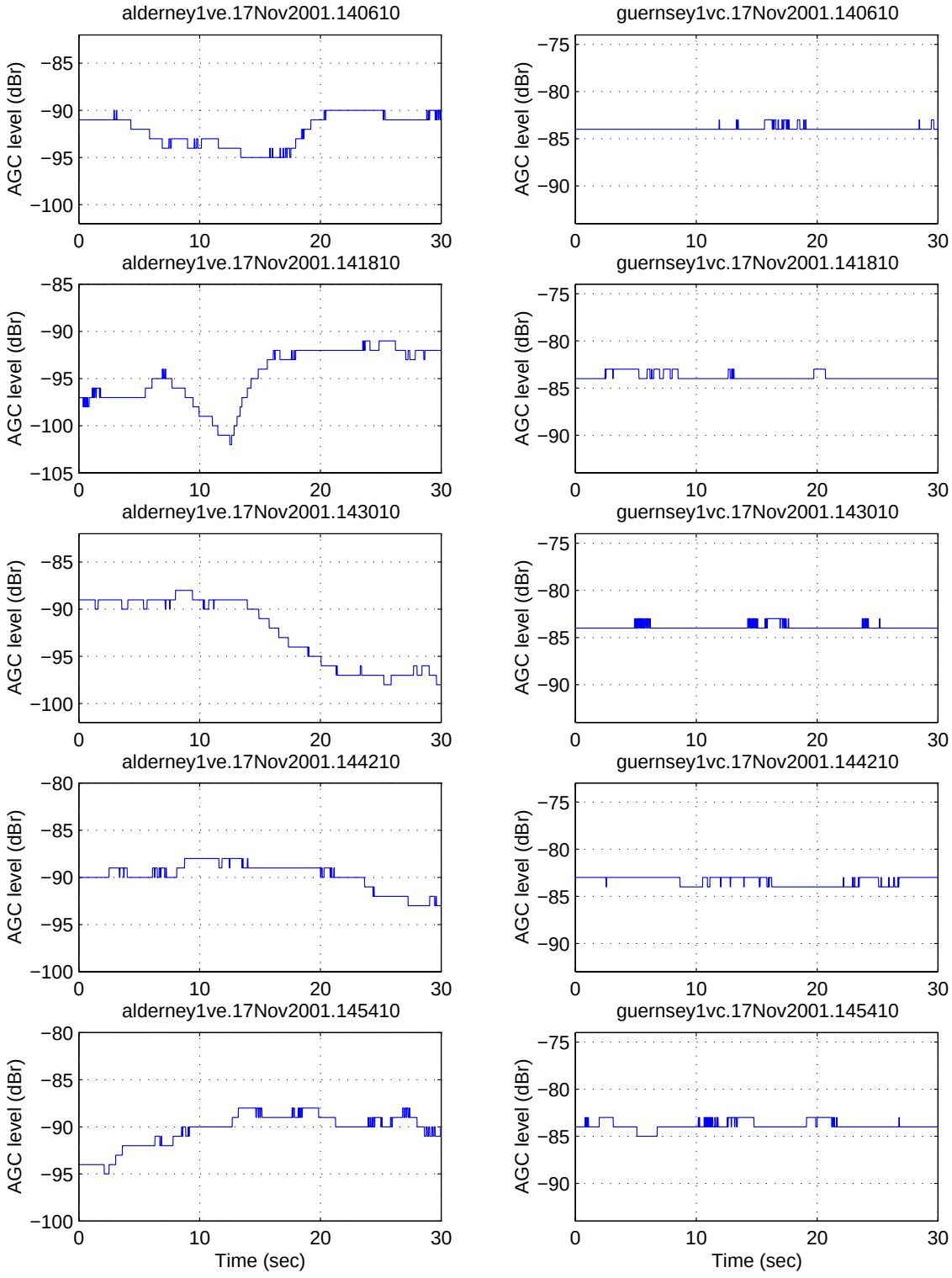

Figure 5.54: Jersey-Guernsey (1) vs. Jersey-Alderney (2) amplitude comparison plot for F1 (Vertical) within an hour period

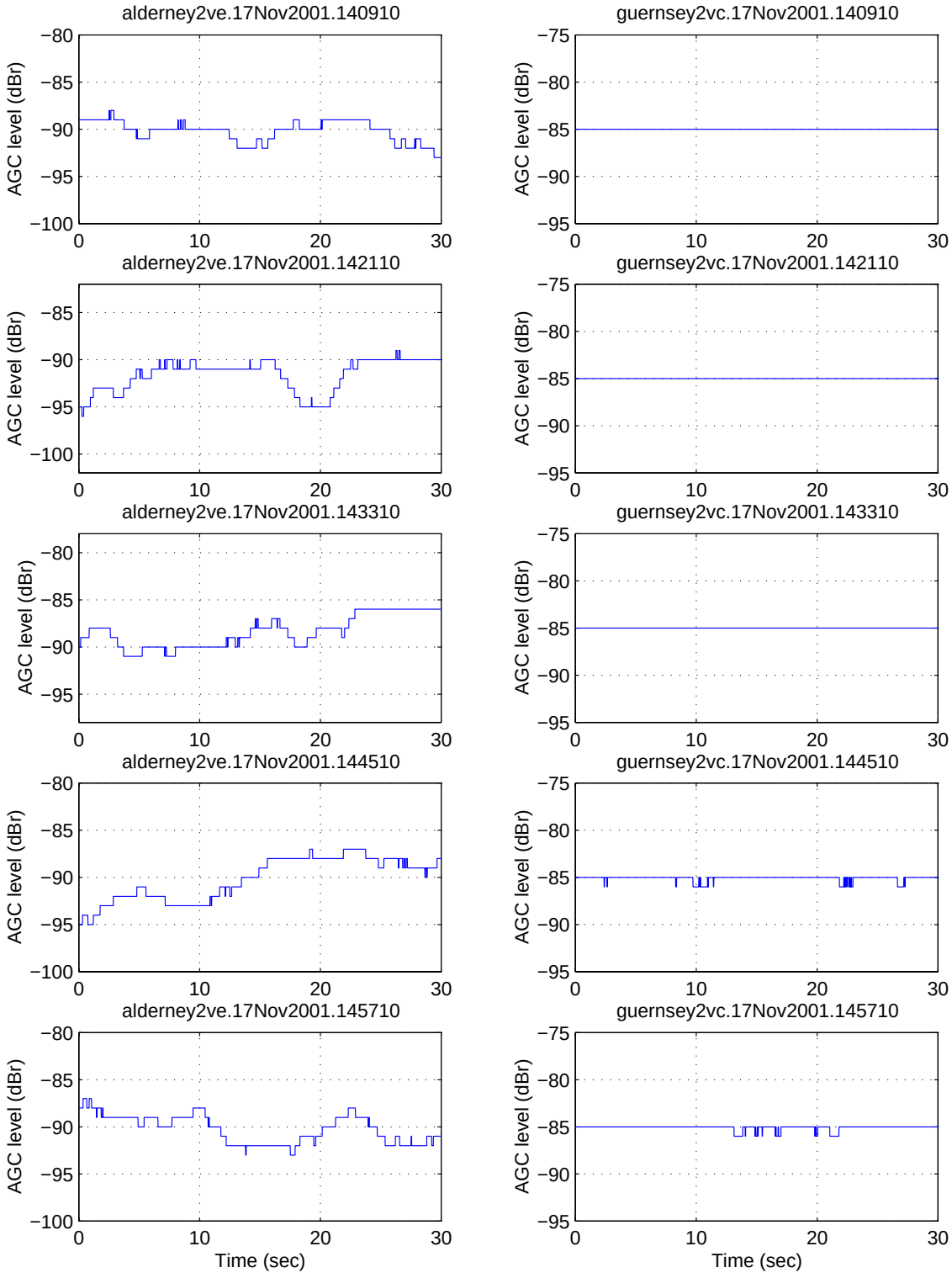

Figure 5.55: Jersey-Guernsey (1) vs. Jersey-Alderney (2) amplitude comparison plot for F2 (Vertically) within an hour period

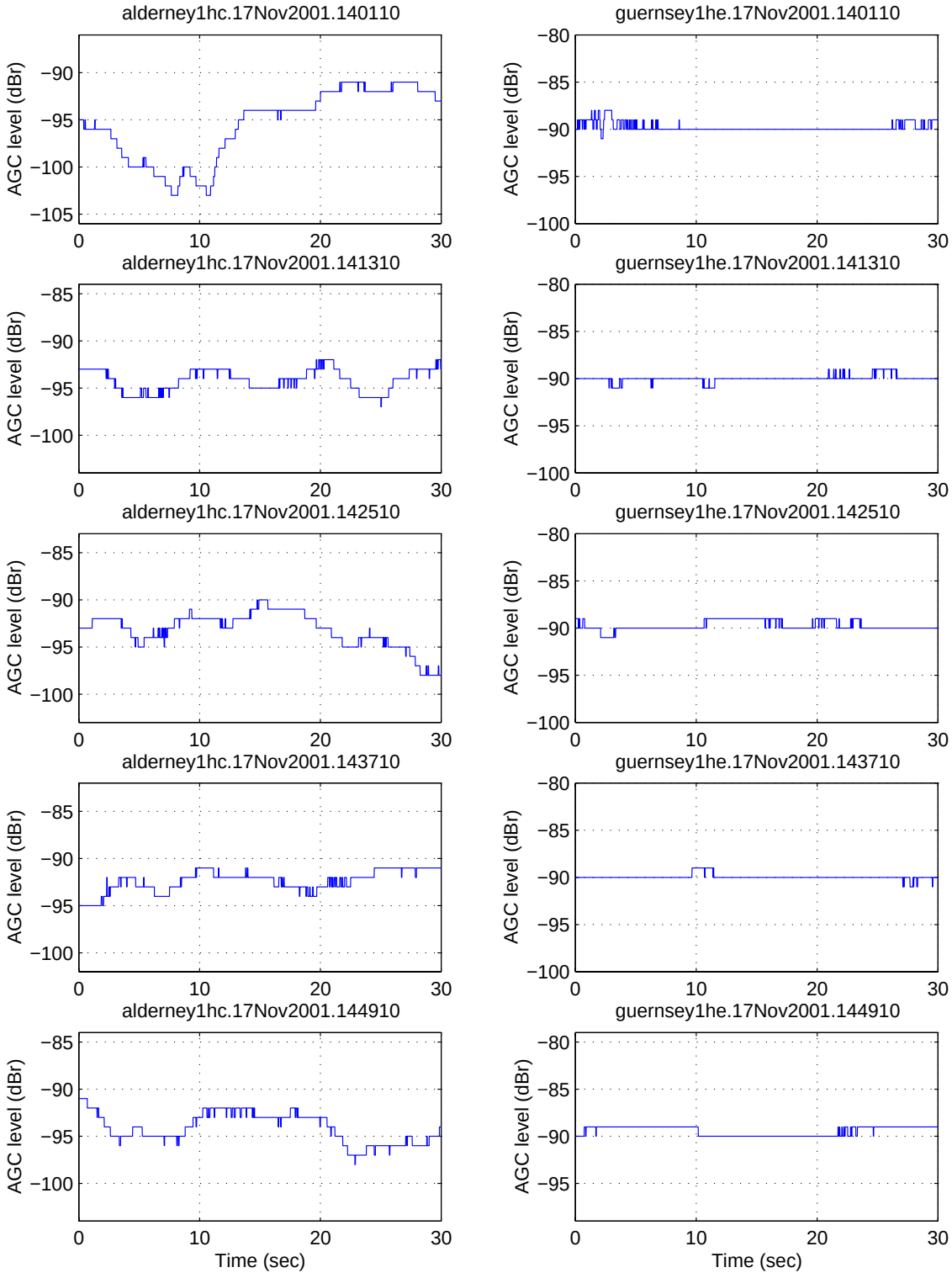

Figure 5.56: Jersey-Alderney (1) (left panel) vs. Jersey-Guernsey (2) (right panel) amplitude comparison plot for F1 (Horizontal) within an hour period

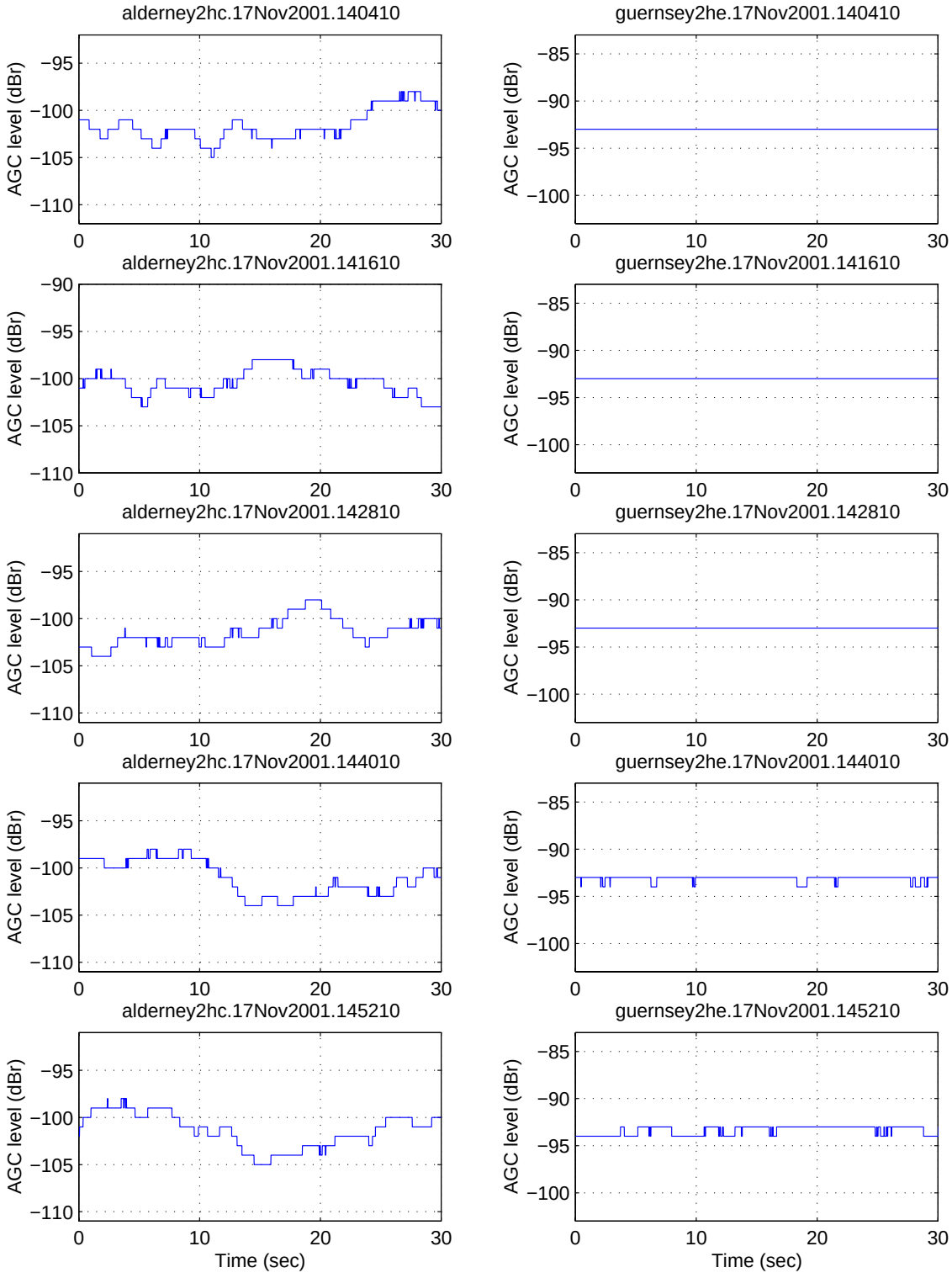

Figure 5.57: Jersey-Alderney (1) vs. Jersey-Guernsey (2) amplitude comparison plot for F2 (Horizontal) within an hour period

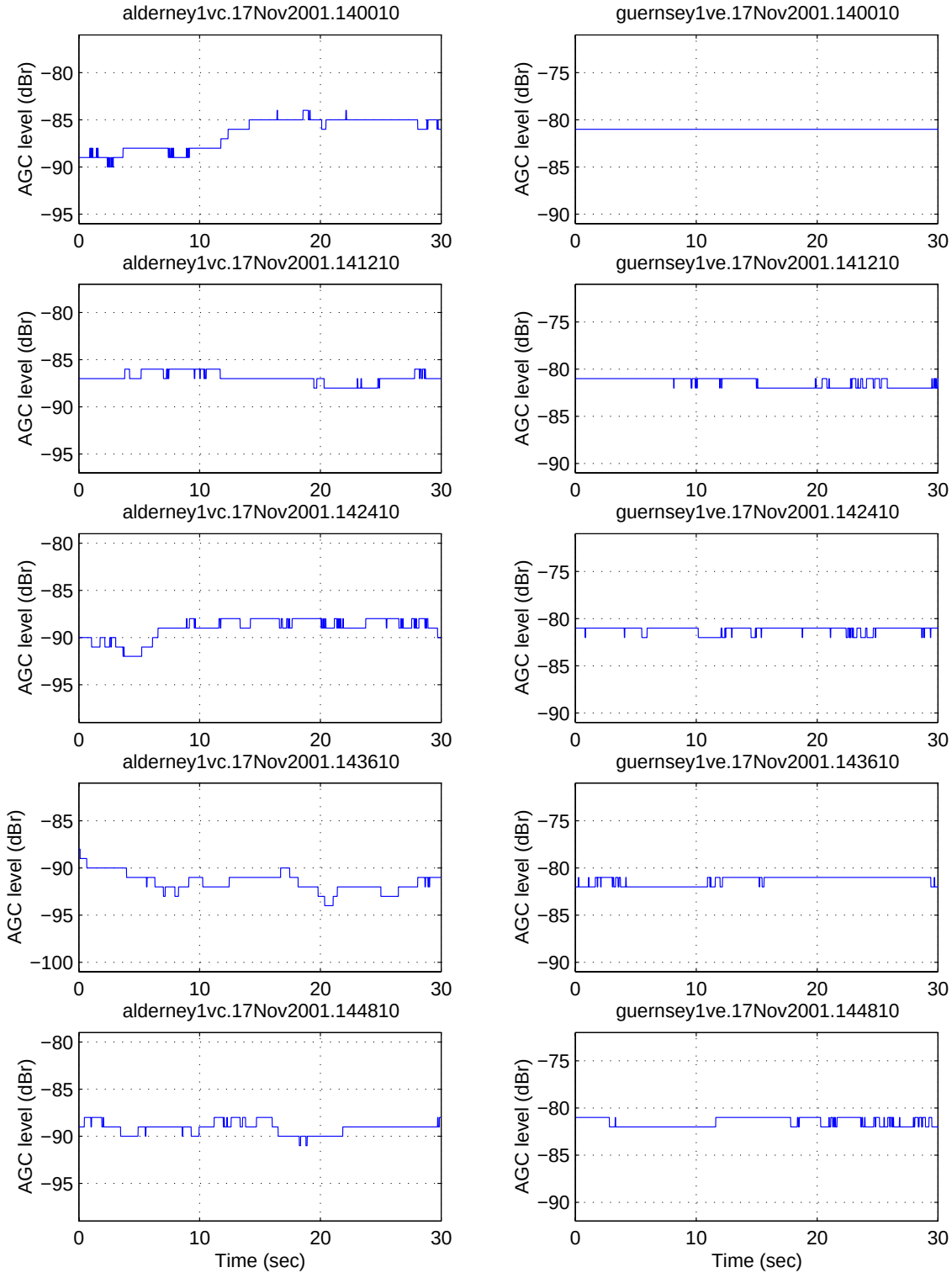

Figure 5.58: Jersey-Alderney (1) vs. Jersey-Guernsey (2) amplitude comparison plot for F1 (Vertical) within an hour period

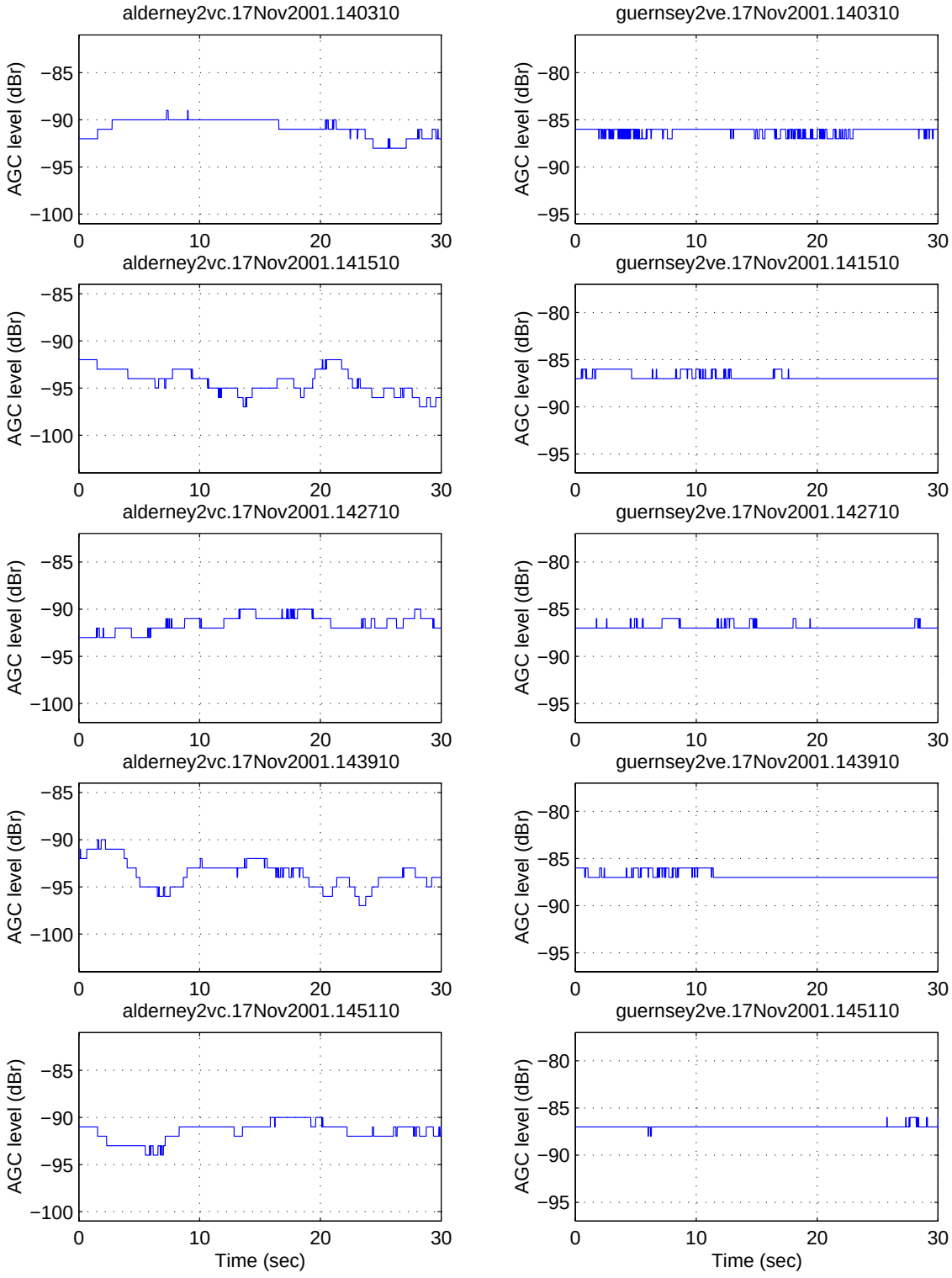

Figure 5.59: Jersey-Alderney (1) vs. Jersey-Guernsey (2) amplitude comparison plot for F2 (Vertical) within an hour period

5.4 An interesting anomaly

Although there are a number of rarely encountered propagation effects observed during this experiment, the total percentage of time they occurred was around 0.01%. One of these anomalous propagation is shown in Figure 5.60 where fast fading is observed during a period of around 13 seconds across the Jersey-Guernsey path. This phenomenon could result due to a low flying plane that flew across the signal path as it is similar to the one observed by Algor [1972] (see Figure 3.8).

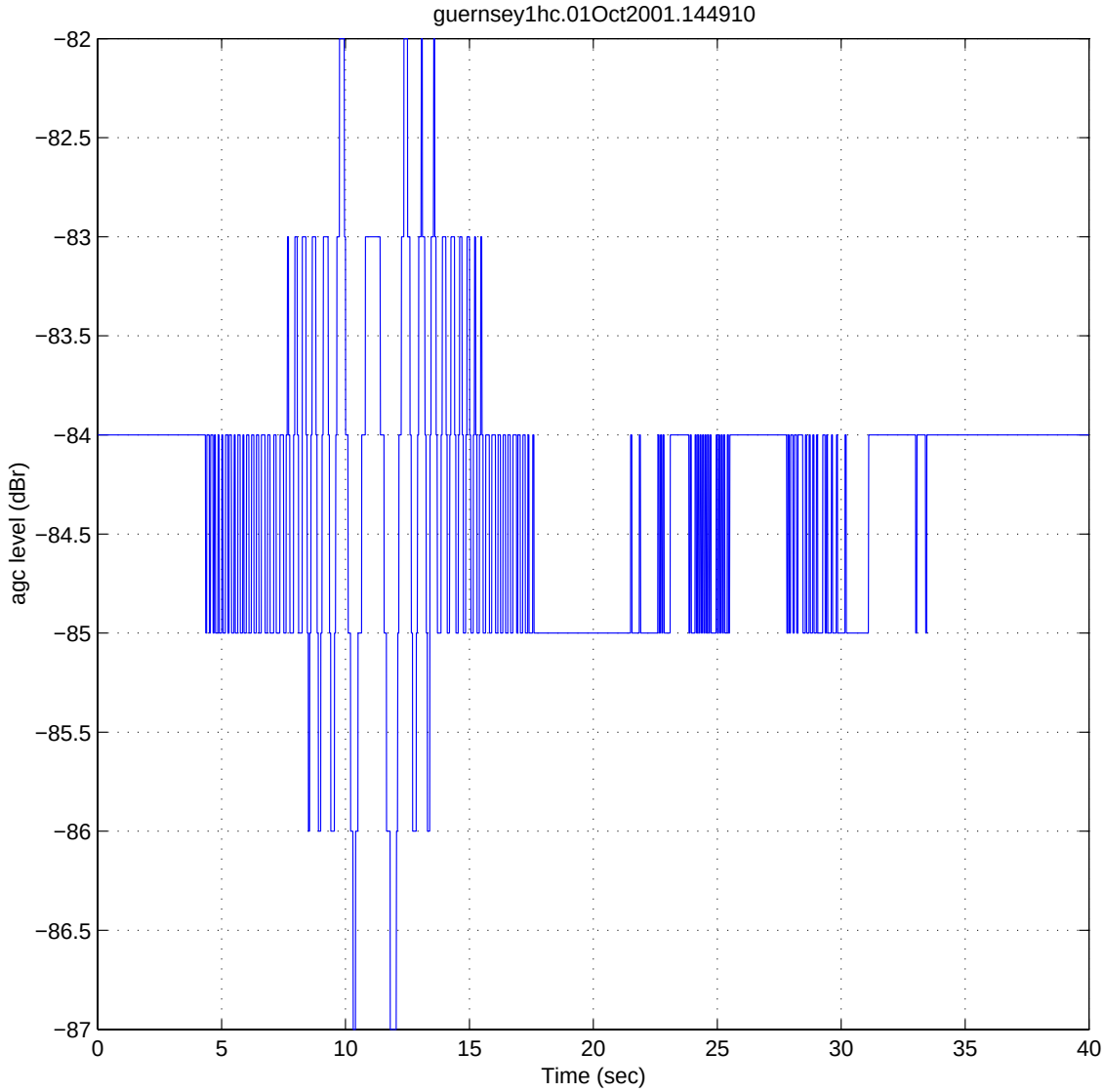

Figure 5.60: Fast fading within a 13 seconds period due to anomalous propagation

5.5 Summary

Data from both the Guernsey and Alderney receiving sites were analysed and the signal amplitude behaviour was discussed in this chapter. These include 17 months of Guernsey data from April 2001 until September 2002 and 8 months of data that were available to the Alderney receiving site from November 2001 until September 2002. Both Jersey-Guernsey and Jersey-Alderney data were divided into a few sections that were investigated and compared with several meteorological effects such as changing sea states, weather condition, season etc.

During times of calm sea state for both Jersey-Guernsey and Jersey-Alderney showed a linear relationship between the signal amplitude and the tide height although the Jersey-Alderney data showed some fluctuation in the signal across the linear region. The signal amplitude decreases as the tide height increases and this accounts for approximately 1.1dB in signal amplitude reduction for every metre of tide height increase. Fading range for Jersey-Guernsey was around 2 dB and in contrast, high fading range of around 10 dB was observed from Jersey-Alderney path. From the statistic, it showed that this high fading phenomenon occurred around 30% of the total time and decreased to around 10% during the period from Nov 2001 until Jan 2002. The statistic also showed that the average high fading period was around 7 seconds, with a maximum fading period and a range of 22 seconds and 12 dB respectively during the autumn period. Further analysis from the FFT plot concluded that multipath propagation was involved, as there were more than one-signal components in the audio signal.

During “rough sea” state for Jersey-Guernsey in spring 2001, on a few occasions (less than 0.1 percentage of the total time), it was observed that the vertically polarised signal was largely affected and the signal strength decreased between 3 to 6 dB. Although the horizontal polarised signal was not much affected during this “rough period”, fast fading with reduction in signal amplitude was observed in excess of 10 dB from F1 (horizontal) during low tidal wave. Although other rough sea days were observed, this phenomenon was not found on these days including Jersey-Alderney for all seasons.

A “cool summer” day for Jersey-Guernsey shown the exact similar signal behaviour during calm sea states in Jersey-Guernsey. Although similar signal characteristic was also observed in Jersey-Alderney, high fading phenomenon was observed mainly during

high tidal periods during spring/summer periods (transmitting and receiving antennas at minimum height above sea level). From the statistic for cool summer day, the average high fading period is around 7 seconds, with maximum fading period and range of 18 seconds and 7.5 dB respectively.

During a “hot summer” day for Jersey-Guernsey, due to an increase in air temperature (with reference to the sea temperature), typical ESS effects enable the signal amplitude to further improve by up to a maximum of 33 dB. The statistic showed that the increase in signal amplitude is around 3 dB (median value) while the upper/lower decile value were 10 and 1 dB respectively. Although the fading range is only around 1dB observed from a 30 seconds period, fading in excess of 20 dB was observed within periods of hours. This ESS effect can last from a few hours to 9 days continuously and in contrast, during "non-summer" or "low temperature" periods such as winter, ESS lasted from a few hours up to a day with signal amplitude improvement up to around 5 dB. Further ESS duration statistic showed that the median duration for ESS was 18 hours and the upper/lower decile values were 24 and 7 hours respectively. Further statistics from Jersey-Guernsey showed that ESS appeared around 45 to 60% of the total time during summer 2001 and around 20 to 35% of the total time during summer 2002. This discrepancy was a result of lower “high temperature” days during summer 2002 as compared to summer 2001. As regard to winter periods, the occurrence of ESS was less than 10% of the total time. Furthermore from the statistic, a threshold temperature (T_d) of 4°C can be applied showing high percentage of ESS occurrence (around 60% of the total summer time during the year 2001) and the evidence showed that ESS occurrence increased dramatically when mean T_{dmax} is more than 4°C.

During a hot summer day for Jersey-Alderney when ESS duration occurred throughout the whole day, the improvement of signal amplitude and the fading characteristic is similar to Jersey-Guernsey. Although there is much similarity (e.g. period of occurrence) between Jersey-Guernsey and Jersey-Alderney during ESS, the differences in signal amplitude improvement on the same day for both receiving sites could be up to 10 dB.

The next chapter contains modelling studies of the data to identify or confirm the propagation mechanisms observed in the measurements presented.

Chapter 6: Theoretical considerations and comparison with observations

6.1 Introduction

Several interesting results from the experiment were described in Chapter 5. These results can be used as a guideline to develop or to compare with the appropriate path loss equations from various authors (e.g. ITU). In order to fully understand the mechanism of over sea propagation especially VHF/UHF, it is important to investigate the direct factors that affect the propagation of the signal. Concepts and theory such as Fresnel zone, effective distance or optical range for line of sight and the "bulge" height of the earth between the propagating path will be investigated thoroughly.

The dominating propagating mechanism for VHF/UHF signals at different antenna heights and distances can be established by evaluating the path loss equations for various mechanisms such as line-of-sight, smooth spherical earth diffraction and tropospheric scattering. The total path loss for VHF/UHF signals over seawater at different antenna heights and distances were simulated and compared with the measurements showed in Chapter 5. This chapter will also include a simplified model for troposhperic ray tracing technique that was derived from Snell's law for spherically stratified medium.

6.2 Path obscuration by the earth's curvature

For a signal to be received with minimum path loss, adequate clearance between the direct path and any obstacle is essential. The necessary clearance is usually expressed in terms of Fresnel zone, that can be defined as the three-dimensional locus of point A such that the difference in path lengths between the reflected wave ($r_1 + r_2$) and the direct wave ($D_1 + D_2$) is an integer number of half-wavelengths as illustrated in Figure6.1 [Griffiths, 1987].

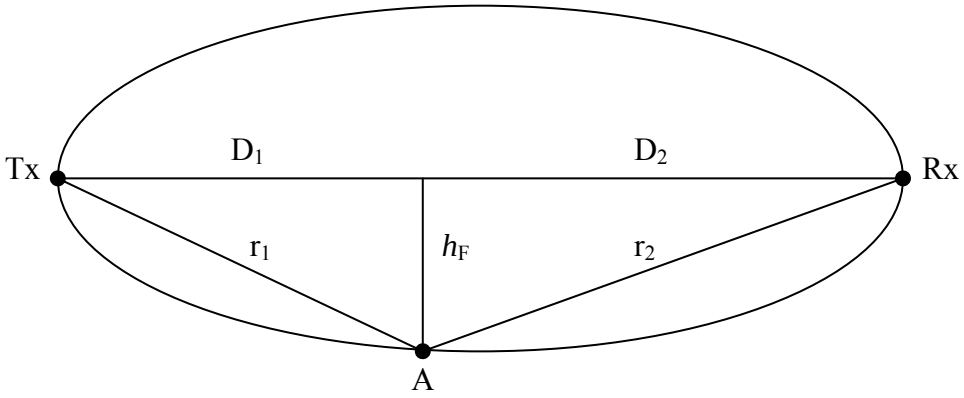

Figure 6.1: Fresnel zone radius [after Griffiths, 1987]

From Figure 6.1, the first Fresnel zone radius (h_F) can be calculated using the below equation 6.01 obtained from Griffiths [1987]:

$$h_F = 31.61\left[\frac{\lambda D_1 D_2}{D_1 + D_2}\right]^{\frac{1}{2}} \qquad (6.01)$$

The wavelength λ is in metre and both D_1 and D_2 are distance in km.

Although there are no fixed obstruction or obstacles along the propagating paths across the sea during the experiment, considering the effect of obstruction such as sea waves or the earth's curvature, the concept of Fresnel zone is still useful. Table 6.1 shows the Fresnel zone radius for both receiving sites with F1 and F2 respectively by assuming both D_1 and D_2 (km) as middle distance between the transmitter and the receiver.

Table 6.1: Fresnel zone radius with respect to both F1 and F2 calculation for both propagating paths

Path Location	Jersey to Guernsey		Jersey to Alderney	
Path length $d_{tx\text{-}rx}$ (km)	33.3		48	
Mid distance $D_1 = D_2$ (km)	16.65		24	
Frequency (MHz)	248.375	341.375	248.375	341.375
Wavelength (m)	1.1514847	0.8377836	1.1514847	0.8377836
Fresnel zone radius h_F (m)	**97.9**	**83.5**	**117.6**	**100.3**

Due to the curvature of the earth, the line-of-sight distance between the transmitter and the receiver without any obstruction is as shown in Figure 6.2. The effective line-of-

sight distance d_{LOS} is d_1+d_2 while the height of both antennas is h_{tx} and h_{rx}. From this figure, by applying Pythagoras theorem, d_{LOS} is given by:

$$d_{LOS} = d_1 + d_2 = \sqrt{2r} \times \left(\sqrt{h_{tx}} + \sqrt{h_{rx}}\right) \qquad (6.02)$$

where r is the earth radius [Griffiths, 1987]. Table 6.2 shows the d_{LOS} for both experimental paths.

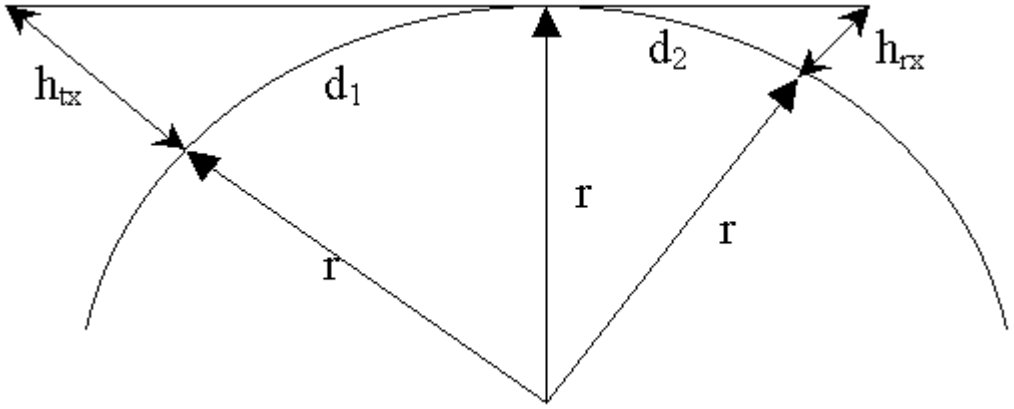

Figure 6.2: Effective range of transmission [after Griffiths, 1987]

Table 6.2: Direct line of sight range with respect to different antenna height

Mean antenna height (m)	10	15	20
Direct line of sight d_{LOS} (m)	**22574**	**27648**	**31925**

*Note that the above assume both transmission and reception antenna heights are the same and r = 6370000 m.

From Figure 6.3, in order to obtain the approximated "bulge" height or heights increment h_{inc} from the curvature of the smooth earth, a few assumptions were made:

- distance $dist_1$ is equal to $dist_2$ (selecting the middle distance)
- distance $dist_1$ or $dist_2$ is approximately equal to half of Jersey-Guernsey (around 16.65 km) or Jersey-Alderney (around 24 km)
- though the changing sea tide (during low tide) could raise the antenna height for both transmitter and receiver to a maximum of around 20 metres, the earth radius r remains as approximately 6370 km

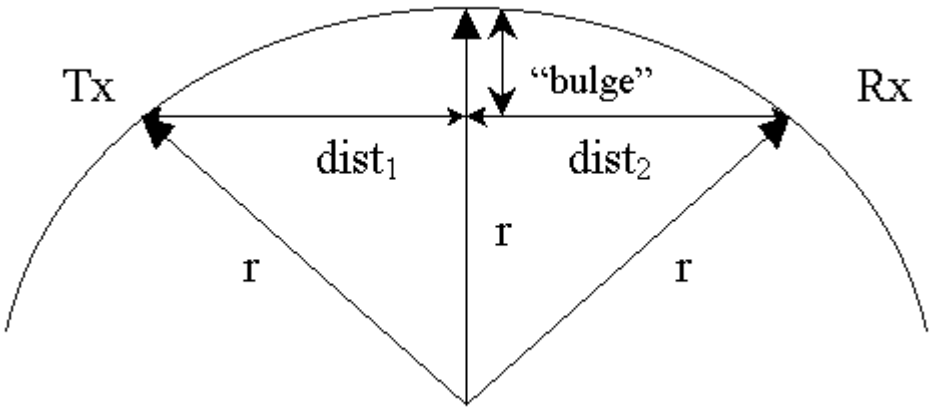

Figure 6.3: "Bulge" height of earth

The approximate curved-Earth geometry equation can be obtained from Hall *et al* [1996] where the approximated "bulge" height (metre) as shown in Figure 6.3 can be determined by:

$$h_{inc} = \frac{dist_1 dist_2}{2r} \qquad (6.03)$$

Considering both the propagating paths in the Channel Island, Table 6.3 below provides the approximated "bulge" height or height increment from the curvature of the earth for both Jersey-Guernsey and Jersey-Alderney paths.

Table 6.3: Approximated "bulge" height of the earth's curvature

Path Location	Jersey to Guernsey	Jersey to Alderney
Path length $d_{tx\text{-}rx}$ (m)	33300	48000
Mid distance $dist_1 = dist_2$ (m)	16650	24000
Earth radius (m)	6370000	6370000
"Bulge" height or h_{inc} (m)	**21.76**	**45.21**

From the above results, it is evident that both receiving paths are not in a direct line-of-sight range, which is a result due to the "bulging" of the curvature of the earth's surface that includes the changing of the sea tide. By comparing the approximated "bulge effect" with the Fresnel zone radius for both experimental paths, the Fresnel zone radius is around 60 metres above the "bulging effect" caused by the curvature of the earth. Therefore, it is evident that both VHF/UHF signals propagated approximately within the first Fresnel zone in this experiment.

6.3 Surface wave attenuation

One means by which the radio wave propagates in the troposphere is by ground wave. In analysing the propagation mechanism near the earth surface, ground waves are often separated into three major propagating mechanisms; direct, reflected and surface wave [Bullington, 1977]. At high frequencies such as VHF/UHF, the surface wave is limited to shorter distances due to an increase in attenuation as it is strongly affected by the electrical properties of the ground.

Bullington [1977] further stated that the surface wave is the major component of ground wave for frequencies of a few MHz, but of secondary importance at VHF and can be ignored at frequencies more than 300 MHz. This is shown in Figure 6.4 obtained from Bullington [1977] where if the antenna height is more than the minimum effective height, surface wave propagation will not be the controlling factor.

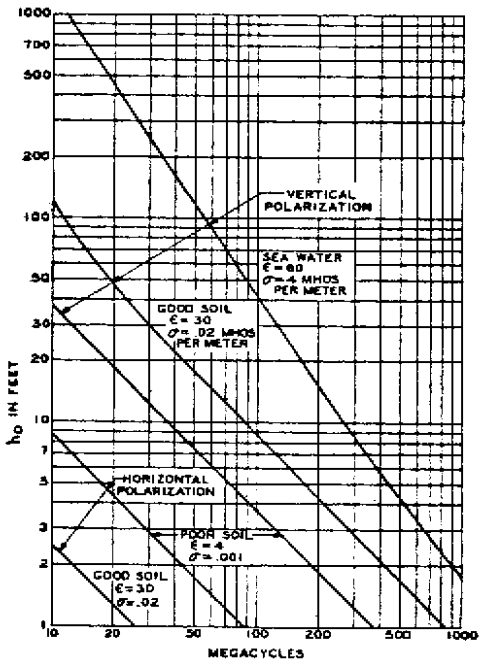

Figure 6.4: Minimum effective height for surface wave propagation [after Bullington, 1965]

From Figure 6.4, by using both F1 (248.375 MHz) and F2 (341.375 MHz) as references, h_o (minimum effective height) are around 3 and 2 metres respectively. In this case, the antenna height for both transmitter and receiver is definitely higher than h_o since both are around 15 metres at mean sea level.

6.4 Diffraction path loss simulation from a smooth spherical earth

Roda [1988] suggested that for a beyond-the-horizon path, at minimum scatter angle (less than 1°), diffraction is the dominant propagation mechanism and is much more stable than troposcatter. Its variations are mainly due to the changing in the refractivity of the air. The differences between diffraction and troposcattering in a beyond-the-horizon path were discussed in Section (2.8).

"The diffraction path loss is considered as the sum of the free-space loss which exists in the absence of obstacles and the diffraction loss introduced by the obstacles" [Roda,1988]. By deriving the formulae obtained from ITU-R P.526-7, the additional transmission loss due to diffraction for a smooth spherical earth (e.g. over the sea) can be determined. The diffraction path loss equations obtained from both ITU-R P.526-7 and Roda [1988] are given below:

The diffraction path loss L_d in dB is given:

$$L_d(\text{dB}) = F(D_n) + G(H_{TX}) + G(H_{RX}) \tag{6.04}$$

The distance term is given by the equation:

$$F(D_n) = 10\log D_n - 17.6D_n + 11 \tag{6.05}$$

D_n is the normalised (with a factor for surface admittance K_n) path length between the antenna at normalised heights H_{tx} and H_{rx} as shown below:

$$D_n = 2.2d_{tx-rx}\left(\frac{f}{r^2}\right)^{1/3} \tag{6.06}$$

where $d_{tx\text{-}rx}$ is in km, f is in MHz and r is the earth radius in km.

Four different height gain terms G(H) for both (H_{TX}) and (H_{RX}) are given by the following formulae:

for $H > 2$: $$G(H) \cong 17.6\left(H - 1.1\right)^{1/2} - 5\log\left(H - 1.1\right) - 8 \tag{6.07}$$

for $10K_n < H < 2$: $$G(H) \cong 20\log\left(H + 0.1H^3\right) \quad (6.08)$$

for $K_n/10 < H < 10K_n$: $$G(H) \cong 2 + 20\log K_n + 9\log\left(\frac{H}{K_n}\right)\left\{\log\left(\frac{H}{K_n}\right) + 1\right\} \quad (6.09)$$

for $H < K_n/10$: $$G(H) \cong 2 + 20\log\left(K_n\right) \quad (6.10)$$

The normalised height H for both transmitter (H_{tx}) and receiver (H_{rx}) is given by the formula:

$$H = 9.6\mathrm{h}\left(\frac{f^2}{r}\right)^{1/3} \times 10^{-3} \quad (6.11)$$

where h is either the height of transmitter (h_{tx}) or receiver (h_{rx}) in metre.

K_n (see equation 6.10) is the normalised factor for surface admittance and can be calculated by the following formulae obtained from ITU-R P.526-7:

for horizontal polarisation: $$K_H = 0.36(rf)^{-1/3}\left[(\varepsilon - 1)^2 + \left(\frac{18000\sigma}{f}\right)^2\right]^{-1/4} \quad (6.12)$$

for vertical polarisation: $$K_V = K_H\left[\varepsilon^2 + \left(\frac{18000\sigma}{f}\right)^2\right]^{1/2} \quad (6.13)$$

ε and σ are 80 and 5 respectively for seawater and the electrical characteristics of the Earth are not important if K_n is less than 0.0001.

From Roda [1988], for frequencies greater than 300 MHz, the maximum value for K_n can be considered as:

$K_V = 4.5 \times 10^{-2}$ for vertically polarised signal on water
$K_H = 2.0 \times 10^{-3}$ for horizontally polarised signal always

The total path attenuation L_p can be considered as:

$$L_p = L_{fs} + L_d \text{ (dB)} \tag{6.14}$$

A very good example on how to use the above diffraction path loss equations is shown in Roda [1988] and he further suggested that Equation 6.09 was suitable for antennas that are installed on an island at a height less than 20 metres.

By using the equations mentioned above, the total path attenuation loss L_p as stated in Equation 6.14 for both receiving sites can be determined. By changing the height of both transmitter (h_{tx}) and receiver (h_{rx}) antennas respectively, the amplitude versus tide height plot for both receiving sites can be determined for different frequencies and polarisation as shown in Figure 6.5 and Figure 6.6. By comparing these two figures with Figure 5.2 and Figure 5.26 (calm sea states for Jersey to Guernsey and Jersey to Alderney) respectively, it is seen that the measurements are consistent with the diffraction path loss equation. For example, the measurements from Figures 5.2 and 5.26 showed around 1.1 dB loss per meter of tide height changes while in comparison, Figures 6.5 and 6.6 show around 1.2 dB loss. Therefore, the diffraction path loss equations obtained from the ITU-R P.526-7 can be applied to this experiment for both VHF/UHF signal across the Channel Islands especially during calm sea states day. This consistency between the measurements and simulated results suggested that the dominating propagation mechanism for Jersey-Guernsey path during calm sea day is smooth earth diffraction.

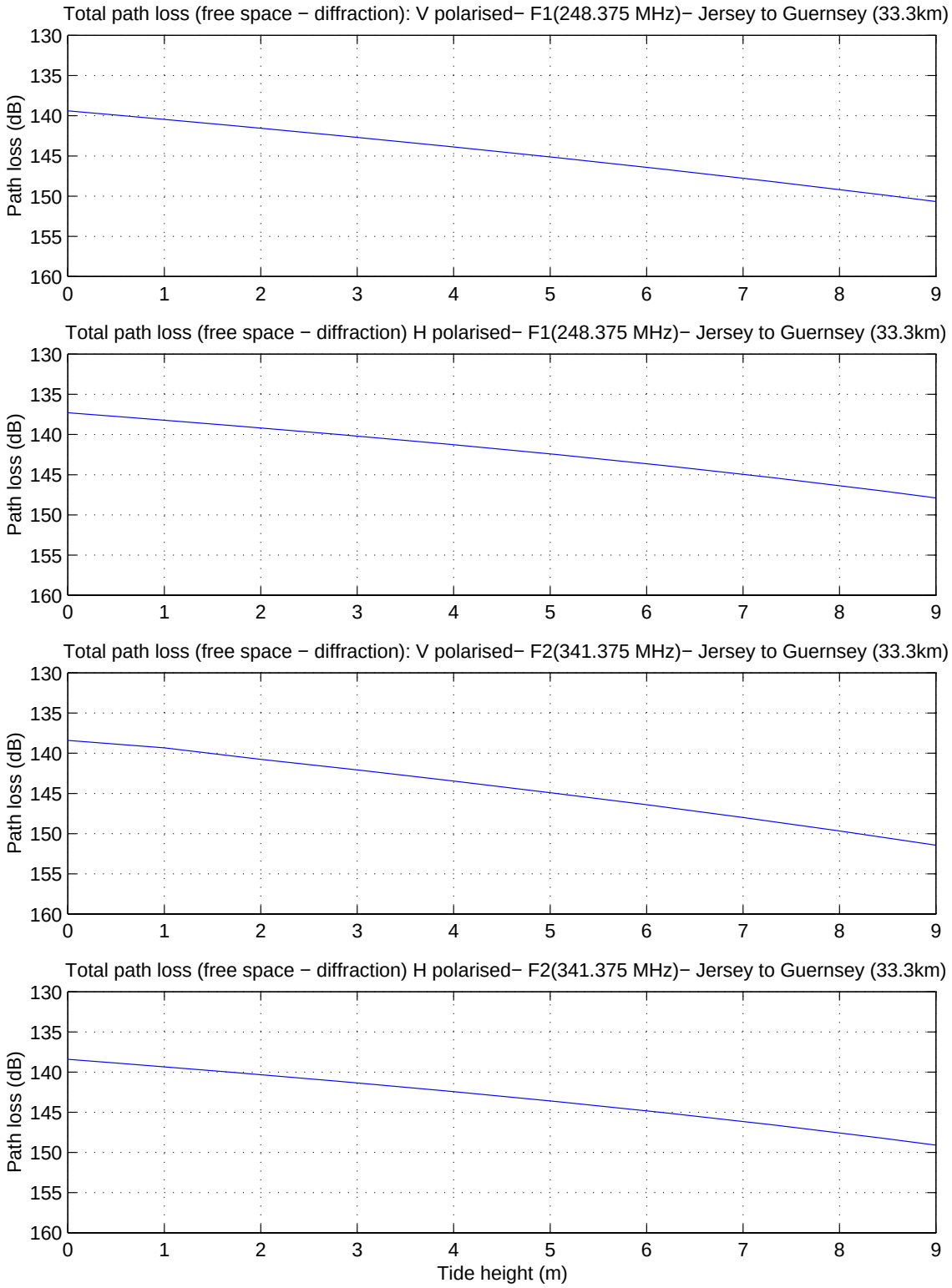

Figure 6.5: Total path attenuation versus tide height plot for Jersey to Guernsey

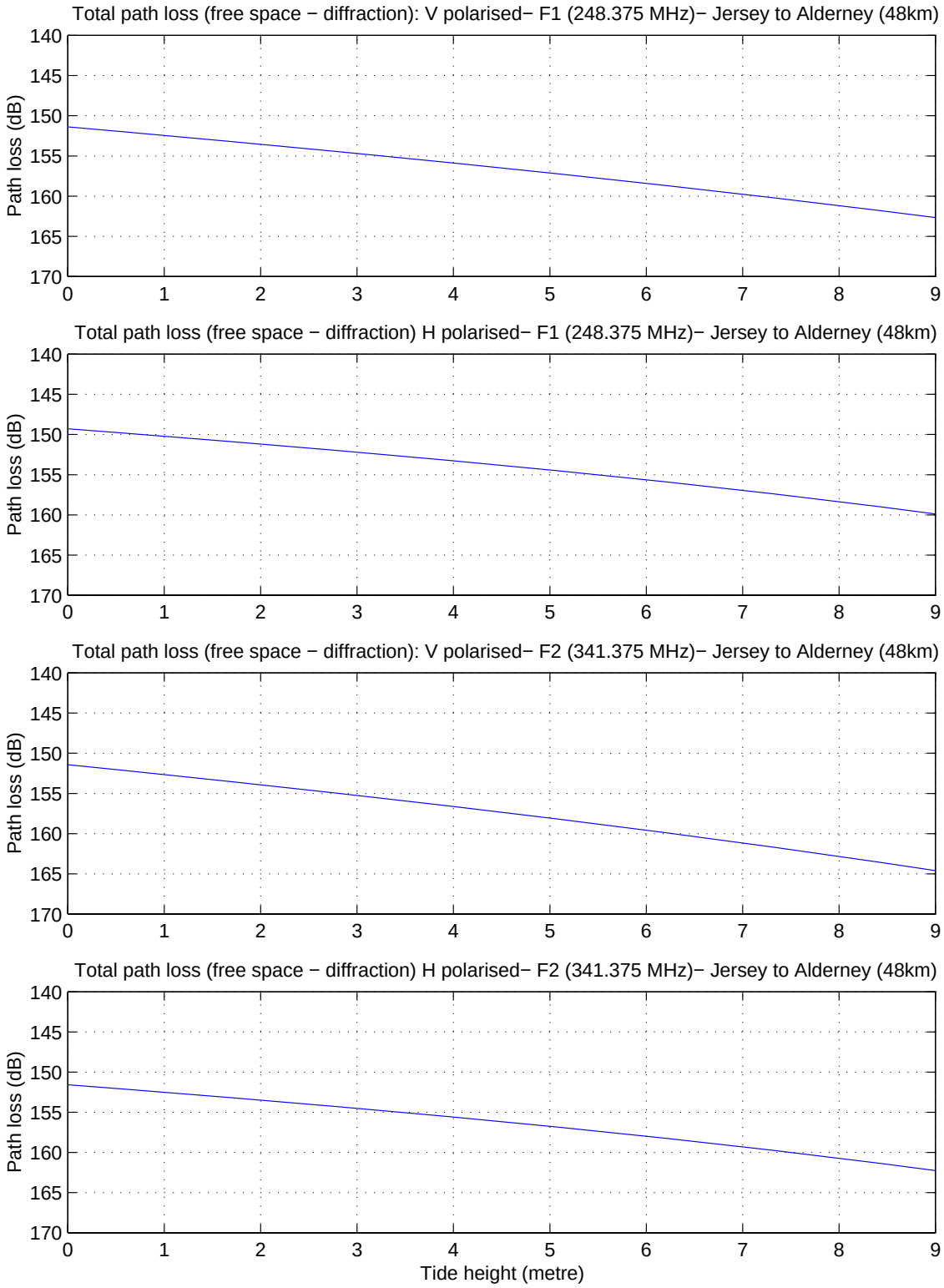

Figure 6.6: Total path attenuation versus tide height plot for Jersey to Alderney

6.5 Tropospheric scattering for VHF/UHF signal propagation

It is important to distinguish or verify that the received signal is a result of the diffraction from the smooth earth, or by scattering due to tropospheric effect which sometimes known as troposcatter [Griffiths, 1987]. At a certain distance far beyond the horizon, diffraction losses become increasingly so high that transmission of signal is impossible. Under these circumstances, troposcatter propagation as discussed in Section 2.7 becomes the dominant propagating mechanism and transmission via troposcatter is possible and reliable under a few conditions, mainly short distances, high pressure, summer period and lower scattering angle (e.g. below 4°) suggested by Griffiths[1987] in order to achieve smooth transmission.

From Griffiths [1987], it suggested that the annual median path loss in dB due to troposcattering effect is:

$$L_{p(sc)} = L_{fs} + L_{sc} + L_c + L_{misc} \tag{6.15}$$

Where L_{fs} is the free space loss, L_{sc} is the scatter loss, L_c is the antenna to medium coupling loss and L_{misc} accounts for the other miscellaneous losses. The scatter loss (dB) is given:

$$L_{sc} = 83 + 0.57\theta_{sc} + 10\log f - 0.2N_s \tag{6.16}$$

where θ_{sc} in mrad is the scattering angle and is given by the formula:

$$\theta_{sc} = 0.118d - 0.485\left(\sqrt{h_{tx}} + \sqrt{h_{rx}}\right) \tag{6.17}$$

The distance from transmitter to receiver d is in km and both antenna heights h_{tx} and h_{rx} are in metres. Frequency f is in MHz and N_s is the surface refractivity.

The antenna to medium coupling losses in dB is given by the formula:

$$L_c = 0.07 \exp\{0.055[G_t + G_r]\} \tag{6.18}$$

as both G_t and G_r are the gains of the transmitting and receiving antennas.

By ignoring both L_c and L_{misc} from equation (6.15) and applying equation (2.07) for L_{fs}, L_{sc} can be considered as:

$$L_{sc} = 115.4 + 0.57\theta_{sc} + 20\log d + 30\log f - 0.2N_s \tag{6.19}$$

By applying the equations from free space, diffraction and scattering losses, the total path attenuation due to free space, diffraction and troposcatter mechanisms can be determined. Note that N_s was assumed to be 320 and the effective earth radius as 8500km.

Figure 6.7 and Figure 6.8 show both the total path attenuation losses L_p, for F1 and F2 (vertical and horizontal wave) respectively, with various distances up to 100 km at different antenna heights (10 to 50 metres) above the earth surface. Every plot shows the path attenuation of the rays at different distances starting from diffraction with free space attenuation until the estimated range when troposcatter effect becomes the dominant mechanism. From these figures, it is evident that greater antenna heights will result in propagation losses much closer to free space losses. In addition, significant troposcattered effects occurred at much shorter distances (around 40 to 50 km) when the antenna heights are low (e.g. 10 metres).

By comparing the above results with the measurements obtained from Jersey-Alderney path, it is suggested that the high fading phenomenon (observed within periods of seconds in Jersey-Alderney) is a result of interference fading between the diffracted wave and troposcatter signal. This is consistent with the measurements from Section 5.3.2 showing the depth of fading (within periods of seconds) decreases with lower tide height (antenna height around 20 metres) as shown in Figures 5.36 and 5.37.

The above results coincide with Gough [1979], concluding that troposcatter will becomes the dominating propagating mechanism if the diffracted signal is 50 dB below L_{fs}.

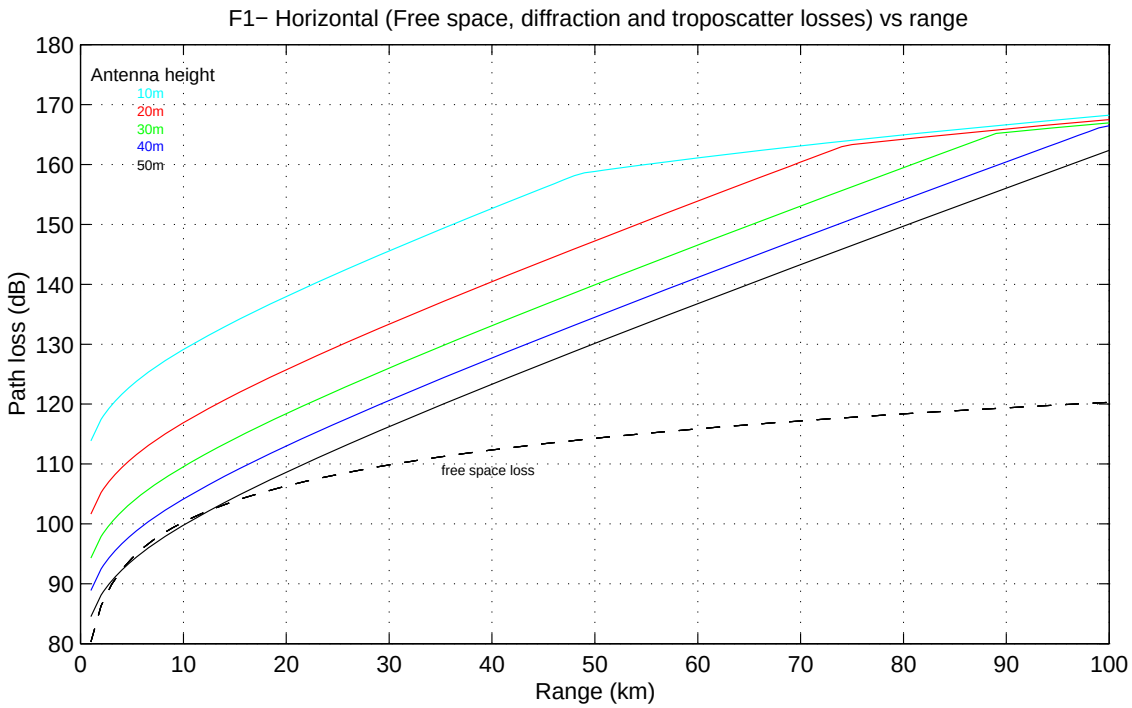

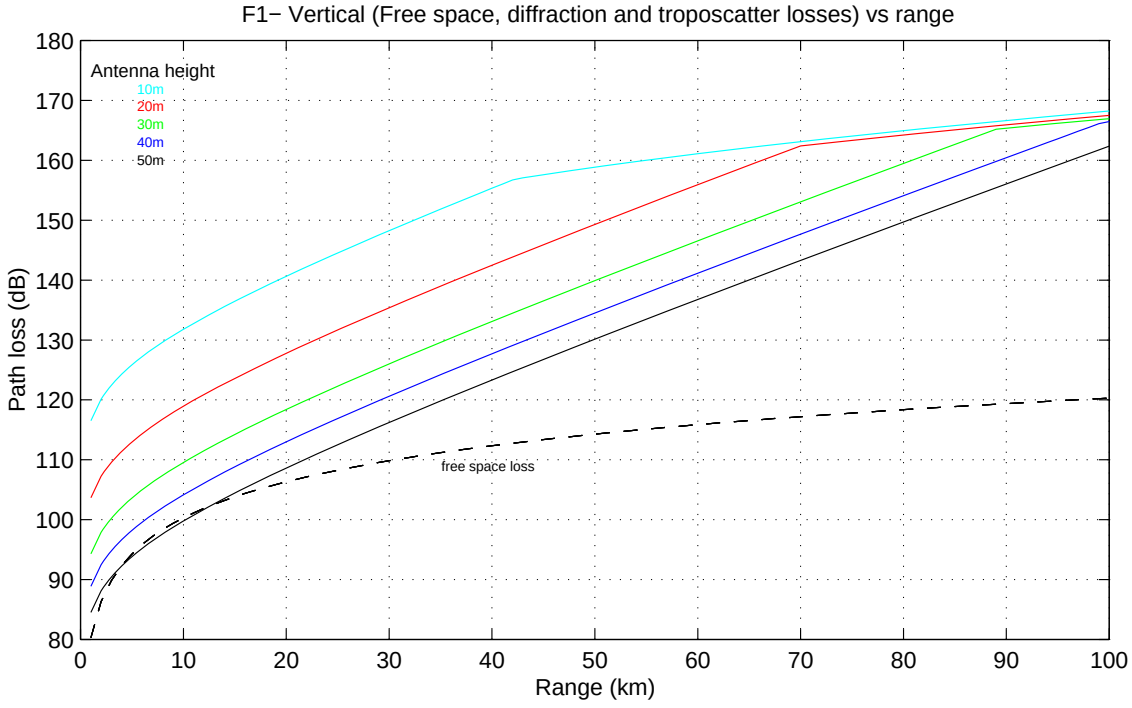

Figure 6.7: F1 path attenuation (free space, diffraction and scattering) versus distances for various antenna heights (top figure: F1- Horizontal and bottom figure: F1- Vertical)

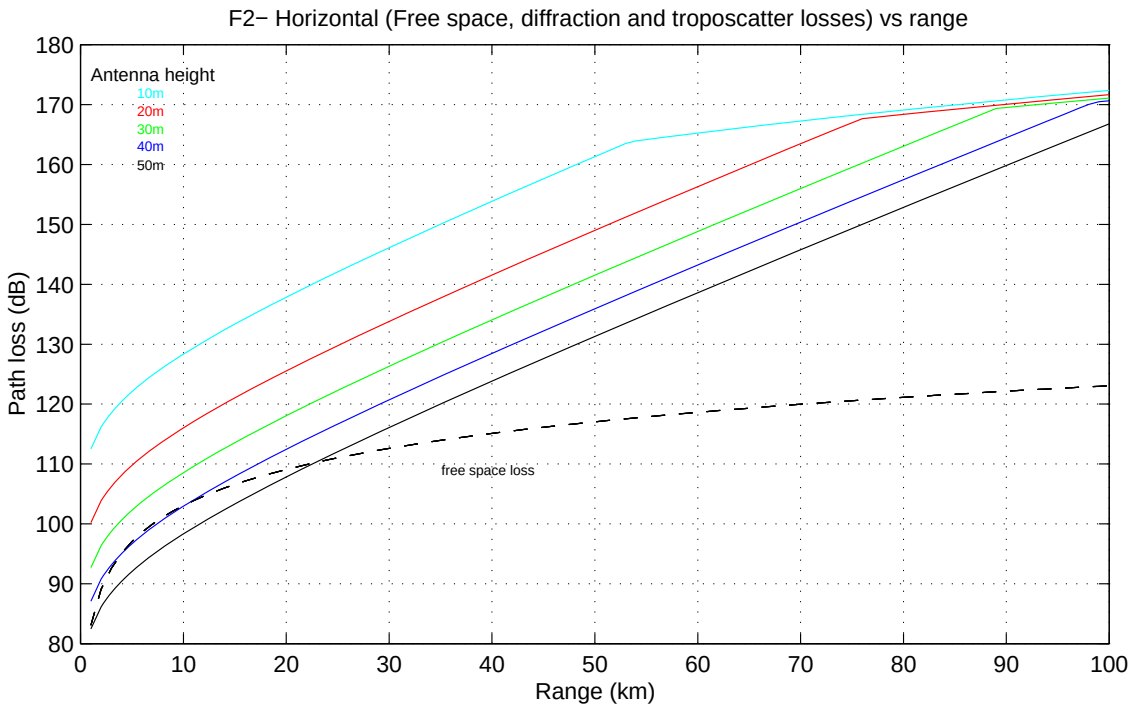

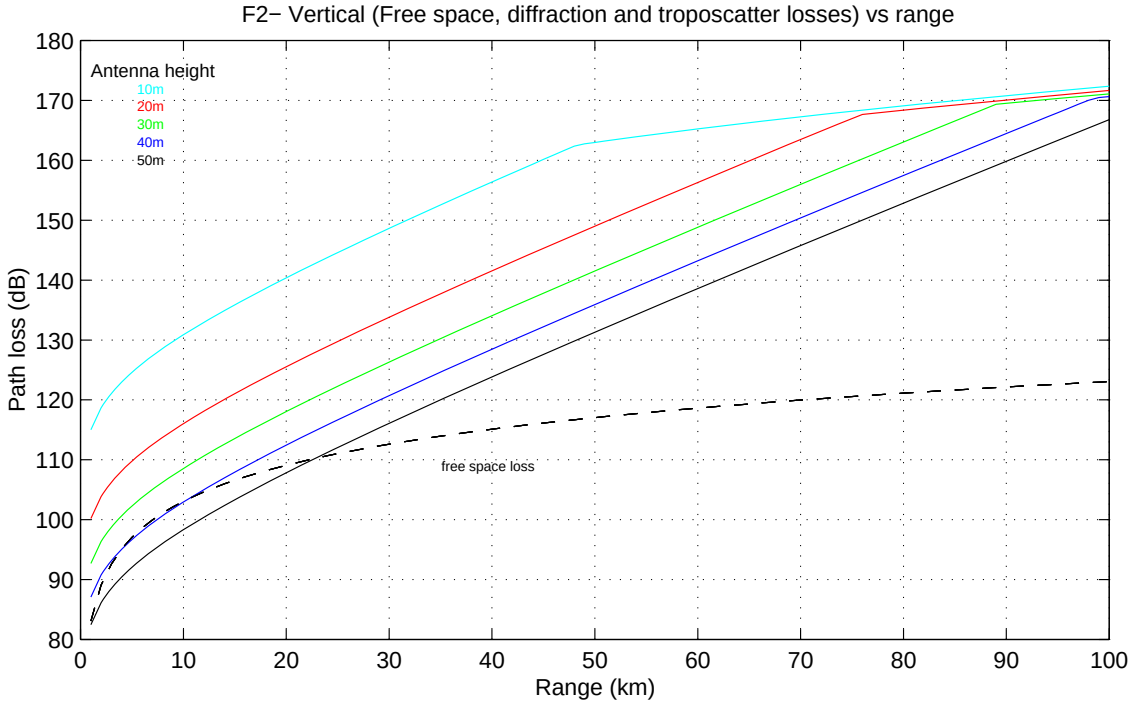

Figure 6.8: F2 path attenuation (free space, diffraction and scattering) versus distances for various antenna heights (top figure: F2- Horizontal and bottom figure: F2- Vertical)

6.6 Ray tracing simulation

Ray tracing programs can be developed to simulate the propagation of the rays that result in creating a more realistic ray propagating images on a computer. Although ray tracing techniques have been widely used for many years and new authors have been including the basic theory of ray tracing (Levy [2000], Lavergnat and Sylvain [2000]), many fail to relate it to VHF/UHF signal propagation over the sea.

This section will begin with the brief discussion from Lavergnat & Sylvain [2000] on the principle on how the changing of atmospheric conditions will lead to situations of abnormal refraction and how this effect can be modelled and predicted. Methods of obtaining the refractive index from the weather parameter acquired from various website, which is vital to the outcome of the propagating ray will be shown. Ray tracing equations derived from Snell's law for a spherically stratified medium will be discussed and simulation results will be shown.

6.6.1 Abnormal refraction and its effect on ray propagation

As discussed in Chapter 2, during unusual atmospheric conditions, the refractive index in the air will change dramatically and this will lead to two types of phenomenon: super-refraction and sub-refraction (see Figure 2.6). The super refraction will increase the radio horizon and in extreme cases, ducting will occur and this will lead to higher signal amplitude. The sub-refraction will shorten the radio horizon, reducing the clearance over terrain along the propagation paths and lead to losses in signal amplitude [Hall *et al*, 1996].

Lavergnat and Sylvain [2000] stated that the behaviour of a propagating ray depends crucially on the relative position of the trajectory of the ray and the atmospheric structure surrounding it at that point. In each of the refraction cases mentioned above, ray-tracing through a horizontally stratified medium can evaluate the propagation effects. Lavergnat and Sylvain [2000] further commented that ray-tracing methods alone are insufficient to fully describe the character of a particular ray propagating across a certain path, but are enough to distinguish the major differences of the phenomenon encountered.

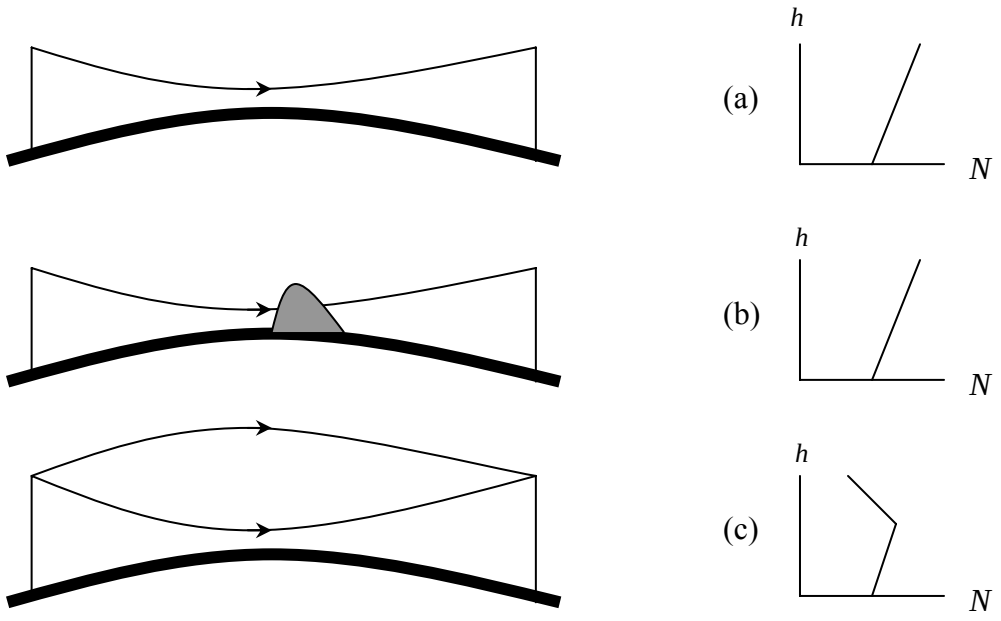

Figure 6.9: Effects of a sub-refracting layer at ground level [after Lavergnat and Sylvain , 2000]

Figure 6.9(a) shows a typical sub-refracting ray as the refractivity (*N*) increases with height *h*. From the above-mentioned figure, when the sub-refracting layer rises from the earth to a height greater than the path of propagating rays, the rays could propagate very close to the earth. Hence, attenuation due to diffraction by the ground has to be taken into consideration. Fading by obstruction is present when there is an obstacle in between the path as shown in Figure 6.9(b). Figure 6.9(c) shows a different scenario when the sub-refracting layer height is less than the propagating path and refraction phenomenon such as "standard" or "super-refraction" occurs. Super-refraction in this case is discussed more thoroughly in Section 2.4.1 and Lavergnat and Sylvain [2000] provided an example on the influences of the relative position of the rays at different refracting layes.

6.6.2 Radio refractive index and water vapour pressure

The propagation velocity in the troposphere is determined by the refractive index, which is dependent on temperature, pressure and relative humidity (Hall *et al* [1996], Biddulph [1993]). By using equation (2.09), the radio refractive index can be obtained. Both the *Pd* (air pressure- millibars) and *T* (air temperature- Kelvin) for both Jersey airport and Channel Lightship Vessel can be obtained from the weather data mentioned in Section4.5.

The actual water vapour pressure e_a can be obtained by using the following equation obtained from Jensen *et al* [1990]:

$$T_{dew} = \frac{116.91 + 237.3\ln(e_a)}{16.78 - \ln(e_a)} \tag{6.20}$$

By revising equation (6.20), the actual water vapour e_a (in millibars) is:

$$e_a = \exp\left(\frac{16.78T_{dew} - 116.91}{237.3 + T_{dew}}\right) \times 10 \tag{6.21}$$

T_{dew} (dew point temperature in degree Celsius) for both Jersey airport and Channel Light Vessel are available in the weather data.

6.6.3 Simple wave trajectory equation for spherically stratified medium

The most efficient and simple way to understand how VHF/UHF propagates in the troposphere is to obtain the wave trajectories of the radio wave. By creating a simple ray-tracing model from equation derived from Snell's Law, it enables the user to make propagation prediction by changing the ray parameters e.g. (refractive index above the sea). The ray trajectory parameters and derivation of the equations for a spherically stratified medium will be discussed in this section. The illustrative results from this model with different ray parameters will be shown in Section 6.6.4.

From both Figure 6.10 and Figure 6.11, by modifying Snell's Law, the following equation is obtained:

$$n(\eta) \times \eta \times \cos\alpha = n(0) \times r_0 \times \cos\alpha_0 \tag{6.22}$$

where $n(\eta)$ is the refractive index in the atmosphere, $n(0)$ is the refractive index at the transmitter antenna (level 0). α_0 is the elevation angle in radians where the ray departs at (level 0) and α is the elevation angle of the ray at the atmosphere at height η. The earth radius r is in metres and $r_0 = r + \Delta H$, where ΔH is the change in antenna height (in metre) due to sea tide.

$n(\eta)$ can also be obtained by:

$$n(\eta) = n(0) + a(\eta - r_0) \tag{6.23}$$

where a is the change in refractive index with respect to the change in height η or $\left(\frac{dn}{d\eta}\right)$.

by substituting (6.22) into (6.23), the height η (in metre) is:

$$\left[n(0) + a \times (\eta - r_0)\right] \times \eta = n(0) \times r_0 \times \frac{\cos\alpha_0}{\cos\alpha} \tag{6.24}$$

by expanding equation (6.24), the following is obtained:

$$a\eta^2 + \eta \times \left[n(0) - ar_0\right] - n(0) \times r_0 \times \frac{\cos\alpha_0}{\cos\alpha} = 0 \tag{6.25}$$

by solving the quadratic equation for η in (6.25), height η is:

$$\eta = \frac{1}{2a}\left\{ar_0 - n(0) \pm \left[\left(n(0) - ar_0\right)^2 + 4a \times n(0) \times r_0 \times \frac{\cos\alpha_0}{\cos\alpha}\right]^{1/2}\right\} \tag{6.26}$$

From Appendix B, the earth angle ζ in radian can be considered as:

$$\zeta = \frac{n(0)\cos\alpha_0}{n(0) + ar_0}(\alpha - \alpha_0) \tag{6.27}$$

therefore, the earth angle ζ_0 in radian where it is the point when the ray is returning to earth at height η_0 in metre is:

$$\zeta_0 = -\frac{n(0)\cos\alpha_0}{n(0) + ar_0}\alpha_0 \tag{6.28}$$

The distance at earth return can be considered as half of the distance between the transmitter and the receiver ($d_{tx\text{-}rx}$) as shown below by using (6.28):

$$\frac{d_{tx-rx}}{2} = r_0\zeta_0 = -\frac{n(0)\cos\alpha_0}{n(0)+ar_0}\times r_0\alpha_0 \tag{6.29}$$

by assuming $\cos\alpha_0$ is ≈ 0, the departing angle α_0 at level 0 can be considered as:

$$\alpha_0 = -\frac{d_{tx-rx}\left(n(0)+ar_0\right)}{2n(0)r_0} \tag{6.30}$$

Reference to Figure 6.11, the following four simplified equations are used to plot both the X and Y axis of both the propagating ray and spherical earth respectively:

$$\mathrm{X}_{\mathrm{ray}} = \left(r_0 - \Delta\mathrm{H}\right)\sin\zeta_0 - \eta\sin\left(\zeta_0 - \zeta\right) \tag{6.31}$$

$$\mathrm{Y}_{\mathrm{ray}} = \eta\times\cos\left(\zeta_0 - \zeta\right) - \left(r_0 - \Delta\mathrm{H}\right)\times\cos\zeta_0 \tag{6.32}$$

$$\mathrm{X}_{\mathrm{earth}} = \left(r_0 - \Delta\mathrm{H}\right)\left[\sin\zeta_0 - \sin\left(\zeta_0 - \zeta\right)\right] \tag{6.33}$$

$$\mathrm{Y}_{\mathrm{earth}} = \left(r_0 - \Delta\mathrm{H}\right)\times\left[\cos\left(\zeta_0 - \zeta\right) - \cos\zeta_0\right] \tag{6.34}$$

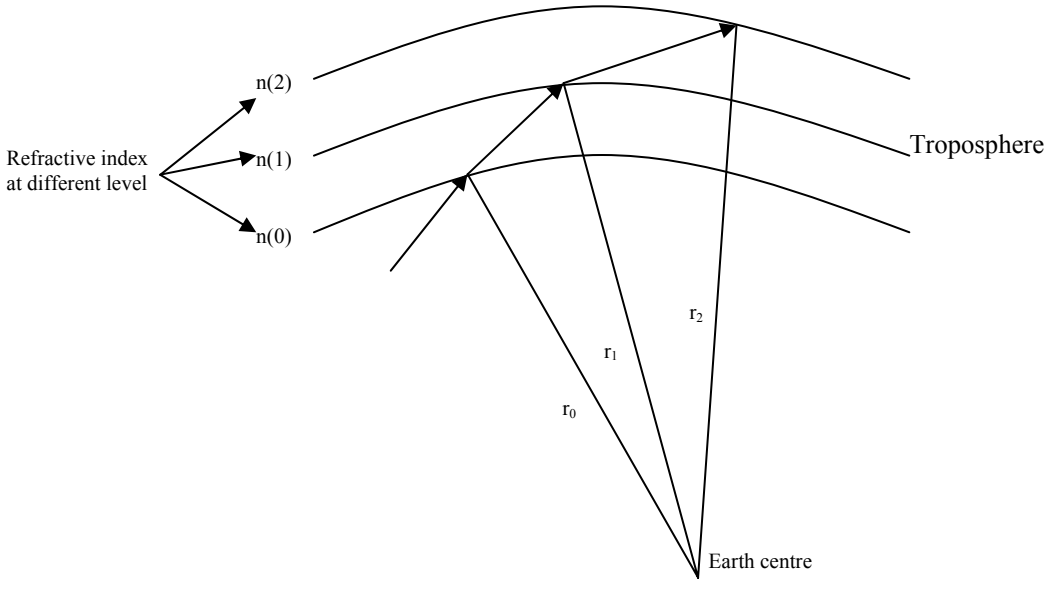

Figure 6.10: Changing refractive index with height in the troposphere

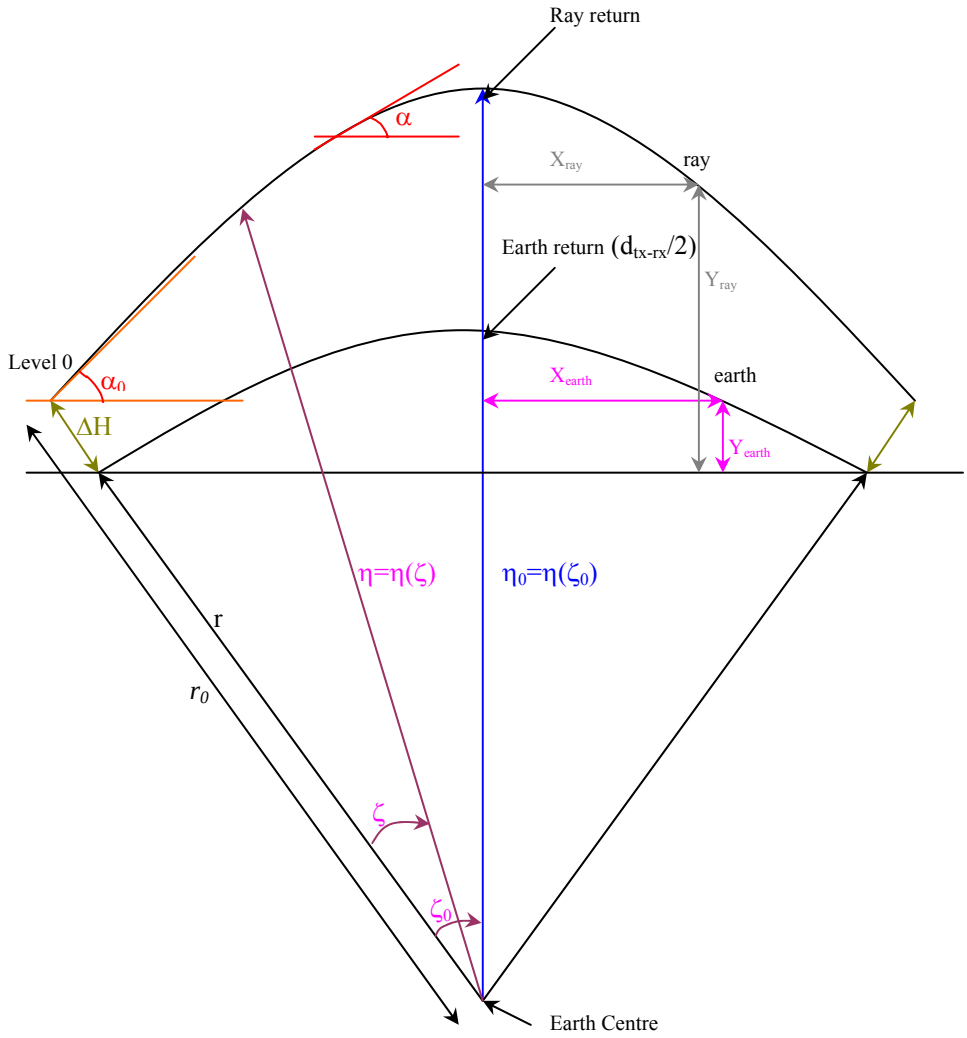

Figure 6.11: Trajectory of ray over the sea in the troposphere

6.6.4 Wave trajectory from Jersey to Guernsey on a spherically stratified medium

The above equations were used to plot the ray from Jersey to Guernsey, a 33.3 km path length. Two assumptions have been made:

(1) both the antennas at Jersey and Guernsey are around 15 metres above the mean sea level without any variation as affected by the sea tide and sea waves.

(2) the height differences between the Jersey airport and Channel Light Vessel is around 85 metres above the mean sea level.

Two measurements will be discussed in this section, a calm sea day during spring on (10^{th} April 2001) and a hot summer day on (26^{th} July 2001).

The equations from Section 6.6.3 show that when α_0 (the elevation angle where the ray departs at level 0) is negative, or when the refractive index of Jersey airport is greater than Channel Light Vessel ($n_J > n_{LS}$), the propagating ray tends to deviate downwards as shown in Figure 6.12. The values for n(Jersey-Lightship) are shown on the top right hand corner of Figure 6.12 together with the values for lapse rate which is:

$$n(\text{Jersey - Lightship}) \times 10^6 \times \frac{1000}{85} (N/\text{km}) \qquad (6.34)$$

From this figure, the propagating ray will approach a straight line when n_J - $n_{LS} \approx 0$ (lapse rate ≈ 0) and deviate downwards even more when lapse rate increased with a positive value. The lapse rate in this case was between 18 to 57 *N*/km. This is consistent with the theories given by Lavergnat and Sylvain [2000] as sub-refraction occurs when refractivity increases with height.

Figure 6.13 showed the ray tracing simulation on a hot summer day from Jersey-Guernsey on 26th July 2001. From the simulated measurement, it is seen that ducting has occurred at a lapse rate of –181 *N*/km at 1400 UT and super-refraction has occurred with lapse rate between –50 to –118 *N*/km on this day. In addition, rays with lapse rate less than –50 *N*/km are likely to be blocked by the bulging of the earth (from Jersey-Guernsey). This is consistent with the data collected on that day as enhanced signal strength (ESS) was observed (see Figure 5.12). Therefore, it can be concluded that ESS phenomenon is mostly due to super-refraction and ducting effect.

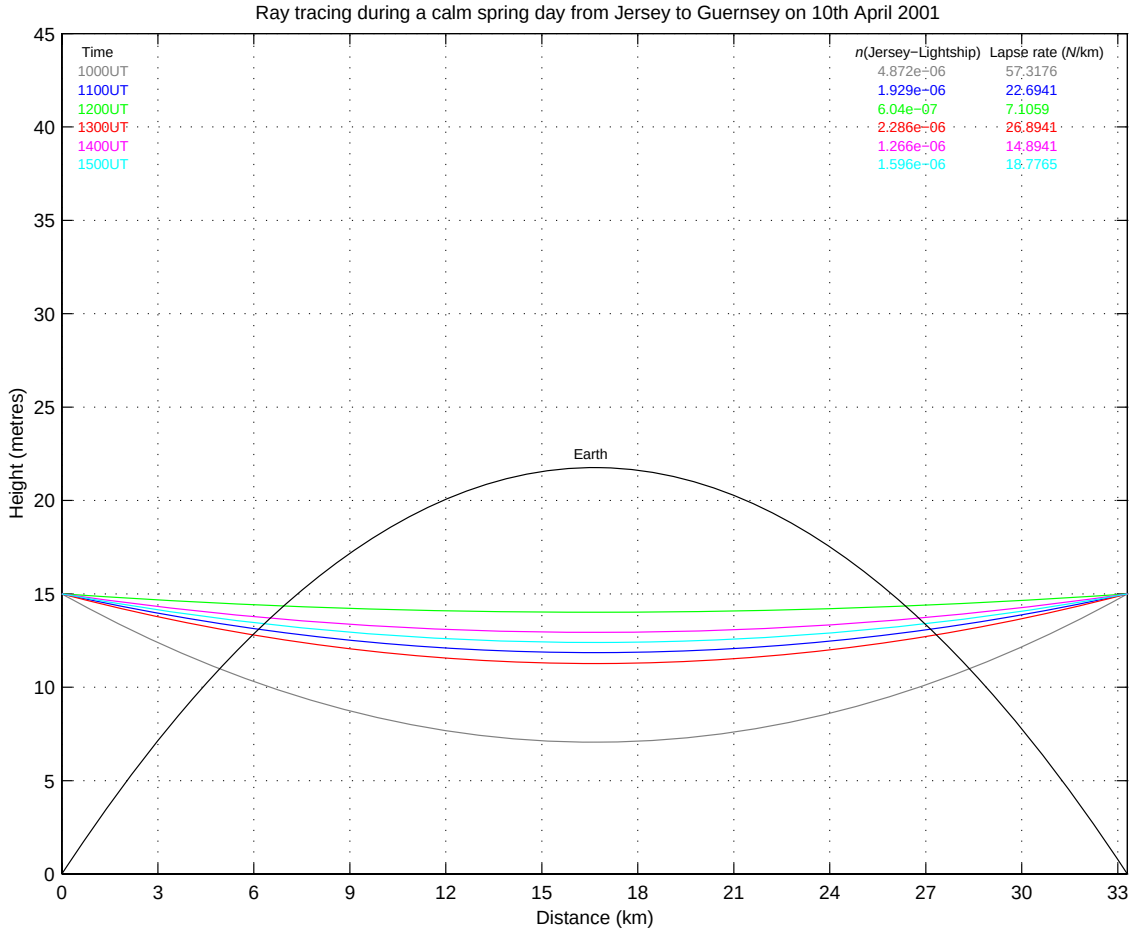

Figure 6.12: Trajectory of ray over the sea (Jersey to Guernsey) during calm spring day on 10th April 2001 [top left corner display the time and top right corner display the resultant refractive index (Jersey airport refractive index subtracted by Channel Light Vessel refractive index)]

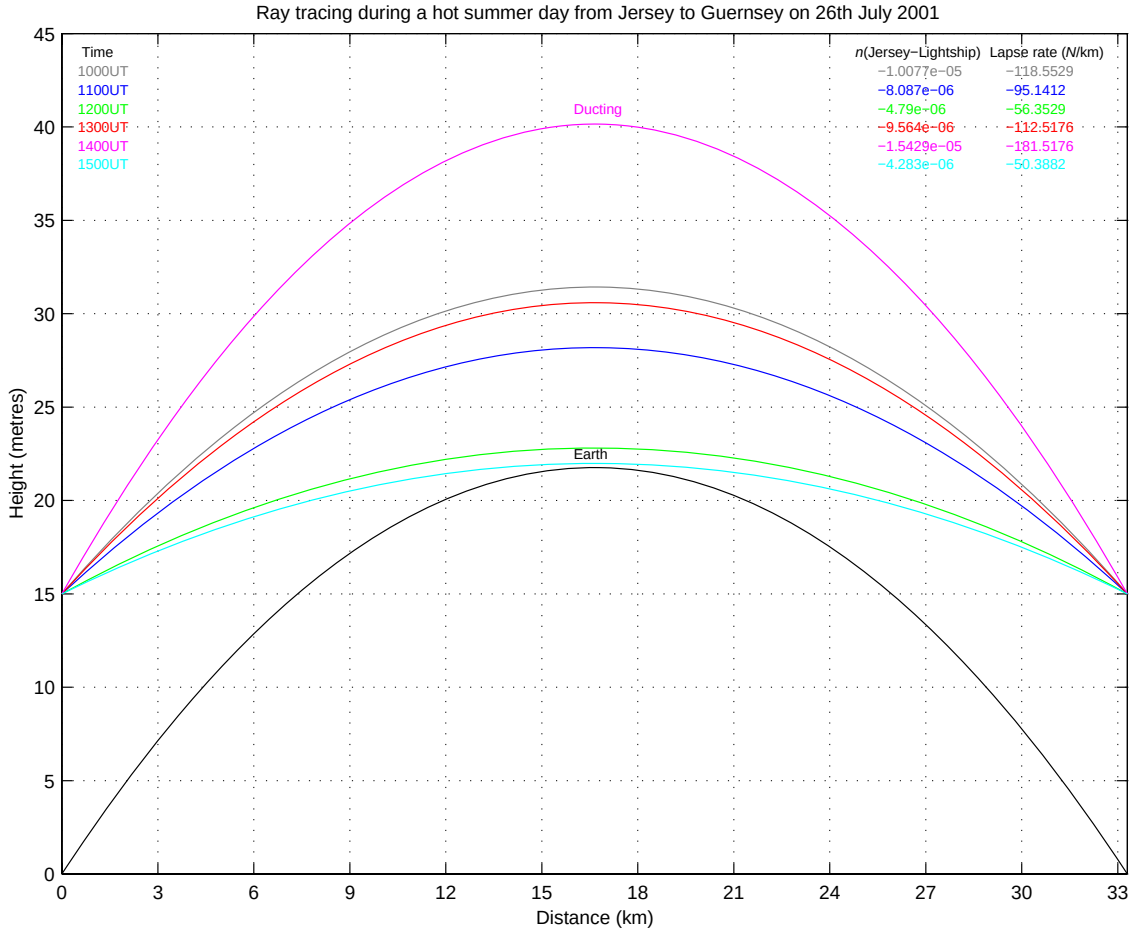

Figure 6.13: Trajectory of ray over the sea (Jersey to Guernsey) during a hot summer day on 26th July 2001

6.6.5 *Wave trajectory from Jersey to Alderney on a spherically stratified medium*

The same equations developed in Section 6.6.3 were used to plot the propagating ray from Jersey to Alderney, a 48 km path with the same assumptions made earlier. Ray tracing plots during autumn and summer day will be discussed in this section. A comparison of propagating rays with signal amplitude from (Jersey to Guernsey) and (Jersey to Alderney) during a "hot summer" day will also be discussed.

On the 18th Nov 2001, the Jersey air temperature was much lower than the Channel Light Vessel sea temperature and the weather parameters showed an average wave height of 1 metre and average wind speed of 12 knots (6.2 m/s). Figure 6.14 shows the ray trajectory from Jersey to Alderney for this day and from this figure, mixtures of standard and sub-refracting rays were shown and the "bulging" earth acted as an obstacle for all these propagating rays. By comparing with the data collected (see Figure5.23) for this day, diffraction is the dominant propagating mechanism with lapse rate between -47 *N*/km to 35 *N*/km. Figure 6.14 also revealed that on this day, most of the sub-refracted rays were below 5 metres with reference to the antenna height at zero level.

Figure 6.15 shows the ray trajectory during a hot summer day (21st Jun2002) for Jersey-Alderney when T_d is around 6°C. From the measurement, lapse rate up to –202 *N*/km was calculated (around 30 metres above the earth's surface) and therefore, it is evident that ducting has occurred and all the propagating rays are in the same Fresnel zone radius (around 100 metres). Figure 6.16 compares both simulated rays propagated from Jersey to both receiving sites (Guernsey and Alderney) during this day. From this figure, it shows that the simulated ray deviates much higher when the path length increases. In addition, it shows that the "bulge" height of the earth (around 45 metres) would obstruct most of the super-refracted rays below lapse rate of around –100 *N*/km for Jersey-Alderney path. For this case, it is evident that all rays propagate in the same Fresnel zone for both Jersey-Guernsey and Jersey-Alderney paths as the Fresnel zone radius is around 100 metres. In comparison, all the rays propagated beyond the earth "bulge" height for Jersey-Guernsey path (around 21 metres) during the same period. By comparing all these measurements with Figure 6.17 (Jersey-Alderney (1) and Jersey-Guernsey (2) amplitude plot) for this day, it is seen that the received signal strength via ducting is not necessarily higher than via super-refraction mode. In addition, Figure6.17

shows that the signal strength received at both locations are different by around 5 dB for this day.

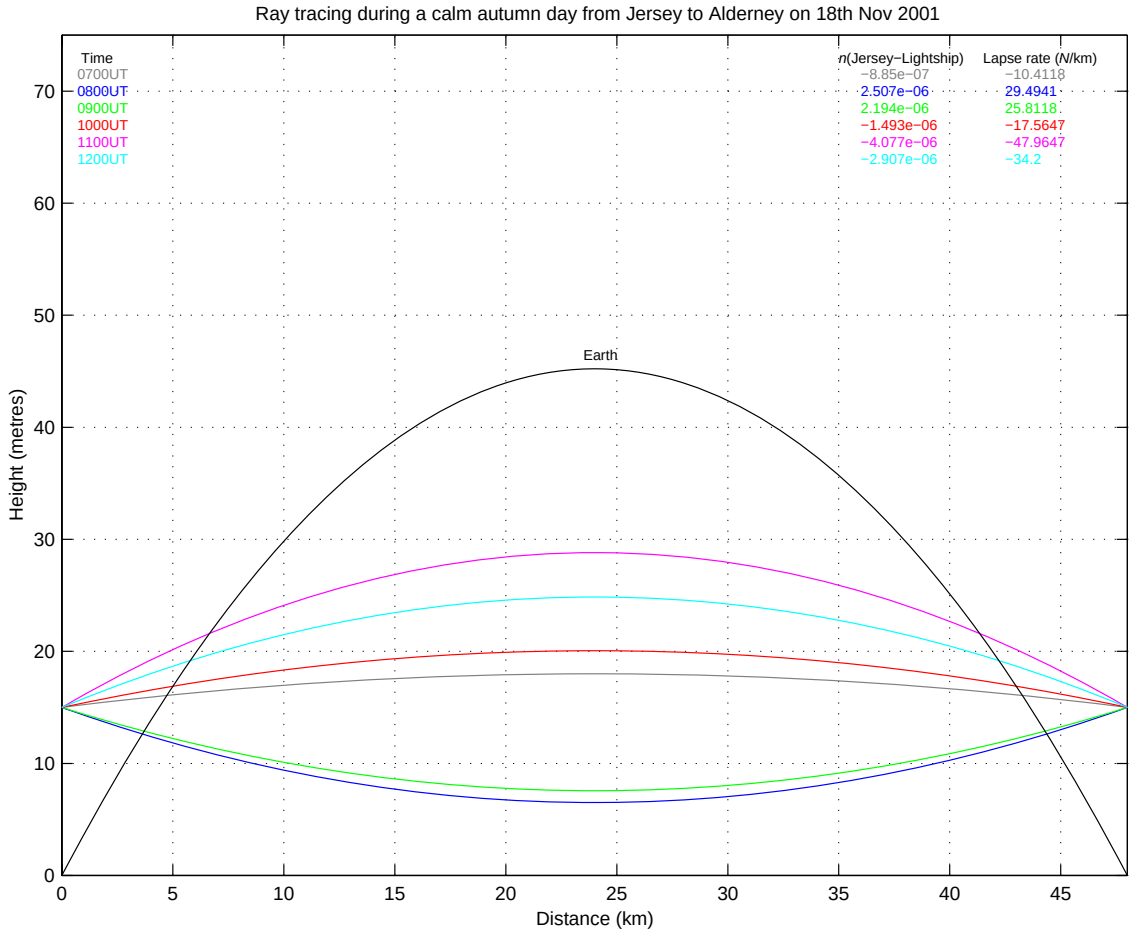

Figure 6.14: Trajectory of ray over the sea (Jersey to Alderney) during a calm autumn day on 18th November 2001

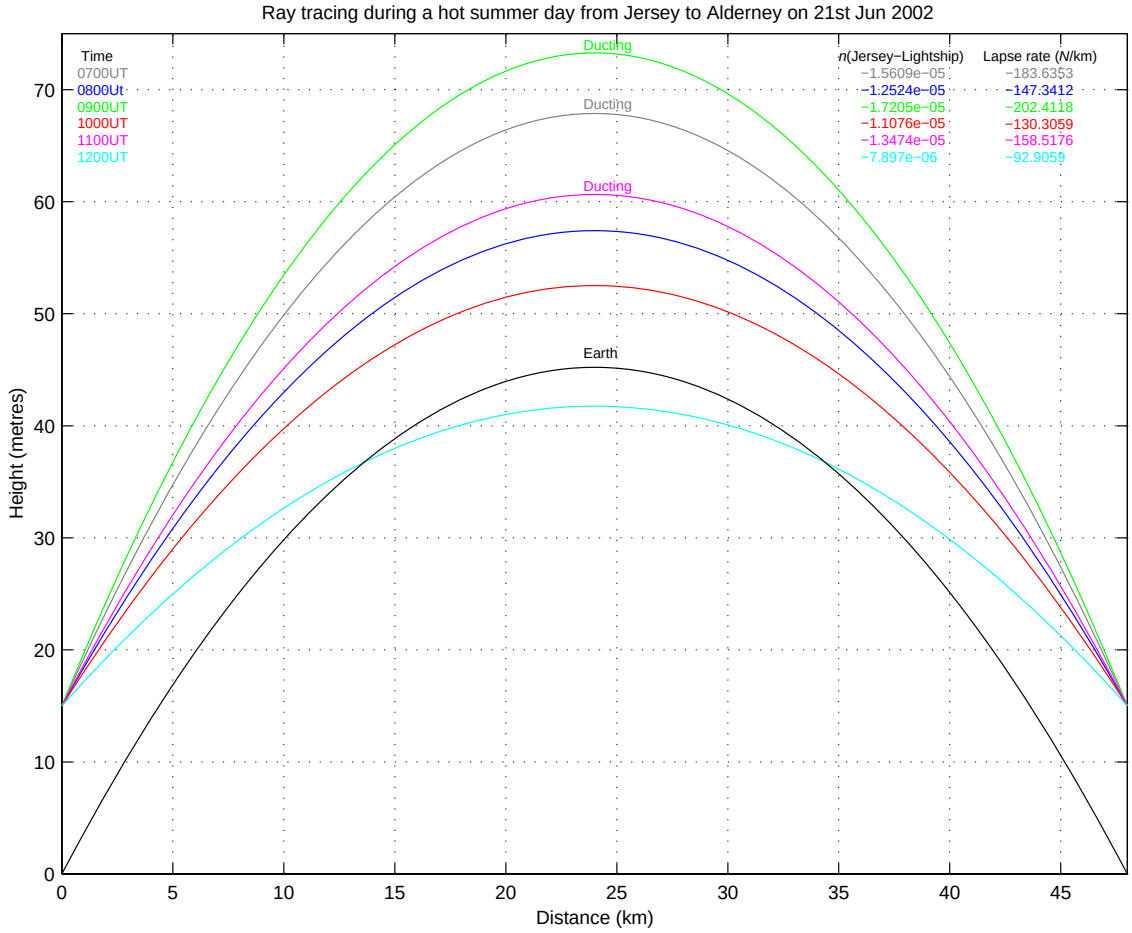

Figure 6.15: Trajectory of ray over the sea (Jersey to Alderney) during a hot summer day on 21st Jun 2002

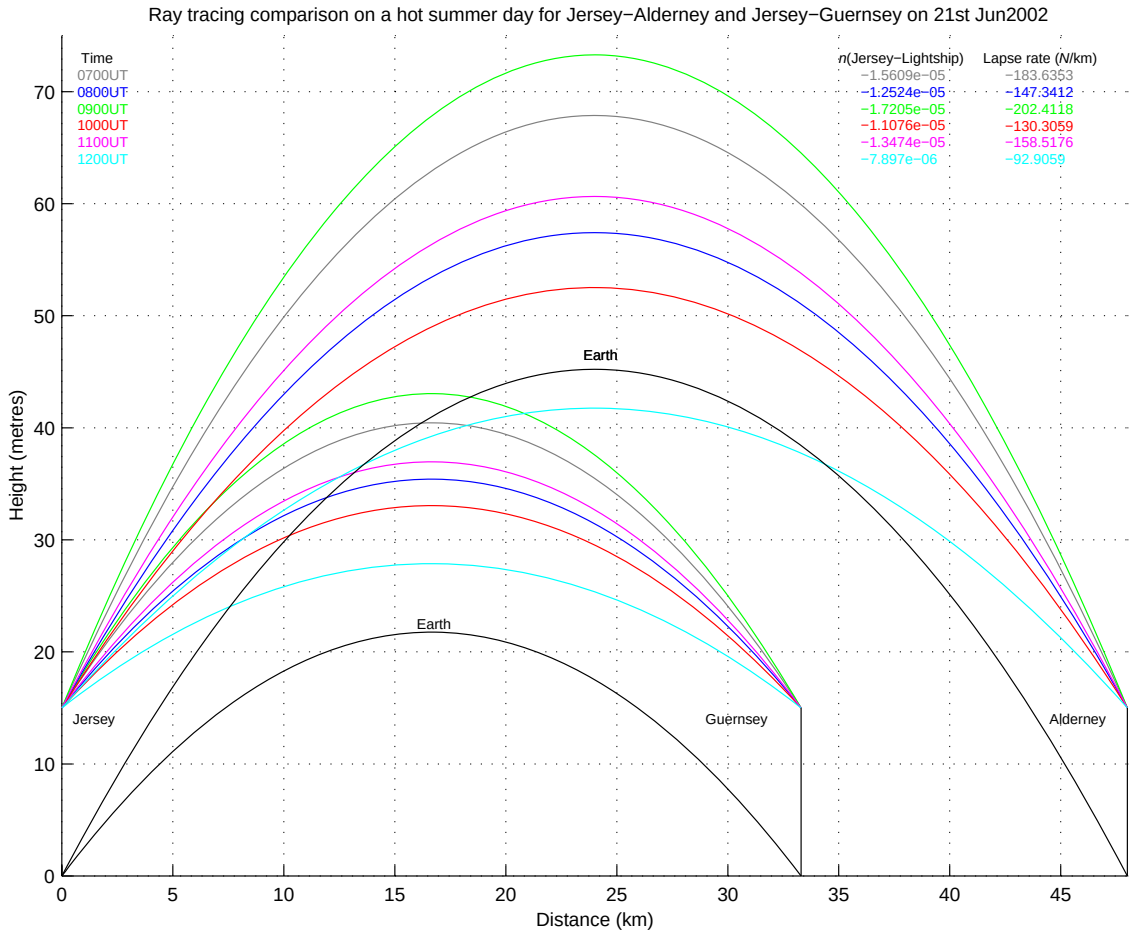

Figure 6.16: Comparison of trajectory of ray over the sea (Jersey to Guernsey & Alderney) during a warm day on 21st Jun 2002

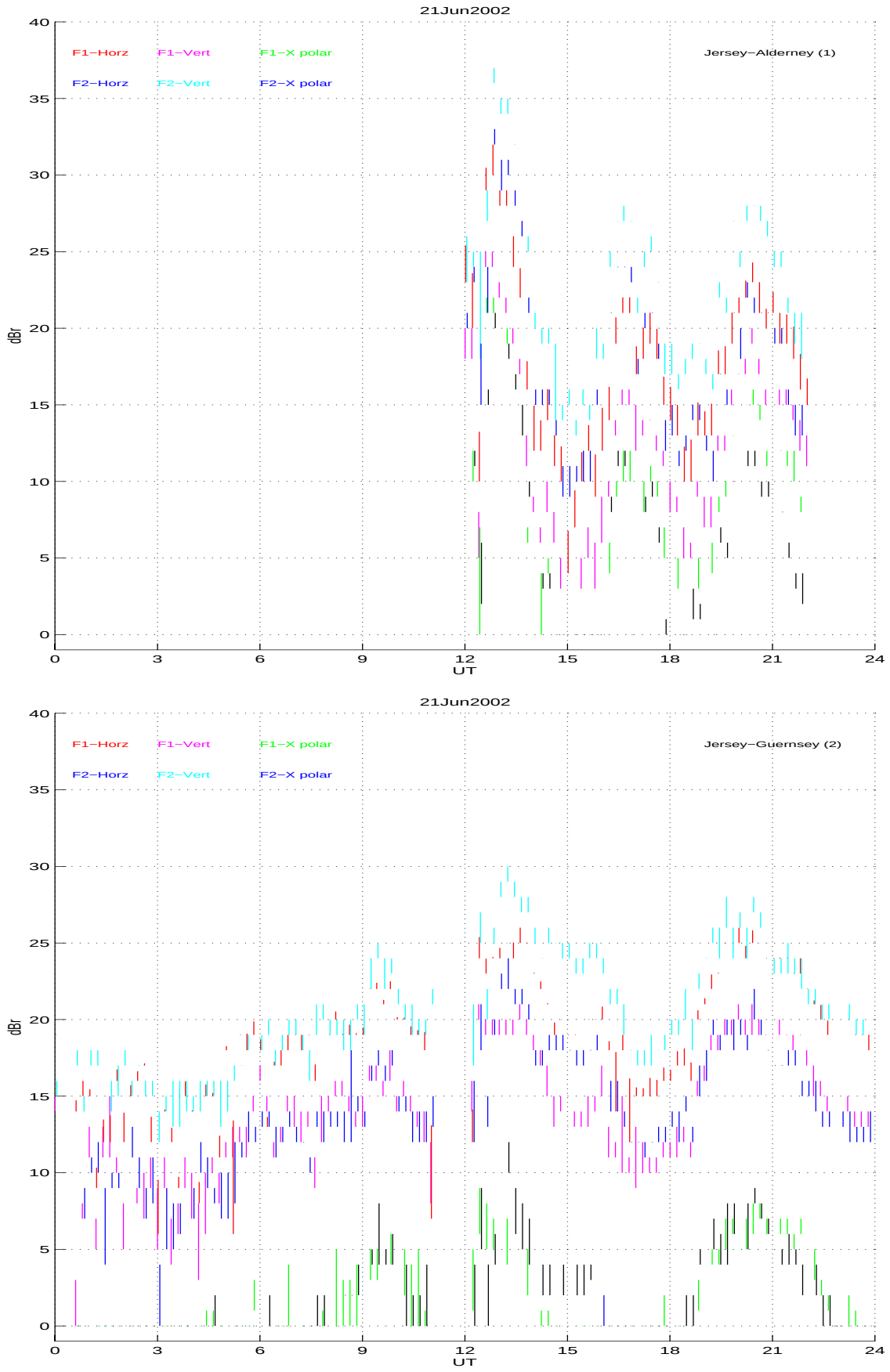

Figure 6.17: Signal amplitude comparison plot for both Jersey-Alderney (1) and Jersey-Guernsey (2) on a hot summer day (21st June 2002)

6.7 Conclusion

This chapter provided several equations and methods (e.g. diffraction, troposcatter and ray tracing equation) in order to understand the propagating mechanism and the ray behaviour for both Jersey-Alderney and Jersey-Guernsey paths with frequency F1 and F2.

By comparing the simulated total path loss (line-of-sight, diffraction and troposcatter) with the measurement results from Chapter 5, it is seen that at around 15 metres antenna height for both transmitter and receiver, smooth earth diffraction is the dominant propagation mechanism for the Jersey-Guernsey path (33.3 km) during calm sea state. For the Jersey-Alderney path (48 km), the high fading phenomenon observed is probably due to interference fading between the diffracted and troposcattered signals. This is consistent with the fluctuated signal observed along the linear region (signal amplitude decreases linearly with tide height increases) on the Jersey-Alderney path and also the increase in fading range when the antenna is at its minimum height at around 10 metres (tide height at maximum around 10 metres). During summer when the signal strength can increase up to 33 dB in maximum, it shows that the increase in signal strength when ESS occurred by whatever phenomenon (super-refraction or ducting), it is not bound by the free space loss as compared with the simulated diffraction loss.

By employing ray tracing technique and lapse rate calculation for both receiving locations, it is seen that on a calm day with "positive" lapse rate, the rays would propagate by a sub-refracting mode due to refractive index increases with height. During a hot summer when the refractive index decreases dramatically with height, both super-refraction and ducting (with a lapse rate more than –157 N/km) were observed. When super-refraction and ducting occurred, the signal would probably propagate above the earth surface reaching the receiving antenna but within the first Fresnel zone radius at around 100 metres. Note that these propagation mechanisms are compromised by the "bulge" height of the earth (both around 21 and 45 metres respectively) along Jersey-Guernsey and Jersey-Alderney paths obstructing rays at lapse rate less than -50 and -100 *N*/km respectively. Therefore, both super-refraction and ducting effects would result in different signal strength for both receiving paths on the same day. This is consistent with the measurement obtained in Chapter 5, as the increased signal amplitudes during hot summer for both receiving paths will no longer follow the usual

linear relationship with the tide height. Instead, it will follow the changes in refractive index of the air that results in phenomenon such as super-refraction or ducting that cause the signal strength to increase by up to 3 dB (median value obtained throughout the whole experiment from Apr 2001 until Sep 2002).

Chapter 7: Conclusions / recommendations and suggestions for further work

The objective of this thesis was to investigate the current understanding of over-sea VHF/UHF propagation at different path lengths, antenna heights, season and weather conditions. Propagation effects that are not attributed to the present understood phenomenon are to be identified. Two propagation paths (33.3 and 48 km) were established between Channel Islands with Jersey (Ronez Quarry) as the transmitting point and Guernsey (St. Peter Port Lighthouse) and Alderney (Isl de Raz) as the receiving points.

The measurements were segregated into two major parts: Jersey-Guernsey and Jersey-Alderney, each contaning statistics of various effects, seasonal and diurnal information, signal amplitude and fading with respect to prevailing weather condition. The results from these measurements and comparison with various theories are discussed below.

Measurements from both receiving sites showed a linear relationship between the signal amplitude and the tide height (approximately 1.1 dB in signal amplitude reduction for every metre of tide height increase). This is consistent with the smooth earth diffraction theory obtained from ITU-R P.526-7, which suggested that smooth earth diffraction (especially over sea) is the dominant propagating effect for distance below 40 km between the transmitter and the receiver. Further analysis from the ray tracing simulation showed that on a calm day when lapse rate is positive, the rays would propagate by a sub-refracting mode due to refractive index increases with height. Note that the fading range during calm sea states for both receiving sites are around 1 to 2 dB with an absence of enhanced signal strength (ESS) or high fading phenomenon observed at Jersey-Alderney path only.

Rougher sea states (around sea state 4) observed on a few occasions from Jersey-Guernsey showed that the signal amplitude of vertically polarised signal was reduced by between 3 and 6 dB. Although horizontally polarised signal amplitude was not much affected, fast fading of up to 15 dB within a short period (30 seconds) was observed during high tide. By applying various parameters (e.g. antenna height, distance, wave height etc.) into the surface theory suggested by Matthew [1965], it is suggested that the sea surface is always calm. Although other rough sea state days were observed from the

weather report, this phenomenon is not seen throughout the year 2002 and on Jersey-Alderney path.

From the statistics and simulation analysis observed/measured from the period April2001 until September 2002 for Jersey-Guernsey path, the following can be concluded:

- During ESS, which is a result due to either super-refraction or ducting (observed by calculating the lapse rate), the fading range is around 1 dB within a 30 seconds period. By comparing with time-scales of tens of minutes, fading range up to 20 dB is commonly observed. The measurements from ray tracing simulation also showed that the refractive index decreases with height when ESS occurred.
- The total percentage of days with ESS during summer 2001 and 2002 are between (55 to 76%) and (31 to 48%) respectively with a threshold temperature (T_d) of 4°C. This indicated that when T_d is equal to or above 4°C, ESS will occur more frequently. This was confirmed by the statistic that showed a mean T_{dmax} of around 4°C during both summers (2001/2002) and further statistic showed that ESS reached zero level when mean T_{dmax} was less than –2°C.
- The total percentage of time (in hours) with ESS during summer 2001 and 2002 are between (43 to 61%) and (19 to 37%) respectively. The total ESS statistics showed a maximum of 409 and 272 hours of ESS occurred in July 2001 and August 2002 respectively. This correlates with the summarised data provided by the Jersey Meteorological office which showed that both the air temperature and sunshine days for summer 2001 was much higher as compared to summer 2000 and summer 2002.
- During winter periods, the total percentage of days and time (in hours) with ESS was below 10%. Although ESS was observed during the winter period in January2002, the signal amplitude was observed to have increased by around 5 dB.
- ESS was observed from a few hours to 9 days continuously. The total statistics for ESS duration for a day showed that the upper/lower decile values to be 24 and 7 hours respectively and the median duration to be 18 hours.
- When ESS occurred, the signal amplitude could increase by an upper/lower decile values of 10 and 1 dB respectively with a median value of 3 dB. The maximum signal amplitude increase was observed to be 33 dB. By comparing these results with the simulated diffraction path loss, the increase in signal amplitude was found not bound by the free space loss.

From the statistics and simulation analysis observed/measured from the period Oct 2001 until September 2002 for Jersey-Alderney path, it showed that:

- Signal fluctuation with high fading phenomenon was observed along the linear region (signal amplitude decrease linearly with increasing tide height) during calm sea state days.
- During spring or summer (especially when ESS was not present), the high fading phenomenon occurred only during high tide (when antenna is at its minimum of 10 metres) adding a few dB into the fast fading signal.
- From the FFT analysis, it showed two or more signal components in the AF measurement that suggested multipath occurrence. These are consistent with the path loss simulation results which showed that the high fading phenomenon is probably due to interference fading between the diffracted wave and troposcatter signal at a distance more than 40 km especially at 10 metres antenna height.
- The statistic showed that the total percentage of time for the occurrence of high fading phenomena decreased from 80 to 30% from November 2001 to January 2002 and between 35 to 55% during the summer period (May to August 2002). The total percentage increased to 66% when it approached September 2002, as lesser ESS occurrence was observed.
- The average fading range for high fading during autumn and summer were around 10 and 7 dB respectively.
- The average fading period for high fading is around 7 seconds although it could increase up to around 20 seconds in maximum.
- Although the fading range during ESS is around 2 dB at Jersey-Alderney, high fading phenomenon will resume itself when ESS is not present or present only for a couple of hours in a day.
- By comparing the ESS occurrence for both Guernsey and Alderney in total time (in hours with references with Alderney total data hours), both receiving locations are seem to coincide very well with each other although the differences in signal amplitude increase could be as high as 10 dB. This could be due to the differences in distance between both Jersey-Guernsey and Jersey-Alderney, which result in different earth “bulge” height (21 and 45 metres respectively). The lapse rate measurements shown that Jersey-Guernsey and Jersey-Alderney rays will be blocked by the “bulge” height of the earth if the lapse rates are less than –50*N*/km and –100 *N*/km respectively.

Further analysis from the ray tracing simulation showed that when super-refraction or ducting occurred, both rays would propagate above the curvature of the earth but within the first Fresnel zone radius at around 100 metres.

The troposcatter mode of propagation enables VHF/UHF signals to be transmitted far beyond the normal line of sight. When the radio wave is transmitted within the line of sight horizon, it experiences little attenuation and when it reaches the horizon, the wave is diffracted and follows the earth's curvature. Beyond the horizon, the rate of attenuation increases very rapidly and signals soon become very weak. In contrast, troposcatter provides a usable signal at distances beyond the point when the diffracted signal wave decreases to an unusable level. Therefore, the recommendations for future work include a third receiving sites in southern UK with a possible range of around 100-km (e.g. Jersey-Weymouth), so as to further investigate the troposcatter effects far beyond the line-of-sight distance. Considering higher antenna heights at 30 or 40 meters, it will provide further information on how the signal wave at F1 and F2 will behave at different antenna heights from 10 to 40 metres as compared to the theory or simulations provided in this thesis. Lastly, if the frequency could be increased up to 2 or 3 GHz, it enables further information such as evaporation ducting to be obtained across the Channel Islands as it only occurred at 2 GHz or higher frequencies across the sea.

References

Algor, M.M.: “Radio-Wave propagation measurements over sea water”. Harry Diamond Laboratories, Washington , D.C., August (1972).

Al’pert, Y.L.: “Radio Wave Propagation and the Ionosphere”. Consultants Bureau, New York, pg. 356-376, (1963).

Ames, L.A., Newman, P., Rogers, T.F.: “VHF Tropospheric Overwater Measurements for Beyond the Radio Horizon”. Proceeding of the IRE, pg. 1369-1436, (1955).

Angling, M.J., Cannon,P.S., Davies, N.C.: “Measurement of Doppler Spread on High Latitude HF path”. Radio Science and Propagation Group (DERA), (2000- Draft).

Barrick, D.E.: “Theory of HF and VHF propagation across the rough sea (1 and 2)”. Radio Science, Volume 6, Number 5, pg. 517-533, May (1971).

Bean, B.R. and Dutton, E.J.: “Radio meteorology”. US National Bureau of Standards, monograph 92, Chapter 1,2,4, (1966).

Bell, C.P.: “A survey of UHF Propagation Measurements carried out by the BBC”. IEE/IERE/IEEE conference on Tropospheri Wave Propagation, London, pg. 101-109, (1968).

Biddulph, D.: “VHF/UHF Hand Book”. RSGB, pg.3.1- 3.20, (1993).

Budden, K.G.: “Radio Wave in the Ionosphere”. Cambridge University Press, pg. 433-434, (1961).

Bullington, K.: “Radio Propagation for Vehicular Communications”. IEEE Transactions on Vehicular Technology, Vol. VT-26, No.4, November (1977).

Castel, F.D. (editor): “Progress in Radio Science”, Elsevier Publishing Company, 1960-1963 Volume 2 – Radio and Troposphere, pg. 127-135, (1965).

Castel, F.D.: “Tropospheric Radio wave Propagation beyond the Horizon”. Pergamon Press Ltd., Pg. 2, Pg. 11-15, Chapter 2-5, (1966).

Crane, R.K.: “Refraction effects in the neutral atmosphere”. Methods of Experimental Physics, Vol.12, Astrohysics, Part B: Radio Telescopes (M.L.Meeks, cd.), New York Academic Press, Pg. 1/6 –200, (1976).

Davies, K.: “Ionospheric Radio”. Peter Peregrinus Ltd, Pg. 1-7, Pg.27-38, Chapter 4, (1969).

Dughherty, H.T. and Hart, B.A.: “Recent progress in duct propagation predictions”. IEEE Trans. Antennas Propagation, Vol. AP-27, pg. 542-548, (July 1979).

Fairall, C.W. and Davison, K.L.: “Evaporation Duct Measurements in the mid-Atlantic”, Rep. 61-78-005, Nav. Postgrad. Sch., Montherey, Calif., (August 1978).

Flock,W.L., Slobin, S.D., and Smith, E.K.: “Propagation effects on radio range and noise in earth-space telecommunications”. Radio Science, Vol. 17, pg.1411-1424, Nov, Dec, (1982).

Gough, M.W.: “UHF Signal Strength Measurement as a guide to Atmospheric Structures”, The Marconi Review, Vol.42, Number 214, pg. 135-152, (1979).

Griffths, H.D, Vinagre, L., Vines, S.B., Bartram, C.P.: “Mearsurements of non line-of-sight VHF propagation over the sea surface”. 10th International Conference on Antennas and Propagation, pg. 2.378- 2.380, (1997).

Griffths, J.: “Radio Wave Propagation and Antennas, An Introduction”. Prentice Hall, pg.74-76, Chapter 4, Chapter 6, 7,(1987).

Hall, M.P.M.: “Effects of the troposphere on radio communication”. Peter Peregrinus Ltd., pg.69-74, pg. 185, Chapter 1,2, (1979).

Hall, M.P.M, Barclay, L.W. and Hewitt, M.T.: “Propagation of Radiowave”. Short Run Press Ltd., Exeter, Chapter 1,4 (D.F.Bacon), Chapter 6 & 8 (K.H.Craig), Chapter 7 (J.W.F.Goddard), (1996).

Hitney, H.V. and Vieth, R.: “Statistic Assessment of Evaporation Duct Propagation”. IEEE Trans. Ant. & Pro, Vol. 38, pg. 794-799, (1990).

Hitney, H.V., Richter, J.H., Pappert, R.A., Anderson, K.D., Baumgartner, G.B.: “Tropospheric Radio Wave Propagation”. Proc. IEEE, Vol. 73, No.2, pg. 265-83, (1985).

ITU-R Recommendation P.453-8: “The radio refractive index: its formula and refractivity data”. pg. 281-307, (2001).

ITU-R Recommendation P.526-7: “propagation by diffraction”, (2001).

Jakes, W.C.: “Microwave Mobile Communication”. John Wiley and Sons, pg. 79-88, (1974).

Janusz, M., Julien, C, Stanisaw, N.: “Analytical Calculation of the Radio Wave Trajectory in the Ionosphere”, IMAPS POLAND Conference 2000, (2000).

Jensen, M.E., Burman, R.D. and Allen, R.G.: “Evapotranspiration and Irrigation Water Requirements”. American Society of Civil Engineers, pg. 177, (1990).

Kallisto Users Guide, Greening technology (Dec 1996).

Kelley, M. C.: “The Earth’s Ionosphere, Plasma Physics and Electrodynamics.” Academic Press, Inc, San Diego, CA, pg. 1-10, (1989).

Lavergnat, J., Sylvain, M.: “Radio wave propagation - principle and techniques”. John Wiley & Sons, Ltd, pg. 115-117, 139-150, 189-192, (2000).

Levy, M.: “Parabolic equation methods for electromagnetic wave propagation”. The institution of Electrical Engineerings, London, Chapter 9 and 10, pg. 64-69, (2000).

Matthew, P.A.: “Radio Wave Propagation V.H.F And Above”. Chapman and Hall Ltd., chapter 2-4,pg. 78-9, pg. 106, pg. 131–151, (1965).

Parson, J.D.: “The mobile Radio Propagation Channel”, 2nd edition, John Wiley & Sons Ltd, chapter 3, (2000).

Patterson, W.L.: “Comparison of Evaporation duct and Path Loss model”, Radio Science, vol. 20, No. 5, Pg. 1061-1068. [Sept- Oct, 1985].

Paulus, R.A.: “Practical Application of an Evaporation Duct Model.” Radio Science, Vol20, No.4, Pg 887-896, [1985].

PCI224/234 Multi-Function Analogue and Digital Input/Output Boards, Instruction Manuel Part No 859 893 94 Issue A1, Amplicon Liveline Limited.

Picquenard, A.: “Radio Wave Propagation”, The Macmillan Press Ltd., chapter 2, pg. 296-302, (1974).

Ratcliff, J.A.: “Sun, Earth and Radio. An introduction to the ionosphere and magnetosphere”. Weidenfeld and Nicolson, pg. 17 – 89, (1972).

Reed, H.R. and Russell, C.M.: “Ultra High Frequency Propagation”, Chapman and Hall Ltd., pg. 1-12, chapter 3–5, (1966).

Rishbeth, H. & Garriott, O.K.: “Introduction to Ionospheric Physics”. Academic Press, New York and London, chapter 1, pg. 50-61, (1969).

Roda, G.: “Troposcatter Radio Links”, Artech House Inc, Chapter 1,3,4 and 6, (1988).

Rotheram, S.: “RadioWave Propagation in the Evaporation Duct”, The Marconi Rev., Vol.37, Pg. 18-40, (1974).

Stark, J.W.: “Simultaneous long distance tropospheric propagation measurements at 560 and 774 MHz over the North Sea”. Radio and Electronic Engineering, Vol.30, pg. 241-255, (October 1965).

Wait, J.R.: “Electromagnetic Waves in Stratified Media”. Pergamon Press, chapter 11, (1962).

Weisbrod, S. and Anderson, L.J.: “Simple methods for computing tropospheric and ionospheric refractive effects on radio waves”. Proc. IRE, Vol. 47, pg. 1770-7, Oct, (1959).

White, I.: “The VHF/UHF Book”. DIR Publishing, chapter 2, (1992).

Wickers, S. and Nilsson, L.: “The Occurrence of Very High Field at beyond the Horizon Propagation Over Sea in the Frequency Range 60 – 5000 MHz”. Conference Proceeding, Number 127, pg. 14/1–14/15, May, (1973).

Web-site references

[1] http://www.gtonline.net/tides/

[2] http://www.ems.psu.edu/cgi-bin/wx/findbuoy.cgi?id=62103

[3] http://weather.noaa.gov/weather/current/EGJJ.html

[4] http://weather.noaa.gov/weather/current/EGJB.html

Appendix A: Matlab Script

Script 1

```
% filename: figure5_1.m
% previousfilename: plot_monthly.m

% modified on 6th Apr/01, added sea pressure plot and arrow direction
% modified on 9th Apr/01, added plotting without going to zero

% plotting Tide Height & wave height
% modified on 27th Apr/01, Plot only Sark tide, enter only 1 data_date.
% modified on 14th July to add in sea /air temperature and multiple axis on the right

clf
clear
orient tall % to change back to landscape - orient landscape

data_date='10Apr2001';

%-------------------------plot Sark sine ----------------------------
%    High      Low       High         Low         high       Low      high
S_t1=-4.16; S_t2=2.38; S_t3=8.10; S_t4=14.73; S_t5=20.45; S_t6=26.98; S_t7=0;
S_h1=9.37; S_h2=0.29; S_h3=9.34; S_h4=0.4; S_h5=9.18; S_h6=0.55;S_h7=0;

S_time1=[S_t1:0.01:S_t2];
S_time2=[S_t2:0.01:S_t3];
S_time3=[S_t3:0.01:S_t4];
S_time4=[S_t4:0.01:S_t5];
S_time5=[S_t5:0.01:S_t6];
S_time6=[S_t6:0.01:S_t7];

%-----------------plot 1st ht------------------------
Sark_ht1=[];

for t = S_t1:0.01:S_t2
    angle = -pi + (t - S_t1)*pi/(S_t2 - S_t1);
    Sark_ht1 =[Sark_ht1 (S_h1 + (S_h2 - S_h1)*(1+cos(angle))/2)];
end
%-----------------------------------------------------
%-----------------plot 2nd ht-------------------------

Sark_ht2=[];

for t = S_t2:0.01:S_t3
    angle = 0 + (t - S_t2)*pi/(S_t3 - S_t2);
    Sark_ht2 =[Sark_ht2 (S_h3 + (S_h2 - S_h3)*(1+cos(angle))/2)];
end
%-----------------------------------------------------
%----------------plot 3rd ht-------------------------

Sark_ht3=[];

for t = S_t3:0.01:S_t4
    angle = -pi + (t - S_t3)*pi/(S_t4 - S_t3);
    Sark_ht3 =[Sark_ht3 (S_h3 + (S_h4 - S_h3)*(1+cos(angle))/2)];

end
%-----------------------------------------------------
%--------------plot 4th ht--------------------------

Sark_ht4=[];

for t = S_t4:0.01:S_t5
    angle = 0 + (t - S_t4)*pi/(S_t5 - S_t4);
    Sark_ht4 =[Sark_ht4 (S_h5 + (S_h4 - S_h5)*(1+cos(angle))/2)];

end
%-----------------------------------------------------
%----------------plot 5rd ht-------------------------

Sark_ht5=[];

for t = S_t5:0.01:S_t6
    angle = -pi + (t - S_t5)*pi/(S_t6 - S_t5);
    Sark_ht5 =[Sark_ht5 (S_h5 + (S_h6 - S_h5)*(1+cos(angle))/2)];
```

```
end
%-----------------------------------------------------
%---------------plot 6th ht--------------------------

Sark_ht6=[];

for t = S_t6:0.01:S_t7
    angle = 0 + (t - S_t6)*pi/(S_t7 - S_t6);
    Sark_ht6 =[Sark_ht6 (S_h7 + (S_h6 - S_h7)*(1+cos(angle))/2)];

end
%-----------------------------------------------------
%plot([S_time1 S_time2 S_time3 S_time4 S_time5 S_time6],[Sark_ht1 Sark_ht2 Sark_ht3
Sark_ht4 Sark_ht5 Sark_ht6]);

%--------------------wave height plot-----------------------------------------
time1=[0:1:24];
wvht=[1.5 1.5 1 1.5 1.5 2 2 2 2 2 2 2 2 1.5 1.5 1.5 1.5 1.5 1.5 2 2 2 2 1.5 1.5];

%-------------------------------------------------------------------------------

S_time_total=[S_time1 S_time2 S_time3 S_time4 S_time5 S_time6];

Sark_ht_total=[Sark_ht1 Sark_ht2 Sark_ht3 Sark_ht4 Sark_ht5 Sark_ht6];

%handle = subplot(4,1,1);plot(Sark_time, Sark_ht, 'c-o',time1, wvht, 'k-*' )

hold on
handle = subplot(4,1,1);plot(S_time_total,Sark_ht_total, 'c',time1, wvht, 'k-*')
hold on

set(handle, 'xtick', [0:3:24],'FontSize',8);
set(handle, 'ytick', [0:1:10],'FontSize',8);
axis([0 24 0 10]);
grid on

date=sprintf('%s%s', data_date,': Sark Tide & Channel Lightship Wave Height');
title(date,'FontSize',8)
ylabel('Height (metre)','FontSize',8)
text(0.5,9.5,'- Tide height','Fontsize',6,'Color','c')
text(3, 9.5,'* Wave height','Fontsize',6,'Color','k')


%aaa=legend('Lightship','Sark', 0);
%set(aaa,'position',[0.2 0.87 0.13 0.04]);
hold off

%-------------------------------------------------------------------------------------------
----
%Plotting Wind Speed with direction

% to obtain wind direct with respect to left arrow angles
N=270;S=90;E=180;W=0;NE=225;SE=135;SW=45;NW=315;
NNE=247.5;NNW=292.5;WNW=337.5;WSW=22.5;SSW=67.5;SSE=112.5;ESE=157.5;ENE=202.5;

o =1; % to declare 1 when no data available from direction

% X axis from 00:00 till 24:00
time2=[0:1:24];

% convert Jersey wind speed from mph to knots
Jersey_wdsp=[20 26 23 23 21 21 20 20 20 19 19 17 17 14 16 13 0 0 0 0 0 0 9 12 12]*0.869;

% Jersey Wind direction
Jersey_wddir=[WNW WNW WNW WNW WNW WNW WNW WNW WNW WNW WNW NW N WNW NW NW o o o o o o NNW
NNW N];

% convert Guernsey wind speed from mph to knots
Guernsey_wdsp=[0 0 0 0 0 24 20 20 19 16 18 18 14 17 12 13 0 0 0 0 0 0 11 12 10]*0.869;

% Guernsey Wind direction
Guernsey_wddir=[o o o o o WNW WNW WNW WNW WNW WNW WNW WNW WNW WNW NW o o o o o o NNW NNW
NNW];

% Channel lightship windspeed
Channel_lightship_wdsp=[28 28 28 28 26 26 29 28 29 26 23 21 18 17 22 21 16 21 25 22 19
21 20 19 19];

orient tall
hold on
```

```
% ------------------to plot all the 3 wind speed-----------------------------
% -------------------to plot Jersey windspeed-------------------------

time3=[0 0];J_speed=[0 0];

for ii=(1:1:24)
   if(Jersey_wdsp(ii)>0.1 & Jersey_wdsp(ii+1)>0.1)
     J_speed(1)=Jersey_wdsp(ii); J_speed(2)=Jersey_wdsp(ii+1);
     time3(1)=time2(ii); time3(2)=time2(ii+1);
     handle =subplot(4,1,2);plot(time3,J_speed,'r-+')
     hold on
   end

   if(Jersey_wdsp(ii)<0.1 & Jersey_wdsp(ii+1)>0.1)
     handle =subplot(4,1,2);plot(time2(ii+1),Jersey_wdsp(ii+1),'r-+')
     hold on
   end

   if(Jersey_wdsp(ii)>0.1 & Jersey_wdsp(ii+1)<0.1)
     handle =subplot(4,1,2);plot(time2(ii),Jersey_wdsp(ii),'r-+')
     hold on
   end
end
%-------------------------------------------------------------------
% -------------------to plot Guernsey windspeed-------------------------

time3=[0 0];G_speed=[0 0];

for ii=(1:1:24)
   if(Guernsey_wdsp(ii)>0.1 & Guernsey_wdsp(ii+1)>0.1)
     G_speed(1)=Guernsey_wdsp(ii); G_speed(2)=Guernsey_wdsp(ii+1);
     time3(1)=time2(ii); time3(2)=time2(ii+1);
     handle =subplot(4,1,2);plot(time3,G_speed,'b-o')
     hold on
   end

   if(Guernsey_wdsp(ii)<0.1 & Guernsey_wdsp(ii+1)>0.1)
     handle =subplot(4,1,2);plot(time2(ii+1),Guernsey_wdsp(ii+1),'b-o')
     hold on
   end

   if(Guernsey_wdsp(ii)>0.1 & Guernsey_wdsp(ii+1)<0.1)
     handle =subplot(4,1,2);plot(time2(ii),Guernsey_wdsp(ii),'b-o')
     hold on
   end
end
%-------------------------------------------------------------------
 % -------------------to plot Channel windspeed-------------------------

handle =subplot(4,1,2);plot(time2,Channel_lightship_wdsp,'k-+' )
hold on

set(handle, 'xtick', [0:3:24], 'FontSize',8);
set(handle, 'ytick', [0:3:42], 'FontSize',8);
axis([0 24 0 42]);
grid on
date1=sprintf('%s%s', data_date,': Jersey, Guernsey and Channel Lightship Wind Speed
with Direction Arrow');
title(date1,'FontSize',8)
%xlabel('hrs')
ylabel('Wind Speed (Knots)','FontSize',8)

%-------------------------------------------------------------------------
%------------------to plot wind direction for Jersey and Guernsey-------------

for iii=[1:1:25]
    if Jersey_wddir(iii) ~= 1
    text(time2(iii),Jersey_wdsp(iii),'\leftarrow','FontSize',
12,'Rotation',Jersey_wddir(iii),'Color','r');
    end
end


for iii=[1:1:25]
    if Guernsey_wddir(iii) ~= 1
    text(time2(iii),Guernsey_wdsp(iii),'\leftarrow','FontSize',
12,'Rotation',Guernsey_wddir(iii),'Color','b');
    end
end
```

```
%-------------------------------------------------------------------------
%---------------- legend in text form-------------------------------------
text(0.5,38,'- Jersey','Fontsize',6,'Color','r')
text(3, 38,'- Guernsey','Fontsize',6,'Color','b')
text(6, 38,'- Lightship','Fontsize',6,'Color','k')

%-------------------------------------------------------------------------
%plot air pressure (Jersey) with multiple axis of sea and air temperature(03/Jul/2001)
orient tall
time_sea=[0 0];pressure=[0 0];
air_pressure=[1016 1016 1017 1017 1017 1017 1018 1018 1018 1019 1019 1020 1020 1021 1021
1022 0 0 0 0 0 0 1024 1024 1025];

for ii=(1:1:24)
   if(air_pressure(ii)>0.1 & air_pressure(ii+1)>0.1)
     pressure(1)=air_pressure(ii); pressure(2)=air_pressure(ii+1);
     time_sea(1)=time2(ii); time_sea(2)=time2(ii+1);
     handle =subplot(4,1,3);plot(time_sea,pressure,'k-*')
     hold on
   end

   if(air_pressure(ii)<0.1 & air_pressure(ii+1)>0.1)
     handle =subplot(4,1,3);plot(time2(ii+1),air_pressure(ii+1),'k-*')
     hold on
   end

   if(air_pressure(ii)>0.1 & air_pressure(ii+1)<0.1)
     handle =subplot(4,1,3);plot(time2(ii),air_pressure(ii),'k-*')
     hold on
   end
end

% input temperature data

sea_temperature=[9.9 9.9 10.0 10.0 10.3 10.2 10.2 10.1 9.9 10.0 9.9 9.9 10.0 9.9 9.9
10.0 10.1 10.2 10.2 10.1 10.1 9.9 9.9 9.9 10.1];

air_temperature=[10.6 10.5 10.1 10.1 9.9 10.0 10.1 9.7 9.7 9.9 10.1 10.1 10.2 10.5 10.6
10.7 10.7 10.7 10.0 10.7 10.5 10.5 10.3 10.0 9.8];

Jersey_air_temperature=[9 9 9 10 10 11 11 11 12 11 11 11 11 10 10 9 0 0 0 0 0 0 8 9 9];

% to find average temp

Avg_temp = (sum(sea_temperature)+sum(air_temperature)+sum(Jersey_air_temperature))/69;
Average_temp =round(Avg_temp); % to get integer value


handle=gca;
set(handle, 'xtick', [0:3:24], 'FontSize',8);
set(handle, 'ytick', [990:5:1035], 'FontSize',8);
axis([0 24 990 1035]);
grid on
date2=sprintf('%s%s', data_date,': Jersey Air pressure/Temperature and Channel Lightship
Sea/Air Temperature');
title(date2,'FontSize',8)
%xlabel('hrs')
ylabel('Pressure (hPa)','FontSize',8)

% Plotting sea and air temperature from right axis

handle1=axes('Position', get(handle,'Position'),...
             'YAxisLocation','right','XAxisLocation','bottom',...
             'YTick',[Average_temp-9:2:Average_temp+9],'xtick',[0:3:24],...
             'Color','none','YColor','r','FontSize',8);


%handle1 =subplot(1,1,1);plot(time2,sea_temperature,'color','c','Parent','handle1');
%plot(time2,sea_temperature,'color','c','Parent',handle1);
%handle1=subplot(1,1,1);plot(time2,sea_temperature,'color','c')

hl2=line(time2,sea_temperature,'Color','m','Parent',handle1);
hl2=line(time2,air_temperature,'Color','r','Parent',handle1);
%hl2=line(time2,Jersey_air_temperature,'Color','b','Parent',handle1);

time3=[0 0];Jersey_air_temp=[0 0];

for ii=(1:1:24)
   if(Jersey_air_temperature(ii)>0.1 & Jersey_air_temperature(ii+1)>0.1)
```

```
     Jersey_air_temp(1)=Jersey_air_temperature(ii);
Jersey_air_temp(2)=Jersey_air_temperature(ii+1);
     time3(1)=time2(ii); time3(2)=time2(ii+1);
     hl2=line(time3,Jersey_air_temp,'Color','b','Parent',handle1);
     hold on
   end

   if(Jersey_air_temperature(ii)<0.1 & Jersey_air_temperature(ii+1)>0.1)
     hl2=line(time2(ii+1),Jersey_air_temperature(ii+1),'Color','b','Parent',handle1);
     hold on
   end

   if(Jersey_air_temperature(ii)>0.1 & Jersey_air_temperature(ii+1)<0.1)
     hl2=line(time2(ii),Jersey_air_temperature(ii),'Color','b','Parent',handle1);
     hold on
   end

end

axis([0 24 Average_temp-9 Average_temp+9]);

ylabel('Temperature (degree celsius)','FontSize',8)
text(6,Average_temp+8,'- Jersey Air Temperature','Fontsize',6,'Color','b')
text(12,Average_temp+8,'- Lightship Sea Temperature','Fontsize',6,'Color','m')
text(18, Average_temp+8,'- Lightship Air Temperature','Fontsize',6,'Color','r')
text(0.1, Average_temp+8,'-* Jersey Air Pressure','Fontsize',6,'Color','k')
%-------------------------------------------------------------------------
%----------------------plot Min and Min data--------------------------

%function plotagc(data_date)

%data_date = '17Apr2001';

dBm = [-107:8];
dBscale = dBm + 107;

agcnum(1,:) = [3 3 3 7 12 19 26 33 40 46 52 57 62 67 71 76 80 84 87   ...
               90 94 98 101 104 107 110 113 115 118 120 123 125 129   ...
               131 133 136 138 140 142 145 147 149 151 153 155 158    ...
               159 161 163 165 167 168 171 173 175 177 178 180 182    ...
               184 186 188 190 192 193 195 197 199 201 203 204 206    ...
               208 210 211 213 215 217 219 221 222 224 226 228 230    ...
               232 233 236 238 239 241 243 245 246 248 248 249 249    ...
               249 250 250 250 250 250 250 250 250 250 250 250 250    ...
               250 250 250 250 250];

agcnum(2,:) = [3 6 12 19 26 33 39 45 51 56 62 66 71 75 79 83 87 91 94 ...
               97 100 104 106 109 112 115 117 120 123 125 128 130 133 ...
               135 137 140 142 144 146 148 151 153 155 157 159 161    ...
               163 165 167 169 171 173 174 176 178 180 182 184 186    ...
               187 189 191 193 195 196 198 200 202 204 205 207 208    ...
               210 212 214 216 218 219 221 223 225 226 228 230 232    ...
               234 236 238 240 241 243 245 246 247 248 249 249 250    ...
               250 250 250 250 250 250 250 250 250 251 251 251 251    ...
               251 251 251 251 251];

for ii = 1:255

  x = find(agcnum(1,:) >= ii);
  if isempty(x)
    agc2dB(1,ii) = dBscale(length(dBm));
  else
    agc2dB(1,ii) = dBscale(x(1));
  end

  x = find(agcnum(2,:) >= ii);
  if isempty(x)
    agc2dB(2,ii) = dBscale(length(dBm));
  else
    agc2dB(2,ii) = dBscale(x(1));
  end

end

orient tall
%handle = axes;
hold on

for hh = 0:23
  for mm = 0:59
```

```
    for ss = [9 10] % 0:59
      time = [num2str(hh,'%2.2d') num2str(mm,'%2.2d') num2str(ss,'%2.2d')];

      for freq = 1:2
        for polar = ['h' 'v' 'x']

          fn = ['/temp/cyds1/Guernsey_Apr2001/10Apr2001/guernsey' num2str(freq) polar
'c.' data_date '.' time];
          if exist(fn,'file')

            [fid, message] = fopen(fn,'r');
             nagc1 = fread(fid,4,'uint8');
             nagc = nagc1(1) + 256*nagc1(2) + 256*256*nagc1(3) + 256*256*256*nagc1(4);
             agc = fread(fid,nagc,'uint8');
             fclose(fid);

             HH = hh + mm/60 + ss/3600;

             switch [num2str(freq) polar]
               case '1h', lcolour = 'r';
               case '1v', lcolour = 'm';
               case '1x', lcolour = 'g';
               case '2h', lcolour = 'b';
               case '2v', lcolour = 'c';
               case '2x', lcolour = 'k';
             end

             if ss==9
               agc1 = agc(25:length(agc));  % Ignore the first 1s for AGC to settle
             else
               agc1 = agc;
             end

             agc1(find(agc1==0)) = 1;  % Don't allow zero values - need a proper fix
later

             if length(agc1)>=2
%               plot(HH,median(agc2dB(freq,agc1)),[lcolour '-']);
               handle = subplot(4,1,4); plot([HH HH],[min(agc2dB(freq,agc1))
max(agc2dB(freq,agc1))],lcolour);
%               plot((HH+(1:length(agc1))/(3600*40)),agc2dB(freq,agc1),lcolour);
               hold on
             end

           end

        end
      end
    end
  end
end

grid on
axis([0 24 dBscale(1)-1 dBscale(1)+60]);
set(handle,'xtick',[0:3:24],'FontSize',8);
set(handle, 'ytick', [0:10:60], 'FontSize',8);

date3=sprintf('%s%s', data_date,': Min and Max Data (F1- 248.375MHz, F2- 341.375MHz)');
title(date3,'FontSize',8)
ylabel('dBr','FontSize',8)
xlabel('UT','FontSize',8)
text(0.5,56,'F1- Horz','Fontsize',6,'Color','r')
text(3, 56,'F1- Vert','Fontsize',6,'Color','m')
text(6, 56,'F1- X-Pole','Fontsize',6,'Color','g')

text(0.5, 52.5,'F2- Horz','Fontsize',6,'Color','b')
text(3, 52.5,'F2- Vert','Fontsize',6,'Color','c')
text(6, 52.5,'F2- X-Pole','Fontsize',6,'Color','k')

%legend('F1 Horz','F1 Vert','F1 X','F2 Horz','F2 Vert','F2 X',0);
%zzz=legend('F1 Horz','F1 Vert','F1 X','F2 Horz','F2 Vert','F2 X',0);
%set(zzz,'position',[0.147 0.25 0.13 0.07]);
%-------------------------------------------------------------------------
%print -dpsc -POldRslColourPS
```

Script 2

```
% filename: figure5_2.m
% modified on 22nd Apr/01 ,plotting of Sark tide Ht vs amplitude only
% modified on 27th Apr/01 , changed data_date
% get Tide Height & wave height data
% new to plot just 6 hrs of data.
% both time_start and time_end is for selection of time
% to plot error bar (in grey) & mean value (11th June2002)
% this file contains error bar

clf
clear
orient landscape % to change back to landscape - orient landscape

data_date='10Apr2001';

time_begin_hr =0; % to select the start time in hr from 00:00:00
time_end_hr=23;% to select the end time in hr till 23:59:00

%-------------------------plot Sark sine ----------------------------
%    High      Low       High         Low         high       Low      high
S_t1=-4.4; S_t2=2.32; S_t3=7.87; S_t4=14.67; S_t5=20.22; S_t6=26.9; S_t7=0;
S_h1=9.37; S_h2=0.29; S_h3=9.34; S_h4=0.40; S_h5=9.18;S_h6=0.55;S_h7=0;

%------need to find out if it is going high to low or low to high tide--------

Sark_ht=[S_h1 S_h2 S_h3 S_h4 S_h5 S_h6 S_h7];
Sark_time=[S_t1 S_t2 S_t3 S_t4 S_t5 S_t6 S_t7];

for i=1:1:7
       if((time_begin_hr-Sark_time(i))<=0) %& (Sark_time(i) >=0
       Sark_ht_begin =Sark_ht(i);
       break
       end
end

for i=1:1:7
       if((time_end_hr-Sark_time(i))<=0) %& (Sark_time(i) >=0)
       Sark_ht_end =Sark_ht(i);
       break
       end
end

if((Sark_ht_begin-Sark_ht_end) <= 0)
   tide=0; % from low to high tide
end

if((Sark_ht_begin-Sark_ht_end) >= 0)
   tide=1; % from high to low tide
end

tide % to show whether the tide from low to high or inverse

S_time1=[S_t1:0.01:S_t2];
S_time2=[S_t2:0.01:S_t3];
S_time3=[S_t3:0.01:S_t4];
S_time4=[S_t4:0.01:S_t5];
S_time5=[S_t5:0.01:S_t6];
S_time6=[S_t6:0.01:S_t7];

%-----------------plot 1st ht------------------------
Sark_ht1=[];

for t = S_t1:0.01:S_t2
    angle = -pi + (t - S_t1)*pi/(S_t2 - S_t1);
    Sark_ht1 =[Sark_ht1 (S_h1 + (S_h2 - S_h1)*(1+cos(angle))/2)];
end
%-----------------------------------------------------
%-----------------plot 2nd ht-------------------------

Sark_ht2=[];

for t = S_t2:0.01:S_t3
    angle = 0 + (t - S_t2)*pi/(S_t3 - S_t2);
    Sark_ht2 =[Sark_ht2 (S_h3 + (S_h2 - S_h3)*(1+cos(angle))/2)];
end
%-----------------------------------------------------
%---------------plot 3rd ht-------------------------
```

```
Sark_ht3=[];

for t = S_t3:0.01:S_t4
    angle = -pi + (t - S_t3)*pi/(S_t4 - S_t3);
    Sark_ht3 =[Sark_ht3 (S_h3 + (S_h4 - S_h3)*(1+cos(angle))/2)];

end
%-----------------------------------------------------
%---------------plot 4th ht--------------------------

Sark_ht4=[];

for t = S_t4:0.01:S_t5
    angle = 0 + (t - S_t4)*pi/(S_t5 - S_t4);
    Sark_ht4 =[Sark_ht4 (S_h5 + (S_h4 - S_h5)*(1+cos(angle))/2)];

end
%-----------------------------------------------------
%---------------plot 5rd ht--------------------------

Sark_ht5=[];

for t = S_t5:0.01:S_t6
    angle = -pi + (t - S_t5)*pi/(S_t6 - S_t5);
    Sark_ht5 =[Sark_ht5 (S_h5 + (S_h6 - S_h5)*(1+cos(angle))/2)];

end
%-----------------------------------------------------
%---------------plot 6th ht--------------------------

Sark_ht6=[];

for t = S_t6:0.01:S_t7
    angle = 0 + (t - S_t6)*pi/(S_t7 - S_t6);
    Sark_ht6 =[Sark_ht6 (S_h7 + (S_h6 - S_h7)*(1+cos(angle))/2)];

end
%-----------------------------------------------------
%plot([S_time1 S_time2 S_time3 S_time4 S_time5 S_time6],[Sark_ht1 Sark_ht2 Sark_ht3
Sark_ht4 Sark_ht5 Sark_ht6]);


S_time_total=[S_time1 S_time2 S_time3 S_time4 S_time5 S_time6];

Sark_ht_total=[Sark_ht1 Sark_ht2 Sark_ht3 Sark_ht4 Sark_ht5 Sark_ht6];


%----------------------get Median data and plot ht vs median data---------

%function plotagc(data_date)

%data_date = '16Apr2001';

dBm = [-107:8];
dBscale = dBm + 107;

agcnum(1,:) = [3 3 3 7 12 19 26 33 40 46 52 57 62 67 71 76 80 84 87   ...
               90 94 98 101 104 107 110 113 115 118 120 123 125 129   ...
               131 133 136 138 140 142 145 147 149 151 153 155 158    ...
               159 161 163 165 167 168 171 173 175 177 178 180 182    ...
               184 186 188 190 192 193 195 197 199 201 203 204 206    ...
               208 210 211 213 215 217 219 221 222 224 226 228 230    ...
               232 233 236 238 239 241 243 245 246 248 248 249 249    ...
               249 250 250 250 250 250 250 250 250 250 250 250 250    ...
               250 250 250 250 250];

agcnum(2,:) = [3 6 12 19 26 33 39 45 51 56 62 66 71 75 79 83 87 91 94 ...
               97 100 104 106 109 112 115 117 120 123 125 128 130 133 ...
               135 137 140 142 144 146 148 151 153 155 157 159 161    ...
               163 165 167 169 171 173 174 176 178 180 182 184 186    ...
               187 189 191 193 195 196 198 200 202 204 205 207 208    ...
               210 212 214 216 218 219 221 223 225 226 228 230 232    ...
               234 236 238 240 241 243 245 246 247 248 249 249 250    ...
               250 250 250 250 250 250 250 250 250 251 251 251 251    ...
               251 251 251 251 251];

for ii = 1:255

  x = find(agcnum(1,:) >= ii);
```

```
  if isempty(x)
    agc2dB(1,ii) = dBscale(length(dBm));
  else
    agc2dB(1,ii) = dBscale(x(1));
  end

  x = find(agcnum(2,:) >= ii);
  if isempty(x)
    agc2dB(2,ii) = dBscale(length(dBm));
  else
    agc2dB(2,ii) = dBscale(x(1));
  end

end


%orient landscape
%handle = axes;
%hold on

%time_1h=[];Array_1h=[];
II=0;JJ=0;KK=0;LL=0;MM=0;NN=0;

for hh = 0:23
  for mm = 0:59
    for ss = [9 10] % 0:59
      time = [num2str(hh,'%2.2d') num2str(mm,'%2.2d') num2str(ss,'%2.2d')];

      for freq = 1:2
        for polar = ['h' 'v' 'x']

          fn = ['/temp/cyds1/Guernsey_Apr2001/10Apr2001/guernsey' num2str(freq) polar
'c.' data_date '.' time];
          if (exist(fn,'file')) & (hh >= time_begin_hr) & (hh <= time_end_hr)

%/ select the correct file name and time of the files
%          time% display time , will cancel off when completion
           [fid, message] = fopen(fn,'r');
            nagc1 = fread(fid,4,'uint8');
            nagc = nagc1(1) + 256*nagc1(2) + 256*256*nagc1(3) + 256*256*256*nagc1(4);
            agc = fread(fid,nagc,'uint8');
            fclose(fid);

            HH = hh + mm/60 + ss/3600;

            switch [num2str(freq) polar]
              case '1h', lcolour = 'r';
              case '1v', lcolour = 'm';
              case '1x', lcolour = 'g';
              case '2h', lcolour = 'b';
              case '2v', lcolour = 'c';
              case '2x', lcolour = 'k';
            end

            if ss==9
              agc1 = agc(25:length(agc));  % Ignore the first 1s for AGC to settle
            else
              agc1 = agc(1:length(agc));
              agc1 = sort(agc1);
              aaa =size(agc1);
              size_of_agc = aaa(1);
              agc_95_percent = round(0.95*(size_of_agc));
              agc_5_percent = round(0.05*(size_of_agc));

            end

            agc1(find(agc1==0)) = 1;  % Don't allow zero values - need a proper fix
later

            if length(agc1)>=2
%              plot(HH,median(agc2dB(freq,agc1)),[lcolour '-']);
%              handle = subplot(4,1,4); plot([HH HH],[min(agc2dB(freq,agc1))
max(agc2dB(freq,agc1))],lcolour);

%-------------------getting median arrays value  -----------------------------
               if lcolour =='r'
                   II=II+1;
                   time_1h(II)=HH;
median_1h(II)=median(agc2dB(freq,agc1));mean_1h(II)=mean(agc2dB(freq,agc1));
                   agcdb_1h_95_percent(II)=agc2dB(freq,agc1(agc_95_percent));
```

```
                    agcdb_1h_5_percent(II)=agc2dB(freq,agc1(agc_5_percent));
                end

                if lcolour =='m'
                    JJ=JJ+1;
                    time_1v(JJ)=HH;
median_1v(JJ)=median(agc2dB(freq,agc1));mean_1v(JJ)=mean(agc2dB(freq,agc1));
                    agcdb_1v_95_percent(JJ)=agc2dB(freq,agc1(agc_95_percent));
                    agcdb_1v_5_percent(JJ)=agc2dB(freq,agc1(agc_5_percent));

                end

                if lcolour =='g'
                    KK=KK+1;
                    time_1x(KK)=HH;
median_1x(KK)=median(agc2dB(freq,agc1));mean_1x(KK)=mean(agc2dB(freq,agc1));
                    agcdb_1x_95_percent(KK)=agc2dB(freq,agc1(agc_95_percent));
                    agcdb_1x_5_percent(KK)=agc2dB(freq,agc1(agc_5_percent));
                end

                if lcolour =='b'
                    LL=LL+1;
                    time_2h(LL)=HH;
median_2h(LL)=median(agc2dB(freq,agc1));mean_2h(LL)=mean(agc2dB(freq,agc1));
                    agcdb_2h_95_percent(LL)=agc2dB(freq,agc1(agc_95_percent));
                    agcdb_2h_5_percent(LL)=agc2dB(freq,agc1(agc_5_percent));
                end

                if lcolour =='c'
                    MM=MM+1;
                    time_2v(MM)=HH;
median_2v(MM)=median(agc2dB(freq,agc1));mean_2v(MM)=mean(agc2dB(freq,agc1));
                    agcdb_2v_95_percent(MM)=agc2dB(freq,agc1(agc_95_percent));
                    agcdb_2v_5_percent(MM)=agc2dB(freq,agc1(agc_5_percent));
                end

                if lcolour =='k'
                    NN=NN+1;
                    time_2x(NN)=HH;
median_2x(NN)=median(agc2dB(freq,agc1));mean_2x(NN)=mean(agc2dB(freq,agc1));
                    agcdb_2x_95_percent(NN)=agc2dB(freq,agc1(agc_95_percent));
                    agcdb_2x_5_percent(NN)=agc2dB(freq,agc1(agc_5_percent));
                end
%-------------------------------------------------------------------------------
%               plot((HH+(1:length(agc1))/(3600*40)),agc2dB(freq,agc1),lcolour);
                hold on
             end
             %end % end for if time >=
           end



        end
      end
    end
  end
end


%--------------------to plot tide ht Vs dBr for Sark tide-------------------

time_1h_Sark_tide_ht=[];time_1v_Sark_tide_ht=[];time_1x_Sark_tide_ht=[];
time_2h_Sark_tide_ht=[];time_2v_Sark_tide_ht=[];time_2x_Sark_tide_ht=[];

%figure(1)
orient tall

[zz1 zz2] =size(S_time_total); % to find out size of S_time_total


% to get 1h (dBm Vs tide height)
[z1 z2]=size(time_1h); %to find out how many of dBm for 1h
for kk=(1:1:z2)
 zzz =0;
  for pp=(1:1:zz2)
    if(zzz==1)
       break;
    end
       if ((time_1h(kk)- S_time_total(pp))<0.01)
         time_1h_Sark_tide_ht(kk)= Sark_ht_total(pp);
```

```
        zzz=1;
        break;
      end
  end
end


% to get 1v (dBm Vs tide height)
[z1 z2]=size(time_1v); %to find out how many of dBm for 1v
for kk=(1:1:z2)
 zzz =0;
  for pp=(1:1:zz2)
    if(zzz==1)
       break;
    end
       if ((time_1v(kk)- S_time_total(pp))<0.01)
         time_1v_Sark_tide_ht(kk)= Sark_ht_total(pp);
         zzz=1;
         break;
       end
  end
end

% to get 1x (dBm Vs tide height)
[z1 z2]=size(time_1x); %to find out how many of dBm for 1v
for kk=(1:1:z2)
 zzz =0;
  for pp=(1:1:zz2)
    if(zzz==1)
       break;
    end
       if ((time_1x(kk)- S_time_total(pp))<0.01)
         time_1x_Sark_tide_ht(kk)= Sark_ht_total(pp);
         zzz=1;
         break;
       end
  end
end

% to get 2h (dBm Vs tide height)
[z1 z2]=size(time_2h); %to find out how many of dBm for 2h
for kk=(1:1:z2)
 zzz =0;
  for pp=(1:1:zz2)
    if(zzz==1)
       break;
    end
       if ((time_2h(kk)- S_time_total(pp))<0.01)
         time_2h_Sark_tide_ht(kk)= Sark_ht_total(pp);
         zzz=1;
         break;
       end
  end
end

% to get 2v (dBm Vs tide height)
[z1 z2]=size(time_2v); %to find out how many of dBm for 2v
for kk=(1:1:z2)
 zzz =0;
  for pp=(1:1:zz2)
    if(zzz==1)
       break;
    end
       if ((time_2v(kk)- S_time_total(pp))<0.01)
         time_2v_Sark_tide_ht(kk)= Sark_ht_total(pp);
         zzz=1;
         break;
       end
  end
end

% to get 2x (dBm Vs tide height)
[z1 z2]=size(time_2x); %to find out how many of dBm for 2x
for kk=(1:1:z2)
 zzz =0;
  for pp=(1:1:zz2)
    if(zzz==1)
       break;
    end
       if ((time_2x(kk)- S_time_total(pp))<0.01)
```

```
         time_2x_Sark_tide_ht(kk)= Sark_ht_total(pp);
         zzz=1;
         break;
       end
  end
end

% subplotting the sark tide ht Vs dBr

handle = axes;

hold on

handle = subplot(3,2,1);plot(time_1h_Sark_tide_ht,median_1h,'r*')
hold on
handle = subplot(3,2,1);plot(time_1h_Sark_tide_ht,mean_1h,'k.','markersize',6)
hold on

%--------------for error bar only---------------
%errorbar(xxx,yyy,zzz), zzz is the deviation
xxx=time_1h_Sark_tide_ht;yyy=(agcdb_1h_95_percent+agcdb_1h_5_percent)/2;
zzz=(agcdb_1h_95_percent-agcdb_1h_5_percent)/2;
h1=errorbar(xxx,yyy,zzz, '.');
%handle =
subplot(3,2,1);errorbar(time_1h_Sark_tide_ht,agcdb_1h_95_percent,agcdb_1h_5_percent,  '.')
set(h1,'markersize',1,'Color',[0.5,0.5,0.5])
%-----------------------------------------------

grid on
axis([0 12 dBscale(1)-1 dBscale(1)+60]);
set(handle, 'xtick', [0:1:12],'FontSize',8);
set(handle, 'ytick', [0:5:60],'FontSize',8);
title1=sprintf('%s%s', data_date, ': F1 Horizontal');
title(title1)
aaa=sort(time_1h_Sark_tide_ht);
%if (tide==0)
%      text(aaa(1),57,[num2str(time_begin_hr),':00 UT'],'Fontsize',6,'Color','k')
%      text(aaa(end),57,[num2str(time_end_hr),':59 UT'],'Fontsize',6,'Color','k')
%end

%if (tide==1)
%      text(aaa(end),57,[num2str(time_begin_hr),':00 UT'],'Fontsize',6,'Color','k')
%      text(aaa(1),57,[num2str(time_end_hr),':59 UT'],'Fontsize',6,'Color','k')
%end
text(9,52.5,'*','Fontsize',16,'Color','r')
text(9.6,54,'median','Fontsize',6,'Color','r')
text(9,52.8,'.','Fontsize',16,'Color','k')
text(9.6,51,'mean','Fontsize',6,'Color','k')
text(9,48,'- Fading Range','Fontsize',6,'Color',[0.5,0.5,0.5])
xlabel('Sark tide height (metre)','FontSize',8)
ylabel('Signal amplitude (dBr)','FontSize',8)


hold on
handle = subplot(3,2,3);plot(time_1v_Sark_tide_ht,median_1v,'m*')
hold on
handle = subplot(3,2,3);plot(time_1v_Sark_tide_ht,mean_1v,'k.','markersize',6)
hold on

%--------------for error bar only---------------
%errorbar(xxx,yyy,zzz), zzz is the deviation
xxx=time_1v_Sark_tide_ht;yyy=(agcdb_1v_95_percent+agcdb_1v_5_percent)/2;
zzz=(agcdb_1v_95_percent-agcdb_1v_5_percent)/2;
h1=errorbar(xxx,yyy,zzz, '.');
set(h1,'markersize',1,'Color',[0.5,0.5,0.5])
%-----------------------------------------------

grid on
axis([0 12 dBscale(1)-1 dBscale(1)+60]);
set(handle, 'xtick', [0:1:12],'FontSize',8);
set(handle, 'ytick', [0:5:60],'FontSize',8);
title1=sprintf('%s%s', data_date, ': F1 Vertical');
title(title1)
aaa=sort(time_1v_Sark_tide_ht);
%if (tide==0)
%      text(aaa(1),57,[num2str(time_begin_hr),':00 UT'],'Fontsize',6,'Color','k')
%      text(aaa(end),57,[num2str(time_end_hr),':59 UT'],'Fontsize',6,'Color','k')
%end

%if (tide==1)
```

```
%      text(aaa(end),57,[num2str(time_begin_hr),':00 UT'],'Fontsize',6,'Color','k')
%      text(aaa(1),57,[num2str(time_end_hr),':59 UT'],'Fontsize',6,'Color','k')
%end
text(9,52.5,'*','Fontsize',16,'Color','m')
text(9.6,54,'median','Fontsize',6,'Color','m')
text(9,52.8,'.','Fontsize',16,'Color','k')
text(9.6,51,'mean','Fontsize',6,'Color','k')
text(9,48,'- Fading Range','Fontsize',6,'Color',[0.5,0.5,0.5])
xlabel('Sark tide height (metre)','FontSize',8)
ylabel('Signal amplitude (dBr)','FontSize',8)

hold on
handle = subplot(3,2,2);plot(time_2h_Sark_tide_ht,median_2h,'b*')
hold on
handle = subplot(3,2,2);plot(time_2h_Sark_tide_ht,mean_2h,'k.','markersize',6)
hold on

%--------------for error bar only---------------
%errorbar(xxx,yyy,zzz), zzz is the deviation
xxx=time_2h_Sark_tide_ht;yyy=(agcdb_2h_95_percent+agcdb_2h_5_percent)/2;
zzz=(agcdb_2h_95_percent-agcdb_2h_5_percent)/2;
h1=errorbar(xxx,yyy,zzz, '.');
set(h1,'markersize',1,'Color',[0.5,0.5,0.5])
%-----------------------------------------------

grid on
axis([0 12 dBscale(1)-1 dBscale(1)+60]);
set(handle, 'xtick', [0:1:12],'FontSize',8);
set(handle, 'ytick', [0:5:60],'FontSize',8);
title1=sprintf('%s%s', data_date, ': F2 Horizontal');
title(title1)
aaa=sort(time_2h_Sark_tide_ht);
%if (tide==0)
%      text(aaa(1),57,[num2str(time_begin_hr),':00 UT'],'Fontsize',6,'Color','k')
%      text(aaa(end),57,[num2str(time_end_hr),':59 UT'],'Fontsize',6,'Color','k')
%end

%if (tide==1)
%      text(aaa(end),57,[num2str(time_begin_hr),':00 UT'],'Fontsize',6,'Color','k')
%      text(aaa(1),57,[num2str(time_end_hr),':59 UT'],'Fontsize',6,'Color','k')
%end
text(9,52.5,'*','Fontsize',16,'Color','b')
text(9.6,54,'median','Fontsize',6,'Color','b')
text(9,52.8,'.','Fontsize',16,'Color','k')
text(9.6,51,'mean','Fontsize',6,'Color','k')
text(9,48,'- Fading Range','Fontsize',6,'Color',[0.5,0.5,0.5])
xlabel('Sark tide height (metre)','FontSize',8)
ylabel('Signal amplitude (dBr)','FontSize',8)

hold on
handle = subplot(3,2,4);plot(time_2v_Sark_tide_ht,median_2v,'c*')
hold on
handle = subplot(3,2,4);plot(time_2v_Sark_tide_ht,mean_2v,'k.','markersize',6)
hold on

%--------------for error bar only---------------
%errorbar(xxx,yyy,zzz), zzz is the deviation
xxx=time_2v_Sark_tide_ht;yyy=(agcdb_2v_95_percent+agcdb_2v_5_percent)/2;
zzz=(agcdb_2v_95_percent-agcdb_2v_5_percent)/2;
h1=errorbar(xxx,yyy,zzz, '.');
set(h1,'markersize',1,'Color',[0.5,0.5,0.5])
%-----------------------------------------------

grid on
axis([0 12 dBscale(1)-1 dBscale(1)+60]);
set(handle, 'xtick', [0:1:12],'FontSize',8);
set(handle, 'ytick', [0:5:60],'FontSize',8);
title1=sprintf('%s%s', data_date, ': F2 Vertical');
title(title1)
aaa=sort(time_2v_Sark_tide_ht);
%if (tide==0)
%      text(aaa(1),57,[num2str(time_begin_hr),':00 UT'],'Fontsize',6,'Color','k')
%      text(aaa(end),57,[num2str(time_end_hr),':59 UT'],'Fontsize',6,'Color','k')
%end

%if (tide==1)
%      text(aaa(end),57,[num2str(time_begin_hr),':00 UT'],'Fontsize',6,'Color','k')
%      text(aaa(1),57,[num2str(time_end_hr),':59 UT'],'Fontsize',6,'Color','k')
%end
text(9,52.5,'*','Fontsize',16,'Color','c')
```

```
text(9.6,54,'median','Fontsize',6,'Color','c')
text(9,52.8,'.','Fontsize',16,'Color','k')
text(9.6,51,'mean','Fontsize',6,'Color','k')
text(9,48,'- Fading Range','Fontsize',6,'Color',[0.5,0.5,0.5])
xlabel('Sark tide height (metre)','FontSize',8)
ylabel('Signal amplitude (dBr)','FontSize',8)

hold on
handle = subplot(3,2,5);plot(time_1x_Sark_tide_ht,median_1x,'g*')
hold on
handle = subplot(3,2,5);plot(time_1x_Sark_tide_ht,mean_1x,'k.','markersize',6)
hold on

%--------------for error bar only---------------
%errorbar(xxx,yyy,zzz), zzz is the deviation
xxx=time_1x_Sark_tide_ht;yyy=(agcdb_1x_95_percent+agcdb_1x_5_percent)/2;
zzz=(agcdb_1x_95_percent-agcdb_1x_5_percent)/2;
h1=errorbar(xxx,yyy,zzz, '.');
set(h1,'markersize',1,'Color',[0.5,0.5,0.5])
%-----------------------------------------------

grid on
axis([0 12 dBscale(1)-1 dBscale(1)+60]);
set(handle, 'xtick', [0:1:12],'FontSize',8);
set(handle, 'ytick', [0:5:60],'FontSize',8);
title1=sprintf('%s%s', data_date, ': F1 Cross Polarisation');
title(title1)
aaa=sort(time_1x_Sark_tide_ht);
%if (tide==0)
%      text(aaa(1),57,[num2str(time_begin_hr),':00 UT'],'Fontsize',6,'Color','k')
%      text(aaa(end),57,[num2str(time_end_hr),':59 UT'],'Fontsize',6,'Color','k')
%end

%if (tide==1)
%      text(aaa(end),57,[num2str(time_begin_hr),':00 UT'],'Fontsize',6,'Color','k')
%      text(aaa(1),57,[num2str(time_end_hr),':59 UT'],'Fontsize',6,'Color','k')
%end
text(9,52.5,'*','Fontsize',16,'Color','g')
text(9.6,54,'median','Fontsize',6,'Color','g')
text(9,52.8,'.','Fontsize',16,'Color','k')
text(9.6,51,'mean','Fontsize',6,'Color','k')
text(9,48,'- Fading Range','Fontsize',6,'Color',[0.5,0.5,0.5])
xlabel('Sark tide height (metre)','FontSize',8)
ylabel('Signal amplitude (dBr)','FontSize',8)

hold on
handle = subplot(3,2,6);plot(time_2x_Sark_tide_ht,median_2x,'k*')
hold on
handle = subplot(3,2,6);plot(time_2x_Sark_tide_ht,mean_2x,'k.','markersize',6)
hold on

%--------------for error bar only---------------
%errorbar(xxx,yyy,zzz), zzz is the deviation
xxx=time_2x_Sark_tide_ht;yyy=(agcdb_2x_95_percent+agcdb_2x_5_percent)/2;
zzz=(agcdb_2x_95_percent-agcdb_2x_5_percent)/2;
h1=errorbar(xxx,yyy,zzz, '.');
set(h1,'markersize',1,'Color',[0.5,0.5,0.5])
%-----------------------------------------------

grid on
axis([0 12 dBscale(1)-1 dBscale(1)+60]);
set(handle, 'xtick', [0:1:12],'FontSize',8);
set(handle, 'ytick', [0:5:60],'FontSize',8);
title1=sprintf('%s%s', data_date, ': F2 Cross Polarisation');
title(title1)
aaa=sort(time_2x_Sark_tide_ht);
%if (tide==0)
%      text(aaa(1),57,[num2str(time_begin_hr),':00 UT'],'Fontsize',6,'Color','k')
%      text(aaa(end),57,[num2str(time_end_hr),':59 UT'],'Fontsize',6,'Color','k')
%end

%if (tide==1)
%      text(aaa(end),57,[num2str(time_begin_hr),':00 UT'],'Fontsize',6,'Color','k')
%      text(aaa(1),57,[num2str(time_end_hr),':59 UT'],'Fontsize',6,'Color','k')
%end
text(9,52.5,'*','Fontsize',16,'Color','k')
text(9.6,54,'median','Fontsize',6,'Color','k')
text(9,52.8,'.','Fontsize',16,'Color','k')
text(9.6,51,'mean','Fontsize',6,'Color','k')
text(9,48,'- Fading Range','Fontsize',6,'Color',[0.5,0.5,0.5])
```

```
xlabel('Sark tide height (metre)','FontSize',8)
ylabel('Signal amplitude (dBr)','FontSize',8)

%print -dpsc -POldRslColourPS
%print -depsc 20010416_ht_vs_amp
%print -djpeg90 20010421_ht_vs_amp.jpg
```

Script 3

```
*filename: figure5_3.m
% previous filename: G_agc_db_30secs_plot.m
%last update: 25th Oct2001 :to plot just agc value from c files (data1hc etc..)
% last upadte: to convert agc to dB value and change the x-axis to secs
% C files contains 40 secs of data, there r roughly 801 agc value in 40 secs
% C files contains 30 secs of data, tehre r roughlu 781 agc values in 30 secs
% last update : 21st May2002, plot Guernsey agc files only for 30 secs files
% to plot only 30secs of data (28th Jun 2002)

clear
%--------------------plot just agc db value from c files freq 1 --------

orient tall

filename1=[ ...

'guernsey1hc.10Apr2001.070110'; ...
'guernsey1hc.10Apr2001.071310'; ...
'guernsey1hc.10Apr2001.072510'; ...
'guernsey1hc.10Apr2001.073710'; ...
'guernsey1hc.10Apr2001.074910'; ...

       ];

aaa=1; % for subplot (see subplot below)

for k=1:(min(5,size(filename1)))

%filename='data1hc.05Oct2001.090110';
fn = ['/temp/cyds1/Guernsey_Apr2001/10Apr2001/'filename1(k,:)];

[fid, message] = fopen(fn,'r');

nagc1 = fread(fid,4,'uint8');
nagc = nagc1(1) + 256*nagc1(2) + 256*256*nagc1(3) + 256*256*256*nagc1(4);

agc = fread(fid,nagc,'uint8');

fclose(fid);

figure(1)

%plot(agc);


% ---ignore the 1st second of agc value ----

[z1 z2] = size(agc); % z1 is the actual size of agc
Agc_1st_sec = round(z1/30);
agc(1:Agc_1st_sec)=[];


[z3 z4]=size(agc);
new_sample = round(3000/z3); % round up the integer value of agc

for i =0:1:(z3-1)
    agc_new(((new_sample*i)+1):(new_sample*(i+1))) =agc(i+1);
end

[z5 z6]=size(agc_new);  % to round up to 3000 sets of samples

if z6 > 3000
  agc_new(3001:z6)=[];
end

if z6 < 3000
  agc_new((z6+1):3000)=agc(z3);
end

% ---- to covert agc value to dBr-------------------------------------

dBm = [-107:8];

% dB value for frequency 1

%below used before 29Jun2001
%agcnum(1,:) = [3 3 3 7 12 19 26 33 40 46 52 57 62 67 71 76 80 84 87   ...
```

```
%               90 94 98 101 104 107 110 113 115 118 120 123 125 129   ...
%               131 133 136 138 140 142 145 147 149 151 153 155 158    ...
%               159 161 163 165 167 168 171 173 175 177 178 180 182    ...
%               184 186 188 190 192 193 195 197 199 201 203 204 206    ...
%               208 210 211 213 215 217 219 221 222 224 226 228 230    ...
%               232 233 236 238 239 241 243 245 246 248 248 249 249    ...
%               249 250 250 250 250 250 250 250 250 250 250 250 250    ...
%               250 250 250 250 250];

% below used after 29Jun2001
agcnum(1,:) = [3 9 12 18 22 31 36 41 46 50 54 59 63 67 71 76 79 82 85   ...
               90 94 98 101 104 107 110 113 115 118 120 123 125 129   ...
               131 133 136 138 140 142 145 147 149 151 153 155 158    ...
               159 161 163 165 167 168 171 173 175 177 178 180 182    ...
               184 186 188 190 192 193 195 197 199 201 203 204 206    ...
               208 210 211 213 215 217 219 221 222 224 226 228 230    ...
               232 233 236 238 239 241 243 245 246 248 248 249 249    ...
               249 250 250 250 250 250 250 250 250 250 250 250 250    ...
               250 250 250 250 250];



for ii = 1:255
  x = find(agcnum(1,:) >= ii);
  if isempty(x)
    agc2dB(1,ii) = dBm(length(dBm));
  else
    agc2dB(1,ii) = dBm(x(1));
  end
end

agc_dBm_value=agc2dB(agc_new);

figure(1)

fig1=agc_dBm_value;

%to convert 3000 to 30 secs
fig1_x= [1:length(fig1)]*1e-2;

subplot(5,2,aaa);plot(fig1_x,fig1)
title(filename1(k,:))
ylabel ('AGC level (dBr)')
%xlabel ('Time (sec)')
axis([0 30 -110 -80])

grid on
hold on

aaa=aaa+2;

end % to end first for lop for freq 1
xlabel ('Time (sec)')



%--------------------start of 2nd plot-------------------------------
%--------------------plot c file agc in db for freq 2---------------

orient tall

filename2=[ ...

'guernsey2hc.10Apr2001.070410'; ...
'guernsey2hc.10Apr2001.071610'; ...
'guernsey2hc.10Apr2001.072810'; ...
'guernsey2hc.10Apr2001.074010'; ...
'guernsey2hc.10Apr2001.075210'; ...
       ];

bbb=2; % for subplot (see subplot below)

for k=1:(min(5,size(filename2)))

%filename='data2hc.05Oct2001.090410';
fn = ['/temp/cyds1/Guernsey_Apr2001/10Apr2001/'filename2(k,:)];

[fid, message] = fopen(fn,'r');

nagc1 = fread(fid,4,'uint8');
```

```
nagc = nagc1(1) + 256*nagc1(2) + 256*256*nagc1(3) + 256*256*256*nagc1(4);

agc = fread(fid,nagc,'uint8');

fclose(fid);


% ------------------- re sample agc samples to 40000 samples----------

% ignore the 1st second of agc value

[z1 z2] = size(agc); % z1 is the actual size of agc
Agc_1st_sec = round(z1/30);
agc(1:Agc_1st_sec)=[];

[z3 z4]=size(agc);
new_sample = round(3000/z3); % round up the integer value of agc

for i =0:1:(z3-1)
    agc_new(((new_sample*i)+1):(new_sample*(i+1))) =agc(i+1);
end

[z5 z6]=size(agc_new);  % to round up to 3000 sets of samples

if z6 > 3000
  agc_new(3001:z6)=[];
end

if z6 < 3000
  agc_new(z6+1:3000)=agc(z3);
end

% ---- to covert agc value to dBr--------------------------------------

dBm = [-107:8];

%dB value for frequency 2
%below used before 29Jun2001
%agcnum(1,:) = [3 6 12 19 26 33 39 45 51 56 62 66 71 75 79 83 87 91 94 ...
%               97 100 104 106 109 112 115 117 120 123 125 128 130 133 ...
%               135 137 140 142 144 146 148 151 153 155 157 159 161    ...
%               163 165 167 169 171 173 174 176 178 180 182 184 186    ...
%               187 189 191 193 195 196 198 200 202 204 205 207 208    ...
%               210 212 214 216 218 219 221 223 225 226 228 230 232    ...
%               234 236 238 240 241 243 245 246 247 248 249 249 250    ...
%               250 250 250 250 250 250 250 250 250 251 251 251 251    ...
%               251 251 251 251 251];



%below used only after 29Jun2001
agcnum(1,:) = [3 3 12 15 26 32 37 41 47 51 56 59 65 69 75 79 83 87 91 94 ...
               97 100 104 106 109 112 115 117 120 123 125 128 130 133 ...
               135 137 140 142 144 146 148 151 153 155 157 159 161    ...
               163 165 167 169 171 173 174 176 178 180 182 184 186    ...
               187 189 191 193 195 196 198 200 202 204 205 207 208    ...
               210 212 214 216 218 219 221 223 225 226 228 230 232    ...
               234 236 238 240 241 243 245 246 247 248 249 249 250    ...
               250 250 250 250 250 250 250 250 250 251 251 251 251    ...
               251 251 251 251];

for ii = 1:255
  x = find(agcnum(1,:) >= ii);
  if isempty(x)
    agc2dB(1,ii) = dBm(length(dBm));
  else
    agc2dB(1,ii) = dBm(x(1));
  end
end

agc_dBm_value=agc2dB(agc_new);

fig3=agc_dBm_value;

%to covert 3000 to 30 secs
fig3_x= [1:length(fig3)]*1e-2;

subplot(5,2,bbb);plot(fig3_x,fig3)
title(filename2(k,:))
ylabel ('AGC level (dBr)')
```

```
%xlabel ('Time (sec)')
axis([0 30 -110 -80])

grid on
hold on

bbb =bbb+2;

end % end of 2nd for loop for Freq 2
xlabel ('Time (sec)')
hold off
```

Script 4

%filename:: figure5_9.m

```
%previous file name : agc_db_fft_G.m
%this file is for ploting Alderney files during 17th Nov2001
%it includes: agc plot, sigmal amplitude plot in dB and fft plot .
%last update : 01 AUG 2002

clear

%--------plot amp X agc value in dBr--------------------------------

filename='guernsey1hb.07Apr2001.173147';
fn = ['/temp/cyds1/Guernsey_Apr2001/07Apr2001/'filename];

[fid, message] = fopen(fn,'r');

nagc1 = fread(fid,4,'uint8');
nagc = nagc1(1) + 256*nagc1(2) + 256*256*nagc1(3) + 256*256*256*nagc1(4);

agc = fread(fid,nagc,'uint8');
%dummy = fread(fid,1,'uint8');

a8 = fread(fid,[2,inf],'uint8');

fclose(fid);

data_length  = size(a8,2);

data = a8(1,1:data_length) ...
     + 256*bitand(a8(2,1:data_length),127) ...
     - 256*bitand(a8(2,1:data_length),128);

X = data - mean(data);   % remove dc component

% X= (abs(X)); % to remove the -ve part

XX = hilbert(data);
amplitude = abs(XX);


%---------------re sample agc sample to 40000 samples-----------------

% ignore 1st second of agc value

[z1 z2] = size(agc); %z1 is the actual size of agc
Agc_1st_sec = round(z1/40);
agc(1:Agc_1st_sec)=[];

[z3 z4]=size(agc);
new_sample = round(100000/z3); %round up the integer value of agc

for i=0:1:(z3-1)
    agc_new(((new_sample*i)+1):(new_sample*(i+1))) = agc(i+1);
end

[z5 z6] = size(agc_new); % to round up to 100000 sets of samples

if z6>100000
   agc_new(100001:z6)=[];
end

if z6<1100000
   agc_new(z6+1:100000)=agc(z3);
end

%-----to convert agc valueto dBr------

dBm= [-107:8];

%dB value for frequency 1

agcnum(1,:) = [3 3 3 7 12 19 26 33 40 46 52 57 62 67 71 76 80 84 87   ...
               90 94 98 101 104 107 110 113 115 118 120 123 125 129   ...
               131 133 136 138 140 142 145 147 149 151 153 155 158    ...
               159 161 163 165 167 168 171 173 175 177 178 180 182    ...
               184 186 188 190 192 193 195 197 199 201 203 204 206    ...
               208 210 211 213 215 217 219 221 222 224 226 228 230    ...
               232 233 236 238 239 241 243 245 246 248 248 249 249    ...
```

```
               249 250 250 250 250 250 250 250 250 250 250 250 250    ...
               250 250 250 250 250];


for ii = 1:255

  x = find(agcnum(1,:) >= ii);
  if isempty(x)
    agc2dB(1,ii) = dBm(length(dBm));
  else
    agc2dB(1,ii) = dBm(x(1));
  end
end


agc_dBm_value=agc2dB(agc_new);

figure(1)

fig1=agc_dBm_value;

%to convert 100000 to 10 secs

fig1_x=[1:length(fig1)]*1e-4;

subplot(3,2,1); plot(fig1_x,fig1)
title(filename)
ylabel('AGC level (dBr)')
xlabel('Time(sec)')
axis([0 10 -110 -80])
grid on
hold on


%------to get the agc linear voltage gain (agc_lvg)---

agc_lvg=10.^(agc_dBm_value/20);
%-------------------------------------------------------

%-----plot amplitude of the signal--------------

Signal_amplitude =(agc_lvg).*(XX);

Signal_Amplitude =abs(Signal_amplitude);%to obtain real signal amplitude

sorted =sort(Signal_Amplitude);

value_at_10_percent=sorted(length(sorted)*0.1);
value_at_90_percent=sorted(length(sorted)*0.9);

Fading_Range=20*log10(value_at_90_percent/value_at_10_percent);

fig2=Signal_Amplitude;

%to convert 100000 to 10 secs and convert to dBm value
fig2_x=[1:length(fig2)]*1e-4;
fig2_y=20*log10(fig2);

subplot(3,2,3);plot(fig2_x,fig2_y)

title(['Signal amplitude with ',num2str(Fading_Range),' dB of fading'])
ylabel('dBr')
xlabel('Time(sec)')
axis([0 10 -90 0])
grid on
hold on


% -----------to get the fft of the signal ---------------

fig2_x_fft=[1:length(fig2)]*0.1; %convert to Hz, note: every step is 0.1Hz
fig2_y_fft=abs(fftshift(fft(fig2)));

subplot(3,2,5);plot(fig2_x_fft,fig2_y_fft)

title('FFT of the signal amplitude')
xlabel('Frequency(Hz)')
axis([5.0001e3 5.005e3 0 2500])
grid on
hold on
```

```
%--------end of 1st plot-----------------------------------------

%---------start of 2nd plot----------------------------------------


%--------plot amp X agc value in dBr-------------------------------

orient tall
figure(1)


filename='guernsey2hb.07Apr2001.173447';
fn = ['/temp/cyds1/Guernsey_Apr2001/07Apr2001/'filename];

[fid, message] = fopen(fn,'r');

nagc1 = fread(fid,4,'uint8');
nagc = nagc1(1) + 256*nagc1(2) + 256*256*nagc1(3) + 256*256*256*nagc1(4);

agc = fread(fid,nagc,'uint8');
%dummy = fread(fid,1,'uint8');

a8 = fread(fid,[2,inf],'uint8');

fclose(fid);

data_length  = size(a8,2);

data = a8(1,1:data_length) ...
     + 256*bitand(a8(2,1:data_length),127) ...
     - 256*bitand(a8(2,1:data_length),128);

X = data - mean(data);   % remove dc component

% X= (abs(X)); % to remove the -ve part

XX = hilbert(data);
amplitude = abs(XX);


%---------------re sample agc sample to 40000 samples-----------------

% ignore 1st second of agc value

[z1 z2] = size(agc); %z1 is the actual size of agc
Agc_1st_sec = round(z1/40);
agc(1:Agc_1st_sec)=[];

[z3 z4]=size(agc);
new_sample = round(100000/z3); %round up the integer value of agc

for i=0:1:(z3-1)
    agc_new(((new_sample*i)+1):(new_sample*(i+1))) = agc(i+1);
end

[z5 z6] = size(agc_new); % to round up to 100000 sets of samples

if z6>100000
   agc_new(100001:z6)=[];
end

if z6<1100000
   agc_new(z6+1:100000)=agc(z3);
end

%-----to convert agc valueto dBr------

dBm= [-107:8];

%dB value for frequency 2

agcnum(1,:) = [3 6 12 19 26 33 39 45 51 56 62 66 71 75 79 83 87 91 94 ...
               97 100 104 106 109 112 115 117 120 123 125 128 130 133 ...
               135 137 140 142 144 146 148 151 153 155 157 159 161    ...
               163 165 167 169 171 173 174 176 178 180 182 184 186    ...
               187 189 191 193 195 196 198 200 202 204 205 207 208    ...
               210 212 214 216 218 219 221 223 225 226 228 230 232    ...
               234 236 238 240 241 243 245 246 247 248 249 249 250    ...
               250 250 250 250 250 250 250 250 250 251 251 251 251    ...
```

```
               251 251 251 251 251];


for ii = 1:255

  x = find(agcnum(1,:) >= ii);
  if isempty(x)
    agc2dB(1,ii) = dBm(length(dBm));
  else
    agc2dB(1,ii) = dBm(x(1));
  end
end


agc_dBm_value=agc2dB(agc_new);

figure(1)

fig3=agc_dBm_value;

%to convert 100000 to 10 secs

fig3_x=[1:length(fig3)]*1e-4;

subplot(3,2,2); plot(fig3_x,fig3)
title(filename)
xlabel('Time(sec)')
ylabel('AGC level (dBr)')
axis([0 10 -110 -80])
grid on
hold on


%------to get the agc linear voltage gain (agc_lvg)---

agc_lvg=10.^(agc_dBm_value/20);
%-------------------------------------------------------

%-----plot amplitude of the signal--------------

Signal_amplitude =(agc_lvg).*(XX);

Signal_Amplitude =abs(Signal_amplitude);%to obtain real signal amplitude

sorted = sort(Signal_Amplitude);

value_at_10_percent=sorted(length(sorted)*0.1);
value_at_90_percent=sorted(length(sorted)*0.9);

Fading_Range=20*log10(value_at_90_percent/value_at_10_percent);

fig4=Signal_Amplitude;

%to convert 100000 to 10 secs and convert to dBm value
fig4_x=[1:length(fig4)]*1e-4;
fig4_y=20*log10(fig4);

subplot(3,2,4);plot(fig4_x,fig4_y)

title(['Signal amplitude with ',num2str(Fading_Range),' dB of fading'])
ylabel('dBr')
xlabel('Time(sec)')
axis([0 10 -90 0])
grid on
hold on


% -----------to get the fft of the signal ---------------

fig4_x_fft=[1:length(fig4)]*0.1; %convert to Hz, note: every step is 0.1Hz
fig4_y_fft=abs(fftshift(fft(fig4)));

subplot(3,2,6);plot(fig4_x_fft,fig4_y_fft)

title('FFT of the signal amplitude')
xlabel('Frequency(Hz)')
axis([5.0001e3 5.005e3 0 2500])
grid on
hold off
```

Script 5

```
% filename: figure5_34.m
% previous filename : plot_10Dec01_FFT_Sounder.m
% 03 & 06 April 2001 - to add in finding the min width with 80%
%                 of total spectrum area.

% put two files in one , update on 30th Jun2002

clear
%--------------------plot FFT -----------------------------

orient tall

filename='alderney1vb.10Dec2001.120047';
fn = ['/temp/cyds1/Alderney_December2001/10Dec2001/'filename];

[fid, message] = fopen(fn,'r');
%[fid, message] =
fopen('/temp/cyds1/Alderney_November2001/17Nov2001/alderney1hb.17Nov2001.110147','r');

nagc1 = fread(fid,4,'uint8');
nagc = nagc1(1) + 256*nagc1(2) + 256*256*nagc1(3) + 256*256*256*nagc1(4);

agc = fread(fid,nagc,'uint8');
%dummy = fread(fid,1,'uint8');

a8 = fread(fid,[2,inf],'uint8');

fclose(fid);

data_length  = size(a8,2);

data = a8(1,1:data_length) ...
     + 256*bitand(a8(2,1:data_length),127) ...
     - 256*bitand(a8(2,1:data_length),128);

X = hilbert(data);
XX = abs(X);

figure(1)

H = abs(fftshift(fft(X)));
fscale = (-5000+(10000/100000)*[1:100000]);

%to calculate 80% of total spectrum
Htotal =0;
 for i=1:1:100000
    Htotal =  Htotal+(H(i)*H(i)*0.1);
 end

H_80percent =0.8*Htotal;
inner_loop =0;

% to find the binary position of max H
[z1 z2]=max(H);
f_max=z2;

% to find the smallest spectrum width with H_80percent

for f_lenght=(0:1:100)
  if (inner_loop == 1)
     break;
  end

    for y=(f_max-50:1:f_max+50) % max of H range from -50 and +50
      if (inner_loop == 1)
      break;
      end

        H_freq_total =0;

        for start = (y:1:(y+f_lenght))
            H_freq_total= H_freq_total +(H(y)*H(y)*0.1);

           if (H_freq_total >= H_80percent)
             a=f_lenght;
             inner_loop =1;
             break;
```

```
             else
             inner_loop =0;

            end
        end
     end
end

f_end =start; f_start=(start-f_lenght);
fend=fscale(start); fstart=fscale(f_start);

subplot(4,1,1);plot(fscale,H)
grid on
hold on
[z1 z2] = max(H);
fmax = fscale(z2);
axis([fmax-10 fmax+10 0 z1*1.05]);

xlabel ('Frequency','Fontsize',9);
ylabel ('ADC Units','Fontsize',9);
title(filename,'Fontsize',9);

text(fmax-9, z1*1,{'fmax='fmax},'Fontsize',6,'Color','r')
text(fmax-9, z1*0.88,{'fstart(80%)='fstart},'Fontsize',6,'Color','b')
text(fmax-9, z1*0.76,{'fend(80%)='fend},'Fontsize',6,'Color','k')
text(fmax+6, z1*0.92,'F1- FFT plot','Fontsize',6,'Color','k')


%-----------------------------------------------------------
% ---------------------plot sounder -------------------

filename='alderney1vd.10Dec2001.120003';
fn = ['/temp/cyds1/Alderney_December2001/10Dec2001/'filename];

[fid, message] = fopen(fn,'r');
%[fid, message] = fopen('/temp/emw/data1vd.01Apr2001.010603','r');

nagc1 = fread(fid,4,'uint8');
nagc = nagc1(1) + 256*nagc1(2) + 256*256*nagc1(3) + 256*256*256*nagc1(4);

agc = fread(fid,nagc,'uint8');
%dummy = fread(fid,1,'uint8');

a8 = fread(fid,[2,inf],'uint8');

fclose(fid);

data_length  = size(a8,2);

data = a8(1,1:data_length) ...
     + 256*bitand(a8(2,1:data_length),127) ...
     - 256*bitand(a8(2,1:data_length),128);

X = hilbert(data);
XX = abs(X);

for ii = 1:10
   YY(ii,:) = XX([1:400]+400*(ii-1));
end

ymean = mean(YY);
ymax=max(YY);
ymin=min(YY);

subplot(4,1,2); plot(ymean);
hold on
plot(ymax, 'r:')
plot(ymin, 'k:')

xlabel ('Number of samples','Fontsize',9);
ylabel ('ADC Units','Fontsize',9);
title(filename,'Fontsize',9);
text(10,7500,'max value','Fontsize',6,'Color','r')
text(20,7500,'mean value','Fontsize',6,'Color','b')
text(30,7500,'min value','Fontsize',6,'Color','k')
text(80,7000,'F1- Sounder plot','Fontsize',6,'Color','k')

axis([0 100 0 8000])
grid on
```

```
%--------------------plot FFT for F2 -----------------------------

filename='alderney2vb.10Dec2001.120347';
fn = ['/temp/cyds1/Alderney_December2001/10Dec2001/'filename];

[fid, message] = fopen(fn,'r');

nagc1 = fread(fid,4,'uint8');
nagc = nagc1(1) + 256*nagc1(2) + 256*256*nagc1(3) + 256*256*256*nagc1(4);

agc = fread(fid,nagc,'uint8');
%dummy = fread(fid,1,'uint8');

a8 = fread(fid,[2,inf],'uint8');

fclose(fid);

data_length  = size(a8,2);

data = a8(1,1:data_length) ...
     + 256*bitand(a8(2,1:data_length),127) ...
     - 256*bitand(a8(2,1:data_length),128);

X = hilbert(data);
XX = abs(X);

figure(1)

H = abs(fftshift(fft(X)));
fscale = (-5000+(10000/100000)*[1:100000]);

%to calculate 80% of total spectrum
Htotal =0;
 for i=1:1:100000
    Htotal =  Htotal+(H(i)*H(i)*0.1);
 end

H_80percent =0.8*Htotal;
inner_loop =0;

% to find the binary position of max H
[z1 z2]=max(H);
f_max=z2;

% to find the smallest spectrum width with H_80percent

for f_lenght=(0:1:100)
  if (inner_loop == 1)
     break;
  end

    for y=(f_max-50:1:f_max+50) % max of H range from -50 and +50
      if (inner_loop == 1)
      break;
      end

        H_freq_total =0;

        for start = (y:1:(y+f_lenght))
            H_freq_total= H_freq_total +(H(y)*H(y)*0.1);

           if (H_freq_total >= H_80percent)
             a=f_lenght;
             inner_loop =1;
             break;

             else
             inner_loop =0;

            end
        end
     end
end

f_end =start; f_start=(start-f_lenght);
fend=fscale(start); fstart=fscale(f_start);

subplot(4,1,3);plot(fscale,H)
grid on
```

```
hold on
[z1 z2] = max(H);
fmax = fscale(z2);
axis([fmax-10 fmax+10 0 z1*1.05]);

xlabel ('Frequency','Fontsize',9);
ylabel ('ADC Units','Fontsize',9);
title(filename,'Fontsize',9);

text(fmax-9, z1*1,{'fmax='fmax},'Fontsize',6,'Color','r')
text(fmax-9, z1*0.88,{'fstart(80%)='fstart},'Fontsize',6,'Color','b')
text(fmax-9, z1*0.76,{'fend(80%)='fend},'Fontsize',6,'Color','k')
text(fmax+6, z1*0.92,'F2- FFT plot','Fontsize',6,'Color','k')


%-----------------------------------------------------------
% --------------------plot sounder -------------------

filename='alderney2vd.10Dec2001.120303';
fn = ['/temp/cyds1/Alderney_December2001/10Dec2001/'filename];

[fid, message] = fopen(fn,'r');
%[fid, message] = fopen('/temp/emw/data1vd.01Apr2001.010603','r');

nagc1 = fread(fid,4,'uint8');
nagc = nagc1(1) + 256*nagc1(2) + 256*256*nagc1(3) + 256*256*256*nagc1(4);

agc = fread(fid,nagc,'uint8');
%dummy = fread(fid,1,'uint8');

a8 = fread(fid,[2,inf],'uint8');

fclose(fid);

data_length  = size(a8,2);

data = a8(1,1:data_length) ...
     + 256*bitand(a8(2,1:data_length),127) ...
     - 256*bitand(a8(2,1:data_length),128);

X = hilbert(data);
XX = abs(X);

for ii = 1:10
   YY(ii,:) = XX([1:400]+400*(ii-1));
end

ymean = mean(YY);
ymax=max(YY);
ymin=min(YY);

subplot(4,1,4); plot(ymean);
hold on
plot(ymax, 'r:')
plot(ymin, 'k:')

xlabel ('Number of samples','Fontsize',9);
ylabel ('ADC Units','Fontsize',9);
title(filename,'Fontsize',9);
text(10,7500,'max value','Fontsize',6,'Color','r')
text(20,7500,'mean value','Fontsize',6,'Color','b')
text(30,7500,'min value','Fontsize',6,'Color','k')
text(80,7000,'F2- Sounder plot','Fontsize',6,'Color','k')
axis([0 100 0 8000])
grid on
hold off
```

Appendix B: Ray tracing equation

The following equations show how to obtain ζ for equation (6.27):

The angle ζ of the earth can be considered as

$$\zeta = \int_{\alpha_0}^{\alpha} \frac{1}{\tan\alpha \bullet \eta} \times \frac{d\zeta}{d\alpha} \tag{1}$$

The change in distance ΔS is:

$$\Delta S = \eta \times d\zeta \tag{2}$$

and,

$$\tan\alpha = \frac{\Delta\eta}{\Delta S} \tag{3}$$

by substituting equation (2) to (3)

$$\tan\alpha = \frac{\Delta\eta}{\eta \bullet d\zeta} \tag{4}$$

therefore,

$$d\zeta = \frac{1}{\tan\alpha} \times \frac{d\eta}{\eta} \tag{5}$$

by substituting (5) into (1),

$$\zeta = \int_{\alpha_0}^{\alpha} \frac{1}{\tan\alpha \bullet \eta} \times \frac{d\zeta}{d\alpha} \tag{6}$$

In order to derive $d\eta/d\alpha$, by expanding equation 6.26,

$$\eta = \frac{r_0}{2} - \frac{n(0)}{2a} \pm \frac{n(0) - ar_0}{2a} \sqrt{1 + \frac{4an(0)r_0 \frac{\cos\alpha_0}{\cos\alpha}}{\left(n(0) - ar_0\right)^2}} \tag{7}$$

If ar_0 is very large, the quadratic equation sign can be consider as + ve.

Assumption can be make that if X is close to 0 (since ar_0 is very large),

$$\sqrt{1+\mathrm{X}} \approx 1+\frac{\mathrm{X}}{2} \approx \left(1+\frac{2an(0)r_0\dfrac{\cos\alpha_0}{\cos\alpha}}{\left(n(0)-ar_0\right)^2}\right) \tag{8}$$

Therefore,

$$\eta=\frac{r_0}{2}-\frac{n(0)}{2a}+\frac{n(0)-ar_0}{2a}\left(1+\frac{2an(0)r_0\dfrac{\cos\alpha_0}{\cos\alpha}}{\left(n(0)-ar_0\right)^2}\right) \tag{9}$$

By expanding the above equation,

$$\eta=\frac{n(0)r_0\dfrac{\cos\alpha_0}{\cos\alpha}}{n(0)-ar_0} \tag{10}$$

Therefore

$$\frac{d\eta}{d\alpha}=\frac{n(0)r_0\cos\alpha_0}{n(0)-ar_0}\times\frac{d\dfrac{1}{\cos\alpha}}{d\alpha}=\frac{n(0)r_0\cos\alpha_0}{n(0)-ar_0}\times\frac{\sin\alpha}{\cos^2\alpha} \tag{11}$$

By substituting (11) to (6),

$$\zeta=\int_{\alpha_0}^{\alpha}\frac{1}{\tan\alpha\eta}\times\frac{n(0)r_0\cos\alpha_0}{n(0)-ar_0}\times\frac{\sin\alpha}{\cos^2\alpha} \tag{12}$$

By expanding (9),

$$\zeta=\int_{\alpha_0}^{\alpha}\frac{1}{\eta}\times\frac{n(0)r_0\cos\alpha_0}{\left(n(0)-ar_0\right)\cos\alpha} \tag{13}$$

If $\eta \approx r_0$, angle $\alpha = 0$ and therefore $\cos\alpha = 1$. Hence,

$$\zeta=\frac{n(0)\cos\alpha_0}{n(0)-ar_0}\left(\alpha-\alpha_0\right) \tag{14}$$

The above equation is also considered as equation 6.27 from Chapter 6.